ETSI TR 102 273-1-1 V1.2.1 (2001-12)

Technical Report

Electromagnetic compatibility and Radio spectrum Matters (ERM); Improvement on Radiated Methods of Measurement (using test site) and evaluation of the corresponding measurement uncertainties; Part 1: Uncertainties in the measurement of mobile radio equipment characteristics; Sub-part 1: Introduction

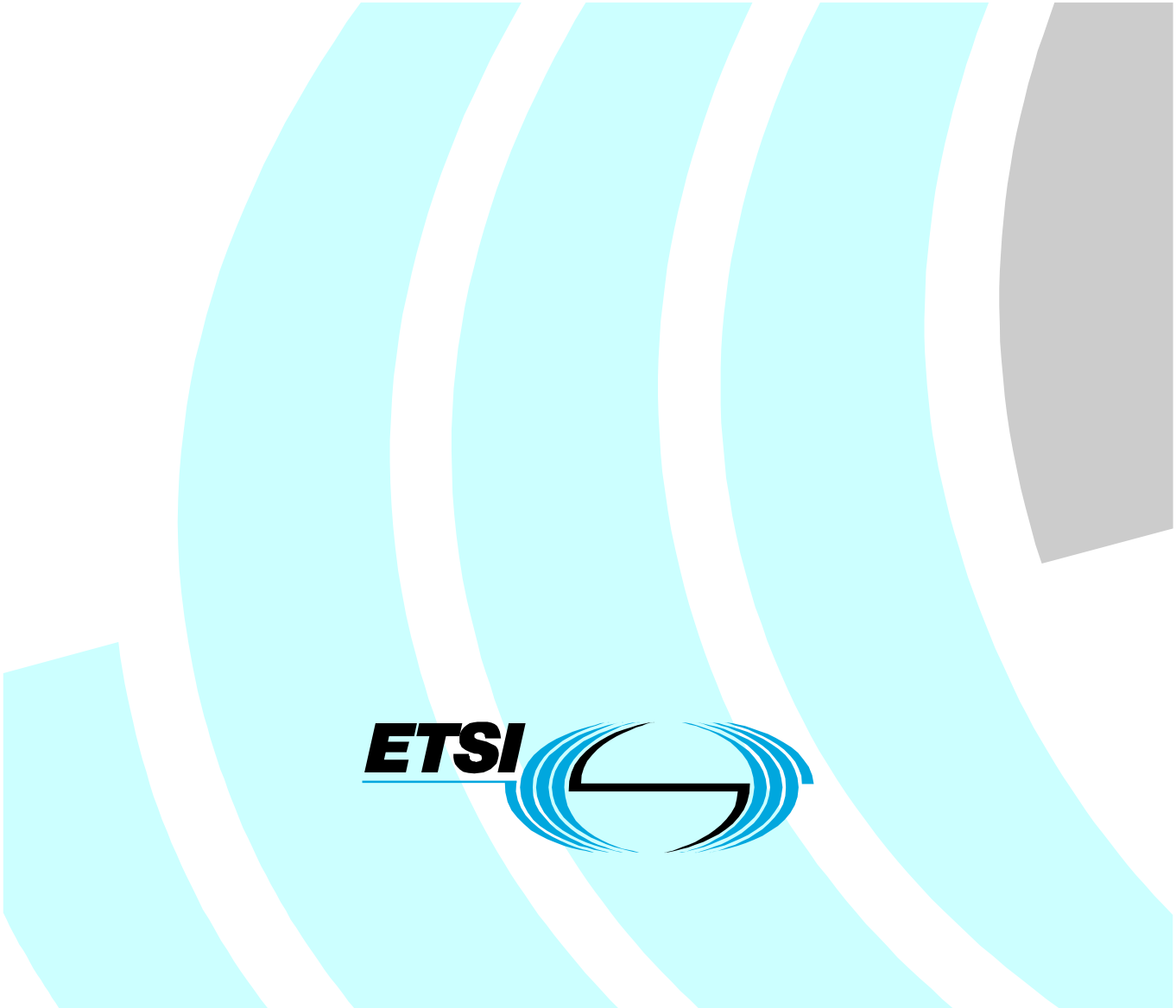

Reference
RTR/ERM-RP02-057-1-1

Keywords
analogue, data, measurement uncertainty,
mobile, radio, testing

ETSI

650 Route des Lucioles
F-06921 Sophia Antipolis Cedex - FRANCE

Tel.: +33 4 92 94 42 00 Fax: +33 4 93 65 47 16

Siret N° 348 623 562 00017 - NAF 742 C
Association à but non lucratif enregistrée à la
Sous-Préfecture de Grasse (06) N° 7803/88

Contents

Intellectual Property Rights

IPRs essential or potentially essential to the present document may have been declared to ETSI. The information pertaining to these essential IPRs, if any, is publicly available for **ETSI members and non-members**, and can be found in ETSI SR 000 314: *"Intellectual Property Rights (IPRs); Essential, or potentially Essential, IPRs notified to ETSI in respect of ETSI standards"*, which is available from the ETSI Secretariat. Latest updates are available on the ETSI Web server (http://webapp.etsi.org/IPR/home.asp).

Pursuant to the ETSI IPR Policy, no investigation, including IPR searches, has been carried out by ETSI. No guarantee can be given as to the existence of other IPRs not referenced in ETSI SR 000 314 (or the updates on the ETSI Web server) which are, or may be, or may become, essential to the present document.

Foreword

This Technical Report (TR) has been produced by ETSI Technical Committee Electromagnetic compatibility and Radio spectrum Matters (ERM).

The present document is part 1 sub-part 1 of a multi-part deliverable covering Improvement on radiated methods of measurement (using test site) and evaluation of the corresponding measurement uncertainties, as identified below:

Part 1: "Uncertainties in the measurement of mobile radio equipment characteristics";

Sub-part 1: "Introduction";

Sub-part 2: "Examples and annexes";

Part 2: "Anechoic chamber";

Part 3: "Anechoic chamber with a ground plane";

Part 4: "Open area test site";

Part 5: "Striplines";

Part 6: "Test fixtures";

Part 7: "Artificial human beings".

Introduction

At the time of publishing Edition 1 of ETR 273 (the original document number for the present document), the uncertainty of radiated tests on radio equipment left something to be desired. It was believed that some measurements may have been subject to as much as ±15 dB uncertainty. This meant that a manufacturer with an equipment which was marginal as far as, for example, spurious emission levels were concerned, could possibly have sent a test item to a number of different test houses in the certain knowledge that one of them would have passed it. As an illustration of the uncertainties existing at that time, a test house invited to participate in Round Robin tests organized as part of the original project, whilst declining the invitation to take part, volunteered the information that they could measure within ±10 dB and they had the results to prove it (i.e. they were proud that they could achieve that uncertainty).

In other cases, engineers have claimed uncertainties of lower magnitudes i.e. 2 or 3 dB for similar tests. An examination of the breakdown of the information available has, however, showed that different uncertaintiy components have been taken into account by the different engineers involved i.e. there has been no standard list of which uncertainty components to include.

The first edition of ETR 273 was the outcome of project team 60V's attempts to address these problems by an investigation into the uncertainties involved in radiated measurements. The information provided was divided as follows:

1) sources of uncertainty are identified for all types of test facility commonly used for radiated tests (i.e. Anechoic Chambers, Anechoic Chambers with Ground Planes, Open Area Test Sites, striplines as well as devices used to assist testing, namely Test Fixtures and Artificial Human Bodies such as salty columns);

2) methods of calculating/deriving the magnitudes of the uncertainties for individual facilities;

3) verification procedures for all test facilities (at the 1,5 m test height);

4) revised radiated test methods (all substitution tests).

This revised 2nd version of ETR 273 (now renumbered TR 102 273) is improved to include in particular:

- new section in part 1, sub-part 1: clause 6.6.6 "Limitations in the applicability of BER uncertainty calculations";
- new section in part 1, sub-part 1: clause 6.8 "Uncertainty of fully automated test systems";
- technical corrections to some values in NSA tables in parts 3 and 4.

1 Scope

The present document provides background to the subject of measurement uncertainty and proposes extensions and improvements relevant to radiated measurements. It also details the methods of radiated measurements (test methods for mobile radio equipment parameters and verification procedures for test sites) and additionally provides the methods for evaluating the associated measurement uncertainties.

The present document provides a method to be used together with all the applicable standards and (E)TRs, supports TR 100 027 [10] and can be used with TR 100 028 [11].

The present document includes a general presentation on the subject of measurement uncertainty.

2 References

For the purposes of this Technical Report (TR), the following references apply:

[1] ANSI C63.5 (1998): "American National Standard for Calibration of Antennas Used for Radiated Emission Measurements in Electromagnetic Interference (EMI) ControlCalibration of Antennas (9 kHz to 40 GHz)".

[2] "Antenna Engineering Handbook", Richard C. Johnson, H. Jasik.

[3] John D. Kraus. "Antennas", third edition, McGraw Hill.

[4] Robert E. Collin. "Antennas and radio wave propagation", 1985, McGraw Hill Series in Electrical Engineering.

[5] Constantine A. Balanis. "Antenna Theory: Analysis and Design", 1996, J. E. Wiley.

[6] ITU-T Recommendation O.41: "Psophometer for use on telephone-type circuits".

[7] ITU-T Recommendation O.153: "Basic parameters for the measurement of error performance at bit rates below the primary rate".

[8] "Control of errors on Open Area Test Sites", A. A. Smith Jnr. EMC technology, October 1982, page 50-58.

[9] EN 55020: "Electromagnetic immunity of broadcast receivers and associated equipment".

[10] ETSI TR 100 027: "Electromagnetic compatibility and Radio spectrum Matters (ERM); Methods of measurement for private mobile radio equipment".

[11] ETSI TR 100 028 (V1.4.1) (parts 1 and 2): "Electromagnetic compatibility and Radio spectrum Matters (ERM); Uncertainties in the measurement of mobile radio equipment characteristics".

[12] ETSI TR 102 273-1-2: "ElectroMagnetic Compatibility and Radio Spectrum Matters (ERM); Improvement on Radiated Methods of Measurement (using test site) and evaluation of the corresponding measurement uncertainties; Part 1: Uncertainties in the measurement of mobile radio equipment characteristics; Sub-part 2: Examples and annexes".

[13] ETSI TR 102 273-5: "ElectroMagnetic Compatibility and Radio Spectrum Matters (ERM); Improvement on Radiated Methods of Measurement (using test site) and evaluation of the corresponding measurement uncertainties; Part 5: striplines".

[14] "Guide to the Expression of Uncertainty in Measurement", International Organization for Standardization, Geneva, Switzerland, 1995.

[15] IEC 60050-161 (1990): "International Electrotechnical Vocabulary. Chapter 161: Electromagnetic compatibility".

[16] The new IEEE standard dictionary of electrical and electronic terms, Fifth edition, IEEE Piscataway, NJ USA 1993.

[17] Recommendation INC-1 (1980): "Expression of experimental uncertainties".

[18] "Wave transmission", F. R. Conner, Arnold 1978.

3 Definitions, symbols and abbreviations

3.1 Definitions

For the purposes of the present document, the following terms and definitions apply:

accuracy: this term is defined, in relation to the measured value, in clause 4.1.1; it has also been used in the remainder of the document in relation to instruments

Audio Frequency (**AF) load:** normally a resistor of sufficient power rating to accept the maximum audio output power from the EUT. The value of the resistor is normally that stated by the manufacturer and is normally the impedance of the audio transducer at 1 000 Hz

NOTE: In some cases it may be necessary to place an isolating transformer between the output terminals of the receiver under test and the load.

AF termination: any connection other than the audio frequency load which may be required for the purpose of testing the receiver. (I.e. in a case where it is required that the bit stream be measured, the connection may be made, via a suitable interface, to the discriminator of the receiver under test)

NOTE: The termination device is normally agreed between the manufacturer and the testing authority and details included in the test report. If special equipment is required then it is normally provided by the manufacturer.

A-M1: a test modulation consisting of a 1 000 Hz tone at a level which produces a deviation of 12 % of the channel separation

A-M2: a test modulation consisting of a 1 250 Hz tone at a level which produces a deviation of 12 % of the channel separation

A-M3: a test modulation consisting of a 400 Hz tone at a level which produces a deviation of 12 % of the channel separation. This signal is used as an unwanted signal for analogue and digital measurements

antenna: that part of a transmitting or receiving system that is designed to radiate or to receive electromagnetic waves

antenna factor: quantity relating the strength of the field in which the antenna is immersed to the output voltage across the load connected to the antenna. When properly applied to the meter reading of the measuring instrument, yields the electric field strength in V/m or the magnetic field strength in A/m

antenna gain: the ratio of the maximum radiation intensity from an (assumed lossless) antenna to the radiation intensity that would be obtained if the same power were radiated isotropically by a similarly lossless antenna

bit error ratio: the ratio of the number of bits in error to the total number of bits

combining network: a network allowing the addition of two or more test signals produced by different sources (e.g. for connection to a receiver input)

NOTE: Sources of test signals are normally connected in such a way that the impedance presented to the receiver is 50 Ω. Combining networks are designed so that effects of any intermodulation products and noise produced in the signal generators are negligible.

correction factor: the numerical factor by which the uncorrected result of a measurement is multiplied to compensate for an assumed systematic error

confidence level: the probability of the accumulated error of a measurement being within the stated range of uncertainty of measurement

directivity: the ratio of the maximum radiation intensity in a given direction from the antenna to the radiation intensity averaged over all directions (i.e. directivity = antenna gain + losses)

DM-0: a test modulation consisting of a signal representing an infinite series of "0" bits

DM-1: a test modulation consisting of a signal representing an infinite series of "1" bits

DM-2: a test modulation consisting of a signal representing a pseudorandom bit sequence of at least 511 bits in accordance with ITU-T Recommendation O.153

D-M3: a test signal agreed between the testing authority and the manufacturer in the cases where it is not possible to measure a bit stream or if selective messages are used and are generated or decoded within an equipment

NOTE: The agreed test signal may be formatted and may contain error detection and correction. Details of the test signal are to be supplied in the test report.

duplex filter: a device fitted internally or externally to a transmitter/receiver combination to allow simultaneous transmission and reception with a single antenna connection

error of measurement (absolute): the result of a measurement minus the true value of the measurand

error (relative): the ratio of an error to the true value

estimated standard deviation: from a sample of n results of a measurement the estimated standard deviation is given by the formula:

$$\sigma = \sqrt{\frac{\sum_{i=1}^{n}(x_i - \bar{x})^2}{n-1}}$$

x_i being the i^{th} result of measurement (i = 1, 2, 3, ..., n) and $\bar{x}$ the arithmetic mean of the n results considered.

A practical form of this formula is:

$$\sigma = \sqrt{\frac{Y - \frac{X^2}{n}}{n-1}}$$

where X is the sum of the measured values and Y is the sum of the squares of the measured values.

The term **standard deviation** has also been used in the present document to characterize a particular probability density. Under such conditions, the term **standard deviation** may relate to situations where there is only one result for a measurement.

expansion factor: multiplicative factor used to change the confidence level associated with a particular value of a measurement uncertainty

NOTE: The mathematical definition of the expansion factor can be found in clause D.5.6.2.2 of TR 100 028-2 [11].

extreme test conditions: conditions defined in terms of temperature and supply voltage

NOTE: Tests are normally made with the extremes of temperature and voltage applied simultaneously. The upper and lower temperature limits are specified in the relevant testing standard. The test report states the actual temperatures measured.

error (of a measuring instrument): the indication of a measuring instrument minus the (conventional) true value

free field: a field (wave or potential) which has a constant ratio between the electric and magnetic field intensities

free Space: a region free of obstructions and characterized by the constitutive parameters of a vacuum

impedance: a measure of the complex resistive and reactive attributes of a component in an alternating current circuit

impedance (wave): the complex factor relating the transverse component of the electric field to the transverse component of the magnetic field at every point in any specified plane, for a given mode

influence quantity: a quantity which is not the subject of the measurement but which influences the value of the quantity to be measured or the indications of the measuring instrument

intermittent operation: operation where the manufacturer states the maximum time that the equipment is intended to transmit and the necessary standby period before repeating a transmit period

isotropic radiator: a hypothetical, lossless antenna having equal radiation intensity in all directions

limited Frequency Range: the limited Frequency Range is a specified smaller frequency range within the full frequency range over which the measurement is made

NOTE: The details of the calculation of the limited Frequency Range are normally given in the relevant testing standard.

maximum permissible frequency deviation: the maximum value of frequency deviation stated for the relevant channel separation in the relevant testing standard

measuring system: a complete set of measuring instruments and other equipment assembled to carry out a specified measurement task

measurement repeatability: the closeness of the agreement between the results of successive measurements of the same measurand carried out subject to all the following conditions:

- the same method of measurement;
- the same observer;
- the same measuring instrument;
- the same location;
- the same conditions of use;
- repetition over a short period of time.

measurement reproducibility: the closeness of agreement between the results of measurements of the same measurand, where the individual measurements are carried out changing conditions such as:

- method of measurement;
- observer;
- measuring instrument;
- location;
- conditions of use;
- time.

measurand: a quantity subjected to measurement

noise gradient of EUT: a function characterizing the relationship between the RF input signal level and the performance of the EUT, e.g., the SINAD of the AF output signal

nominal frequency: one of the channel frequencies on which the equipment is designed to operate

nominal mains voltage: the declared voltage or any of the declared voltages for which the equipment was designed

normal test conditions: the conditions defined in terms of temperature, humidity and supply voltage stated in the relevant testing standard

normal deviation: the frequency deviation for analogue signals which is equal to 12 % of the channel separation

psophometric weighting network: as described in ITU-T Recommendation O.41 [6].

polarization: for an electromagnetic wave, the figure traced as a function of time by the extremity of the electric vector at a fixed point in space

quantity (measurable): an attribute of a phenomenon or a body which may be distinguished qualitatively and determined quantitatively

rated audio output power: the maximum audio output power under normal test conditions, and at standard test modulations, as declared by the manufacturer

rated radio frequency output power: the maximum carrier power under normal test conditions, as declared by the manufacturer

shielded enclosure: a structure that protects its interior from the effects of an exterior electric or magnetic field, or conversely, protects the surrounding environment from the effect of an interior electric or magnetic field

SINAD sensitivity: the minimum standard modulated carrier-signal input required to produce a specified SINAD ratio at the receiver output

stochastic (random) variable: a variable whose value is not exactly known, but is characterized by a distribution or probability function, or a mean value and a standard deviation (e.g. a measurand and the related measurement uncertainty)

test load: 50 Ω substantially non-reactive, non-radiating power attenuator which is capable of safely dissipating the power from the transmitter

test modulation: a baseband signal which modulates a carrier and is dependent upon the type of EUT and also the measurement to be performed

trigger device: a circuit or mechanism to trigger the oscilloscope timebase at the required instant

NOTE: It may control the transmit function or inversely receive an appropriate command from the transmitter.

uncertainty (random): a component of the uncertainty of measurement which, in the course of a number of measurements of the same measurand, varies in an unpredictable way (to be considered as a component for the calculation of the combined uncertainty when the effects it corresponds to have not been taken into consideration otherwise)

uncertainty (systematic): a component of the uncertainty of measurement which, in the course of a number of measurements of the same measurand remains constant or varies in a predictable way

uncertainty (limits of uncertainty of a measuring instrument): the extreme values of uncertainty permitted by specifications, regulations etc. for a given measuring instrument

NOTE: This term is also known as "tolerance".

uncertainty (standard): an expression characterizing, for each individual uncertainty component, the uncertainty for that component

NOTE: It is the standard deviation of the corresponding distribution.

uncertainty (combined standard): the combined standard uncertainty is calculated by combining appropriately the standard uncertainties for each of the individual contributions identified in the measurement considered or in the part of it, which has been considered

NOTE: In the case of additive components (linearly combined components where all the corresponding coefficients **are equal to one**) and when all these contributions are independent of each other (stochastic), this combination is calculated by using the Root of the Sum of the Squares (the RSS method). A more complete methodology for the calculation of the combined standard uncertainty is given in annex D of TR 100 028-2 [11], see in particular, clause D.3.12.

uncertainty (expanded): the expanded uncertainty is the uncertainty value corresponding to a specific confidence level different from that inherent to the calculations made in order to find the combined standard uncertainty

NOTE: The combined standard uncertainty is multiplied by a constant to obtain the expanded uncertainty limits (see clauses 5.3 of TR 100 028-1 [11] and D.5 of TR 100 028-2 [11], (and more specifically clause D.5.6.2).

upper specified AF limit: the maximum audio frequency of the audio pass-band. It is dependent on the channel separation

wanted signal level: for conducted measurements a level of +6 dBμV emf referred to the receiver input under normal test conditions. Under *extreme test conditions* the value is +12 dBμV emf

NOTE: For analogue measurements the wanted signal level has been chosen to be equal to the limit value of the measured usable sensitivity. For bit stream and message measurements the wanted signal has been chosen to be +3 dB above the limit value of measured usable sensitivity.

3.2 Symbols

For the purposes of the present document, the following symbols apply:

β	2π/λ (radians/m)
γ	incidence angle with ground plane (°)
λ	wavelength (m)
ϕ_H	phase angle of reflection coefficient (°)
η	120π Ω - the intrinsic impedance of free Space (Ω)
μ	permeability (H/m)
AF_R	antenna factor of the receive antenna (dB/m)
AF_T	antenna factor of the transmit antenna (dB/m)
AF_{TOT}	mutual coupling correction factor (dB)
c	calculated on the basis of given and measured data
C_{cross}	cross correlation coefficient
d	derived from a measuring equipment specification
$D(\theta,\phi)$	directivity of the source
d	distance between dipoles (m)
δ	skin depth (m)
d_1	an antenna or EUT aperture size (m)
d_2	an antenna or EUT aperture size (m)
d_{dir}	path length of the direct signal (m)
d_{refl}	path length of the reflected signal (m)
E	electric field intensity (V/m)
E_{DH}^{max}	calculated maximum electric field strength in the receiving antenna height scan from a half wavelength dipole with 1 pW of radiated power (for horizontal polarization) (μV/m)
E_{DV}^{max}	calculated maximum electric field strength in the receiving antenna height scan from a half wavelength dipole with 1 pW of radiated power (for vertical polarization) (μV/m)
e_{ff}	antenna efficiency factor
ϕ	angle (°)
Δf	bandwidth (Hz)
f	frequency (Hz)
$G(\theta,\phi)$	gain of the source (which is the source directivity multiplied by the antenna efficiency factor)
H	magnetic field intensity (A/m)
I_0	the (assumed constant) current (A)
I_m	the maximum current amplitude
k	2π/λ
k	a factor from Student's t distribution
k	Boltzmann's constant (1,38 x 10-23 Joules/° Kelvin)
K	relative dielectric constant
l	the length of the infinitesimal dipole (m)
L	the overall length of the dipole (m)
l	the point on the dipole being considered (m)
m	measured
p	power level value
$Pe_{(n)}$	probability of error n

$Pp_{(n)}$	probability of position n
P_r	antenna noise power (W)
P_{rec}	power received (W)
P_t	power transmitted (W)
θ	angle (°)
ρ	reflection coefficient
r	the distance to the field point (m)
ρ_g	reflection coefficient of the generator part of a connection
ρ_l	reflection coefficient of the load part of the connection
R_s	equivalent surface resistance (Ω)
σ	conductivity (S/m)
σ	standard deviation
r	indicates rectangular distribution
SNR_{b*}	Signal to Noise Ratio at a specific BER
SNR_b	Signal to Noise Ratio per bit
T_A	antenna temperature (° Kelvin)
u	indicates U-distribution
U	the expanded uncertainty corresponding to a confidence level of x %: $U = k \times u_c$
u_c	the combined standard uncertainty
u_i	general Type A standard uncertainty
u_{i01}	random uncertainty
u_j	general Type B uncertainty
u_{j01}	reflectivity of absorbing material: EUT to the test antenna
u_{j02}	reflectivity of absorbing material: substitution or measuring antenna to the test antenna
u_{j03}	reflectivity of absorbing material: transmitting antenna to the receiving antenna
u_{j04}	mutual coupling: EUT to its images in the absorbing material
u_{j05}	mutual coupling: de-tuning effect of the absorbing material on the EUT
u_{j06}	mutual coupling: substitution, measuring or test antenna to its image in the absorbing material
u_{j07}	mutual coupling: transmitting or receiving antenna to its image in the absorbing material
u_{j08}	mutual coupling: amplitude effect of the test antenna on the EUT
u_{j09}	mutual coupling: de-tuning effect of the test antenna on the EUT
u_{j10}	mutual coupling: transmitting antenna to the receiving antenna
u_{j11}	mutual coupling: substitution or measuring antenna to the test antenna
u_{j12}	mutual coupling: interpolation of mutual coupling and mismatch loss correction factors
u_{j13}	mutual coupling: EUT to its image in the ground plane
u_{j14}	mutual coupling: substitution, measuring or test antenna to its image in the ground plane
u_{j15}	mutual coupling: transmitting or receiving antenna to its image in the ground plane
u_{j16}	range length
u_{j17}	correction: off boresight angle in the elevation plane
u_{j18}	correction: measurement distance
u_{j19}	cable factor
u_{j20}	position of the phase centre: within the EUT volume
u_{j21}	positioning of the phase centre: within the EUT over the axis of rotation of the turntable
u_{j22}	position of the phase centre: measuring, substitution, receiving, transmitting or test antenna
u_{j23}	position of the phase centre: LPDA
u_{j24}	stripline: mutual coupling of the EUT to its images in the plates
u_{j25}	stripline: mutual coupling of the three-axis probe to its image in the plates
u_{j26}	stripline: characteristic impedance
u_{j27}	stripline: non-planar nature of the field distribution
u_{j28}	stripline: field strength measurement as determined by the 3-axis probe
u_{j29}	stripline: transform factor

u_{j30} stripline: interpolation of values for the transform factor
u_{j31} stripline: antenna factor of the monopole
u_{j32} stripline: correction factor for the size of the EUT
u_{j33} stripline: influence of site effects
u_{j34} ambient effect
u_{j35} mismatch: direct attenuation measurement
u_{j36} mismatch: transmitting part
u_{j37} mismatch: receiving part
u_{j38} signal generator: absolute output level
u_{j39} signal generator: output level stability
u_{j40} insertion loss: attenuator
u_{j41} insertion loss: cable
u_{j42} insertion loss: adapter
u_{j43} insertion loss: antenna balun
u_{j44} antenna: antenna factor of the transmitting, receiving or measuring antenna
u_{j45} antenna: gain of the test or substitution antenna
u_{j46} antenna: tuning
u_{j47} receiving device: absolute level
u_{j48} receiving device: linearity
u_{j49} receiving device: power measuring receiver
u_{j50} EUT: influence of the ambient temperature on the ERP of the carrier
u_{j51} EUT: influence of the ambient temperature on the spurious emission level
u_{j52} EUT: degradation measurement
u_{j53} EUT: influence of setting the power supply on the ERP of the carrier
u_{j54} EUT: influence of setting the power supply on the spurious emission level
u_{j55} EUT: mutual coupling to the power leads
u_{j56} frequency counter: absolute reading
u_{j57} frequency counter: estimating the average reading
u_{j58} Salty man/Salty-lite: human simulation
u_{j59} Salty man/Salty-lite: field enhancement and de-tuning of the EUT
u_{j60} Test Fixture: effect on the EUT
u_{j61} Test Fixture: climatic facility effect on the EUT
V_{direct} received voltage for cables connected via an adapter (dBµV/m)
V_{site} received voltage for cables connected to the antennas (dBµV/m)
W_0 radiated power density (W/m^2)

3.3 Abbreviations

For the purposes of the present document, the following abbreviations apply:

AF Audio Frequency
BER Bit Error Ratio
CB Citizens' Band
emf electromotive force
EUT Equipment Under Test
FSK Frequency Shift Keying
GMSK Gaussian Minimum Shift Keying
GSM Global System for Mobile telecommunication (Pan European digital telecommunication system)
IF Intermediate Frequency
LPDA Log Periodic Dipole Antenna
m measured
NaCl Sodium chloride
NSA Normalized Site Attenuation

r	indicates rectangular distribution
RF	Radio Frequency
rms	root mean square
RSS	Root-Sum-of-the-Squares
TEM	Transverse Electro-Magnetic
u	indicates U-distribution
VSWR	Voltage Standing Wave Ratio

4 Introduction to measurement uncertainty

This clause gives the general background to the subject of measurement uncertainty and is the basis of the present document. It covers methods of evaluating both individual components and overall system uncertainties and ends with a discussion of the generally accepted present day approach to the calculation of overall measurement uncertainty.

For further details and for the basis of a theoretical approach, please see annex D of TR 100 028-2 [11].

An outline of the extensions and improvements recommended is also included in this clause.

This clause should be viewed as introductory material for clauses 5 and 6.

4.1 Background to measurement uncertainty

4.1.1 Commonly used terms

UNCERTAINTY is that part of the expression of the result of a measurement which states the range of values within which the true value is estimated to lie.

ACCURACY is an estimate of the closeness of the measured value to the true value. An accurate measurement is one in which the uncertainties are small. This term is not to be confused with the terms PRECISION or REPEATABILITY which characterize the ability of a measuring system to give identical indications or responses for repeated applications of the same input quantity.

Measuring exactly a quantity (referred to as the measurand) is an ideal which cannot be attained in practical measurements. In every measurement a difference exists between the TRUE VALUE and the MEASURED VALUE. This difference is termed "THE ABSOLUTE ERROR OF THE MEASUREMENT". This error is defined as follows:

Absolute error = the measured value - the true value

Since the true value is never known exactly, it follows that the absolute error cannot be known exactly either. The above formula is the defining statement for the terms of ABSOLUTE ERROR and TRUE VALUE, but, as a result of neither ever being known, it is recommended that these terms are never used.

In practice, many aspects of a measurement can be controlled (e.g. temperature, supply voltage, signal generator output level, etc.) and by analysing a particular measurement set-up, the overall uncertainty can be assessed, thereby providing upper and lower UNCERTAINTY BOUNDS within which the true value is believed to lie.

The overall uncertainty of a measurement is an expression of the fact that the measured value is only one of an infinite number of possible values dispersed (spread) about the true value.

This is further developed in clause D.5.6 of TR 100 028-2 [11].

4.1.2 Assessment of upper and lower uncertainty bounds

One method of providing upper and lower bounds is by straightforward arithmetic calculation in the worst case condition, using the individual uncertainty contributions. This method can be used to arrive at a value each side of the measured result within which, there is utmost confidence (100 %) that the true value lies (see also clause D.5.6.1 of TR 100 028-2 [11]).

When estimating the measurement uncertainty in the worst case e.g. by simply adding the uncertainty bounds (in additive situations), (extremely) pessimistic uncertainty bounds are often found. This is because the case when all the individual uncertainty components act to their maximum effect in the same direction at the same time is, in practice, very unlikely to happen (it has to be noted, however, that the usage of expansion factors in order to increase the confidence levels (see also clauses 5.3.1, D.5.6.2.2 and D.3.3.5.2 of TR 100 028-2 [11]) may have a balancing effect).

To overcome this (very) pessimistic calculation of the lower and upper bounds, a more realistic approach to the calculation of overall uncertainty needs to be taken (i.e. a probabilistic approach).

The method presented in the present document is based on the approach to expressing uncertainty in measurement as recommended by the Comite International des Poids et Mesures (CIPM) in 1981. This approach is founded on Recommendation INC-1 [17] of the Working Group on the Statement of Uncertainties. This group was convened in 1980 by the Bureau International des Poids et Mesures (BIPM) as a consequence of a request by the Comite that the Bureau study the question of reaching an international consensus on expressing uncertainty in measurement. Recommendation INC-1 [17] led to the development of the *Guide to the Expression of Uncertainty in Measurement* [15] (the Guide), which was prepared by the *International Organization for Standardization Technical Advisory Group 4 (ISOTAG 4)*, Working Group 3. The Guide had been the most complete reference on the general application of the BIPM approach to expressing measurement uncertainty. Further theoretical analysis has been introduced in the third edition of the TR 100 028 [11] (see, in particular, annexes D and E in TR 100 028-2 [11]).

Although the Guide represented the current international view of how to express uncertainty it is a rather lengthy document that is not easily interpreted for radiated measurements. The guidance given in the present document is intended to be applicable to radio measurements but since the Guide itself is intended to be generally applicable to measurement results, it should be consulted for additional details, if needed.

The method in both the present document and the Guide apply statistical/probabilistic analysis to estimate the overall uncertainties of a measurement and to provide associated confidence levels. They depend on knowing the magnitude and distribution of the individual uncertainty components. This approach is commonly known as the BIPM method.

Basic to the BIPM method is the representation of each individual uncertainty component that contributes to the overall measurement uncertainty by an estimated standard deviation, termed **standard uncertainty**, with suggested symbol u.

All individual uncertainties are categorized as either Type A or Type B. Type A uncertainties, symbol u_i, are estimated by statistical methods applied to repeated measurements, whilst Type B uncertainties, symbol u_j, are estimated by means of available information and experience.

The **combined standard uncertainty,** symbol u_c, of a measurement is calculated by combining the standard uncertainties for each of the individual contributions identified. In the case where the underlying physical effects are additive, this is done by applying the "Root of the Sum of the Squares (the RSS)" method (see also clause D.3.3 of TR 100 028-2 [11]) under the assumption that all contributions are stochastic i.e. independent of each other.

The table included in clause D.3.12 of TR 100 028-2 [11] provides the way in which should be handled contributions to the uncertainty which correspond to physical effects which are not additive. Clause D.5 of the same annex provides an overview of several general methods.

The resulting combined standard uncertainty can then be multiplied by a constant k_{xx} to give the uncertainty limits (bounds), termed **expanded uncertainty**, in order to provide a confidence level of *xx* %. This is further discussed in clause D.5.6.2 of TR 100 028-2 [11].

One of the main assumptions when calculating uncertainty using the basic BIPM method is that the combined standard uncertainty of a measurement has a Normal (also called Gaussian) distribution (see also clause D.1.3.4 of TR 100 028-2 [11]) with an associated standard deviation. This may be true when there is an infinite number of contributions in the uncertainty, which is generally not the case in the examples discussed in the present document (an interesting example is provided in clause D.3.3.5.2.2 of TR 100 028-2 [11]).

Should the combined standard uncertainty correspond to a Normal distribution, then the multiplication by the appropriate constant (expansion factor) will provide the sought confidence level.

The case where the combined standard uncertainty corresponds to non-Gaussian distributions is also considered in clauses D.5.6.2.3 and D.5.6.2.4 of TR 100 028-2 [11].

The Guide defines the combined standard uncertainty for this distribution $u_{c,}$ as equal to the standard deviation of a corresponding Normal distribution. The mean value is assumed to be zero as the measured result is corrected for all known errors. Based on this assumption, the uncertainty bounds corresponding to any confidence level can be calculated as $k_{xx} \times u_c$ (see also clause D.5.6.2 of TR 100 028-2 [11]).

To illustrate the true meaning of a typical final statement of measurement uncertainty using this method, if the combined standard uncertainty is associated with a Normal distribution, confidence levels can be assigned as follows:

- 68,3 % confidence level that the true value is within bounds of $1{,}00 \times u_c$;
- 95,0 % confidence within $\pm 1{,}96 \times u_c$;
- 95,45 % confidence within $\pm 2{,}00 \times u_c$, etc.

Care must be taken in the judgement of which unit is chosen for the calculation of the uncertainty bounds. In some types of measurements the correct unit is logarithmic (dB); in other measurements it is linear (i.e. V or %). The choice depends on the model and architecture of the test system. In any measurement there may be a combination of different types of unit. The present document breaks new ground by giving methods for conversion between units (e.g. dB into V %, power % into dB, etc.) thereby allowing all types of uncertainty to be combined. Details of the conversion schemes are given in clause 5, and theoretical support in annexes D and E of TR 100 028-2 [11].

4.1.3 Combination of rectangular distributions

The following example shows that the overall combined uncertainty of a measurement, when all contributions of that measurement have the **same** rectangular distribution, approaches a Normal distribution.

The case of a discrete approach to a rectangularly distributed function, (the outcome of throwing a die), is shown and how, with up to 6 individual events simultaneously, (6 dice thrown at the same time) the events combine together to produce an output increasingly approximating a Normal distribution.

Initially with 1 die the output mean is 3,5 with a rectangularly distributed "error" of ±2,5. With 2 dice the output is 7 ± 5 and is triangularly distributed see figure 1.

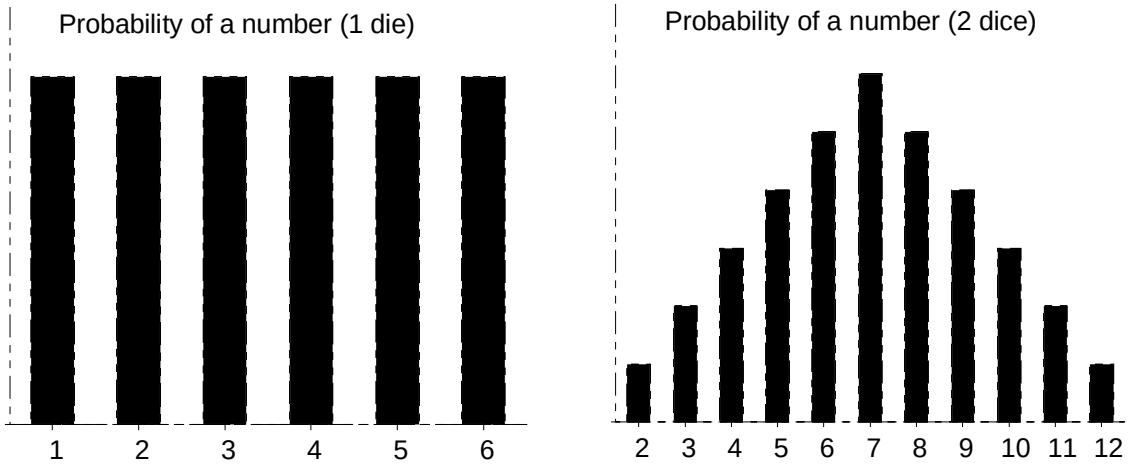

Figure 1: One and two die outcomes

By increasing the number of dice further through 3, 4, 5 and 6 dice it can be seen from figures 2 and 3, that there is a central value (most probable outcome) respectively for 2, 3, 4, 5 and 6 dice of (7), (10,5), (14), (17,5) and (21) and an associated spread of the results that increasingly approximates a Normal distribution. It is possible to calculate the mean and standard deviation for these events.

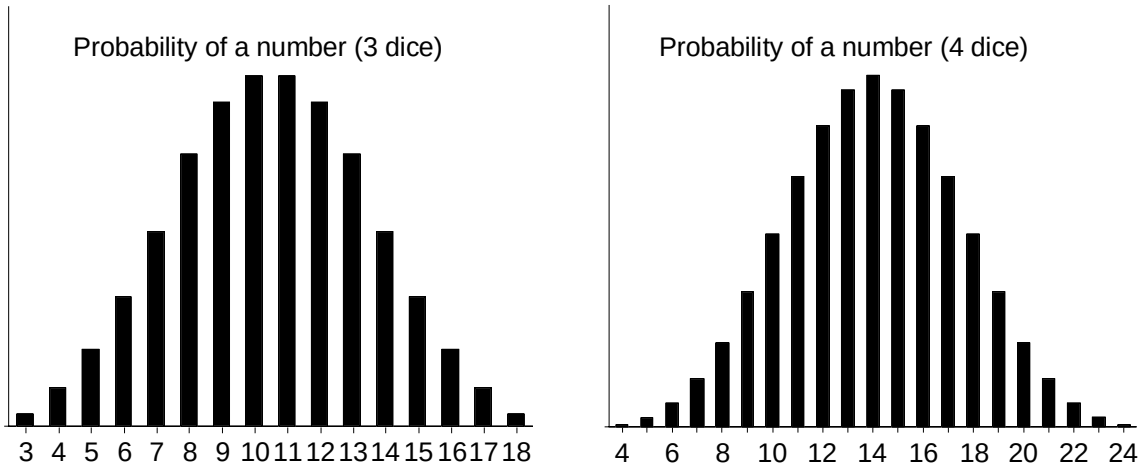

Figure 2: Three and four die outcomes

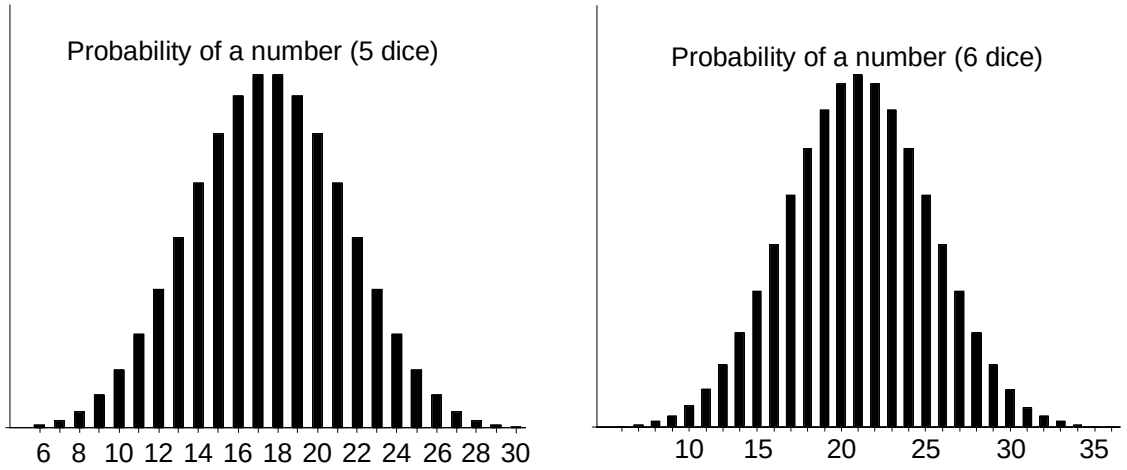

Figure 3: Five and six die outcomes

The practical interpretation of the standard deviation of a Normally distributed quantity is that 68,3 % of all its possible values will lie within ±1 standard deviation of the mean value, 95,45 % will lie within ±2 standard deviations. Another way to regard these standard deviations is "as confidence levels", e.g. a confidence level of 68,3 % attaches to one standard deviation, 95,45 % to two standard deviations.

Using the mathematical definition of a Gaussian (see annex D of TR 100 028-2 [11]), it is possible to calculate the expanded measurement uncertainty for other confidence levels.

This illustration shows that in the case of individual throws of a die (which corresponds to a set of identical rectangular distributions since any of the values 1 to 6 is equally likely) the overall probability curve approximates closer and closer that of a Normal distribution as more dice are used.

The BIPM method extends this principle by combining the individual standard uncertainties to derive a combined standard uncertainty. The standard uncertainties (corresponding to the distributions of the individual uncertainties) are all that need to be known (or assumed) to apply this approach. From the assumption that the final combined standard uncertainty corresponds to a Normal distribution, it is possible to calculate the expanded uncertainty for a given confidence level.

The confidence level should always be stated in any test report, in the case where the resulting distribution is Gaussian. In such case, it makes it possible for the user of the measured results to calculate expanded uncertainty figures corresponding to other confidence levels.

For similar reasons, in the case where there is no evidence that the distribution corresponding to the combined uncertainty is Normal, the expansion factor, k_{xx}, should be stated in the test report, instead.

Usually, for the reasons stated above, k_{xx} = 1,96 is used (see also clause D.5.6.2 of TR 100 028-2 [11])… this factor providing a confidence level of 95 %, should the corresponding distribution be Normal.

Another example: an expansion factor, k_{xx} = 2,00 would have provided a confidence level of 95,45 %, should the corresponding distribution be Normal.

NOTE: In some countries, an expansion factor of k_{xx} = 2,00 is used by accreditation organizations, as they consider that k_{xx} = 2,00 provides a "confidence level of approximately 95 %".

4.1.4 Main contributors to uncertainty

The main contributors to the overall uncertainty of a measurement comprise:

- systematic uncertainties: those uncertainties inherent in the test equipment used (instruments, attenuators, cables, amplifiers, etc.), and in the method employed. These uncertainties cannot always be eliminated (calculated out) although they may be constant values, however they can often be reduced;
- uncertainties relating to influence quantities i.e. those uncertainties whose magnitudes are dependent on a particular parameter or function of the EUT. The magnitude of the uncertainty contribution can be calculated, for example, from the slope of "dB RF level" to "dB SINAD" curve for a receiver or from the slope of a power supply voltage effect on the variation of a carrier output power or frequency;
- random uncertainties: those uncertainties due to chance events which, on average, are as likely to occur as not to occur and are generally outside the engineer's control.

NOTE: When making a measurement care must be taken to ensure that the measured value is not affected by unwanted or unknown influences. Extraneous influences (e.g. ambient signals on an Open Area Test Site) should be eliminated or minimized by, for example, the use of screened cables.

4.1.5 Other contributors

Other contributors to the overall uncertainty of a measurement can relate to the standard itself:

- the type of measurement (direct field, substitution or conducted) and the test method have an effect on the uncertainty. These can be the most difficult uncertainty components to evaluate. As an illustration, if the same measurand is determined by the same method in different laboratories (as in a round robin) or alternatively by different methods either in the same laboratory or in different laboratories, the results of the testing will often be widely spread, thereby showing the potential uncertainties of the different measurement types and test methods;
- a direct field measurement involves only a single testing stage in which the required parameter (ERP, sensitivity, etc.) is indirectly determined as the received level on a receiving device, or as the output level of a signal generator, etc., and is subsequently converted to ERP, field strength, etc., by a calculation involving knowledge of antenna gain, measurement distance, etc. This method, whilst being of short time duration, offers no way of allowing for imperfections (reflections, mutual coupling effects, etc.) in the test site and can results in large overall uncertainty values;
- the substitution technique, on the other hand, is a two-stage measurement in which the unknown performance of an EUT (measured in one stage) is directly compared with the "known" performance of some standard (usually an antenna) in the other stage. This technique therefore subjects both the EUT and the known standard to (hopefully) the same external influences of reflections, mutual coupling, etc., whose effects on the different devices are regarded as identical. As a consequence, these site effects are deemed to cancel out (this has also been addressed in clause D.5.3.2 of TR 100 028-2 [11]). Some residual effects do remain however, (due to different elevation beamwidths, etc.) but these tend to be small compared to the uncertainties in the direct field method. All the test methods in the present document are substitution measurements;
- for their part, test methods can contain imprecise and ambiguous instructions which could be open to different interpretations;

- an inadequate description of the measurand can itself be a source of uncertainty in a measurement. In practice a measurand cannot be completely described without an infinite amount of information. Because this definition is incomplete it therefore introduces into the measurement result a component of uncertainty that may or may not be significant relative to the overall uncertainty required of the measurement. The definition of the measurand may, for example, be incomplete because:

  - it does not specify parameters that may have been assumed, unjustifiably, to have negligible effect (i.e. coupling to the ground plane, reflections from absorbers or that reference conditions remain constant);

  - it leaves many other matters in doubt that might conceivably affect the measurement (i.e. supply voltages, the layout of power, signal and antenna cables);

  - it may imply conditions that can never be fully met and whose imperfect realization is difficult to take into account (i.e. an infinite, perfectly conducting ground plane, a free Space environment) etc.

Maximum acceptable uncertainties and confidence levels (or expansion factors) are both defined in most ETSI standards.

4.2 Evaluation of individual uncertainty components

As discussed in clause 4.1.4, uncertainty components can be categorized either as "random" or "systematic". Such categorization of components of uncertainty can be ambiguous if they are applied too rigorously. For example, a "random" component of uncertainty in one measurement may become a "systematic" component of uncertainty in another measurement e.g. where the result of a first measurement is used as a component of a second measurement. Categorizing the methods of evaluating the uncertainty components rather than the components themselves avoids this ambiguity.

Instead of "systematic" and "random" uncertainty the types of uncertainty contribution are grouped into two categories:

- Type A: those which are evaluated by statistical methods;

- Type B: those which are evaluated by other means.

The classification into Type A and Type B is not meant to indicate that there is any difference in the nature of the components, it is simply a division based on their means of evaluation. Both types will possess probability distributions (although they may be governed by different rules), and the uncertainty components resulting from either type may be quantified by standard deviations.

4.2.1 Evaluation of Type A uncertainties

When we carry out a measurement more than once and find the results are different, the following questions arise:

- What to do with the results?

- How much variation is acceptable?

- When do we suspect the measuring system is faulty?

- Are the conditions repeatable?

Variations in these repeated measurements are assumed to be due to influence and random quantities that affect the measurement result and cannot be held completely constant. Therefore none of the results is necessarily correct. In practice, repeated measurements of the same measurand can help us evaluate these Type A uncertainties. By treating the results statistically, we can derive the mean (the best approximation to the "true value") and standard deviation values. The standard deviation can then be incorporated as a standard uncertainty into the calculation of combined standard uncertainty, when the corresponding component is part of some measurement system.

Uncertainties determined from repeated measurements are often thought of as statistically rigorous and therefore absolutely correct. This implies, sometimes wrongly, that their evaluation does not require the application of some judgement. For example:

- When carrying out a series of measurements do the results represent completely independent repetitions or are they in some way biased?

- Are we trying to assess the randomness of the measurement system, or the randomness in an individual EUT, or the randomness in all of the EUT produced?
- Are the means and standard deviations constant, or is there perhaps a drift in the value of an unmeasured influence quantity during the period of repeated measurements?
- Are the results stable with ambient conditions?

If all of the measurements are on a single EUT, whereas the requirement is for sampling, then the observations have not been independently repeated. An estimate of the standard uncertainty arising from possible differences among production EUT should, in this case, be incorporated into the combined standard uncertainty calculation along with the calculated standard uncertainty of the repeated observations made on the single equipment (e.g. for characterizing a set of pieces of equipment).

If an instrument is calibrated against an internal reference as part of the measurement procedure, (such as the "cal out" reference on a spectrum analyser), then the calibration should be carried out as part of every repetition, even if it is known that the drift is small during the period in which observations are made.

If the EUT is rotated during a radiated test on a test site and the azimuth angle read, it should be rotated and read for each repetition of the measurement, for there may be a variation both in received level and in azimuth reading, even if everything else is constant.

If a number of measurements have been carried out on the same EUT/types of EUT, but in two groups spaced apart in time, the arithmetic means of the results of the first and second groups of measurements and their experimentally derived means and standard deviations may be calculated and compared. This will enable a judgement to be made as to whether any time varying effects are statistically significant.

4.2.2 Evaluation of Type B uncertainties

Some examples of Type B uncertainties are:

- mismatch;
- losses in cables and components;
- non-linearities in instruments;
- antenna factors.

Type B uncertainties do not reveal themselves as fluctuations as do Type A uncertainties; they can only be assessed by careful analysis of test and calibration data.

For incorporation into an overall analysis, the magnitudes and distributions of Type B uncertainties can be estimated based on:

- manufacturers' information/specification about instruments and components in the test set-up;
- data in calibration certificates (if the history of the instrument is known);
- experience with the behaviour of the instruments.

4.2.3 Uncertainties relating to influence quantities

Uncertainties relating to influence quantities are, as a result of the way they are treated in the present document, regarded as a subgroup of Type B uncertainties. Some examples of influence quantities are:

- power supply;
- ambient temperature;
- time/duty cycle.

Their effect is evaluated using some relationship between the measured parameter e.g. output power and the influence quantity e.g. supply voltage.

Dependency functions (e.g. the relationship between output power and the fluctuating quantity), as those given in the present document, should be used to calculate the properties corresponding to the effect considered.

A theoretical approach to influence quantities and dependency functions can be found in clause D.4 of TR 100 028-2 [11].

4.3 Methods of evaluation of overall measurement uncertainty

The uncertainty of the measurement is a combination of many components.

Some of these components may be evaluated from the statistical distributions of the results of a series of measurements (Type A uncertainty) whilst other components are evaluated from assumed probability distributions based on experience or other information (Type B uncertainty).

The exact error of a result of a measurement is, in general, unknown and unknowable. All that can be done is to estimate the values of all quantities likely to contribute to the combined standard uncertainty, including those uncertainties associated with corrections for recognized systematic offset effects. With knowledge of the magnitudes of their individual standard uncertainties, it is then possible to calculate the combined standard uncertainty of the measurement.

At present the assessment of the number of uncertainty components for any particular test is very variable. Whilst some general agreement has been reached on the manner in which individual uncertainties should be combined (the BIPM method, see also the discussion of such methods in annex D of TR 100 028-2 [11], in particular, in clause D.5), no such agreement has been arrived at concerning the identity of those individual components. Consequently, it is left to the particular test house/engineer/etc. to decide the contributory uncertainties, and to assess which are independent and which are not. This can lead to considerable test house to test house variation for the same test and is heavily dependent, in general, on the experience of the test engineer.

A model of the measurement can assist in the evaluation of combined standard uncertainty since it will enable all known individual components of uncertainty to be rigorously included in the analysis, and correctly combined (see annex D of TR 100 028-2 [11], and, in particular, the table in clause D.3.12).

For all the radiated measurements detailed in parts 2 to 7 of the present document, comprehensive tables of individual uncertainty components are given.

4.4 Summary

The measured result can be affected by many variables, some of which are shown in figure 4.

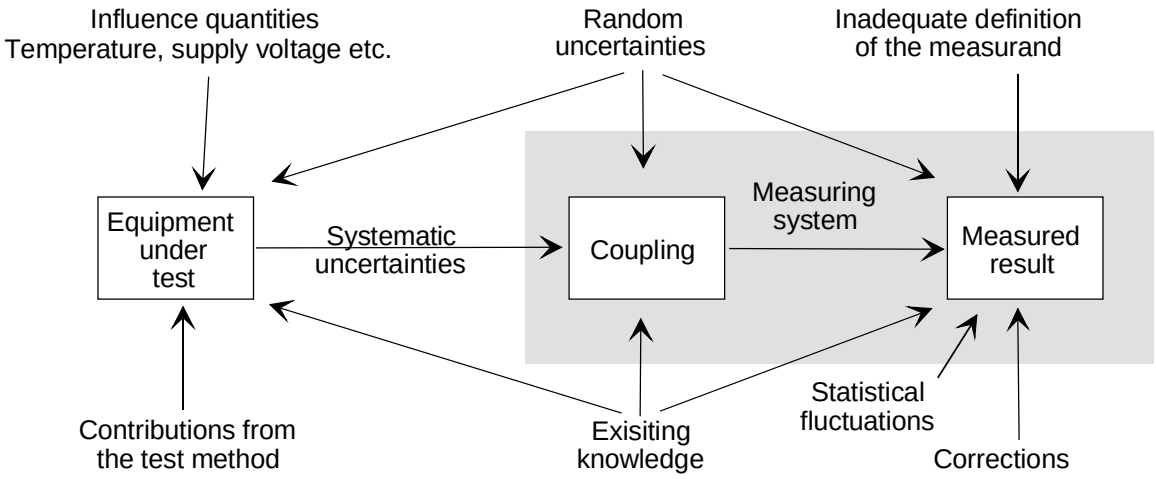

Figure 4: The measurement model

4.5 Overview of the approach of the present document

The present document proposes an approach to the calculation of the combined standard uncertainty of a measurement which includes solutions to the present day imperfections.

For example, in clause 5, a technique is put forward for converting linear standard deviations into logarithmic ones (and vice versa) so that all uncertainty contributions for a particular test can be combined in the same units (dB, Voltage % or Power %), and as stated above, comprehensive lists of the individual uncertainty sources for all tests are attached to the test methods presented in parts 2, 3, 4, 5, 6 and 7. Also the instructions within the test methods have been made more detailed and thereby less ambiguous.

A global approach for the analysis of the uncertainties corresponding to a complete measurement set up (i.e. "a complete system") is also proposed in clause D.5 of TR 100 028-2 [11]. This approach addresses, in particular, the concept of "sub-systems" and how to combine the uncertainties relating to each "sub-system". Clause 6.8 of the present part uses these concepts. Such an approach could also help in cases where different units are to be used (e.g. dBs in one sub-system, linear terms in another).

A set of files (spread sheets) has been included in TR 100 028 [11], in order to support some of the examples given in that report and to help the user in the implementation of his own methodology.

5 Analysis of measurement uncertainty

This clause develops the approach to measurement uncertainty beyond the introduction given in clause 4. It details the improvements to the analysis which the present document is proposing and presents solutions for all the identified problems associated with the BIPM method for calculating measurement uncertainty in radiated measurements. Clause 6 presents numerous worked examples which illustrate the application of the proposed new techniques.

In the beginning of this clause, a review is given of the BIPM method, along with an outline of where it is inadequate for radiated measurements. The means of evaluation of Type A and Type B uncertainties are also given.

This is followed by a discussion of the units in which the uncertainties are derived and the technique for converting standard deviations from logarithmic (dB) to linear quantities (% voltage or % power and vice versa) is presented. The conversion technique allows all the individual uncertainty components in a particular test to be combined in the same units and overcomes a major current day problem of asymmetric uncertainty limits (e.g. x + 2, -3 dB, as found in edition 2 of ETR 028 [11]).

The clause concludes with text relating to deriving the expanded uncertainties in the case of Normal distributions, how influence quantities are dealt with, calculating the standard deviation of random effects and an overall summary.

Theoretical and mathematical support for this clause can be found in annex D of TR 100 028-2 [11].

5.1 The BIPM method

Basic to the BIPM method is the representation of each individual uncertainty component that contributes to the overall measurement uncertainty by an estimated standard deviation, termed **standard uncertainty** [14], with suggested symbol u.

All individual uncertainties are categorized as either Type A or Type B.

Type A uncertainties, symbol u_i, are estimated by statistical methods applied to repeated measurements, whilst Type B uncertainties, symbol u_j, are estimated by means of available information and experience.

The **combined standard uncertainty** [14], symbol u_c, of a measurement is calculated by combining the standard uncertainties for each of the individual contributions identified. In the case where the underlying physical effects are additive, this is done by applying the Root of the Sum of the Squares (the RSS) method under the assumption that all contributions are stochastic i.e. independent of each other.

Table B.1 of TR 102 273-1-2 [12]), provides the way in which contributions to the uncertainty, corresponding to physical effects that are not additive, should be handled. Clause D.5 of TR 100 028-2 [11] provides an overview of several more general methods.

The resulting combined standard uncertainty can then be multiplied by a constant k_{xx} to give uncertainty limits (bounds), termed **expanded uncertainty** [14]. When the combined standard uncertainty corresponds to a Normal distribution (see clause 4.1.3) the expanded uncertainty corresponds to a confidence level of *xx* %.

This is the broad outline of the analysis technique employed in the present document, but there are numerous practical problems when applying the basic BIPM rules to measurements, such as:

- how uncertainty contributions in different units (dB, % voltage, % power) can be combined;
- whether individual uncertainties are functions of the true value (e.g. Bit error ratios);
- how to deal with asymmetrically distributed individual uncertainties;
- how to evaluate confidence levels for those standard uncertainties which are not Normal by nature (see also clause D.5.6.2 of TR 100 028-2 [11]).

These problem areas are discussed below and have resulted in modifications and extensions to the BIPM method. For most cases, examples are given in clause 6. Additional supporting theory can be found in annex D of TR 100 028-2 [11].

In order to help understand some of these questions and to bring some more theoretical support, annexes D and E (found in TR 100 028-2 [11]) have been added to the third edition of that document. Clause D.3 of TR 100 028-2 [11] supports various combinations (e.g. additive, multiplicative, etc.), conversions (e.g. to and from dBs) and functions (see clauses D.3.9 and D.3.11 of TR 100 028-2 [11]). A complete approach, encompassing the "BIPM method" is included in clause D.5 of TR 100 028-2 [11].

5.1.1 Type A uncertainties and their evaluation

Type A uncertainties are evaluated by statistical methods, estimating their standard deviations (corresponding to "standard uncertainties").

Annex D of TR 100 028-2 [11] shows that, in most cases, it is only the standard uncertainty that needs to be known in order to find the combined uncertainty. In the BIPM approach, the shape of the individual distributions is considered as being relatively unimportant. However, annex D of TR 100 028-2 [11] shows how to combine the various individual distributions, when needed, and that the result of a combination does not necessarily correspond to a Normal distribution. In such a case, the actual shape of the resulting distribution may be fully relevant (see, in particular, clauses D.5.6.2.3 and D.5.6.2.4 of TR 100 028-2 [11]).

5.1.2 Type B uncertainties and their evaluation

Type B uncertainties are estimated by various methods.

Figure 5 illustrates a selection of uncertainty distributions which can often be identified in RF measurements.

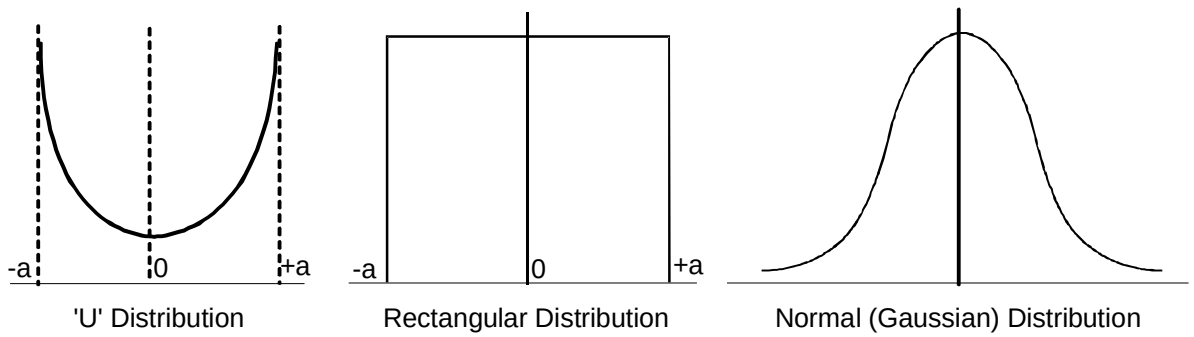

Figure 5: Types of uncertainty distribution

Mismatch uncertainties have the "U" distribution, see annex D of TR 102 273-1-2 [12]. The value of the uncertainty contribution is more likely to be near the limits than to be small or zero. If the limits are ±a, the standard uncertainty is:

$\frac{a}{\sqrt{2}}$ (see TR 102 273-1-2 [12], annex B)

Systematic uncertainties (e.g. those associated with the loss in a cable) are, unless the actual distribution is known, assumed to have a rectangular distribution. The result of this assumption is that the uncertainty can take any value between the limits with equal probability. If the limits are ±a, the standard uncertainty is:

$\frac{a}{\sqrt{3}}$ (see TR 102 273-1-2 [12], annex B)

If the distribution used to model the uncertainty is a Normal distribution, it is characterized by its standard deviation (standard uncertainty) (see annex D of TR 100 028-2 [11]).

In the present document the standard uncertainties are symbolized by $u_{j\ xx}$ or $u_{j\ description}$.

In all cases where the distribution of the uncertainty is unknown, the rectangular distribution should be taken as the default model.

It will be noted that all the distributions illustrated in figure 5 are symmetrical about zero (see clause D.1 of TR 100 028-2 [11], addresses also distributions showing an offset and/or which are not symmetrical). An unexpected complication in combining standard uncertainty contributions may result from the use of different units, since a symmetrical standard uncertainty in % voltage is asymmetrical in dB (and vice versa); similarly for % power. This "major" complication (for any particular test, the contributions may be in a variety of units) is the subject of clause 5.2. See also clause D.3 and in particular clause D.3.10.7 of TR 100 028-2 [11].

5.2 Combining individual standard uncertainties in different units

The BIPM method for calculating the combined standard uncertainty of any test involves combining the individual standard uncertainties by the RSS method. If there are n individual standard uncertainty contributions to be combined, the combined standard uncertainty is:

$$u_c = \sqrt{u_{j1}^2 + u_{j2}^2 + u_{j3}^2 + ... + u_{j(n-1)}^2 + u_{jn}^2 + ... + u_{i1}^2 + u_{i2}^2 + u_{i3}^2 + ... + u_{i(n-1)}^2 + u_{in}^2} \quad (5.1)$$

However, this is correct only if all the individual contributions, represented by their standard uncertainties:

1) combine by addition; and

2) are expressed in the same units.

It does not matter whether the contributions are expressed in percent or logarithmic terms or any other terms as long as these two conditions are fulfilled… noting that the result of the corresponding combination will be expressed in the same way (see also conversions in clause D.3 and the discussion on the concept of sub-systems in clause D.5 of TR 100 028-2 [11]).

To use formula 5.1 for standard uncertainties of individual contributions which combine by **addition**, linear terms only i.e. voltage, percentage, etc., should be used. This is essential for the RSS combination to be valid. This is the case in many measuring instruments.

To use formula 5.1 for standard uncertainties of individual contributions which combine by **multiplication**, logarithmic terms only i.e. dB should be used as they can then be combined by addition. This is essential for the RSS combination to be valid where uncertainty multiplication occurs. This is the case where gains and/or losses (i.e. attenuators, amplifiers, antennas, etc.) are involved as well as under mismatch conditions where modules (i.e. attenuators, cables, RF measuring instruments, etc.) are interconnected in RF measurements.

If all parameters and their associated standard uncertainties in a measurement are in the same unit and combine by addition, the RSS method can be applied directly. For other cases, refer to annex D of TR 100 028-2 [11].

For small (<30 % or 2,5 dB) standard uncertainties however, both additive and multiplicative contributions can be incorporated into the same calculation (with negligible error) provided they are converted to the same units prior to calculating the combined standard uncertainty. The conversion factors are given in table 1. This is supported by the theoretical analysis provided in clause D.3 and annex E of TR 100 028-2 [11].

Annex C of TR 102 273-1-2 [12] gives the justification for this statement by firstly mathematically converting the distribution of an individual uncertainty from logarithmic to linear (and vice versa) and secondly comparing the standard deviation of the two distributions before and after the conversion. One of the outcomes of annex C is that the conversion between linear and logarithmic standard uncertainties can, under some conditions, be approximated by the first order mathematical functions given in table 1.

As can be seen from annex C of TR 102 273-1-2 [12] there are, however, some problems involved in converting distributions:

- It is not a linear procedure; the conversion factor is not only dependent on the magnitude of the standard uncertainty, but it is also dependent on the shape of the distribution.

- The mean value of the converted uncertainty distribution is not necessarily zero, even if that was the case before the conversion. However if the **standard uncertainties** to be converted are less than 2,5 dB, 30 % (voltage), or 50 % (power) the errors arising may be considered as negligible.

Table 1 shows the multiplicative factors to be used when converting **standard uncertainties with a first order approximation**. As an example, if the **standard uncertainty** is 1,5 dB then this, converted to voltage %, gives a corresponding **standard uncertainty** of $1,5 \times 11,5\ \% = 17,3\ \%$.

Table 1: Standard uncertainty conversion factors

Converting from standard uncertainties in ...:	Conversion factor multiply by:	To standard uncertainties in:
dB	11,5	voltage %
dB	23,0	power %
power %	0,0435	dB
power %	0,5	voltage %
voltage %	2,0	power %
voltage %	0,0870	dB

It should be noted after any conversions that may be necessary before using equation 5.1, that the combined standard uncertainty, u_c, which results from the application of equation 5.1, does not, by itself give the expanded uncertainty limits for a measurement.

When u_c corresponds to a Normal distribution, these can be calculated (see clause 5.3) from u_c (assumed in this case to be in units of dB) as the 95 % confidence limits in dB of $\pm 1,96 \times u_c$ (which is very asymmetric in linear terms).

Similarly, in voltage as $\pm 1,96 \times u_c \times 11,5\ \%$ (which is very asymmetric in dB terms). The major factor determining whether the combined standard uncertainty, u_c, will have the symmetrical dB interval or the symmetrical % interval (or somewhere in-between) is whether the individual uncertainties combine by multiplication or by addition. In radiated measurements as well as most conducted measurements where the RF level is of importance, the overwhelming majority of the uncertainties combine by multiplication. It is, therefore, safe to assume that, in general, the resulting uncertainty limits are symmetrical in logarithmic terms (dB). This assumption has been confirmed by computer simulations on a large number of measurement models. This is also clear from the relations found in annex D of TR 100 028-2 [11].

As shown in annex C of TR 102 273-1-2 [12], the shapes of the individual distributions only matter if they are very large (compared to the rest).

5.3 Calculation of the expanded uncertainty values and Student's t-distribution

This clause discusses two different problems, both relating to the handling of uncertainties, which have to be very clearly identified and handled separately. Unfortunately, in the previous edition of the present document, this clause had not been subdivided into two clauses.

The two clauses address:

- the situation where the **statistical properties of a number of samples** are to be evaluated; in this case, the **Student's t-distribution** is a powerful tool allowing the evaluation of the performance of those properties; it can be helpful in supporting the evaluation of properties of "type A uncertainties";
- the situation where **only one measurement** is performed, in conditions where the various sources of uncertainty have been evaluated; as a result, the combined standard uncertainty of that measurement may be evaluated (see clause D.5 of TR 100 028-2 [11]), and **the knowledge of the shape of the distribution** corresponding to that combined uncertainty **allows for changes in the confidence level**.

5.3.1 Student's t-distribution

The Student's t-distribution gives coverage factors (i.e. multipliers) for measurements, whereby the confidence level of a series of measurements can be calculated from a limited number of samples, assuming those samples have been taken from a Normal distribution. The fewer the number of samples, the bigger the coverage factor for a given confidence level.

For example:

- if a type A standard deviation is calculated on only 3 samples and the required confidence level is 95 % the appropriate Student's t-factor is 3,18;
- if the standard deviation had been based on 20 samples, the factor would have been 2,09;
- for an infinite number of samples the multiplier would have been 1,96.

When using such an approach, any measurement should be repeated a large number of times.

In radio measurements, however, by using the approach recommended in the present document, only one measurement is usually performed. As a result, the Student's t-distribution is of no help.

The Student's t-distribution can, however, be very useful for the statistical evaluation of the properties of individual uncertainty components (i.e. type A uncertainties which may happen to be part of some test set up).

5.3.2 Expanded uncertainties

When the combined standard uncertainty, u_c, has been calculated from equation 5.1 (or by any other method) and it can be expected that the corresponding distribution is Normal, then, the uncertainty limits relate to a confidence level of 68,3 % (due to the properties of the Gaussian curve).

By multiplying u_c by "a coverage factor" (or "an expansion factor") other confidence levels may be obtained when the distribution corresponding to the combined standard uncertainty, u_c, is Normal. Why?

When:

- all the individual sources of uncertainty are identified for all the tests;
- the distributions of the uncertainties of the individual sources are all known (or assumed);
- the maximum, worst-case values of all of the individual uncertainties are known.

Then, under these conditions, annex D of TR 100 028-2 [11] applies and the combined standard uncertainty can be calculated (see clause D.5 of TR 100 028-2 [11]).

Assuming that the combined standard uncertainty corresponds to a Normal distribution then the magic factor of 1,96 applies: this is due to the shape of the Gaussian curve used to describe the distribution corresponding to the combined uncertainty (see the interpretation in clause D.5.6.2 of TR 100 028-2 [11]).

As already indicated above (see clause 4.1.3), for a Gaussian shaped curve:

- a surface of 68 % (2 x 34 %, the value which can be found in some tables) corresponds to one standard deviation (i.e. a combined standard deviation);
- a surface of 95 % (2 x 47,5 %, the value which can be found in some tables) corresponds to two standard deviations (more precisely 1,96 standard deviations);

and the surface referred to above can be interpreted as the probability of the true value being within the stated uncertainty bounds.

The probability of remaining inside this surface is, by definition, the confidence level.

It has to be made clear that, when the combination of the various components of the uncertainty correspond to a distribution which is not Normal, then other expansion factors apply in order to convert from one confidence level to another. The values of these factors depend on the mathematical properties (i.e. the shape) of the corresponding distribution.

It has to be made clear also that, as indicated in particular in annex D of TR 100 028-2 [11], when the number of components added (or combined linearly) in order to obtain the uncertainty can be considered as an infinity, and under some other conditions, then the distribution can be considered as Normal (based on the "Central Limit Theorem"). Under such conditions, the factor 1,96 is valid (for a 95% confidence level). This is why it has been used extensively in the examples given in the present document.

The usage of a value of 2,00 for this expansion factor has also been suggested (this would provide a confidence level of 95,45 % in the case of Normal distributions).

The tools given in annex D of TR 100 028-2 [11] could allow for the calculation of the actual distribution corresponding to the combination of various components for the uncertainty. Under such conditions, the appropriate expansion factors could also be calculated, in the case where the distribution found would not have happened to be Normal.

5.4 Combining standard uncertainties of different parameters, where their influence on each other is dependant on the EUT (influence quantities)

In many measurements, variations in the influence quantities, intermediate test results or test signals can affect the uncertainty of the measurand in ways that may be functions of the characteristics of the EUT and other instrumentation.

It is not always possible to fully characterize test conditions, signals and measurands. Uncertainties are related to each of them. These uncertainties may be well known, but their influence on the combined standard uncertainty depends on the EUT. Uncertainties related to general test conditions are:

- ambient temperature;
- the effect of cooling and heating;
- power supply voltage;
- power supply impedance;
- impedance of test equipment connectors (VSWR).

Uncertainties related to applied test signals and measured values are:

- level;
- frequency;
- modulation;

- distortion;
- noise.

The effect of such uncertainties on the test results can vary from one EUT to another. Examples of the characteristics that can affect the calculation of the uncertainties are:

- receiver noise dependency of RF input signal levels;
- impedance of input and output connectors (VSWR);
- receiver noise distribution;
- performance dependency of changes of test conditions and test signals;
- modulator limiting function e.g. maximum deviation limiting;
- system random noise.

If the appropriate value for each characteristic has not been determined for a particular case, then the values listed in table F.1 of TR 100 028-2 [11] should be used. These values are based on measurements made with several pieces of equipment and are stated as mean values associated with a standard uncertainty reflecting the spread from one EUT to another.

When the EUT dependent uncertainties add to the combined standard uncertainty, the RSS method of combining the standard uncertainties is used, but in many calculations the EUT dependency is a function that converts uncertainty from one part of the measurement configuration to another. In most cases the EUT dependency function can be assumed to be linear; therefore the conversion is carried out by multiplication as shown in the theoretical analysis provided in clause D.4 of TR 100 028-2 [11].

The standard uncertainty to be converted is $u_{j\,1}$. The mean value of the influence quantity is A and its standard uncertainty is $u_{j\,a}$. The resulting standard uncertainty $u_{j\,converted}$ of the conversion is:

$$u_{jconverted} = \sqrt{u_{j1}^2 (A^2 + u_{ja}^2)} \qquad (5.2)$$

The standard uncertainty of this contribution is then looked upon as any other individual component and is combined accordingly (see annex D of TR 100 028-2 [11]). A fully worked example of an influence quantity is given in clause 6.4.6. The conditions under which the expression 5.2 is valid can also be found in clause D.4 of TR 100 028-2 [11].

If the function is not linear another solution must be found:

- the theoretical relation between the influence quantity and its effect has to be determined;
- the expressions providing the conversion can then be found based on the table contained in clause D.3.12of TR 100 028-2 [11]).

When the theoretical relation between the influence quantity and its effect is not known, the usage of a simple mathematical model can be tried. In this case, an attempt can be made in order to determine the numerical values of the parameters of the model by some statistical method (see also clause D.5.4 of TR 100 028-2 [11]).

In all cases, it is recommended to determine first the mathematical relation between the parameters, and only after try and find the appropriate numerical values. As a consequence, tables similar to table F.1 in annex F (part 2) should also include the mathematical relation between the parameters for each entry (for further details, see clause D.4.2.1.2 in TR 100 028-2 [11]).

5.5 Uncertainties and randomness

The major difficulty behind this clause is to understand exactly what "randomness uncertainty" is supposed to cover in this context (i.e. what this clause or contribution is expected to cover): the BIPM method and the corresponding analysis is supposed to cover all components of the uncertainty, so it is fundamental to understand what is left over for the "uncertainty of randomness", in order to avoid taking into account the same effects twice, under different names (in a complex set up).

The standard uncertainty of randomness can be evaluated by repeating a measurement (e.g. of a particular component of the measurement uncertainty).

The first step is to calculate the arithmetic mean or average of the results obtained.

The spread in the measured results reflects the merit of the measurement process and depends on the apparatus used, the method, the sample and sometimes the person making the measurement. A more useful statistic, however, is the standard uncertainty σ_i of the sample. This is the root mean square of the differences between the measured values and the arithmetic mean of the samples.

If there are n results for x_m where m = 1, 2, ..., n and the sample mean is $\bar{x}$, then the standard deviation σ_i is:

$$\sigma_i = \sqrt{\frac{1}{n}\sum_{m=1}^{n}\left(x_m - \bar{x}\right)^2} \tag{5.3}$$

This should not be confused with the standard deviation of the A uncertainty being investigated. It only covers *n* samples.

If further measurements are made, then for each sample of results considered, different values for the arithmetic mean and standard deviation will be obtained. For large values of n these mean values approach a central limit value of a distribution of all possible values. This distribution can usually be assumed, for practical purposes, to be a Normal distribution.

From the results of a relatively small number of measurements an estimate can be made of the standard deviation of the whole population of possible values, of which the measured values are a sample.

Estimate of the standard deviation σ_i':

$$\sigma_i' = \sqrt{\left(\frac{1}{n\text{-}1}\right)\sum_{m=1}^{n}\left(x_m - \bar{x}\right)^2} \tag{5.4}$$

A practical form of this formula is:

$$\sigma_i' = \sqrt{\frac{Y - \frac{X^2}{n}}{n - 1}} \tag{5.5}$$

where *X* is the sum of the measured values and *Y* is the sum of the squares of the measured values.

It will be noted that the only difference between σ_i' and σ_i is in the factor 1/ (n-1) in place of 1/n, so that the difference becomes smaller as the number of measurements is increased. A similar way of calculating the standard deviation of a discrete distribution can be derived from this formula.

In this case *X* is the sum of the individual values from the distribution times their probability, and *Y* is the sum of the square of the individual values times their probability.

If the distribution has m values x_i, each having the probability p (x_i):

$$X = \sum_{i=1}^{m} x_i\, p(x_i) \tag{5.6}$$

and

$$Y = \sum_{i=1}^{m} x_i^2\, p(x_i) \tag{5.7}$$

The standard uncertainty is then:

$$\sigma_i = \sqrt{Y - X^2} \quad (5.8)$$

When a measured results is obtained as the arithmetic mean of a series of *n* (independent) measurements the standard uncertainty is reduced by a factor $\sqrt{n}$ thus:

$$\sigma_i = \frac{\sigma_1'}{\sqrt{n}} \quad (5.9)$$

This is an efficient method of reducing measurement uncertainty when making noisy or fluctuating measurements, and it applies both for random uncertainties in the measurement configuration and the EUT. Having established the standard deviation, this is directly equated to the standard uncertainty:

$u_i = \sigma_i$

As the uncertainty due to random uncertainty is highly dependent on the measurement configuration and the test method used it is not possible to estimate a general value.

Each laboratory must by means of repetitive measurements estimate their own standard uncertainties characterizing the randomness involved in each measurement. Once having done this, the estimations may be used in future measurements and calculations.

NOTE: See also the note found in clause 6.4.7 concerning the usage of this component.

5.6 Summary of the recommended approach

The basic BIPM method, with specific modifications, remains the adopted approach used for the calculation of combined standard and expanded uncertainty in the examples given in this report for radiated measurements. That is to say that once all the individual standard uncertainties in a particular measurement have been identified and given values, they are combined by the RSS method provided they combine by addition and are expressed in the same units (otherwise, methods such as those detailed in annex D of TR 100 028-2 [11], e.g. in clause D.5, have to be used).

In order to ensure that this proviso is satisfied as often as possible, the present document supplies the factors necessary to convert standard uncertainties in linear units to standard uncertainties in logarithmic units (and vice versa). The present document also shows that additive standard uncertainties (% V, % power) can be combined with small multiplicative standard uncertainties once converted into dBs in the RSS manner with, hopefully, negligible error.

Having derived the combined standard uncertainty, an expanded uncertainty for 95 % confidence levels can then be derived, when the corresponding distribution is Normal, by multiplying the result by the expansion factor of 1,96. The multiplication by this factor (or simply by a factor equal to 2) is to be done in all cases, in order to obtain the expanded uncertainty. However, if the corresponding distribution is not Normal, then the resulting confidence level is not necessarily 95 % (see clause D.5.6.2 of TR 100 028-2 [11]). In all cases, however, the actual confidence level can be calculated, once the distribution corresponding to the combination of all uncertainty components has been calculated. clause D.3 of TR 100 028-2 [11], provides the equations allowing for the calculation of this combined distribution.

The practical implementation of this modified BIPM approach, adopted throughout the present document, is for each test method (including the verification procedures) to have appended to it a complete list of the individual uncertainty sources that contribute to each stage of the test. Magnitudes of the standard uncertainties can then be assigned to these individual contributions by consulting annex A of TR 102 273-1-2 [12] (converting from linear units to dB, if necessary). All uncertainties are in dB units since the great majority of the individual contributions in radiated measurements are multiplicative i.e. they add in dB terms.

In those cases in which annex A of TR 102 273-1-2 [12] instructs that the values of the uncertainty contributions be taken from a manufacturer's data sheet, that data should be taken over as broad a frequency band as possible. This type of approach avoids the necessity of calculating the combined standard uncertainty every time the same test is performed for different EUT.

6 Examples of uncertainty calculations specific to radio equipment

6.1 Mismatch

In the following the Greek letter Γ means the complex reflection coefficient. ρ_x is the magnitude of the reflection coefficient:

$$\rho_x = |\Gamma_x|$$

Where two parts or elements in a measurement configuration are connected, if the matching is not ideal, there will be an uncertainty in the level of the RF signal passing through the connection. The magnitude of the uncertainty depends on the VSWR at the junction of the two connectors.

The uncertainty limits of the mismatch at the junction are calculated by means of the following formula:

$$\text{Mismatch limits} = |\Gamma_{\text{generator}}| \times |\Gamma_{\text{load}}| \times |S_{21}| \times |S_{12}| \times 100\ \%\ \text{Voltage} \quad (6.1)$$

where:

$|\Gamma_{generator}|$ is the modulus of the complex reflection coefficient of the signal generator;

$|\Gamma_{load}|$ is the modulus of the complex reflection coefficient of the load (receiving device);

$|S_{21}|$ is the forward gain in the network between the two reflection coefficients of interest;

$|S_{12}|$ is the backward gain in the network between the two reflection coefficients of interest.

NOTE: S_{21} and S_{12} are set to 1 if the two parts are connected directly. In linear networks S_{21} and S_{12} are identical.

The distribution of the mismatch uncertainty is U-shaped, If the uncertainty limits are ±a, the standard uncertainty is:

$$u_{j\ mismatch:individual} = \frac{|\Gamma_{generator}| \times |\Gamma_{load}| \times |S_{21}| \times |S_{12}| \times 100\%}{\sqrt{2}} Voltage\% \quad (6.2)$$

This can be converted into equivalent dB by dividing by 11,5 (see clause 5.2):

$$u_{j\ mismatch:individual} = \frac{|\Gamma_{generator}| \times |\Gamma_{load}| \times |S_{21}| \times |S_{12}| \times 100\%}{\sqrt{2} \times 11{,}5} \text{dB} \quad (6.3)$$

If there are several connections in a test set-up, they will all interact and contribute to the combined mismatch uncertainty. The method of calculating the combined mismatch uncertainty is fully explained in annex D of TR 102 273-1-2 [12].

In conducted measurements, when calculating the mismatch uncertainty at the antenna connector of the EUT, the reflection coefficient of the EUT is required. In this case, the laboratory should either measure it in advance or use the reflection coefficients given in TR 100 028 [11].

6.2 Attenuation measurement

In many measurements the absolute level of the RF signal is part of the measured result. The RF signal path attenuation has to be known in order to apply a systematic correction to the result. The RF signal path can be characterized using the manufacturers' information about the components involved, but this method can result in unacceptably large uncertainties.

Another method is to measure the attenuation directly by using, for example, a signal generator and a receiving device. To measure the attenuation, connect the signal generator to the receiving device and read the reference level (A), see figure 6, and then insert the unknown attenuation, repeat the measurement and read the new level (B), see figure 7.

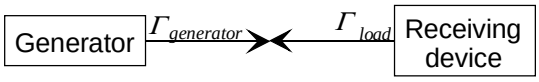

Figure 6: Measurement of level (A)

In figure 6, $\Gamma_{generator}$ is the complex reflection coefficient of the signal generator and Γ_{load} is the complex reflection coefficient of the load (receiving device);

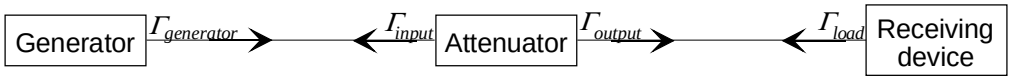

Figure 7: Measurement of level (B)

In figure 7, $\Gamma_{generator}$ is the complex reflection coefficient of the signal generator, Γ_{load} is the complex reflection coefficient of the load (receiving device), Γ_{input} is the complex reflection coefficient of the attenuator input, Γ_{output} is the complex reflection coefficient of the attenuator output.

The attenuation is calculated as A/B if the readings are linear values or A-B if the readings are in dB.

Using this method, four uncertainty sources need to be considered. Two sources concern the receiving device, namely its absolute level (if the input attenuation range has been changed) and its linearity. The other two sources are the stability of the signal generator output level (which contributes to both stages of the measurement) and mismatch caused by reflections at both the terminals of the network under test and the instruments used. The absolute level, linearity and stability uncertainties can be obtained from the manufacturers data sheets, but the mismatch uncertainty has to be estimated by calculation.

For this example, we assume that an attenuator of nominally 20 dB is measured at a frequency of 500 MHz by means of a signal generator and a receiving device. The magnitude of the reflection coefficient of the generator $|\Gamma_{generator}|$ is 0,2, the magnitude of the reflection coefficient of the receiving device $|\Gamma_{load}|$ is 0,3 and the magnitude of the reflection coefficients of the attenuator $|\Gamma_{input}|$ and $|\Gamma_{output}|$ are 0,05.

Since the mismatch uncertainty of the attenuation measurement is different in figure 7 to that in figure 6, it therefore has to be calculated (for figure 6 and figure 7) and both values included in the combined mismatch uncertainty as shown below.

Mismatch uncertainty:

Reference measurement: The signal generator is adjusted to 0 dBm and the reference level A is measured on the receiving device. Using equation 6.1 with $S_{21} = S_{12} = 1$, and taking the standard uncertainty, $u_{j\ mismatch:\ reference\ measurement}$

$$u_{j\ mismatch:referencemeasurement} = \frac{0{,}2 \times 0{,}3 \times 100}{\sqrt{2}}\ \% = 4{,}24\ \% \approx \frac{4{,}24}{11{,}5} = 0{,}37\ \text{dB} \qquad (6.4)$$

Attenuator measurement: The attenuator is inserted and a level (B) = -20,2 dB is measured after an input attenuation range change on the receiving device.

NOTE: The measured attenuation is 20,2 dB, for which $S_{21} = S_{12} = 0{,}098$.

The following three components comprise the uncertainty in this part of the measurement:

The standard uncertainty of the mismatch between the signal generator and the attenuator:

$$u_{j\ mismatch:generatortoattenuator} = \frac{0{,}2 \times 0{,}05 \times 100}{\sqrt{2}}\ \% = 0{,}71\%$$

The standard uncertainty of the mismatch between the attenuator and the receiving device:

$$u_{j\ mismatch:attenuatortoreceivingdevice} = \frac{0{,}3 \times 0{,}05 \times 100}{\sqrt{2}}\ \% = 1{,}06\,\%$$

The standard uncertainty of the mismatch between the signal generator and the receiving device:

$$u_{j\ mismatch:generatortoreceivingdevice} = \frac{0{,}3 \times 0{,}2 \times 0{,}098^2 \times 100}{\sqrt{2}}\% = 0{,}041\,\%$$

The combined standard uncertainty of the mismatch of the attenuation measurement $u_{c\ mismatch:\ att.\ measurement}$, is calculated by RSS (see clause 5.2) of the individual contributions.

$$u_{c\ mismatch:att.measurement} = \sqrt{0{,}71^2 + 1{,}06^2 + 0{,}041^2} = 1{,}28\,\% \approx \frac{1{,}28}{11{,}5} = 0{,}11\,\text{dB}$$

A comparison of $u_{j\ mismatch:\ reference\ measurement}$ (0,37 dB) and $u_{c\ mismatch:\ att.\ measurement}$ (0,11 dB) shows clearly the impact of inserting an attenuator between two mismatches.

Other components of uncertainty:

Reference measurement: The stability of the signal generator provides the only other uncertainty in this part. The receiving device contributes no uncertainty here since only a reference level is being set for comparison in the attenuation measurement stage.

The output level stability of the signal generator is taken from the manufacturer's data sheet as 0,10 dB which is assumed (since no information is given) to be rectangularly distributed (see clause 5.1). Therefore the standard uncertainty, $u_{j\ signal\ generator\ stability}$, is:

$$u_{j\ signalgeneratorstability} = \frac{0{,}10}{\sqrt{3}} = 0{,}06\,\text{dB}$$

Therefore, the combined standard uncertainty, $u_{c\ reference\ measurement}$, for the reference measurement is:

$$u_{c\ referencemeasurement} = \sqrt{u^2_{jmismatch:referencemeasurement} + u^2_{jsignalgeneratorstability}} = \sqrt{0{,}37^2 + 0{,}06^2} = 0{,}37\,\text{dB}$$

Attenuation measurement: Here the output stability of the signal generator as well as absolute level uncertainty of the receiving device (the input attenuation range has changed) contribute to the uncertainty. However as a range change has occurred there is no linearity contribution as this is included in the absolute level uncertainty of the receiver.

The signal generator stability, $u_{j\ signal\ generator\ stability}$, has the same value as for the reference measurement, whilst the uncertainty for the receiving device is given in the manufacturer's data sheet as 1,0 dB absolute level accuracy. A rectangular distribution is assumed for the absolute level accuracy so the standard uncertainty, $u_{j\ signal\ generator\ level}$, of its uncertainty contribution is:

$$u_{j\ signalgeneratorlevel} = \frac{1{,}00}{\sqrt{3}} = 0{,}58\,\text{dB}$$

The uncertainty contribution of the linearity of the receiving device $u_{j\ linearity}$ is zero.

Therefore the combined standard uncertainty, $u_{c\ att.\ measurement}$, for the attenuation measurement is:

$$u_{c\ att.measurement} = \sqrt{u^2_{c\ mismatch:att.measurement} + u^2_{j\ signalgeneratorstability} + u^2_{j\ signalgeneratorlevel} + u^2_{j\ linearity}}$$

$$= \sqrt{0{,}08^2 + 0{,}06^2 + 0{,}58^2 + 0{,}00^2} = 0{,}59\,\text{dB}$$

So, for the complete measurement, the combined standard uncertainty, $u_{c\ measurement}$, is given by:

$$u_{cmeasurement} = \sqrt{u_{c\ referencemeasurement}{}^2 + u_{c\ att.measurement}{}^2} = \sqrt{0{,}37^2 + 0{,}59^2} = 0{,}70\ \text{dB}$$

The expanded uncertainty is ±1,96 × 0,70 = ±1,37 dB at a 95 % confidence level.

This is an exaggerated example. Smaller uncertainty is possible if a better receiving device is used.

6.3 Calculation involving a dependency function

The specific dependency function is the relationship between the RF signal level at the EUT antenna connector (dB) to the uncertainty of the measurement of SINAD at the EUT's audio output i.e. how does SINAD measurement uncertainty relate to RF level uncertainty at the EUT antenna connector.

The following example is based on a typical TR 100 028 [11] type (conducted) RF measurement for clarity. The sensitivity of a receiving EUT is measured. The outline of the measurement is as follows. The RF level at the input of the receiver is continuously reduced until a SINAD measurement of 20 dB is obtained, see figure 8.

The result of the measurement is the RF signal level causing 20 dB SINAD at the audio output of the receiver.

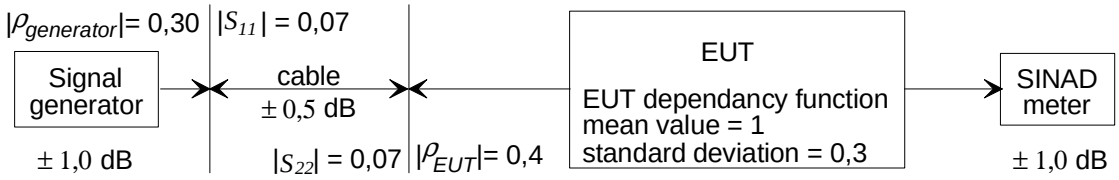

Figure 8: Typical measurement configuration

The combined standard uncertainty is calculated as follows:

For the mismatch uncertainty (annex D):

Generator:	Output reflection coefficient: $\lvert\rho_{generator}\rvert$	= 0,30
Cable:	Input and output reflection coefficients: $\lvert S_{11}\rvert$ and $\lvert S_{22}\rvert$	= 0,07
	Attenuation: 1 dB = $\lvert S_{21}\rvert = \lvert S_{12}\rvert$	= 0,891
EUT:	Input reflection coefficient: $\lvert\rho_{EUT}\rvert$	= 0,4

All these contributions are U distributed. There are three contributions:

The standard uncertainty of the mismatch between the signal generator and the cable:

$$u_{j\ mismatch:signal generator to cable} = \frac{0{,}30 \times 0{,}07 \times 100\,\%}{\sqrt{2} \times 11{,}5} = 0{,}13\ \text{dB}$$

The standard uncertainty of the mismatch between the cable and the EUT:

$$u_{j\ mismatch:cable to EUT} = \frac{0{,}4 \times 0{,}07 \times 100\,\%}{\sqrt{2} \times 11{,}5} = 0{,}17\ \text{dB}$$

The standard uncertainty of the mismatch between the signal generator and the EUT:

$$u_{j\ mismatch:signal generator to EUT} = \frac{0{,}3 \times 0{,}4 \times 0{,}891^2 \times 100\,\%}{\sqrt{2} \times 11{,}5} = 0{,}59\ \text{dB}$$

The combined standard uncertainty of the mismatch:

$$u_{c\ mismatch} = \sqrt{0{,}13^2 + 0{,}17^2 + 0{,}59^2} = 0{,}63\text{dB}$$

$$u_{c\ mismatch} = 0{,}63\ \text{dB}$$

The uncertainty due to the absolute output level of the signal generator is taken as ±1,0 dB (from manufacturers data). As nothing is said about the distribution, a rectangular distribution in logs is assumed (see clause 5.1), and the standard uncertainty is:

$$u_{j\ signal\ generator\ level} = 0{,}58\ \text{dB}$$

The uncertainty due to the output level stability of the signal generator is taken as ±0,02 dB (from manufacturer's data). As nothing is said about the distribution, a rectangular distribution in logs is assumed (see clause 5.1), and the standard uncertainty is:

$$u_{j\ signal\ generator\ stability} = 0{,}01\ \text{dB}$$

The uncertainty due to the insertion loss of the cable is taken as ±0,5 dB (from calibration data). As nothing is said about the distribution, a rectangular distribution in logs is assumed, and the standard uncertainty is:

$$u_{j\ cable\ loss} = 0{,}29\ \text{dB}$$

Dependency function uncertainty calculation:

The uncertainty due to the SINAD measurement corresponds to an RF signal level uncertainty at the input of the receiving EUT.

The SINAD uncertainty from the manufacturer's data is ±1 dB which is converted to a standard uncertainty of 0,577 dB. The dependency function converting the SINAD uncertainty to RF level uncertainty is found from table F1 of TR 100 028-2 [11]. It is given as a conversion factor of 1,0 % (level)/ % (SINAD) with an associated standard uncertainty of 0,3. The SINAD uncertainty is then converted to RF level uncertainty using formula 5.2:

$$u_{j\ RF\,level(converted)} = \sqrt{0{,}577^2 \times \left(1{,}0^2 + 0{,}3^2\right)} = 0{,}60\,\text{dB}$$

The RF level uncertainty caused by the SINAD uncertainty and the RF level uncertainty at the input of the receiver is then combined using the square root of the sum of the squares method to give the combined standard uncertainty.

$$u_{c\ measurement} = \sqrt{u^2_{c\ mismatch} + u^2_{j\ signal generator level} + u^2_{j\ signal generator stability} + u^2_{j\ cable loss} + u^2_{j\ RF level(converted)}}$$

$$= \sqrt{0{,}63^2 + 0{,}58^2 + 0{,}01^2 + 0{,}29^2 + 0{,}60^2} = 1{,}08\,\text{dB}$$

The expanded uncertainty is ±1,96 × 1,08 = ±2,12 dB at a 95 % confidence level.

6.4 Measurement of carrier power

The example test is a conducted measurement.

6.4.1 Measurement set-up

The EUT is connected to the power meter via a coaxial cable and two power attenuators, one of 10 dB and one of 20 dB (see figure 9).

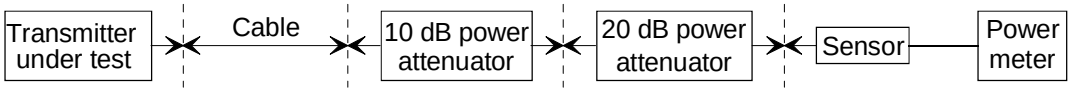

Figure 9: Measurement set-up

The nominal carrier power is 25 W, as a result the power level at the input of the power sensor is (nominally) 25 mW. The carrier frequency is 460 MHz and the transmitter is designed for continuous use.

6.4.2 Method of measurement

The transmitter is in an environmental chamber adjusted to +55 °C. The attenuators and the power sensor are outside the chamber.

Prior to the power measurement the total insertion loss of cable and attenuators is measured.

The attenuation measurements are done using a generator and a measuring receiver and two 6 dB attenuators with small VSWR.

Also the power sensor is calibrated using the built in power reference.

The result of the measurement is the power found as the average value of 9 readings from the power meter, corrected for the measured insertion loss.

6.4.3 Power meter and sensor module

The power meter uses a thermocouple power sensor module and contains a power reference.

Power reference level:

Power reference level uncertainty: ±1,2 % power.

As nothing is stated about the distribution it is assumed to be rectangular and the standard uncertainty is converted from % power to dB by division with 23,0 (see clause 5.2).

Standard uncertainty $u_{j\ referencelevel} = \frac{1,2}{\sqrt{3} \times 23,0} = 0,030\,\text{dB}$

Mismatch whilst measuring the reference:

Reference source VSWR: 1,05 (d): $\rho_{reference\ source} = 0,024$

Power sensor VSWR: 1.15 (d): $\rho_{load} = 0,07$

Using formula 6.3 the standard uncertainty of the mismatch is:

$$u_{j\ mismatch:reference} = \frac{0,024 \times 0,07 \times 100\ \%}{\sqrt{2} \times 11,5} = 0,010\,\text{dB}$$

Calibration factors:

Calibration factor uncertainty = ±2,3 % power

As nothing is stated about the distribution it is assumed to be rectangular. The standard uncertainty is converted from % power to dB by division with 23,0.

Standard uncertainty $u_{j\ calibration\ factor} = \frac{2,3}{\sqrt{3} \times 23,0} = 0,058\,\text{dB}$

Range to range change:

Range to range uncertainty (one change) = ±0,25 % power.

As nothing is stated about the distribution it is assumed to be rectangular. The standard uncertainty is converted from % power to dB by division with 23,0.

Standard uncertainty $u_{j rangechange} = \frac{0,25}{\sqrt{3} \times 23,0} = 0,006\,\text{dB}$

Noise and drift is negligible at this power level and can be ignored.

Combined standard uncertainty of the power meter and sensor:

Using formula 5.1:

$$u_{c\ meter\ and\ sensor} = \sqrt{u_{j\ reference level}^2 + u_{j\ mismatch:reference}^2 + u_{j\ calibration\ factor}^2 + u_{j\ range change}^2}$$

$$u_{c\ meter\ and\ sensor} = \sqrt{0{,}03^2 + 0{,}010^2 + 0{,}058^2 + 0{,}006^2} = 0{,}066\ \text{dB}$$

6.4.4 Attenuator and cabling network

Standing wave ratios involved in the attenuation measurement (taken from manufacturers data):

- Signal generator: VSWR ≤ 1,5 ρ = 0,200;
- Power sensor: VSWR ≤ 1,15 ρ = 0,070;
- 6 dB attenuators: VSWR ≤ 1,2 ρ = 0,091;
- 10 dB power attenuator: VSWR ≤ 1,3 ρ = 0,130;
- 20 dB attenuator: VSWR ≤ 1,25 ρ = 0,111;
- Cable: VSWR ≤ 1,2 ρ = 0,091.

Nominal attenuations converted to linear values:

- 6 dB = $|S_{21}| = |S_{12}| = 0{,}500$;
- 10 dB = $|S_{21}| = |S_{12}| = 0{,}316$;
- 20 dB = $|S_{21}| = |S_{12}| = 0{,}100$;
- 0,3 dB = $|S_{21}| = |S_{12}| = 0{,}966$ (assumed cable attenuation in the uncertainty calculations).

The attenuation measurement is carried out using a signal generator and a measuring receiver. In order to have a low VSWR two 6 dB attenuators with low reflection coefficients are inserted.

The measurement of the attenuation in the attenuator and cabling network is carried out by making a reference measurement (see figure 10). The measurement receiver reading is "A" dBm.

Then the cables and the attenuators are inserted. First the cable and the 10 dB power attenuator is inserted between the two 6 dB attenuators, and a new reading "B" dBm is recorded (see figure 11).

Finally the 20 dB attenuator is inserted between the two 6 dB attenuators, and the reading "C" dBm is recorded (see figure 12).

The total attenuation is then ("A"-"B") dB + ("A"-"C") dB.

6.4.4.1 Reference measurement

Figure 10 details the components involved in this reference measurement.

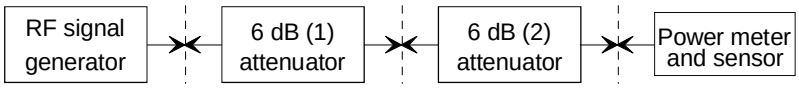

Figure 10: The reference measurement

The individual mismatch uncertainties between the various components in figure 10 are calculated using formula 6.3:

The standard uncertainty of the mismatch between the signal generator and 6 dB attenuator (1):

$$u_{j\ mismatch:generatorto6dBatt.} = \frac{0{,}2 \times 0{,}091 \times 100\,\%}{\sqrt{2} \times 11{,}5} = 0{,}112\,\text{dB}$$

The standard uncertainty of the mismatch between the 6 dB attenuator (1) and 6 dB attenuator (2):

$$u_{j\ mismatch:6dBatt.1to6dBatt.2} = \frac{0{,}091 \times 0{,}091 \times 100\,\%}{\sqrt{2} \times 11{,}5} = 0{,}051\,\text{dB}$$

The standard uncertainty of the mismatch between the 6 dB attenuator (2) and power sensor:

$$u_{j\ mismatch:6dBatt.to\ powersensor} = \frac{0{,}091 \times 0{,}07 \times 100\,\%}{\sqrt{2} \times 11{,}5} = 0{,}039\,\text{dB}$$

The standard uncertainty of the mismatch between the signal generator and 6 dB attenuator (2):

$$u_{j\ mismatch:generatorto6dBatt.2} = \frac{0{,}2 \times 0{,}091 \times 0{,}5^2 \times 100\,\%}{\sqrt{2} \times 11{,}5} = 0{,}028\,\text{dB}$$

The standard uncertainty of the mismatch between the 6 dB attenuator (1) and power sensor:

$$u_{j\ mismatch:6dBatt.1to\ powersensor} = \frac{0{,}091 \times 0{,}07 \times 0{,}5^2 \times 100\,\%}{\sqrt{2} \times 11{,}5} = 0{,}010\,\text{dB}$$

The standard uncertainty of the mismatch between the signal generator and power sensor:

$$u_{j\ mismatch:generatorto\ powersensor} = \frac{0{,}2 \times 0{,}07 \times 0{,}5^2 \times 0{,}5^2 \times 100\,\%}{\sqrt{2} \times 11{,}5} = 0{,}005\,\text{dB}$$

It can be seen that the mismatch uncertainty between the RF signal generator and the 6 dB attenuator (1) $u_{j\ generator\ to\ 6\ dB\ att\ 1}$, and the mismatch uncertainty between the 6 dB attenuator (2) and the power sensor $u_{j\ 6\ dB\ att.\ 2\ to\ power\ sensor,}$ add to both the reference measurement and the measurements with the unknown attenuators inserted.

It is the result of the methodology adopted in annex D that these terms cancel and hence do not contribute to the combined standard uncertainty of the final result. The reference measurement mismatch uncertainty $u_{j\ mismatch:\ reference}$ (formula 5.1):

$$u_{j\ mismatch:reference} = \sqrt{u^2_{j\ 6dBatt.1to6dBatt.2} + u^2_{j\ generatorto6dBatt.2} + u^2_{j\ 6dBatt.1to\ powersensor} + u^2_{j\ generatorto\ powersensor}}$$

$$u_{j\ mismatch:reference} = \sqrt{0{,}051^2 + 0{,}028^2 + 0{,}010^2 + 0{,}005^2} = 0{,}059\,\text{dB}$$

NOTE: If the two uncertainties of the generator and the power sensor did not cancel due to the methodology, the calculated reference measurement uncertainty would have been 0,131 dB.

6.4.4.2 The cable and the 10 dB power attenuator

Figure 11 shows the section of the reference set-up which concerns this part of the calculation.

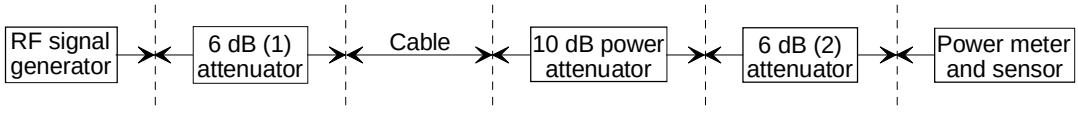

Figure 11: The cable and the 10 dB power attenuator

The individual uncertainties are calculated using formula 6.3:

The standard uncertainty of the mismatch between the signal generator and 6 dB attenuator (1):

$$u_{j\ mismatch:generator to 6dBatt.} = \frac{0{,}2 \times 0{,}091 \times 100\,\%}{\sqrt{2} \times 11{,}5} = 0{,}112\,\text{dB}$$

The standard uncertainty of the mismatch between the 6 dB attenuator (1) and cable:

$$u_{j\ mismatch:6dBatt.1 to cable} = \frac{0{,}091 \times 0{,}091 \times 100\,\%}{\sqrt{2} \times 11{,}5} = 0{,}051\,\text{dB}$$

The standard uncertainty of the mismatch between the cable and 10 dB power attenuator:

$$u_{j\ mismatch:cable to 10dBatt.} = \frac{0{,}091 \times 0{,}130 \times 100\,\%}{\sqrt{2} \times 11{,}5} = 0{,}073\,\text{dB}$$

The standard uncertainty of the mismatch between the 10 dB attenuator and the 6 dB attenuator (2):

$$u_{j\ mismatch:10dBatt.to 6dBatt.2} = \frac{0{,}130 \times 0{,}091 \times 100\,\%}{\sqrt{2} \times 11{,}5} = 0{,}073\,\text{dB}$$

The standard uncertainty of the mismatch between the 6 dB attenuator (2) and power sensor:

$$u_{j\ mismatch:6dBatt.to\ power sensor} = \frac{0{,}091 \times 0{,}07 \times 100\,\%}{\sqrt{2} \times 11{,}5} = 0{,}039\,\text{dB}$$

The standard uncertainty of the mismatch between the signal generator and cable:

$$u_{j\ mismatch:generator to cable} = \frac{0{,}200 \times 0{,}091 \times 0{,}5^2 \times 100\,\%}{\sqrt{2} \times 11{,}5} = 0{,}028\,\text{dB}$$

The standard uncertainty of the mismatch between the 6 dB attenuator (1) and 10 dB power attenuator:

$$u_{j\ mismatch:6dBatt.1 to 10dBatt.} = \frac{0{,}091 \times 0{,}130 \times 0{,}966^2 \times 100\,\%}{\sqrt{2} \times 11{,}5} = 0{,}068\,\text{dB}$$

The standard uncertainty of the mismatch between the cable and 6 dB attenuator (2):

$$u_{j\ mismatch:cable to 6dBatt.2} = \frac{0{,}091 \times 0{,}091 \times 0{,}316^2 \times 100\,\%}{\sqrt{2} \times 11{,}5} = 0{,}005\,\text{dB}$$

The standard uncertainty of the mismatch between the 10 dB power attenuator and the power sensor:

$$u_{j\ mismatch:10dBatt.to\ power sensor} = \frac{0{,}130 \times 0{,}070 \times 0{,}500^2 \times 100\,\%}{\sqrt{2} \times 11{,}5} = 0{,}014\,\text{dB}$$

The standard uncertainty of the mismatch between the signal generator and 10 dB power attenuator:

$$u_{j\ mismatch:generator to 10dBatt.} = \frac{0{,}200 \times 0{,}130 \times 0{,}500^2 \times 0{,}966^2 \times 100\,\%}{\sqrt{2} \times 11{,}5} = 0{,}037\,\text{dB}$$

The standard uncertainty of the mismatch between the 6 dB attenuator (1) and 6 dB attenuator (2):

$$u_{j\ mismatch:6dBatt.1 to 6dBatt.2} = \frac{0{,}091 \times 0{,}091 \times 0{,}966^2 \times 0{,}316^2 \times 100\,\%}{\sqrt{2} \times 11{,}5} = 0{,}005\,\text{dB}$$

The standard uncertainty of the mismatch between the cable and power sensor:

$$u_{j\ mismatch:cable\ to\ power\ sensor} = \frac{0{,}091 \times 0{,}070 \times 0{,}316^2 \times 0{,}500^2 \times 100\,\%}{\sqrt{2} \times 11{,}5} = 0{,}001\,\text{dB}$$

The standard uncertainty of the mismatch between the signal generator and 6 dB attenuator (2):

$$u_{j\ mismatch:generator\ to\ 6dB\ Batt.2} = \frac{0{,}200 \times 0{,}091 \times 0{,}500^2 \times 0{,}966^2 \times 0{,}316^2 \times 100\,\%}{\sqrt{2} \times 11{,}5} = 0{,}003\,\text{dB}$$

The standard uncertainty of the mismatch between the 6 dB attenuator (1) and power sensor:

$$u_{j\ mismatch:6dB\ Batt.1\ to\ power\ sensor} = \frac{0{,}091 \times 0{,}070 \times 0{,}966^2 \times 0{,}316^2 \times 0{,}500^2 \times 100\,\%}{\sqrt{2} \times 11{,}5} = 0{,}001\,\text{dB}$$

The standard uncertainty of the mismatch between the signal generator and power sensor:

$$u_{j\ mismatch:generator\ to\ power\ sensor} = \frac{0{,}200 \times 0{,}070 \times 0{,}500^2 \times 0{,}966^2 \times 0{,}316^2 \times 0{,}500^2 \times 100\,\%}{\sqrt{2} \times 11{,}5} = 0{,}000\,\text{dB}$$

The combined mismatch uncertainty when measuring the power level when the cable and the 10 dB power attenuator is inserted is the RSS of all these components except $u_{j\ mismatch:\ generator\ to\ 6\ dB\ attenuator}$ and $u_{j\ mismatch:\ 6\ dB\ attenuator\ to\ power\ sensor:}$

$$u_{c\ mismatch:10dB\ and\ cable} = \sqrt{u^2_{j\ mismatch:6dB\ Batt.1\ to\ cable} + \ldots\ldots + u^2_{j\ mismatch:generator\ to\ power\ sensor}}$$

$$u_{c\ mismatch:10dB\ and\ cable} = \sqrt{0{,}051^2 + 0{,}073^2 + \ldots. + 0{,}001^2 + 0{,}000^2} = 0{,}142\,\text{dB}$$

The combined standard uncertainty of the mismatch when measuring the 10 dB attenuator and cable is:

$$u_{c\ mismatch:10dB\ and\ cable\ measurement} = \sqrt{u^2_{c\ mismatch:10dB\ Batt\ and\ cable} + u^2_{c\ mismatch:reference}}$$

$$u_{c\ mismatch:10dB\ and\ cable\ measurement} = \sqrt{0{,}142^2 + 0{,}059^2} = 0{,}154\,\text{dB}$$

The combined standard uncertainty of the mismatch $u_{c\ mismatch:\ 10\ dB\ and\ cable}$ is 0,154 dB.

NOTE: The result would have been the same if only the 6 dominant terms were taken into account. This illustrates that combinations of reflection coefficients separated by attenuations of 10 dB or more can normally be neglected. The exceptions may be in cases where one or both of the reflection coefficients involved are approaching 1,0 - which can be the case with filters or antennas outside their working frequencies.

6.4.4.3 The 20 dB attenuator

Figure 12 shows the section of the set-up which concerns this part of the calculation.

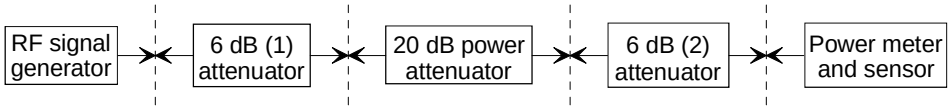

Figure 12: The 20 dB attenuator

In this part only terms separated by less than 10 dB are taken into account.

The individual uncertainties are calculated using formula 6.3:

The standard uncertainty of the mismatch between the signal generator and 6 dB attenuator (1):

$$u_{j\ mismatch:generatorto6dBatt.} = \frac{0{,}2 \times 0{,}091 \times 100\,\%}{\sqrt{2} \times 11{,}5} = 0{,}112\ \text{dB}$$

The standard uncertainty of the mismatch between the 6 dB attenuator (1) and 20 dB attenuator:

$$u_{j\ mismatch:6dBatt.1to20dBatt.} = \frac{0{,}091 \times 0{,}111 \times 100\,\%}{\sqrt{2} \times 11{,}5} = 0{,}062\ \text{dB}$$

The standard uncertainty of the mismatch between the 20 dB attenuator and 6 dB attenuator (2):

$$u_{j\ mismatch:20dBatt.to6dBatt.2} = \frac{0{,}111 \times 0{,}091 \times 100\,\%}{\sqrt{2} \times 11{,}5} = 0{,}062\ \text{dB}$$

The standard uncertainty of the mismatch between the 6 dB attenuator (2) and power sensor:

$$u_{j\ mismatch:6dBatt.to\ powersensor} = \frac{0{,}091 \times 0{,}07 \times 100\,\%}{\sqrt{2} \times 11{,}5} = 0{,}039\ \text{dB}$$

The standard uncertainty of the mismatch between the signal generator and 20 dB attenuator:

$$u_{j\ mismatch:generaorto20dBatt.} = \frac{0{,}200 \times 0{,}111 \times 0{,}500^2 \times 100\,\%}{\sqrt{2} \times 11{,}5} = 0{,}034\ \text{dB}$$

The standard uncertainty of the mismatch between the 20 dB attenuator and power sensor:

$$u_{j\ mismatch:20dBatt.to\ powersensor} = \frac{0{,}111 \times 0{,}070 \times 0{,}500^2 \times 100\,\%}{\sqrt{2} \times 11{,}5} = 0{,}012\ \text{dB}$$

The rest of the combinations are not taken into account because the insertion losses between them are so high, that the values are negligible:

- 6 dB attenuator (1) and 6 dB attenuator (2);
- signal generator and 6 dB attenuator (2);
- 6 dB attenuator (1) and measuring receiver;
- signal generator and measuring receiver.

The combined standard uncertainty of the mismatch when measuring the attenuation of the 20 dB attenuator is the RSS of these 4 individual standard uncertainty values.

$$u_{j\ mismatch:20dB} = \sqrt{0{,}062^2 + 0{,}062^2 + 0{,}034^2 + 0{,}012^2} = 0{,}095\ \text{dB}$$

The combined standard uncertainty of the mismatch involved in the 20 dB attenuator measurement is:

$$u_{c\ mismatch:20dBmeasurement} = \sqrt{u^2_{c\ mismatch:20dB} + u^2_{c\ mismatch:reference}}$$

$$u_{c\ mismatch:20dBmeasurement} = \sqrt{0{,}095^2 + 0{,}059^2} = 0{,}112\ \text{dB}$$

NOTE: If the two 6 dB attenuators had not been inserted, the result would have been 0,265 dB.

6.4.4.4 Instrumentation

Linearity of the measuring receiver is ±0,04 dB (from manufacturers data) as nothing is said about the distribution, a rectangular distribution in a logarithmic scale is assumed and the standard uncertainty is calculated:

$$u_{j\ receiverlinearity} = \frac{0{,}04}{\sqrt{3}} = 0{,}023\,\text{dB}$$

6.4.4.5 Power and temperature influences

Temperature influence: 0,0001 dB/degree (from manufacturers data), which is negligible, the power influence for the 10 dB attenuator is 0,0001 dB/dB × Watt (from manufacturers data) which gives 0,0001 × 25 × 10 = 0,025 dB as nothing is said about the distribution, a rectangular distribution in logs is assumed and the standard uncertainty is calculated:

$$u_{j\ powerinfluence10dB} = \frac{0{,}025}{\sqrt{3}} = 0{,}014\,\text{dB}$$

The power influence for the 20 dB attenuator is 0,001 dB/dB × Watt (from manufacturers data) which gives 0,001 × 2,5 × 20 = 0,05 dB as nothing is said about the distribution, a rectangular distribution in a logarithmic scale is assumed and the standard uncertainty is calculated:

$$u_{j\ powerinfluence20dB} = \frac{0{,}050}{\sqrt{3}} = 0{,}028\,\text{dB}$$

6.4.4.6 Collecting terms

10 dB attenuator and cabling network uncertainty:

$$u_{c\ 10dBattenuatorandcable} = \sqrt{u^2_{c\ mismatch} + u^2_{j\ receiverlinearity} + u^2_{j\ powerinfluence10dB}}$$

$$u_{c\ 10dBattenuatorandcable} = \sqrt{0{,}154^2 + 0{,}04^2 + 0{,}014^2} = 0{,}160\,\text{dB}$$

20 dB attenuator and cabling network uncertainty:

$$u_{c\ 20dBattenuator} = \sqrt{u^2_{c\ mismatch} + u^2_{j\ receiverlinearity} + u^2_{j\ powerinfluence20dB}}$$

$$u_{c\ 20dBattenuator} = \sqrt{0{,}112^2 + 0{,}04^2 + 0{,}028^2} = 0{,}122\,\text{dB}$$

The combined standard uncertainty of the attenuator and cabling network uncertainty:

$$u_{c\ attenuationandcabling} = \sqrt{u^2_{c\ 10dBattenuatorandcable} + u^2_{c\ 20dBattenuator}}$$

$$u_{c\ attenuationandcabling} = \sqrt{0{,}160^2 + 0{,}122^2} = 0{,}201\,\text{dB}$$

6.4.5 Mismatch during measurement

Standing wave ratios involved in the power measurement:

- EUT: ρ = 0,200;
- Power sensor: VSWR ≤ 1,15 ρ = 0,070;
- 10 dB power attenuator: VSWR ≤ 1,3 ρ = 0,130;
- 20 dB attenuator: VSWR ≤ 1,25 ρ = 0,111;

- Cable: VSWR ≤ 1,2 ρ = 0,091.

The mismatch uncertainties are calculated using formula 6.3 for the individual mismatch uncertainties between:

The standard uncertainty of the mismatch between the EUT and cable:

$$u_{j\ mismatch:EUT to cable} = \frac{0{,}200 \times 0{,}091 \times 100\ \%}{\sqrt{2} \times 11{,}5} = 0{,}112\ \text{dB}$$

The standard uncertainty of the mismatch between the cable and 10 dB power attenuator:

$$u_{j\ mismatch:cable to 10dBatt.} = \frac{0{,}091 \times 0{,}130 \times 100\ \%}{\sqrt{2} \times 11{,}5} = 0{,}073\ \text{dB}$$

The standard uncertainty of the mismatch between the 10 dB power attenuator and 20 dB attenuator:

$$u_{j\ mismatch:10dBatt.to 20dBatt.} = \frac{0{,}130 \times 0{,}111 \times 100\ \%}{\sqrt{2} \times 11{,}5} = 0{,}089\ \text{dB}$$

The standard uncertainty of the mismatch between the 20 dB attenuator and power sensor:

$$u_{j\ mismatch:20dBatt.to\ power\ sensor} = \frac{0{,}111 \times 0{,}070 \times 100\ \%}{\sqrt{2} \times 11{,}5} = 0{,}048\ \text{dB}$$

The standard uncertainty of the mismatch between the EUT and 10 dB power attenuator:

$$u_{j\ mismatch:EUT to 10dBatt.} = \frac{0{,}200 \times 0{,}130 \times 0{,}966^2 \times 100\ \%}{\sqrt{2} \times 11{,}5} = 0{,}149\ \text{dB}$$

The standard uncertainty of the mismatch between the cable and 20 dB attenuator:

$$u_{j\ mismatch:cable to 20dBatt.} = \frac{0{,}091 \times 0{,}111 \times 0{,}966^2 \times 0{,}316^2 \times 100\ \%}{\sqrt{2} \times 11{,}5} = 0{,}058\ \text{dB}$$

The standard uncertainty of the mismatch between the EUT and 20 dB attenuator:

$$u_{j\ mismatch:EUT to 20dBatt.} = \frac{0{,}200 \times 0{,}111 \times 0{,}966^2 \times 0{,}316^2 \times 100\ \%}{\sqrt{2} \times 11{,}5} = 0{,}013\ \text{dB}$$

The rest of the combinations:

- 10 dB attenuator to power sensor
- cable to power sensor
- EUT to power sensor

are neglected. The combined standard uncertainty of the mismatch during the measurement is the RSS of the individual components:

$$u_{c\ mismatch} = \sqrt{0{,}112^2 + 0{,}073^2 + 0{,}089^2 + 0{,}048^2 + 0{,}149^2 + 0{,}058^2 + 0{,}013^2} = 0{,}232\ \text{dB}$$

In the case where all contributions are considered as independent.

6.4.6 Influence quantities

The two influence quantities involved in the measurement are ambient temperature and supply voltage.

Temperature uncertainty: ±1,0 °C.

Supply voltage uncertainty: ±0,1 V.

Uncertainty caused by the temperature uncertainty: Dependency function (from TR 100 028 [11]): Mean value 4 %/°C and standard deviation: 1,2 %/°C.

Standard uncertainty of the power uncertainty caused by ambient temperature uncertainty (formula 5.2, see also clause D.4.2.1 of TR 100 028-2 [11]):

$$u_{j\ power\ /\ temperature} = \frac{1}{23{,}0}\sqrt{\frac{1{,}0^2}{3}\left(4{,}0^2 + 1{,}2^2\right)} = 0{,}105\,\text{dB}$$

Uncertainty caused by supply voltage uncertainty: Dependency function (from table F.1 of TR 100 028-2 [11]): Mean: 10 %/V and standard deviation: 3 %/V power, standard uncertainty of the power uncertainty caused by power supply voltage uncertainty (formula 5.2, see also clause D.4.2.1 of TR 100 028-2 [11]):

$$u_{j\ power/voltage} = \frac{1}{23{,}0}\sqrt{\frac{0{,}1^2}{3}\left(10^2 + 3^2\right)} = 0{,}026\,\text{dB}$$

$$u_{cinfluence} = \sqrt{u^2_{j\ power/temperature} + u^2_{j\ power/voltage}} = \sqrt{0{,}105^2 + 0{,}026^2} = 0{,}108\,\text{dB}$$

6.4.7 Random

The measurement was repeated 9 times. The following results were obtained (before correcting for cabling and attenuator network insertion loss):

21,8 mW; 22,8 mW; 23,0 mW; 22,5 mW; 22,1 mW; 22,7 mW; 21,7 mW; 22,3 mW; 22,7 mW

The two sums *X* and *Y* are calculated:

X = the sum of the measured values = 201,6 mW

Y = the sum of the squares of the measured values = 4 517,5 mW^2

$$u_{c\ random} = \sqrt{\frac{Y - \frac{X^2}{n}}{n-1}} = \sqrt{\frac{4517{,}5 - \frac{201{,}6^2}{9}}{9-1}} = 0{,}456\ \text{mW (formula 5.5)}$$

Mean value = 22,4 mW

As the result is obtained as the mean value of 9 measurements the standard uncertainty (converted to dB by division with 23,0) of the random uncertainty is:

$$u_{c\ random} = \frac{0{,}456}{22{,}4} \times \frac{100}{23{,}0} = 0{,}089\,\text{dB}$$

NOTE: It is important to identify whether this value (the random uncertainty) corresponds to the effect of other uncertainties already taken into account in the calculations (e.g. uncertainties due to the instrumentation) or whether this is a genuine contribution of randomness. Obviously there are uncertainties in all measurements, so it has to be expected that performing the same measurement a number of times may provide a set of different results. When a contribution due to randomness has to be taken into account, then the method of evaluating the random uncertainty component provided in the present clause is to be used. Care should be taken to ensure the measurement conditions are kept constant, as far as possible, through out the repetition of the measurements.

6.4.8 Expanded uncertainty

The combined standard uncertainty for the carrier power measurement is the RSS of all the calculated part standard uncertainties:

$$u_{ccarrier\,power} = \sqrt{u^2_{c\,meter\,and\,sensor} + u^2_{c\,attenuation\,and\,cabling} + u^2_{c\,mismatch} + u^2_{c\,in\,fluence} + u^2_{c\,random}}$$

$$u_{ccarrier\,power} = \sqrt{0{,}066^2 + 0{,}201^2 + 0{,}232^2 + 0{,}108^2 + 0{,}089^2} = 0{,}344\,\text{dB}$$

Assuming a Normal distribution, the expanded uncertainty is ±1,96 × 0,344 dB = ±0,67 dB at a 95 % confidence level (this is further discussed in clause D.5.6 of TR 100 028-2 [11]).

The dominant part of this expanded uncertainty is mismatch uncertainty. In the calculations all the mismatch uncertainties were based on manufacturers data, which are normally very conservative. The relevant reflection coefficients could be measured by means of a network analyser or reflection bridge. This would probably give lower reflection coefficients thereby reducing the overall uncertainty.

NOTE: In the case where these coefficients are measured a number of times, under conditions where it can be considered that the measurements are independent, then the comments found in clauses 5.3.1 and 6.4.7 may be relevant.

6.5 Uncertainty calculation for measurement of a receiver (third order intermodulation)

Before starting we need to know the architecture and the corresponding noise behaviour of the receiver.

6.5.1 Noise behaviour in different receiver configurations

The effect of noise on radio receivers is very dependant on the actual design. A radio receiver has (generally) a front end and demodulation stages according to one of the possibilities presented in figure 13. This simplified diagram (for AM and FM/PM systems) illustrates several possible routes from the front end to the "usable output".

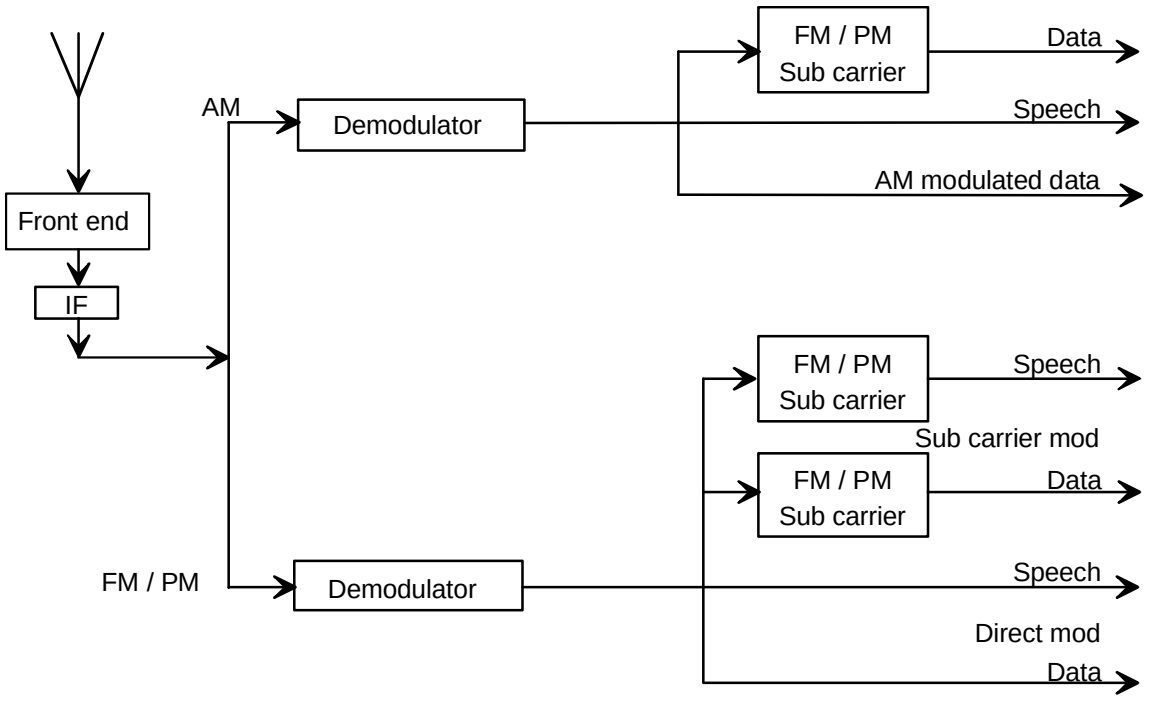

Figure 13: Possible receiver configurations

The Amplitude Modulation route involves a 1:1 conversion after the front end and the amplitude demodulation information is available immediately (analogue) or undergoes data demodulation.

The frequency modulation / phase modulation route introduces an enhancement to the noise behaviour in non-linear (e.g. FM/PM) systems compared to linear (e.g. AM) systems, see figure 14, until a certain threshold or lower limit (referred to as the knee-point) is reached. Below this knee-point the demodulator output signal to noise ratio degrades more rapidly for non-linear systems than the linear system for an equivalent degradation of the carrier to noise ratio, this gives rise to two values for the slope: one value for C/N ratios above the knee and one value for C/N ratios below the knee.

A similar difference will occur in data reception between systems which utilize AM and FM/PM data. Therefore "Noise Gradient" corresponds to several entries in TR 100 028 [11], in particular table F.1 of TR 100 028-2 [11].

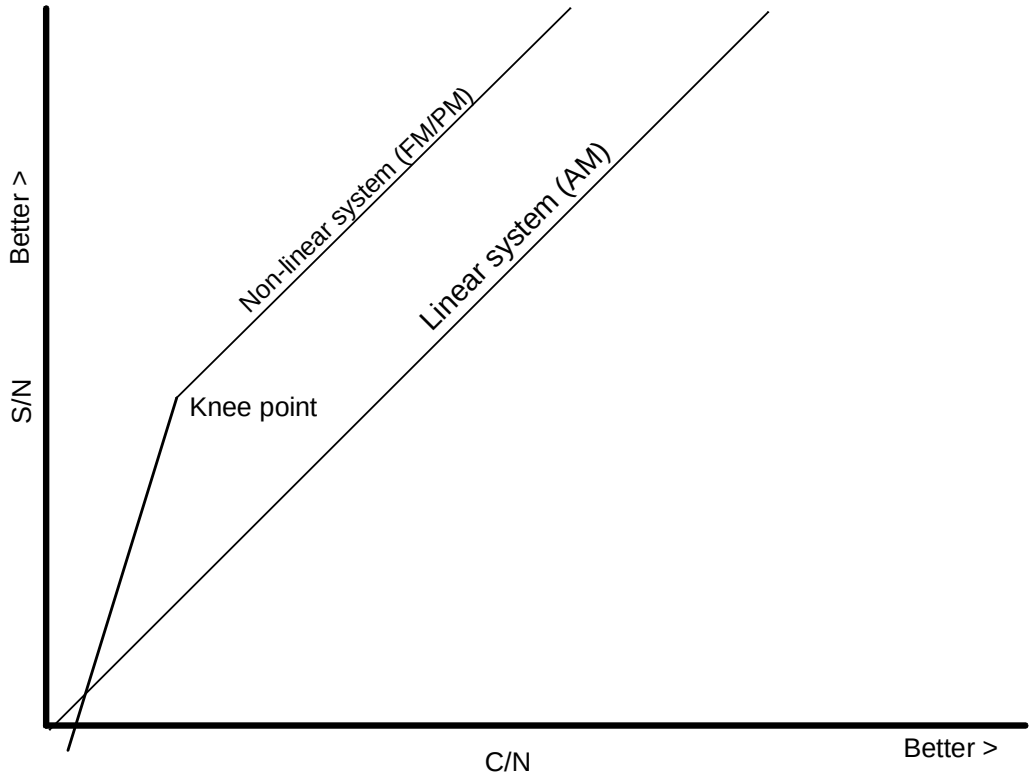

Figure 14: Noise behaviour in receivers

6.5.2 Sensitivity measurement

The sensitivity of a receiver is usually measured as the input RF signal level which produces a specific output performance which is a function of the base band signal-to-noise ratio in the receiver.

This is done by adjusting the RF level of the input signal at the RF input of the receiver.

What is actually done is that the RF signal-to-noise ratio at the input of the receiver is adjusted to produce a specified signal-to-noise ratio dependant behaviour at the output of the receiver, i.e. SINAD, BER, or message acceptance.

An error in the measurement of the output performance will cause a misadjustment of the RF level and thereby the result.

In other words any uncertainty in the output performance is converted to signal-to-noise ratio uncertainty at the input of the receiver. As the noise does not change it causes an uncertainty in the adjusted level.

For an analogue receiver, the dependency function to transform the SINAD uncertainty to the RF input level uncertainty is the slope of the noise function described above in clause 6.5.1 and depends on the type of carrier modulation.

The dependency function involved when measuring the sensitivity of an FM/PM receiver is the noise behaviour usually below the knee-point for a non-linear system, in particular in the case of data equipment. This function also affects the uncertainty when measuring sensitivity of an FM/PM based data equipment.

This dependency function has been empirically derived at *0,375* dB $_{RF\ i/p\ level}$ / dB $_{SINAD}$ associated with a standard uncertainty of 0,075 dB $_{RF\ i/p\ level}$ / dB $_{SINAD}$ and is one of the values stated in table F.1 of TR 100 028-2 [11].

If the receiver is for data the output performance is a specified BER. BER measurements are covered by clause 6.6.

In some standards the sensitivity is measured as the output performance at a specified input level. In this case the dependency functions converting input level uncertainty to output performance uncertainty are the inverse of the functions previously described.

6.5.3 Interference immunity measurements

Interference immunity (i.e. co-channel rejection, adjacent channel rejection) is measured by adjusting the RF level of the wanted signal to a specified value. Then the RF level of the interfering signal is adjusted to produce a specified performance at the output of the receiver.

The interfering signal is normally modulated. Therefore for measurement uncertainty purposes it can be regarded as white noise in the receiving channel.

The uncertainty analysis is therefore covered by clause 6.5.2.

6.5.4 Blocking and spurious response measurements

These measurements are similar to interference immunity measurements except that the unwanted signal is without modulation.

Even though the unwanted signal (or the derived signal in the receive channel caused by the unwanted signal) cannot in every case be regarded as white noise, the present document does not distinguish. The same dependency functions are used.

6.5.5 Third order intermodulation

When two unwanted signals *X* and *Y* occur at frequency distance *d(X)* and *2d(Y)* from the receiving channel a disturbing signal *Z* is generated in the receiving channel due to non linearities in filters, amplifiers and mixers.

The physical mechanism behind the intermodulation is the third order component of the non-linearity of the receiver: $K \times X^3$.

When two signals - *X* and *Y* - are subject to that function, the resulting function will be:

$$K(X + Y)^3 = K(X^3 + Y^3 + 3X^2Y\ 3XY^2)$$

where the component $Z = 3X^2Y$ is the disturbing intermodulation product in the receiving channel.

If *X* is a signal $I_x\ sin(2\pi(f_o+d)t)$ and *Y* is a signal $I_y\ sin(2\pi(f_o+2d)t)$, the component

$$Z = K \times 3X^2Y$$

will generate a signal having the frequency f_o and the amplitude $K \times 3I_x^2I_y$.

(A similar signal $Z' = 3XY^2$ is generated on the other side of the two signals *X* and *Y*, as shown in figure 15).

The predominant function is a third order function:

$$I_z = I_c + 2I_x + I_y \qquad (6.4)$$

where l_z is the level of the intermodulation product *Z*, I_c is a constant, I_x and I_y are the levels of *X* and *Y*. All terms are logarithmic.

6.5.5.1 Measurement of third order intermodulation

The measurement is normally carried out as follows:

Three signal generators are connected to the input of the EUT.

Generator 1 is adjusted to a specified level at the receiving frequency f_o (the wanted signal W).

Generator 2 is adjusted to frequency $f_o + \delta$ (unwanted signal *X*) and generator 3 is adjusted to frequency $f_o + 2\delta$ (unwanted signal *Y*). The level of *X* and *Y* (I_x and I_y) are maintained equal during the measurement.

I_x and I_y are increased to level *A* which causes a specified degradation of AF output signal (SINAD) or a specific bit error ratio (BER) or a specific acceptance ratio for messages.

Both the SINAD, BER and message acceptance ratio are a function of the signal-to-noise ratio in the receiving channel.

The level of the wanted signal *W* is A_w (see figure 15). The measured result is the difference between the level of the wanted signal A_w and the level of the two unwanted signals *A*. This is the ideal measurement.

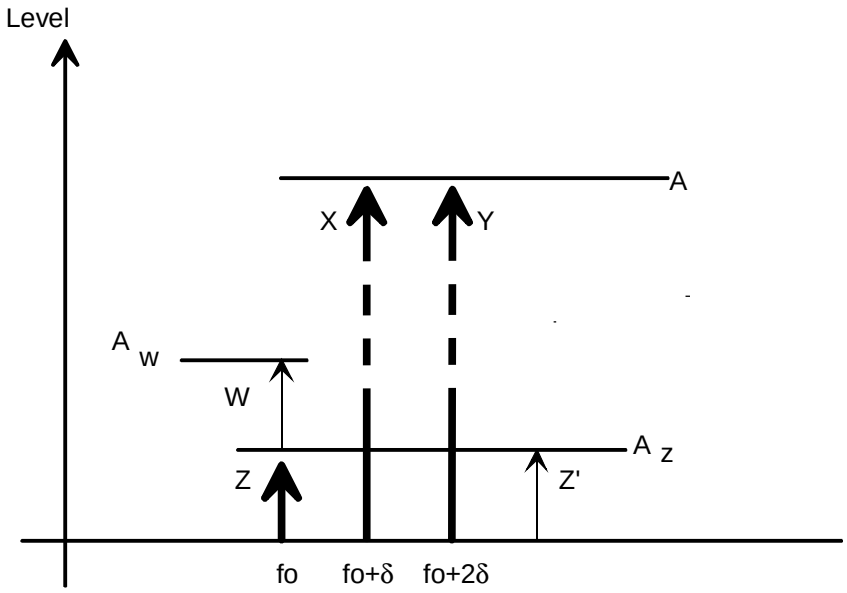

Figure 15: Third order intermodulation components

When looked upon in logarithmic terms a level change δI_x dB in *X* will cause a level change of $2 \times \delta I_x$ dB in *Z*, and a level change δI_y dB in *Y* will cause the same level change δI_z dB in *Z*.

If the levels of both *X* and *Y* are changed by δI dB, the resulting level change of *Z* is $3 \times \delta I$ dB.

Since *X* is subject to a second order function, any modulation on *X* will be transferred with double uncertainty to *Z* (see also clauses D.3.2, D.3.4 and D.5 of TR 100 028-2 [11]), whereas the deviation of any modulation on *Y* will be transferred unchanged to *Z*.

Therefore, as *Y* is modulated in the measurement, the resulting modulation of *Z* will be the same as with *Y*.

6.5.5.2 Uncertainties involved in the measurement

The predominant uncertainty sources related to the measurement are the uncertainty of the levels of the applied RF signals and uncertainty of the degradation (the SINAD, BER, or message acceptance measurement). The problems about the degradation uncertainty are exactly the same as those involved in the co-channel rejection measurement if the intermodulation product Z in the receiving channel is looked upon as the unwanted signal in this measurement. Therefore the noise dependency is the same, but due to the third order function the influence on the total uncertainty is reduced by a factor of 3 (see also clauses D.3.2 and D.5 of TR 100 028-2 [11]).

It is in the following assumed that the distance to the receiver noise floor is so big that the inherent receiver noise can be disregarded.

6.5.5.2.1 Signal level uncertainty of the two unwanted signals

A is the assumed level of the two unwanted signals (the indication of the two unwanted signal generators corrected for matching network attenuations).

A_x is the true level of *X* and A_y is the true level of *Y*. (A_x is $A + \delta x$ and A_y is $A + \delta y$) see figure 16.

A_z is the level of *Z* (the same as in the ideal measurement).

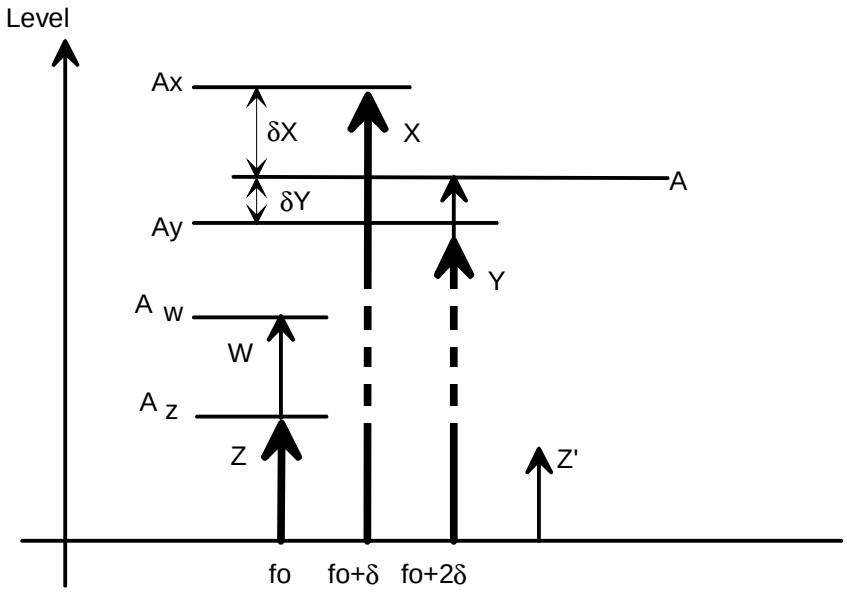

Figure 16: Level uncertainty of two unwanted signals

If A_x and A_y were known the correct measuring result would be obtained by adjusting the two unwanted signals to the level A_t (true value) which still caused the level A_z of *Z*.

If there is an error δx of the level of signal *X*, the error of the level of the intermodulation product will be $2 \times \delta x$ (see also clauses D.3.2 and D.5 of TR 100 028-2 [11]); to obtain the wanted signal-to-noise ratio the two unwanted levels are reduced by $2 \times \delta x/3$.

In other words the dependency function of generator *X* is 2/3.

In the same way if there is an error δy of the level of signal *Y*, the error of the level of the intermodulation product will be δy; to obtain the wanted signal-to-noise ratio the two unwanted signals are be reduced by $\delta y/3$.

In other words the dependency function of generator *Y* is 1/3.

When looking at the problem in linear terms, the dependency functions are valid for small values of δx and δy due to the fact that the higher order components of the third order function can be neglected.

δx and δy are the relative RF level uncertainties at the input of the EUT. They are combinations of signal generator level uncertainty, matching network attenuation uncertainty and mismatch uncertainties at the inputs and the output of the matching network.

The standard uncertainties of the levels of *X* and *Y* are $u_{j\,x}$ and $u_{j\,y}$.

The standard uncertainty $u_{j\ unwanted\ signals}$ related to the uncertainty caused by level uncertainty of the two unwanted signals is thus:

$$u_{j\ unwanted signals} = \sqrt{\left(\frac{2}{3}u_{j\,x}\right)^2 + \left(\frac{1}{3}u_{j\,y}\right)^2} \qquad (6.5)$$

6.5.5.2.2 Signal level uncertainty of the wanted signal

Under the assumption that equal change of both the level of the wanted signal and the intermodulation product will cause no change of the SINAD, (or the BER, or the message acceptance) the error contribution from the uncertainty of the level of the wanted signal can be calculated.

If there is an error δ_w on the wanted signal, the two unwanted signal levels are be adjusted by $1/3 \times \delta_w$ to obtain the wanted signal-to-noise ratio. The dependency function of generator *W* is therefore 1/3 and assuming the same types of uncertainties as previously the standard uncertainty, $u_{j\ wanted\ signal}$, is (see also clause D.3.2.3 of TR 100 028-2 [11]):

$$u_{j\ wanted signal} = \left(\frac{1}{3}u_{j\ unwanted signals}\right) \qquad (6.6)$$

6.5.5.3 Analogue speech (SINAD) measurement uncertainty

Sensitivity is normally stated as an RF input level in conducted measurements.

For analogue systems this is stated as at a specified SINAD value.

For an analogue receiver, the dependency function to transform the SINAD uncertainty to the RF input level uncertainty is the slope of the noise function described above in clause 6.5.1 and depends on the type of carrier modulation.

The dependency function involved when measuring the sensitivity of an FM/PM receiver is the noise behaviour usually below the knee-point for a non-linear system, in particular in the case of data equipment. This function also affects the uncertainty when measuring sensitivity of an FM/PM based data equipment.

This dependency function has been empirically derived at *0,375* dB $_{RF\ i/p\ level}$ / dB $_{SINAD}$ associated with a standard uncertainty of 0,075 dB $_{RF\ i/p\ level}$ / dB $_{SINAD}$ and is one of the values stated in table F.1 of TR 100 028-2 [11].

The SINAD measurement uncertainty also contributes to the total measurement uncertainty.

If the receiver is working beyond the demodulator knee point any SINAD uncertainty corresponds to an equal uncertainty (in dB) of the signal-to-noise ratio.

If the receiver is working below the knee point the corresponding uncertainty of the signal-to-noise ratio will be in the order of 1/3 times the SINAD uncertainty (according to TR 100 028 [11]).

Any signal-to-noise ratio uncertainty causes 1/3 times that uncertainty in the combined uncertainty: the unwanted signal levels should be adjusted by 1/3 of the signal-to-noise ratio error to obtain the correct value.

Therefore if the receiver is working above the knee point the SINAD dependency function is 1/3, and if the receiver is working below the knee point the dependency function is in the order of 1/9.

6.5.5.4 BER and message acceptance measurement uncertainty

Any BER (or message acceptance) uncertainty will influence the total uncertainty by the inverse of the slope of the appropriate BER function at the actual signal-to-noise ratio.

As the BER function is very steep, the resulting dependency function is small, and it is sufficient to use the differential coefficient as an approximation.

If the signalling is on a subcarrier, the relation between the signal-to-noise ratio of the subcarrier should be dealt with in the same way as with other receiver measurements. See clause 6.6.3.

6.5.5.5 Other methods of measuring third order intermodulation

Some test specifications specify other methods of measuring the intermodulation rejection:

The measured result is the SINAD, BER, or message acceptance at **fixed** test signal levels. This is the case with some digital communication equipment like DECT and GSM.

In these measurements the uncertainty should be calculated in 3 steps:

1) the uncertainty of the resulting signal-to-noise ratio is calculated;
2) this uncertainty is then applied to the appropriate SINAD, BER, or message acceptance function;
3) and then combined with the measurement uncertainty of the SINAD, BER, or message acceptance measurement.

The uncertainty of the signal-to-noise ratio due to uncertainty of the level of the test signals is:

$$u_{j\,SNR} = \sqrt{(2u_{j\,x})^2 + u_{j\,y}{}^2 + u_{j\,w}^2}$$

This uncertainty is then transformed to the measured parameter.

If the measured value is a SINAD value and the receiver is working beyond the knee point the SINAD uncertainty is identical, but if the receiver is working below the knee point the dependency function is in the order of 3,0.

If the measurand is a BER or a message acceptance, the dependency function is too non linear to be regarded as a first order function.

The total uncertainty should then be calculated as described in clause 6.6.4.3.

6.6 Uncertainty in measuring continuous bit streams

6.6.1 General

If an EUT is equipped with data facilities, the characteristic used to assess its performance is the Bit Error Ratio (BER).

The BER is the ratio of the number of bits in error to the total number of bits in a received signal and is a good measure of receiver performance in digital radio systems just as SINAD is a good measure of receiver performance in analogue radios. BER measurements, therefore, are used in a very similar way to SINAD measurements, particularly in sensitivity and immunity measurements.

6.6.2 Statistics involved in the measurement

Data transmissions depend upon a received bit actually being that which was transmitted. As the level of the received signal approaches the noise floor (and therefore the signal to noise ratio decreases), the probability of bit errors (and the BER) increases.

The first assumption for this statistical analysis of BER measurements is that each bit received (with or without error) is independent of all other bits received. This is a reasonable assumption for measurements on radio equipment, using binary modulation, when measurements are carried out in steady state conditions. If, for instance, fading is introduced, it is not a reasonable assumption.

The measurement of BER is normally carried out by comparing the received data with that which was actually transmitted. The statistics involved in this measurement can be studied using the following population of stones: one black and (1/BER)-1 white stones. If a stone is taken randomly from this population, its colour recorded and the stone replaced *N* times, the black stone ratio can be defined as the number of occurrences of black stones divided by *N*. This is equivalent to measuring BER.

The statistical distribution for this measurement is the binomial distribution. This is valid for discrete events and gives the probability that *x* samples out of the *N* stones sampled are black stones (or *x* bits out of *N* received bits are in error) given the BER:

$$P_{(x)} = \frac{N!}{x!(N-x)!} \times BER^{x} (1 - BER)^{N-x} \quad (6.7)$$

The mean value of this distribution is $BER \times N$ and the standard deviation is:

$$\sqrt{BER \times (1 - BER)} \times \sqrt{N} \quad (6.8)$$

and for large values of *N* the shape of the distribution approximates a Gaussian distribution.

Normalizing the mean value and standard uncertainty (by dividing by *N*) gives:

$$Mean\ value = BER \quad (6.9)$$

$$u_{jBER} = \sqrt{\frac{BER(1 - BER)}{N}} \quad (6.10)$$

From these two formulas it is easy to see that the larger number of bits, the smaller the random uncertainty, and the relation between number of bits and uncertainty is the same as for random uncertainty in general. By means of formula 6.10 it is possible to calculate the number of bits needed to be within a specific uncertainty.

EXAMPLE: A BER in the region of 0,01 is to be measured.

a) If the standard uncertainty, due to the random behaviour discussed above, is to be 0,001, then the number of bits to be compared, *N*, in order to fulfil this demand is calculated from the rearranged formula (6.10):

$$N = \frac{BER(1 - BER)}{u_{jBER}^{2}} = \frac{0{,}01 \times 0{,}99}{0{,}001^{2}} = 9900$$

b) If the number of bits compared, *N*, is defined, e.g. 2 500 then the standard uncertainty is given directly by formula (6.10):

$$u_{jBER} = \sqrt{\frac{0{,}01(1 - 0{,}01)}{2500}} = 0{,}002$$

As stated earlier the binomial distribution can be approximated by a Normal distribution. This is not true when the BER is so small that only a few bit errors (<10) are detected within a number of bits. In this case the binomial distribution is skewed as the p (BER < 0) = 0.

Another problem that occurs when only few bit errors are detected, and the statistical uncertainty is the dominant uncertainty (which does not happen in PMR measurements, but it does, due to the method, occur in DECT and GSM tests) is that the distribution of the true value about the measured value can be significantly different from an assumed Normal distribution.

6.6.3 Calculation of uncertainty limits when the distribution characterizing the combined standard uncertainty cannot be assumed to be a Normal distribution

In the calculations of uncertainty there is usually no distinction between the distribution of a measured value about the true value, and the distribution of the true value about a measured value. The assumption is that they are identical.

This is true in the cases where the standard uncertainty for the distribution of the measured value about the true value is independent of the true value - which usually is the case. But if the standard uncertainty is a function of the true value of the measurand (**not** the measured value), the resulting distribution of the measurement uncertainty will not be a Normal distribution even if the measured value about the true value is.

This is illustrated by the following (exaggerated) example:

A DC voltage is to be measured. We assume that there is only one uncertainty contribution which comes from the voltmeter used for the measurement.

In the manufacturers data sheet for the voltmeter it is stated that the measured value is within ±25 % of the true value.

If the true value is 1,00 V then the measured value lies between 0,75 V and 1,25 V. However, if the measured value is 0,75 V and the true value is still 1,0 V corresponding to 1,333 3 times the measured value. Similarly, If the measured value is 1,25 V and the true value is still 1,0 V this corresponds to 0,8 times the measured value.

Therefore the limits are asymmetric for the true value about the measured value (-20 % and +33,33 %).

When looking at the standard deviations, the error introduced is small. In the previous example the standard deviation of the measured value about the true value is 14,43 %. The standard deviation of the related true value about the measured value is 15,36 %. As the difference is small, and the distribution of the measured value about the true value is based on an assumption anyway, the present document suggests that it can be used directly.

NOTE: The average value, however, is no longer zero, but in this case is approximately 4,4 %.

Alternatively, also in this example, x_t is the true value and x_m is the measured value. Any parameter printed in square brackets, e.g. $[x_m]$, is considered to be constant.

The distribution of the measured value x_m about the true value x_t is given by the function $p(x_m, [x_t])$.

Based on this function the distribution $p1(x_t, [x_m])$ of the true value x_t about the measured value x_m can be derived.

The intermediate function is $p(x_t, [x_m])$ which is the same as the previous; the only difference being that x_t is the variable and x_m is held constant. This function is not a probability distribution as the integral from $-\infty$ to $+\infty$ is not unity. To be converted to the probability function $p1(x_t, [x_m])$ it should be normalized.

Therefore:

$$p1(x_t,[x_m]) = \frac{p(x_t,[x_m])}{\int_{-\infty}^{\infty} p(x,[x_m])dx} \qquad (6.11)$$

As this distribution is not Normal, the uncertainty limits need to be found by other means than by multiplication with a coverage factor from Student's t-distribution. How the actual limits are calculated in practise depends on the actual distribution.

An example: If the true BER of a radio is 5×10^{-6} and the BER is measured over 10^6 bits, the probability of detecting 0 bits is 0,674 %. On the other hand if the BER in a measurement is measured as 5×10^{-6} the true value cannot be 0.

If the uncertainty calculations are based on the assumption of a Gaussian distribution, the lower uncertainty limit becomes negative (which of course does not reflect reality, and provides evidence that not all distributions are Normal):

The standard uncertainty based on the measured value $3{,}0 \times 10^{-6}$:

$$u_j = \sqrt{\frac{3{,}0\times10^{-6}\left(1-3{,}0\times10^{-6}\right)}{10^6}} = 1{,}73\times10^{-6}$$

The expanded uncertainty is $\pm 1{,}96 \times 1{,}73 \times 10^{-6} = \pm 3{,}39 \times 10^{-6}$ at a 95 % confidence level.

The correct distribution $p1(x_t)$ is the continuous function in figure 17.

NOTE: The true value is not BER, but number of bit errors, where BER= (bit errors/number of bits tested). The binomial function $p(x_m)$ based on the true value = 3 bit errors (corresponding to BER = 3×10^{-6}) is the discrete function shown.

The distribution p (x_t) (based on the binomial distribution with 3 bit errors and 10^6 bits tested):

$$p(x_t) = 100 \times k \times \left(\frac{x_t}{10^6}\right)^3 \times \left(1 - \frac{x_t}{10^6}\right)^{\left(10^6 - 3\right)} \%$$

where $k = \frac{10^6!}{3! \times \left(10^6 - 3\right)!} = 1{,}67 \times 10^{17}$

The integral from - ∞ to + ∞ of p (x_t) is very close to 1. Therefore p (x_t) is a good approximation to the correct distribution p1 (x_t).

By means of numerical methods the 95 % error limits are found to be +5,73 and -1,91 corresponding to +5,73 $\times 10^{-6}$ and -1,91 $\times 10^{-6}$.

Figure 17 shows the discrete distribution giving the probabilities of measuring from 0 to 14 bit errors when the true value is 3 bit errors corresponding to BER = 3×10^{-6}, and the continuous distribution giving the probability function for the true value when the measured value is 3 bit errors corresponding to BER = 3×10^{-6}.

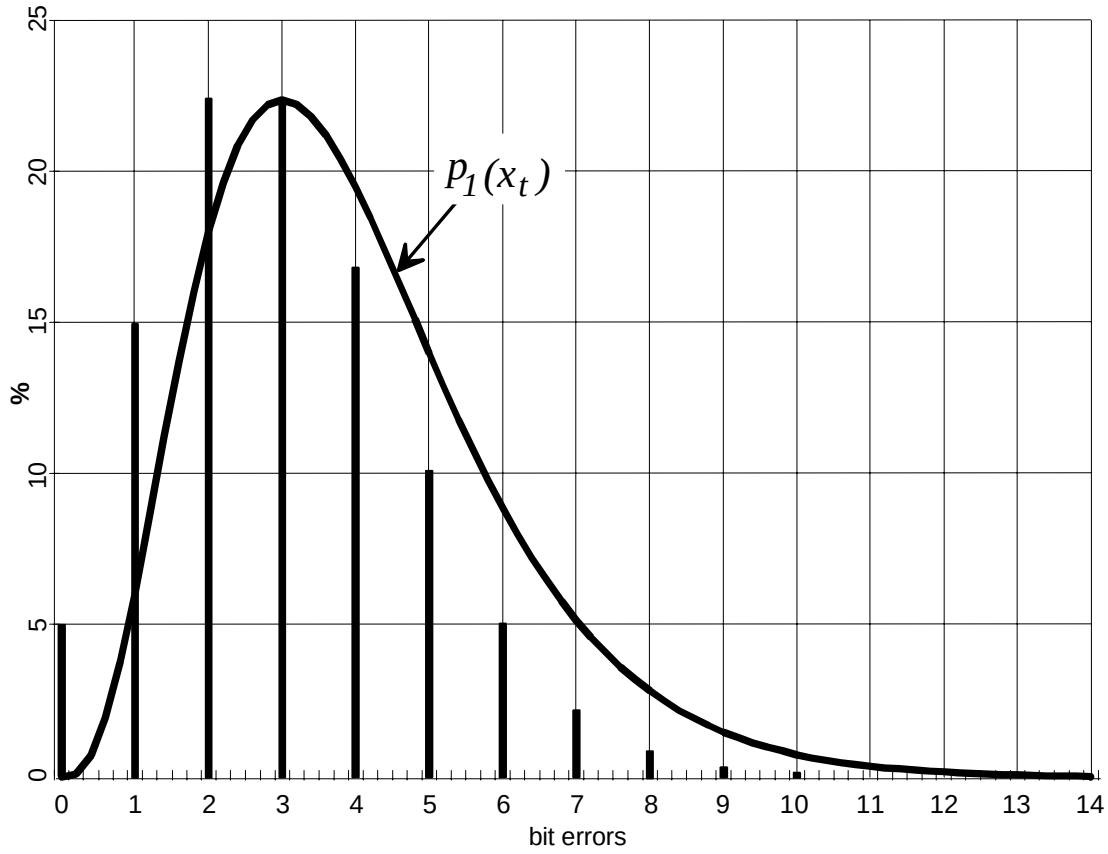

Figure 17: BER uncertainty

6.6.4 BER dependency functions

As in SINAD measurements, the BER of a receiver is a function of the signal to noise ratio of the RF signal at the input of the receiver.

Several modulation and demodulation techniques are used in data communication and the dependency functions are related to these techniques.

This clause covers the following types of modulation:

- coherent modulation/demodulation of the RF signal;

- non coherent modulation/demodulation of the RF signal;
- FM modulation.

The following assumes throughout that the data modulation uncertainty combines linearly to the carrier to noise ratio uncertainty. The uncertainty calculations are based on ideal receivers and demodulators where correctly matched filters are utilized.

The characteristics of practical implementations may differ from the theoretical models thereby having BER dependency functions which are different from the theoretical ones. The actual dependency functions can, of course, be estimated individually for each implementation. This, however, would mean additional measurements. Instead the theoretically deduced dependency functions may be used in uncertainty calculations.

6.6.4.1 Coherent data communications

Coherent demodulation techniques are techniques which use absolute phase as part of the information. Therefore the receiver has to be able to retrieve the absolute phase from the received signal. This involves very stable oscillators and sophisticated demodulation circuitry, but there is a gain in performance under noise conditions compared to non coherent data communication. Coherent demodulation is used, for example, in the GSM system with Gaussian Minimum Shift Keying (GMSK).

6.6.4.2 Coherent data communications (direct modulation)

The BER as a function of SNR_b, the signal to noise ratio per bit for coherent binary systems is:

$$\text{BER}\,(\text{SNR}_\text{b}) = 0{,}5 \times \text{erfc}\,(\sqrt{\text{SNR}_\text{b}}) \tag{6.12}$$

where *erfc (x)* is defined as:

$$erfc(x)=\frac{2}{\sqrt{\pi}}\int_{x}^{\infty} e^{-t^2}\,dt \tag{6.13}$$

It is not possible to calculate the integral part of formula (6.11) analytically, but the BER as a function of the signal to noise ratio is shown in figure 18 together with the function for non coherent binary data communication.

There are different types of coherent modulation and the noise dependency of each varies, but the shape of the function remains the same. The slope, however, is easily calculated and, although it is negative, the sign has no meaning for the following uncertainty calculations:

$$\frac{d(BER)}{d(SNR_b)} = \frac{1}{2\sqrt{\pi \times SNR_b}} \times e^{-SNR_b} \tag{6.14}$$

For the purpose of calculating the measurement uncertainty, this can be approximated:

$$\frac{d(BER)}{d(SNR_b)} \approx 1{,}2 \times BER \tag{6.15}$$

If the aim is to transform BER uncertainty to level uncertainty - which is the most likely case in PMR measurements, the inverse dependency function will be used (the result is in percentage power terms as it is normalized by division with SNR_{b*}):

$$u_{\,j\ level\,due\,to\,BER\,uncertainty} = \left[\frac{u_{\,jBER}}{\frac{d(BER)}{d(SNR_b)} \times SNR_{b*}}\right] 100\,\% \approx \frac{u_{\,jBER}}{1{,}2 \times BER \times SNR_{b*}} \times 100\,\% \tag{6.16}$$

The SNR_b* is a theoretical signal to noise ratio read from figure 19. It may not be the signal to noise ratio at the input of the receiver but the slope of the function is assumed to be correct for the BER measured.

For example: The sensitivity of a receiver is measured. The RF input level to the receiver is adjusted to obtain a BER of 10^{-2}. The measured result is the RF level giving this BER. The BER is measured over a series of 25 000 bits. The resulting BER uncertainty is then calculated using formula (6.10):

$$u_{j\,BER} = \sqrt{\frac{0{,}01(1-0{,}01)}{25000}} = 6{,}29\times10^{-4}$$

The uncertainty of the RF signal at the input is 0,7 dB (u_j). The signal to noise ratio giving this BER is then read from figure 18: SNR_b*(0,01) = 2,7 and the dependency function at this level is:

$$\frac{d(BER(2{,}7))}{d(SNR_b)} = 1{,}2\times BER = 1{,}2\times1\times10^{-2} = 1{,}2\times10^{-2}$$

The BER uncertainty is then transformed to level uncertainty using formula (6.16):

$$u_{j\,level} = \left[\frac{6{,}29\times10^{-4}}{1{,}2\times10^{-2}\times2{,}7}\right]\times100\,\% = 1{,}95\,\%\ \text{power} \approx \frac{1{,}95}{23{,}0}\,\text{dB} = 0{,}085\,\text{dB}$$

$$u_{j\,RF\,level} = \sqrt{0{,}7^2 + 0{,}085^2 + ...}$$

There is an additional uncertainty component due to resolution of the readout of the measured BER. If the RF input level has been adjusted to give a reading of 0,01 and the resolution of the BER meter is 0,001 the correct lies between 0,0095 and 0,0105 with equal probability.

The standard deviation is therefore:

$$u_{j\,BER\,resolution} = \frac{0{,}5\times10^{-3}}{\sqrt{3}} = 2{,}89\times10^{-4}$$

This standard deviation is then by means of formula 6.16 converted to level uncertainty:

$$u_{j\,level\,due\,to\,BER\,resolution} = \frac{u_{j\,BER\,resolution}}{\frac{d(BER)}{d(SNR_b)}\times SNR_b}\times100\%$$

$$u_{j\,level\,due\,to\,BER\,resolution} = \frac{0{,}289\times10^{-4}}{1{,}2\times0{,}01\times2{,}7}\times100\% = 0{,}089\% \approx \frac{0{,}089}{23{,}0}\,dB = 0{,}004dB$$

The total uncertainty of the sensitivity level is then:

$$u_{c\,RF\,level} = \sqrt{u^2_{j\,level}u^2_{j\,level\,due\,to\,BER\,resolution} + u^2_j} = \sqrt{0{,}085^2 + 0{,}004^2 + 0{,}7^2} = 0{,}71\text{dB}$$

As can be seen the BER statistical uncertainty and the BER resolution only plays a minor role.

6.6.4.3 Coherent data communications (subcarrier modulation)

If a subcarrier frequency modulation is used in the data communication the functions related to direct coherent data communication apply, but in this case they give the relationship between BER and the signal to noise of the subcarrier. To be able to transform BER uncertainty to RF input level uncertainty the relationship between the subcarrier signal to noise ratio and the RF carrier signal to noise ratio need to be calculated.

If the BER is measured at a RF level much higher than the sensitivity this relation is assumed to be 1:1 as described in clause 6.5.

In FM systems, if the BER is measured in the sensitivity region (below the knee point) the relationship as for analogue receivers is assumed and the same value taken from table F.1 of TR 100 028-2 [11]: *0,375* dB $_{RF\ i/p\ level}$/dB $_{SINAD}$ and standard uncertainty 0,075 dB $_{RF\ i/p\ level}$/dB $_{SINAD}$ (see clause 6.5).

EXAMPLE: The sensitivity of an FM receiver is measured. The RF input level to the receiver is adjusted to obtain a BER of 10^{-2}. The measured result is the RF level giving this BER. The BER is measured over a series of 2 500 bits. The uncertainty of the RF signal at the input is 0,5 dB (u_j).

The resulting BER uncertainty is then calculated using formula (6.10):

$$u_{j\,BER} = \sqrt{\frac{0{,}01(1-0{,}01)}{2500}} = 2{,}0\times10^{-3}$$

The signal to noise ratio giving this BER is then read from figure 18: SNR_b*(0,01) = 2,7. The dependency function at this level is:

$$\frac{d(BER(2{,}7))}{d(SNR_b)} = 1{,}2\times BER = 1{,}2\times1{,}0\times10^{-2} = 1{,}2\times10^{-2}$$

The BER uncertainty is then transformed to level (or SNR_b) uncertainty using formula (6.16):

$u_{j\,SNR_b} = \left[\frac{2{,}0\times10^{-3}}{1{,}2\times10^{-2}\times2{,}7}\right]\times100\ \% = 6{,}17\ \%$ power, which is equal to (6,17/23,0) = 0,27 dB.

This uncertainty is then by means of formula (5.2) and the relationship taken from TR 100 028 [11] converted to RF input level uncertainty (as SINAD and SNR_b is considered to be equivalent in this case). The dependency function is: mean = 0,375 dB $_{RF\ i/p\ level}$/dB $_{SINAD}$ and standard uncertainty 0,075 dB $_{RF\ i/p\ level}$/dB $_{SINAD}$

$$u_{j\,level} = \sqrt{0{,}27^2\times\left(0{,}38^2+0{,}08^2\right)} = 0{,}102\ \text{dB} \qquad \text{(formula 5.2)}$$

This RF level uncertainty is then combined with the uncertainty of the level of the input signal to obtain the total uncertainty of the sensitivity:

$$u_{j\,sensitivity} = \sqrt{0{,}5^2+0{,}10^2} = 0{,}51\,\text{dB}$$

In this example the uncertainty due to meter resolution is assumed to be negligible.

6.6.4.4 Non coherent data communication

Non coherent modulation techniques disregard absolute phase information. Communications based on non coherent modulation tend to be more sensitive to noise, and the techniques used may be much simpler. A typical non coherent demodulation technique is used with FSK, where only the information of the frequency of the signal is required.

6.6.4.5 Non coherent data communications (direct modulation)

The BER as a function of the SNR_b in this case is:

$$BER(SNR_b) = \frac{1}{2}e^{-\frac{SNR_b}{2}} \qquad (6.17)$$

provided that the cross correlation coefficient c_{cross} between the two frequencies defining the zeros and the ones is 0. The cross correlation coefficient c_{cross} of two FSK signals with frequency separation f_δ and the bit time T is:

$$|c_{cross}| = \left|\frac{\sin(\pi\times T\times f_\delta)}{\pi\times T\times f_\delta}\right| \qquad (6.18)$$

It is assumed that the cross correlation coefficient for land mobile radio systems is so small that the formulas for c_{cross} = 0 apply, and as c_{cross} is 0 the BER, as a function of the SNR_b for non coherent modulation is as shown in formula 6.15.

The slope of the function is negative, but the sign is of no interest for the uncertainty calculation. The BER (SNR_b) function for non coherent data communication is shown in figure 19.

The inverse function is:

$$SNR_b\,(BER) = -2 \times \ln\,(2 \times BER) \tag{6.19}$$

From (6.17) the slope of SNR_b (BER) is:

$$\frac{d(SNR_b)}{d(BER)} = -\frac{2}{BER} \tag{6.20}$$

The slope of the function is the inverse of (6.18):

$$\frac{d(BER)}{d(SNR_b)} = \frac{BER}{2} \tag{6.21}$$

The SNR_b can be calculated by means of formula (6.19) or read from the function shown in figure 19. If the aim is to transform BER uncertainty to level uncertainty - which is generally the case in PMR measurements - formula (6.16) is used.

$$u_{j\,level} = \frac{u_{j\,BER}}{\frac{d(BER)}{d(SNR_b)} \times SNR_{b*}}$$

Before it can be combined with the other part uncertainties at the input of the receiver it should be transformed to linear voltage terms.

EXAMPLE: The sensitivity of a receiver is measured. The RF input level to the receiver is adjusted to obtain a BER of 10^{-2}. The measured result is the RF level giving this BER. The BER is measured over a series of 2 500 bits. The uncertainty of the RF signal at the input is 0,6 dB (u_j).

The resulting BER uncertainty is then calculated using formula (6.10):

$$u_{j\,BER} = \sqrt{\frac{0{,}01 \times 0{,}99}{2500}} = 2{,}00 \times 10^{-3}$$

The signal to noise ratio giving this BER is then calculated using formula (6.19):

$SNR_b\,(0{,}01) = -2 \times \ln\,(2 \times 0{,}01) = 7{,}824$

The dependency function at this level is (formula (6.21)):

$$\frac{d(BER(7{,}824))}{d(SNR_b)} = 0{,}5 \times 0{,}01$$

The BER uncertainty is then transformed to level uncertainty using formula (6.16):

$$u_{j\,level} = \left[\frac{2{,}00 \times 10^{-3}}{0{,}5 \times 10^{-2} \times 7{,}824}\right] \times 100\,\% = 5{,}11\ \%\ \text{power}$$

which is equal to 5,11/23,0 dB = 0,22 dB (u_j) in voltage terms. This RF level uncertainty is then combined with the rest of the uncertainty contribution to give the combined standard uncertainty of the RF level.

$$u_{c\,RF\,level} = \sqrt{(0{,}6)^2 + (0{,}22)^2} = 0{,}64\ \text{dB}$$

6.6.4.6 Non coherent data communications (subcarrier modulation)

If a subcarrier modulation is used in the data communication the functions related to direct non coherent data communications apply, but in this case they give the relation between BER and signal to noise ratio of the subcarrier. To be able to transform BER uncertainty to RF input level uncertainty the relationship between the subcarrier signal to noise ratio and the RF carrier signal to noise ratio should be calculated. If the BER is measured at a RF level much higher than the sensitivity this relationship is assumed to be 1:1 as described in clause 6.5.

In FM systems, If the BER is measured in the sensitivity region (below the knee point) the relationship as for analogue receivers is assumed and the same value taken from table F.1 of TR 100 028-2 [11]: 0,375 $dB_{RF\ i/p\ level}/dB_{SINAD}$ and standard uncertainty 0,075 $dB_{\ RF\ i/p\ level}/dB_{\ SINAD}$ (see clause 6.5).

EXAMPLE: The sensitivity of an FM receiver is measured. The RF input level to the receiver is adjusted to obtain a BER of 10^{-2}. The measured result is the RF level giving this BER. The BER is measured over a series of 2 500 bits. The uncertainty of the RF signal at the input is 0,6 dB (u_j). The resulting BER uncertainty is then calculated using formula (6.11):

$$u_{j\,BER} = \sqrt{\frac{0{,}01 \times 0{,}99}{2\,500}} = 2{,}00 \times 10^{-3}$$

The signal to noise ratio giving this BER is then calculated using formula (6.19):

$SNR_b*(0{,}01) = -2 \times \ln(2 \times 0{,}01) = 7{,}824$

The dependency function at this level is:

$$\frac{d\left(BER\left(7{,}824\right)\right)}{d\left(SNR_b\right)} = \frac{0{,}01}{2}$$

This BER uncertainty is then transformed to level uncertainty using formula (6.16):

$$u_{j\ level} = \left[\frac{2{,}00 \times 10^{-3}}{0{,}5 \times 10^{-2} \times 7{,}824}\right] \times 100\,\% = 5{,}11\%\ \text{power}$$

which is equal to 5,11/23,0 = 0,22 dB ($u_{j\ level}$). This subcarrier level uncertainty is then transformed to RF level uncertainty.

$$u_{j\ RF\,level\,transformed} = \sqrt{(0{,}22)^2 \times \left(\left(0{,}375_{dB_{RF}/dB_{SINAD}}\right)^2 + \left(0{,}075_{dB_{RF}/dB_{SINAD}}\right)^2\right)} = 0{,}08\,\text{dB}$$

NOTE: As the uncertainty is small the dependency function can be used directly without transforming to dB.

This RF level uncertainty is then combined with the uncertainty of the level of the input signal to obtain the total uncertainty of the sensitivity:

$$u_{j\ sensitivity} = \sqrt{(0{,}6)^2 + (0{,}08)^2} = 0{,}61\,\text{dB}$$

The uncertainty due to meter resolution is assumed to be negligible.

6.6.5 Effect of BER on the RF level uncertainty

The SNR_b to BER function is used to transform BER uncertainty to RF input level uncertainty. In the measurements on PMR equipment the RF input level is adjusted to obtain a specified BER. A sufficiently large number of bits are examined to measure the BER, but still there is a (small) measurement uncertainty contribution $u_{j\ BER}$.

6.6.5.1 BER at a specified RF level

If the purpose is to measure the BER at a specific input level, the transformation is more of a problem. The BER function is so non-linear that the approximation where (dBER)/(dSNR$_B$) is used as the dependency function is no longer sufficient.

One approach is to calculate the uncertainty limits of the RF input level at the wanted confidence level, and then apply these limits directly to the BER function. In this case the statistical uncertainty in the BER measurement is ignored, but as the following example shows, the uncertainty due to this is negligible.

For example: The BER of a receiver is measured with the RF input level adjusted to the sensitivity limit. A BER of $0{,}75 \times 10^{-2}$ is measured over a series of 25 000 bits. The uncertainty of the RF signal at the input is 1,1 dB (u_j). The resulting BER uncertainty is then calculated using formula (6.11):

$$u_{j\,BER} = \sqrt{\frac{0{,}0075(1-0{,}0075)}{25\,000}} = 5{,}45\times10^{-4} \text{ corresponding to } 7{,}3\ \%$$

The straightforward procedure of calculating the combined standard uncertainty by applying a 1st order dependency function to the standard uncertainty of the RF input level uncertainty does not reflect reality due to the non linearity of the BER function. This is shown in the following calculation:

The dependency function is $1{,}2 \times 0{,}75 \times 10^{-2} = 0{,}9 \times 10^{-2}$ found by formula 6.3. The SNR$_b$ at BER = 0,0075 is read to be 2,9 from figure 18. The level uncertainty of 1,1 dB corresponds to $1{,}1 \times 23{,}0$ % (p) = 25,5 % (u_j). This is transformed to SNR$_b$ uncertainty: $0{,}255 \times 2{,}9 = 0{,}74$ (u_j). The level uncertainty is then transformed to BER uncertainty by means of the dependency function:

$$u_{j\,BER} = 0{,}74 \times 0{,}9 \times 10^{-2} = 0{,}666 \times 10^{-2}$$

The expanded uncertainty = $\pm 1{,}96 \times 0{,}666 \times 10^{-2} = \pm 1{,}31 \times 10^{-2}$ at a 95 % confidence level. This expanded uncertainty would give a **negative** bit error ratio as the lower limit. The reason is the non-linearity of the BER function (see also the discussion on confidence levels and their relations with the actual distributions, in clause D.5.6.2 of TR 100 028-2 [11]).

Therefore another method should be applied:

The expanded uncertainty should be expressed at a 95 % confidence level. Therefore the input level uncertainty limits are found to be $\pm 1{,}96 \times 1{,}1$ dB = ±2,16 dB. This corresponds to 1,64 and 0,608 (power values). The values corresponding to the 95 % confidence level is then $2{,}9 \times 1{,}64 = 4{,}76$ and $2{,}9 \times 0{,}608 = 1{,}76$.

By means of figure 18 the BER uncertainty limits at 95 % confidence level are read to be $3{,}0 \times 10^{-2}$ and $1{,}0 \times 10^{-3}$ corresponding to +300 % and -87 %.

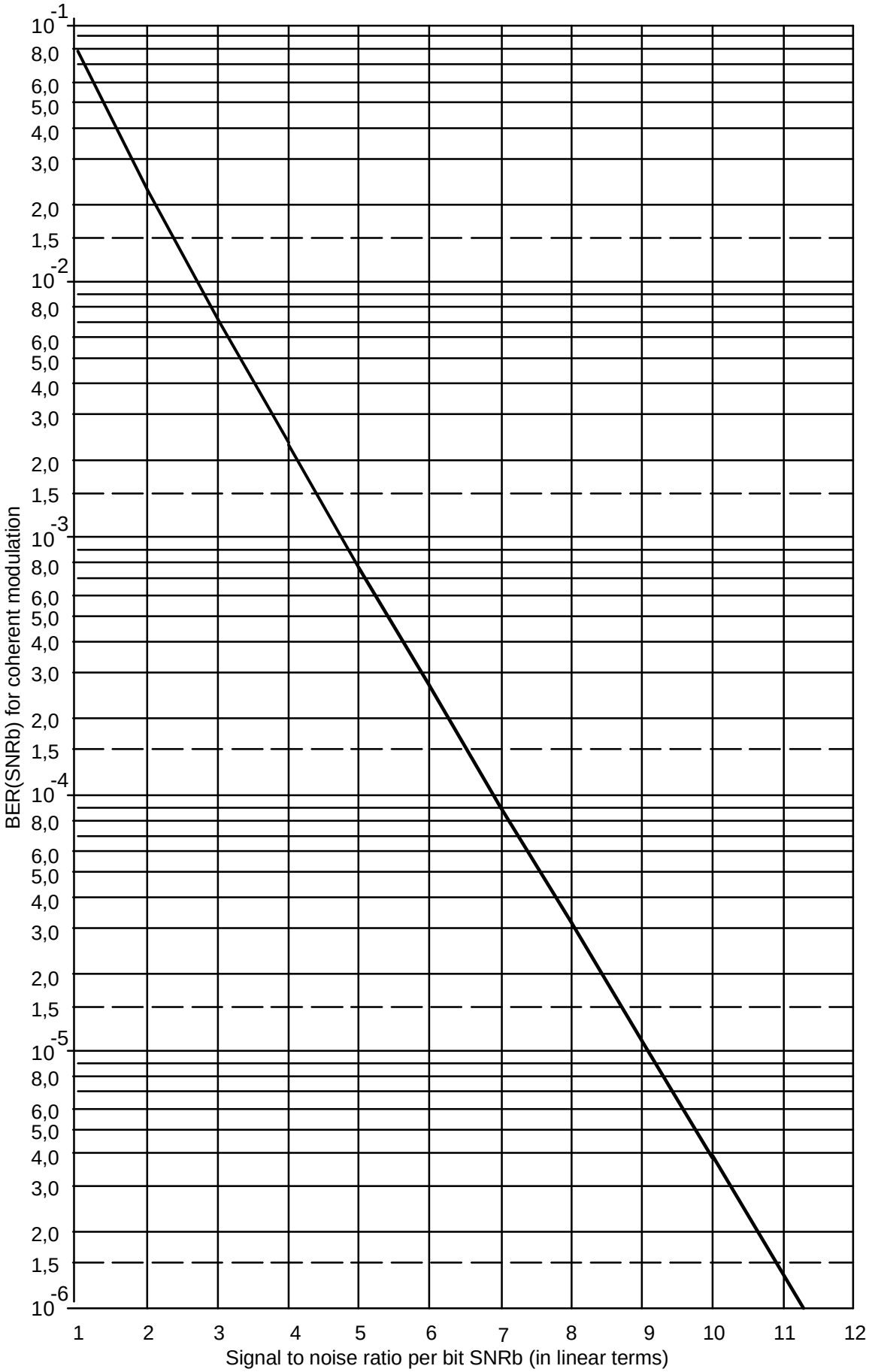

Figure 18: BER (SNR_b) against SNR_b

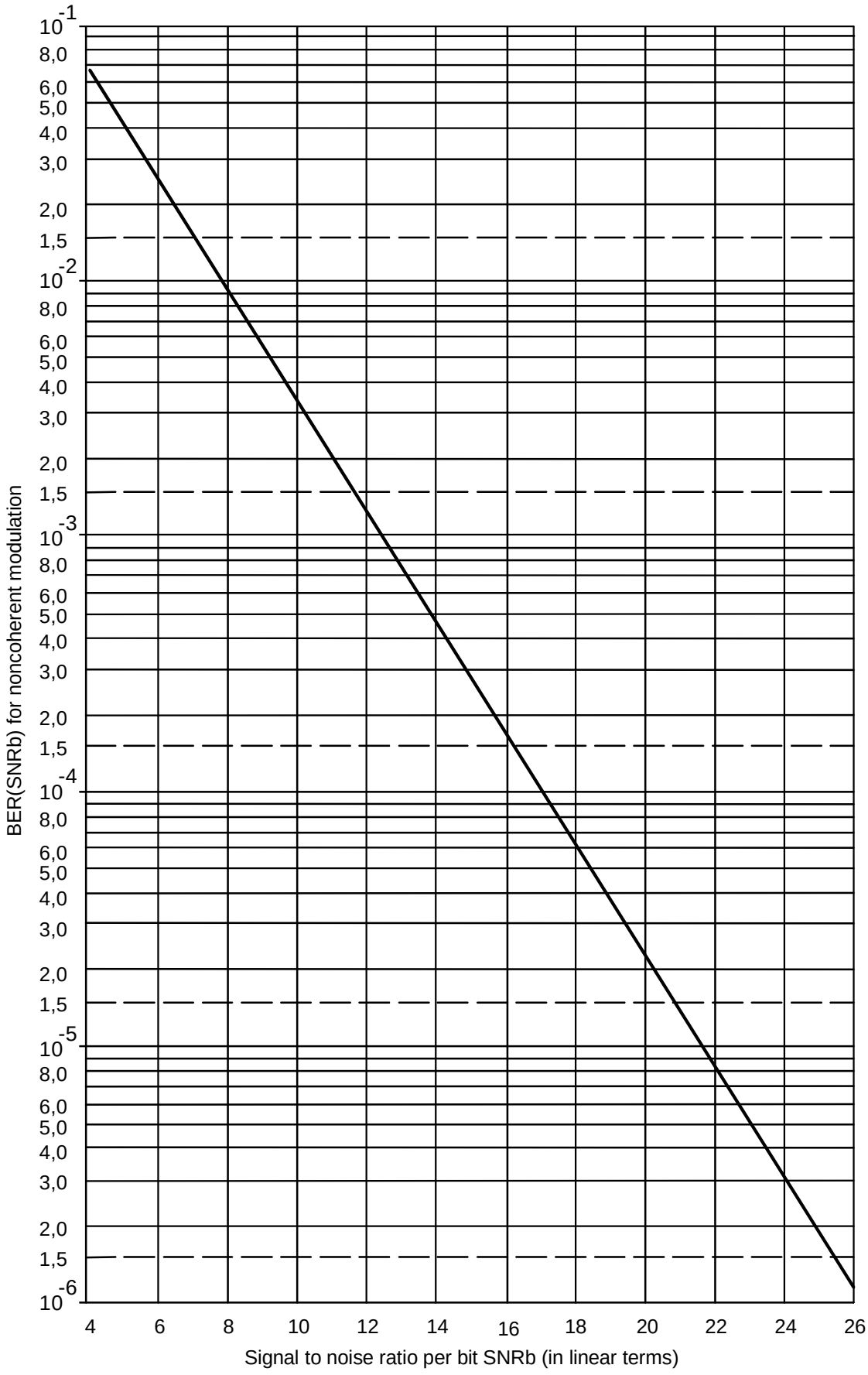

Figure 19: BER (SNR_b) against SNR_b

6.6.6 Limitations in the applicability of BER uncertainty calculations

As mentioned earlier the above figures and formulas are not applicable to all BER measurements; the conditions for applicability are:

- the noise is white Gaussian noise;
- the signal-to-noise ratio is constant;
- each bit error is statistically independent;
- the transmission channel delay is constant.

These 4 conditions apply to most normal receiver measurements covered by the present document, but the blocking measurement (and any variant where the unwanted signal is un-modulated) does not satisfy the first condition about white Gaussian noise. Therefore the formulas do not apply to this measurement.

The receiver is normally not as sensitive to a single frequency component as to a broadband signal with the same power.

In some technologies (for instance GSM) data is protected by error correcting signalling schemes. The data is usually transmitted in packets with extra information for the error correction attached to the packet, so that up to a specified number of bit errors within a packet can be corrected. When this limit is exceeded the number of bits will increase dramatically because the error correction procedures will generate more bit errors than actually received. The result is that the BER will be less sensitive to noise at moderate signal-to-noise ratios, but the dependency function will be steeper at lower signal-to-noise ratios. The reception of the data packet also relies on the recognition of the packet's preamble or synchronization pattern. If this is not received and accepted all data is lost. The dependency function depends very much on the error correction algorithm and must be analysed and derived in each case.

In some technologies receiver characteristics are measured under fading and multipath conditions which means that the signal-to-noise ratio is not constant. Multipath conditions also add other errors like distortion and timing errors to the transmitted signal. It also causes the bit errors to appear as bursts rather than independent errors.

In all the cases above the BER dependency functions derived previously do not apply, as one or more of the conditions are not fulfilled. In these cases, the dependency functions must be derived or estimated by other means. A simple approach would be to estimate the dependency function by measuring the BER at different signal-to-noise ratios, for instance by changing the level of the wanted signal 1 dB up and down. However, the dependency functions estimated for one receiver will not necessarily apply to the next receiver even within the same technology.

6.7 Uncertainty in measuring messages

6.7.1 General

If the EUT is equipped with message facilities the characteristic used to assess the performance of the equipment is the message acceptance ratio. The message acceptance ratio is the ratio of the number of messages accepted to the total number of message sent.

Normally it is required to assess the receiver performance at a message acceptance ratio of 80 %. The message acceptance ratio is used as a measure of receiver performance in digital radio systems in a similar way that SINAD and BER ratios are used as a measure of receiver performance in analogue and bit stream measurements, particularly in sensitivity and immunity measurements.

6.7.2 Statistics involved in the measurement

When considering messages, parameters such as message length (in bits), type of modulation (direct or sub-carrier, coherent or non-coherent), affect the statistics that describe the behaviour of the receiver system.

Performance of the receiver is assessed against a message acceptance ratio set by the appropriate standard and/or methodology used. To assess the uncertainty the cumulative probability distribution curves for message acceptance are required, these can be calculated from (6.20).

$$Pe_{(0)} + Pe_{(1)} + Pe_{(2)} + Pe_{(3)} + Pe_{(n)} \quad (6.22)$$

where:

n is the message length.

$Pe_{(0)}$ is the probability of 0 errors;

$Pe_{(1)}$ is the probability of 1 errors;

$Pe_{(2)}$ is the probability of 2 errors;

$Pe_{(3)}$ is the probability of 3 errors;

$Pe_{(n)}$ is the probability of n errors.

The individual contribution of each probability $Pe_{(x)}$ in formula (6.22) is calculated using formula (6.8). Curves for a theoretical 50 bit system with 1, 2, 3, 4, 5 and 6 bits of error correction are shown in figure 20.

As the number of bits of error correction increase so does the slope of the relevant portion of the cumulative probability density function, and as the slope increases less carrier to noise (or RF input level) variation is required to cause the message acceptance ratio to vary between 0 % and 100 %.

This effect is increased in non-linear systems by a factor of approximately 3:1. Due to the increased slope associated with sub-carrier modulation, as a result of this in our theoretical 50 bit system, 6 bits of error correction will result in a very well defined level of 0 % acceptance to 100 % acceptance, (with 1 dB level variation), however, with no error correction, the level variation between 0 % and 100 % acceptance will be several dB.

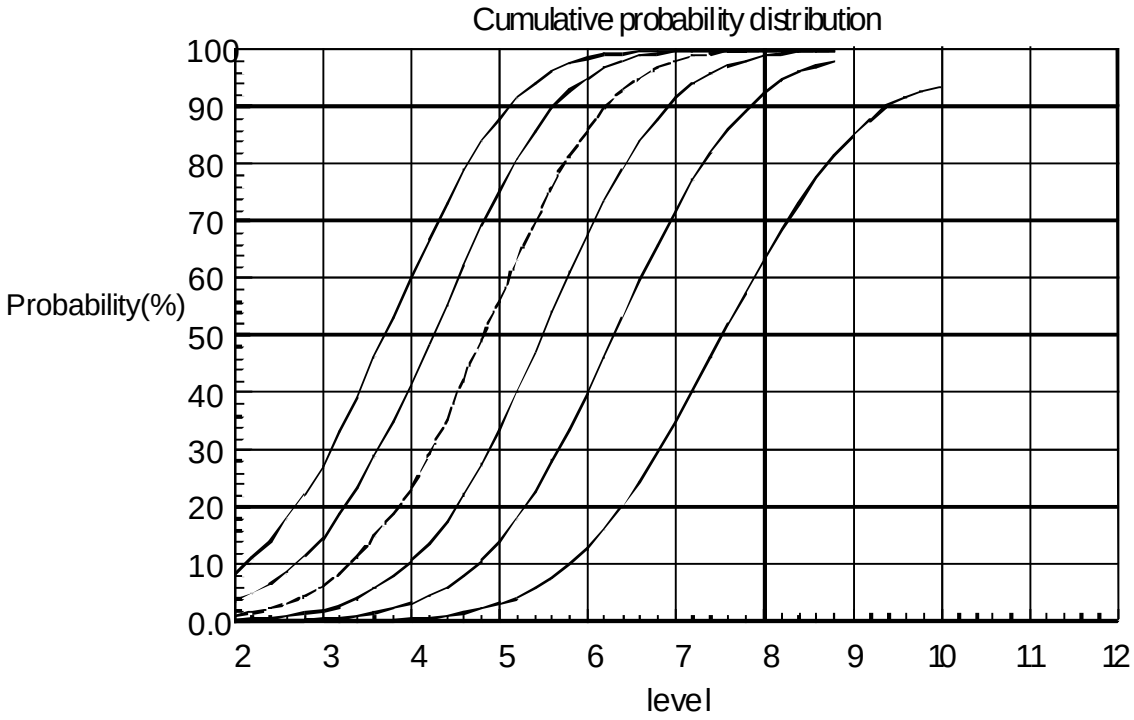

Figure 20: Cumulative probability (error correction for messages)

As a method of testing receivers the "up-down" method is used. The usage of the up down method will result in a series of transmissions using a limited number of RF levels.

6.7.3 Analysis of the situation where the up down method results in a shift between two levels

With some systems (e.g. 6 bits of error correction) the up-down method will typically result in a pattern shifting between two levels, where at the lower level the message acceptance ratio will approach zero and at the higher level (+1 dB) the message acceptance ratio will approach 100 %. In this case the measurement uncertainty is of the simplest form for this contribution.

The RF is switching between two levels, the mean value is calculated, usually from 10 or 11 measurements. The measurement uncertainty cannot be calculated as though random, independent sources are involved. The RF is switching between two output levels of the same signal generator, the levels therefore are correlated and only have two values (upper and lower), hence the standard uncertainty for a signal generator with output level uncertainty of ±1 dB is:

$$u_{j\ outputlevel} = \frac{1{,}0}{\sqrt{3}} = 0{,}58\,\text{dB}$$

Also there is a quantization uncertainty associated with half of the step size (in this case 1 dB which gives ±0,5 dB).

$$u_{j\ quantisiation} = \frac{0{,}5}{\sqrt{3}} = 0{,}29\,\text{dB}$$

Therefore the combined standard uncertainty of this step will be:

$$u_{ctwolevelshift} = \sqrt{u^2_{j\ outputlevel} + u^2_{j\ quantisation}} = \sqrt{0{,}58^2 + 0{,}29^2} = 0{,}65\,\text{dB}$$

For the case of no error correction the pattern of the measured results will spread beyond a single dB step and measurement uncertainty calculations are more complex.

6.7.4 Detailed example of uncertainty in measuring messages

For this example a theoretical system with 50 bit message length and 1 bit error correction will be considered, although the principles can be applied to all practicable message and correction lengths.

a) Calculate the message acceptance ratio (formula (6.22)) for the given message length and given number of bit error corrections, using bit error ratios corresponding to a convenient step size (in this case 1 dB) using either formula (6.18) for non-coherent, or, formula (6.12) for coherent, and if sub-carrier modulation is used, use the appropriate SINAD conversion in table F.1 of TR 100 028-2 [11].

b) Now the probability of being at a given point on the curve is to be assessed. For example the probability of being at a particular point (in figure 20) is:

   - the probability of being below a particular point times the probability of going up from this point, plus
   - the probability of being above a particular point times the probability of going down from this point.

The method requires three successful responses, therefore the probability of going up is:

$$Pp_{(up)} = 1 - (\text{Message Acceptance})^3 = 1 - (MA)^3 \qquad (6.23)$$

and the probability of going down is:

$$Pp_{(down)} = (\text{Message Acceptance})^3 = (MA)^3 \qquad (6.24)$$

($Pe_{(0)} + Pe_{(1)}$) = Probability of 0 errors + the probability of 1 error (see formula (6.24)). These calculations are shown in table 2.

Table 2: Probability of going up or down from a given position

dB	Linear	BER	$(Pe_{(0)}+Pe_{(1)})$ %	$Pp_{(up)}=1-(MA)^3$	$Pp_{(down)}=(MA)^3$
+2	12,679	$0,8826 \times 10^{-3}$	99,91	$2,698 \times 10^{-3}$	$997,3 \times 10^{-3}$
+1	10,071	$3,251 \times 10^{-3}$	98,83	$34,69 \times 10^{-3}$	$965,3 \times 10^{-3}$
0	8,000	$9,158 \times 10^{-3}$	92,30	$213,7 \times 10^{-3}$	$786,3 \times 10^{-3}$
-1	6,355	$20,84 \times 10^{-3}$	72,02	$626,4 \times 10^{-3}$	$373,6 \times 10^{-3}$
-2	5,048	$40,07 \times 10^{-3}$	39,95	$936,2 \times 10^{-3}$	$63,76 \times 10^{-3}$
-3	4,010	$67,33 \times 10^{-3}$	14,13	$997,2 \times 10^{-3}$	$2,821 \times 10^{-3}$
-4	3,185	$101,7 \times 10^{-3}$	3,123	1,000	$30,46 \times 10^{-6}$
-5	2,530	$141,1 \times 10^{-3}$	0,459	1,000	$96,55 \times 10^{-9}$

Based on equations (6.21) and (6.22), and the fact that the sum of all probabilities equals 1, the individual probabilities of being at each step of the signal to noise ratio per bit (SNR_b) can be calculated.

Assuming that at SNR_b greater than +1 dB all messages are accepted (therefore can only move down from here) and Assuming that at SNR_b less than -4 dB all messages are rejected (therefore can only move up from here), this gives rise to two boundary positions -5 dB and +2 dB.

The probability of being at any one of the points -5, -4, -3, -2, -1, 0, +1, +2 is Pp_{-5}, Pp_{-4}, Pp_{-3}, Pp_{-2}, Pp_{-1}, Pp_0, Pp_{+1}, and Pp_{+2} respectively.

The analysis of the possible transitions between these points provide:

$Pp_{-5} = (Pp_{-4} + 30,46 \times 10^{-6}) + (Pp_{-6} \times 1)$

$Pp_{-4} = (Pp_{-3} \times 2,821 \times 10^{-3}) + (Pp_{-5} \times 1)$

$Pp_{-3} = (Pp_{-2} \times 63,76 \times 10^{-3}) + (Pp_{-4} \times 1)$

$Pp_{-2} = (Pp_{-1} \times 373,6 \times 10^{-3}) + (Pp_{-3} \times 997,2 \times 10^{-3})$

$Pp_{-1} = (Pp_0 \times 786,3 \times 10^{-3}) + (Pp_{-2} \times 936,2 \times 10^{-3})$

$Pp_0 = (Pp_{+1} \times 965,3 \times 10^{-3}) + (Pp_{-1} \times 626,4 \times 10^{-3})$

$Pp_{+1} = (Pp_{+2} \times 1) + (Pp_0 \times 213,7 \times 10^{-3})$

$Pp_{+2} = (Pp_{+3} \times 1) + (Pp_{+1} \times 34,69 \times 10^{-3})$

NOTE: The probability of being at point Pp_{-6} or Pp_{+3} is zero, hence $Pp_{-6} \times 1$ and $Pp_{+3} \times 1$ are both equal to zero.

Based on seven out of these eight equations and the fact that the sum of Pp_{-5} to Pp_{+2} is one, each individual probability Pp_{-5} to Pp_{+2} is calculated as follows:

rearranging the above equations gives:

$Pp_{-6} \times 1 - Pp_{-5} + Pp_{-4} \times 30,46 \times 10^{-6} = 0$

$Pp_{-5} \times 1 - Pp_{-4}\, Pp_{-3} \times 2,821 \times 10^{-3} = 0$

$Pp_{-4} \times 1 - Pp_{-3} + Pp_{-2} \times 63,76 \times 10^{-3} = 0$

$Pp_{-3} \times 997,3 \times 10^{-3} - Pp_{-2} + Pp_{-1} \times 373,6 \times 10^{-3} = 0$

$Pp_{-2} \times 936,2 \times 10^{-3} - Pp_{-1} + Pp_0 \times 786,3 \times 10^{-3} = 0$

$Pp_{-1} \times 626{,}4 \times 10^{-3} - Pp_0 + Pp_{+1} \times 965{,}3 \times 10^{-3} = 0$

$Pp_0 \times 213{,}7 \times 10^{-3} - Pp_{+1} + Pp_{+2} \times 1 = 0$

$Pp_{+1} \times 34{,}69 \times 10^{-3} - Pp_{+2} + Pp_{+3} \times 1 = 0$

$Pp_{-5} + Pp_{-4} + Pp_{-3} + Pp_{-2} + Pp_{-1} + Pp_0 + Pp_{+1} + Pp_{+2} = 1$

$Pp_{-6} = Pp_{+3} = 0$

	Pp_{-5}	**Pp_{-4}**	**Pp_{-3}**	**Pp_{-2}**	**Pp_{-1}**	**Pp_0**	**Pp_{+1}**	**Pp_{+2}**	
1	1	-1	$2{,}821 \times 10^{-3}$						
2		1	-1	$63{,}76 \times 10^{-3}$					
3			$997{,}3 \times 10^{-3}$	-1	$373{,}6 \times 10^{-3}$				
4				$936{,}2 \times 10^{-3}$	-1	$786{,}3 \times 10^{-3}$			
5					$626{,}4 \times 10^{-3}$	-1	$965{,}3 \times 10^{-3}$		
6						$213{,}7 \times 10^{-3}$	-1	1	
7							$34{,}69 \times 10^{-3}$	-1	
8	1	1	1	1	1	1	1	1	1

solving this by means of row operations on row 8, gives:

1	**1**	**-1**	**$2{,}821 \times 10^{-3}$**						
2		1	-1	$63{,}76 \times 10^{-3}$					
3			$997{,}3 \times 10^{-3}$	-1	$373{,}6 \times 10^{-3}$				
4				$936{,}2 \times 10^{-3}$	-1	$786{,}3 \times 10^{-3}$			
5					$626{,}4 \times 10^{-3}$	-1	$965{,}3 \times 10^{-3}$		
6						$213{,}7 \times 10^{-3}$	-1	1	
7							$34{,}69 \times 10^{-3}$	-1	
8								392,91	1

From this we have: $392{,}91 \times Pp_{+2} = 1$; Therefore $Pp_{+2} = 2{,}545 \times 10^{-3}$

this is then used in row 7 to determine Pp_{+1}: $Pp_{+1} = \frac{2{,}545 \times 10^{-3}}{34{,}69 \times 10^{-3}} = 73{,}36 \times 10^{-3}$

this is used in row 6 to determine Pp_0: $Pp_0 = \frac{0{,}07336 - \left(2{,}545 \times 10^{-3} \times 1\right)}{213{,}7 \times 10^{-3}} = 331{,}38 \times 10^{-3}$

this is used in row 5 to determine Pp_{-1}: $Pp_{-1} = \frac{331{,}38 \times 10^{-3} - \left(73{,}36 \times 10^{-3} \times 965{,}3 \times 10^{-3}\right)}{626{,}4 \times 10^{-3}} = 415{,}97 \times 10^{-3}$

this is used in row 4 to determine Pp_{-2}: $Pp_{-2} = \frac{415{,}97 \times 10^{-3} - (0{,}33138 \times 0{,}7863)}{0{,}9362} = 166{,}0 \times 10^{-3}$

this is used in row 3 to determine Pp_{-3}: $Pp_{-3} = \frac{166{,}00 \times 10^{-3} - (0{,}41597 \times 0{,}3736)}{0{,}9973} = 10{,}622 \times 10^{-3}$

this is used in row 2 to determine Pp_{-4}: $Pp_{-4} = \frac{10{,}622 \times 10^{-3} - \left(0{,}1660 \times 63{,}76 \times 10^{-3}\right)}{1} = 37{,}84 \times 10^{-6}$

this is used in row 1 to determine Pp_{-5}: $Pp_{-5} = \frac{37{,}84 \times 10^{-6} - \left(10{,}622 \times 10^{-3} \times 2{,}821 \times 10^{-3}\right)}{1} = 7{,}87 \times 10^{-6}$

There are, of course, other ways of solving the equations.

After having calculated the probabilities it should always be checked that the sum of all probabilities is 1. If the sum is not 1 (to within (0,001) it can cause major uncertainties in the calculation of the resulting standard uncertainty of the distribution.

Based on these probabilities the standard uncertainty of the distribution is calculated:

$$X = \sum_{i=-5}^{i=2} Pp_i \times i = -0{,}70 \qquad \text{(formula 5.6)}$$

$$Y = \sum_{i=-5}^{i=2} Pp_i \times i^2 = 1{,}26 \qquad \text{(formula 5.7)}$$

then:

$$u_j = \sqrt{Y - X^2} = \sqrt{1{,}26 - (-0{,}70)^2} = 0{,}88\,\text{dB} \qquad \text{(formula 5.8)}$$

and the standard uncertainty for the measurement (as the result is the average value of 10 samples):

$$\frac{0{,}88}{\sqrt{10}} = 0{,}28\,\text{dB} \qquad \text{(formula 5.9)}$$

The expanded uncertainty is ±1,96 × 0,28 = ±0,54 dB at a 95 % confidence level.

Therefore the methodology introduces an additional ±0,54 dB of uncertainty to the level.

6.8 Uncertainty of fully automated test systems

So far the uncertainty calculations for manual measurements have been examined.

But in many radio technologies testing is performed using fully automated test systems. In technologies such as GSM, DECT and Bluetooth, certification and type approval is based on measurements using such test systems. This gives an improvement in reproducibility and test time compared to manual measurements, but the measurement uncertainty for such test systems has yet to be documented.

One major reason is that the procedures and calculations outlined for the simpler test methods do not cover fully automated test systems due to the complexity, even though the basic principles still apply.

The measurements are basically carried out in the same way as the manual measurements. A conducted power measurement is still performed by connecting the EUT to a power measuring instrument through a combining network consisting of cables, attenuators and maybe filters. Then a power measurement is carried out, and a correction factor is applied to the reading of the instrument to get the final test result.

Similarly a receiver measurement is done by connecting one or more RF signal generators to an EUT through a combining network and adjusting the output levels from the generators each time using correction factors.

The major difference between the manual measurement and the fully automated test system measurement is how this correction factor is derived. For fully automated systems this is normally done by executing **Path Compensation** procedures.

The purpose of path compensation procedures is (as mentioned) to generate correction factors, and in a well designed test system these correction factors eliminate all errors leaving "only" some irreducible stability and mismatch errors.

In most fully automated test systems the path compensation procedures are a combination of measurements performed at the same time as the actual measurement as well as periodic measurements on sub parts of the test system, but to have a full picture of the uncertainties involved the path compensation and the actual measurement should be seen as one procedure. With a well designed overall path compensation procedure it is easy to see that if all instruments and components were stable and linear and had an impedance of exactly 50 Ω then the only uncertainty contribution would be the absolute uncertainty of the power meter.

But as with the manual measurements the instruments are not totally stable, and there are mismatch uncertainties due to non-ideal coaxial components.

6.8.1 Test system properties

A fully automated test system normally consists of a set of test instruments (usually exactly the same as the ones used in the manual measurements), but in addition it contains a switch unit. The purpose of the switch unit is to create the correct set-ups using attenuators, power combiners, filters, amplifiers, and cables. The set-ups inside the switch unit is then realized using RF switches controlled by a system controller - normally a PC with appropriate test software. A switch unit often consists of more than 100 components.

A fully automated test system can perform all the common radio tests: Transmitter tests including output power, timing, modulation, output spectrum, and spurious emissions, and receiver tests including 1, 2, and 3 signal measurements as the test system contains 3 RF signal generators. The BER measurement or the signal-to-noise measurement is not shown. It is assumed to be either a part of signal generator 1 or some external equipment connected to the base band output of the EUT. It is not important for the analysis of the test system because once the level uncertainties are calculated, the rest (BER, signal-to-noise, modulation, or timing) are the same as with the manual measurements.

Signal generator 1 generates the wanted signal.

Signal generator 2 generates the low frequency unwanted signal.

Signal generator 3 generates the high frequency unwanted signal.

(Both signal generator 2 and 3 can also produce in-band signals for 3 signal measurements).

The signal analyser is capable of measuring both power, frequency, and modulation, but for the purpose of this analysis only power is considered.

Tests are normally carried out as follows: The EUT is connected to a specific EUT connector on the test system. Then the test operator selects and activates some tests, and some test results are produced by the test system. Depending on the degree of automation the operator may be prompted to control the EUT from time to time - for instance to set up a connection with the EUT or to switch the EUT to a different channel.

It is normally not visible to the operator how the tests are carried out by the test system, but this is often described in the test system documentation. As a part of a test the path compensation related to that test can be run prior to the actual testing. This depends on the flexibility and complexity of the switch unit and the test software.

6.8.2 General aspects of the measurement uncertainty

As indicated previously, the main difference between manual testing and a fully automated test system is how the correction factors are generated. From a measurement uncertainty point of view this is very important because this is X one of the major contributions to the overall RF level uncertainty of the actual measurement. The other contributions are:

- Instruments stability.
- Instruments linearity.
- Mismatch between the EUT and the test system.
- RF switch repeatability.

Often it is the power meter that is the essential instrument in the path compensation, and the one which provides the traceability to external standards.

The uncertainty of the correction factor is very dependant on how the correction factor is measured. The contributions to the uncertainty are:

- Absolute power meter uncertainty.
- Instruments stability.
- Instruments linearity.

- Mismatch between the instruments and the individual components of the switch unit.
- Errors due to interpolation between correction factors at different frequencies.

As will be shown, the mismatch uncertainty is the most complex component of the overall measurement uncertainty. It can for complex fully automated systems be the combination of several thousands of individual mismatch contributions. The amount of contributions can, however, be reduced by disregarding very small contributions.

The contributions tend to be greater than with the manual measurements because more cables and switches are necessary to provide the needed flexibility.

For the purpose of the measurement uncertainty analysis, two fully automated test systems will be considered: a "simple" test system, and a "complex" test system.

6.8.3 The "simple" test system

The test system is shown in figure 21:

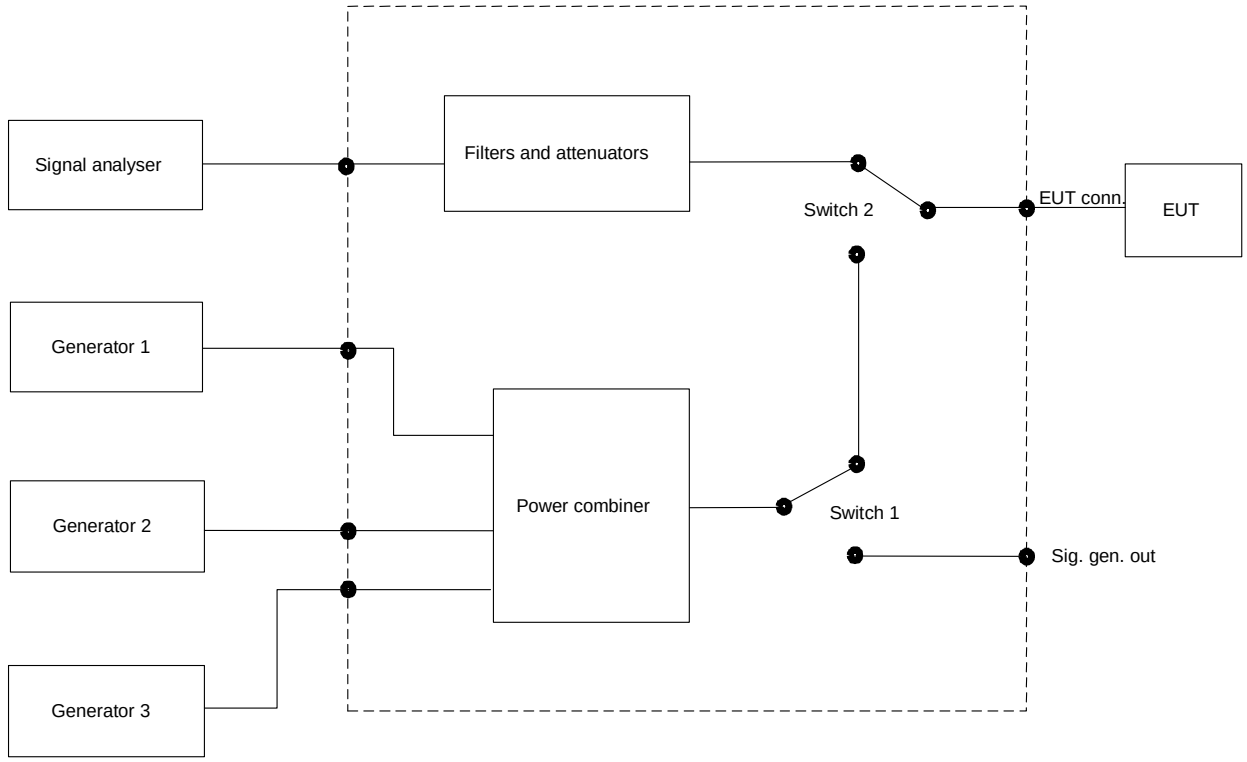

Figure 21: The "simple" test system

6.8.3.1 Transmitter measurement

For the "simple" test system the path compensation procedures and the actual measurement for transmitter measurements using the correction factors, are as follows:

The path compensation is performed as follows:

Switch 1 is set so the generators are connected to the Sig. gen. out connector.

Switch 2 is set so the signal analyser is connected to the EUT connector.

Measurement 1:

A power meter is connected to the RF out connector through a cable and a 10 dB attenuator.

The RF generators are in turn adjusted to a suitable level which gives a reading in the operational range of the power meter. When one generator is active the others are turned down, so they do not contribute to the measurement, but their output impedance is still 50 Ω. A series of measurements covering the frequency range of interest is carried out and for each frequency the reading is stored by the test system.

Measurement 2:

The power meter is removed and the open end of the 10 dB attenuator is connected to the EUT connector. For all the frequencies and generator level settings in step 4 the power level is measured by the signal analyser. This is preferably done with the same analyser setting as the one used in the actual EUT measurement. The readings are stored by the test system. For each frequency the correction factor is calculated as the difference (in dB) between the signal analyser reading XX and the power meter XX.

Measurement 3 (the actual measurement):

The EUT is connected to the EUT connector.

The power level of the signal generated by the EUT is measured, and the signal analyser reading is stored by the test system.

The final result is then calculated as the reading from step 2 (in dBm) minus the correction factor calculated in the path compensation procedure at the appropriate frequency. (If a correction factor at the measuring frequency does not exist it is found by interpolation between the two correction factors at the nearest frequencies on each side).

6.8.3.1.1 Error analysis

The combined path compensation procedure and the actual test consist of 3 individual measurements as shown in figure 22: two measurements in the path compensation part and one in the actual measurement.

In each of the 3 measurements a signal source is connected to a measuring instrument through a network consisting of several components and a level is measured.

In the following the total procedure is analysed.

The following assumptions apply for the analysis:

- The generator has a static error of **Egen** dB in measurement 1 (compared to the setting of the generator level).
- Between measurement 1 and measurement 2 there is a generator drift error **dEgen** dB.
- The attenuation between the generator and the sig. gen. out connector is **Att1** dB.
- Between measurement 1 and measurement 2 there is an attenuation change in the network between the generator and the sig. gen. out. connector of **dAtt1** dB.
- The attenuation of the external cable and attenuator is **Att2** dB.
- Between measurement 1 and measurement 2 there is an attenuation change in the external cable and attenuator of **dAtt2** dB.
- There is a static error of **Epow** dB in power measurements using the power meter.
- The attenuation between the EUT connector and the signal analyser i **Att3** dB.
- Between measurement 2 and measurement 3 there is an attenuation change in the network between the EUT connector and the signal analyser of **dAtt3** dB.
- There is a static error of **Esa** dB in the power measurement in measurement 2 using the signal analyser.
- Between measurement 2 and measurement 3 there is a signal analyser drift error **dEsa** dB.
- The EUT has an output power of **Pout** dBm.
- The generator level is set to **Pgen** dBm in measurement 1 and 2.

- If the value read from the signal analyser in measurement 3 differs from the value in measurement 2 there is a signal analyser linearity (or log fidelity) error **dElog**.

In measurement 1 the reading on the power meter is:

P1 = Pgen + Egen - Att1 - Att2 + Epow dBm

In measurement 2 the reading on the signal analyser is:

P2 = Pgen + Egen + dEgen - Att1 - dAtt1 - Att2 - dAtt2 - Att3 + Esa dBm

The correction factor is:

Ccorr = P2 - P1 =

(Pgen + Egen + dEgen - Att1 - dAtt1 - Att2 - dAtt2 - Att3 + Esa) - (Pgen + Egen - Att1 - Att2 + Epow) =

dEgen - dAtt1 - dAtt2 - Att3 + Esa - Epow dB

In measurement 3 the reading from the signal analyser is:

P3 = Pout - (Att3 + dAtt3) + Esa + dEsa + dElog dBm

The measured result after having applied the correction factor to the reading from measurement 3 is:

Pmeas = P3 - Ccorr =

Pout - (Att3 + d Att3) + Esa + dEsa + dElog - (dEgen - dAtt1 - dAtt2 - Att3 + Esa - Epow) =

Pout + dAtt3 + dEsa + dElog - dEgen + dAtt1 + dAtt2 + Epow dBm

As can be seen from the calculated result all static errors in the combined measurement except the power meter error have cancelled. Apart from that only the drift and linearity errors remain.

The remaining errors are:

- the absolute uncertainty of the power meter;
- the linearity (or log fidelity) of the signal analyser due to the fact that the level measured by the signal analyser in actual measurement may be different from the level measured in the path compensation;
- signal analyser drift between the different measurements;
- signal generator drift between the different measurements;
- repeatability of the switches in the switch unit;
- change of the insertion losses between the different measurements.

Since the path compensation is performed at descrete frequencies there is an additional error

- error due to interpolation between correction factors at different frequencies.

Finally, in addition to the uncertainties mentioned there is a mismatch uncertainty in each measurement.

The mismatch uncertainty is analysed in clause 6.8.3.1.2.

6.8.3.1.2 Mismatch uncertainty

For each measurement there is a mismatch uncertainty which is the combination of all the mismatch uncertainties between all of the parts in the path between the signal source and the measuring instrument.

Fortunately many of the mismatch uncertainties are cancelled due to the total procedure.

Firstly the two measurements involved in the path compensation procedure are considered. The correction factor is the difference between the two values measured; this means that the total error is the difference between the errors in the two measurements, so all errors which are identical cancel.

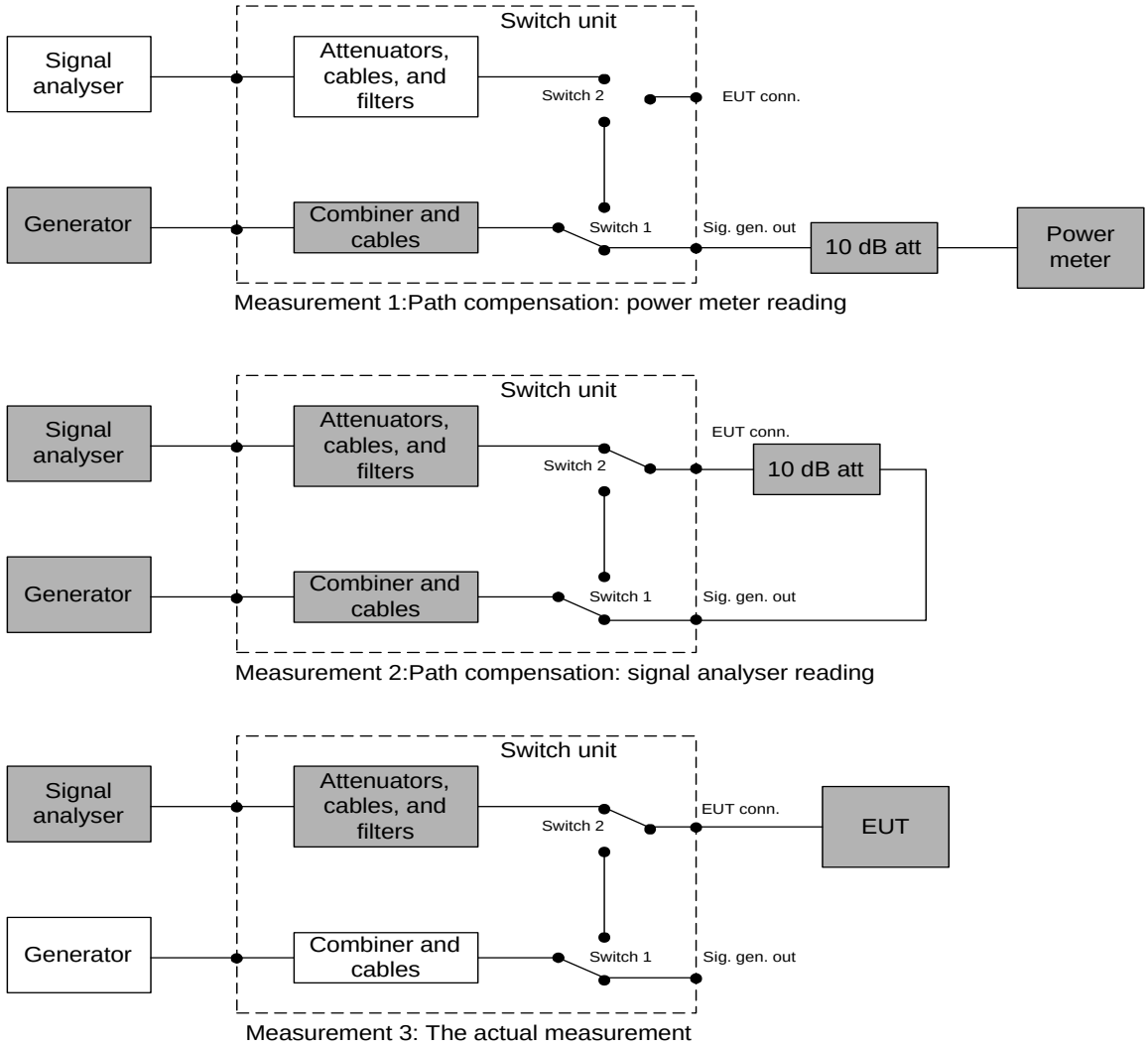

Figure 22: The three set-ups in the transmitter measurement

From figure 22 it can be seen that all the mismatch uncertainties from the path between the 10 dB attenuator and the RF signal generators cancel because they are present in both measurements 1 and 2.

In measurement 1 all the mismatch uncertainties associated with the power meter remain. The rest are cancelled.

In measurement 2 all mismatch uncertainties from the path between the 10 dB attenuator and the signal analyser remain, as they only appear here. For the same reason all the mismatch uncertainties where one of the parts is to the right of the EUT connector, and the other part is to the left of the EUT connector remain.

Then when measurement 3 (the actual measurement) is taken into account it can be seen that parts of the mismatch uncertainties from measurement 2 cancel, since they are also present in measurement 3: all the uncertainties from the path between the EUT connector and the signal analyser.

What is left in measurement 3 are all the mismatch uncertainties where the EUT is one of the parts. The rest cancel with measurement 2.

The total mismatch uncertainty in the total measurement including the path compensation is then the combination of the following part uncertainties:

1) all mismatch uncertainties where the power sensor is one of the parts (measurement 1)

2) all mismatch uncertainties where the two parts are on each side of the EUT conn. (measurement 2)

3) all mismatch uncertainties where the EUT is one of the parts (measurement 3)

Based on this the calculation of the total mismatch uncertainty can be done in two ways.

If all VSWRs and insertion losses (or gains) of the individual components in the test system are known all the contributions can be calculated and combined.

But a more simple approach is to measure (or estimate by other methods) the reflection coefficient **Rg** of the free end of the 10 dB attenuator, measure (or take from the specification sheet) the reflection coefficient **Rp** of the power meter, measure the reflection coefficient **Ri** of the EUT connector, and measure (or estimate) the reflection coefficient **Reut** of the EUT.

If these 4 reflection coefficients are known, the total uncertainty is the combination of:

- **Ri*Rp/√2** (from measurement 1)
- **Rg*Ri//√2** (from measurement 2)
- **Reut*Ri//√2** (from measurement 3)

This is exactly the same result as if the measurement had been done manually with a generator, a power meter, and a signal analyser if the switch unit paths are considered as parts of the individual instruments.

But the method of analysing the "simple" test system is important, because the same method is used in the "complex" test system, and here the result are not similar to any simple manual measurement.

6.8.3.2 Receiver measurements

For the "simple" test system the path compensation procedures for receiver measurements and the actual measurement using the correction factors, are as follows:

The path compensation (measurement 1) is done as follows:

Switch 1 and switch 2 is set so the generators are connected to the EUT connector.

Then the power meter is connected to the EUT connector.

The RF generators are in turn adjusted to a suitable level which gives a reading in the operational range of the power meter. When one generator is active the others are turned down, so they do not contribute to the measurement, but their output impedance is still 50 Ω. A series of measurements covering the frequency range of interest is done and for each frequency the reading are stored by the test system.

For each frequency point the correction factor is calculated as the difference (in dB) between the power meter reading and the generator setting.

The actual measurement (measurement 2) is done as follows:

The EUT is connected to the EUT connector.

The generator is set to the wanted signal level (in dBm) minus the correction factor at the appropriate frequency. (If a correction factor at the measuring frequency does not exist it is found by interpolation between the two correction factors at the nearest frequencies on each side).

Then the appropriate receiver measurement is done (BER or signal-to-noise ratio).

6.8.3.2.1 Error analysis

The combined path compensation procedure and the actual test consist of 2 individual measurements as shown in figure 23: two measurements in the path compensation part and one in the actual measurement.

In each of the 2 measurements a signal source is connected to a measuring instrument through a network consisting of several components and a level is measured.

In the following the total procedure is analysed.

The following assumptions apply for the analysis:

- The generator has a static error of **Egen** dB in measurement 1(compared to the setting of the generator level)

- The generator has a linearity/log fidelity error of **Elog** dB between the levels in measurement 1 and measurement 2
- Between measurement 1 and measurement 2 there is a generator drift error **dEgen** dB
- The attenuation between the generator and the EUT connector is **Att1** dB in measurement 1
- Between measurement 1 and measurement 2 there is an attenuation change in the network between the generator and the EUT connector of **dAtt1** dB
- There is a static error of **Epow** dB in the power meter measurement in measurement 1
- The generator level is set to **Pgen1** dBm in measurement 1
- The wanted level at the EUT connector is **Pwanted** dBm in the actual measurement

In measurement 1 the reading on the power meter is:

P1 = Pgen1 + Egen - Att1 + Epow dBm

The correction factor is calculated to be **Ccorr = Pgen1 - P1 =**

Pgen1 - (Pgen1 + Egen - Att1 + Epow) = -Egen + Att1 - Epow

In measurement 2 the generator level is set to **Pgen2 = Pwanted + Ccorr =**

Pwanted -Egen + Att1 - Epow dBm

The level at the EUT connector in the actual measurement is

Peut = Pgen2 + Egen + dEgen + Elog - Att1 - dAtt1 =

Pwanted - Egen + Att1 - Epow + Egen + dEgen + Elog - Att1 - dAtt1 =

Pwanted - Epow + dEgen + Elog - dAtt1

As can be seen from the calculated result, again all static errors in the combined measurement except the power meter error have cancelled. Apart from that only the drift and linearity errors remain.

The remaining errors are:

- the absolute uncertainty of the power meter;
- the linearity (or log fidelity) of the signal generator due to the fact that the level setting of the generator in actual measurement may be different from the level setting in the path compensation;
- change of the insertion loss between the path compensation and the actual measurement including repeatability of the switches in the switch unit.

Since the path compensation is performed at descrite frequencies there is an additional error

- error due to interpolation between correction factors at different frequencies.

Finally, in addition to the uncertainties mentioned there is a mismatch uncertainty in each measurement.

The mismatch uncertainty is analysed in clause 6.8.3.2.2.

6.8.3.2.2 Mismatch uncertainty

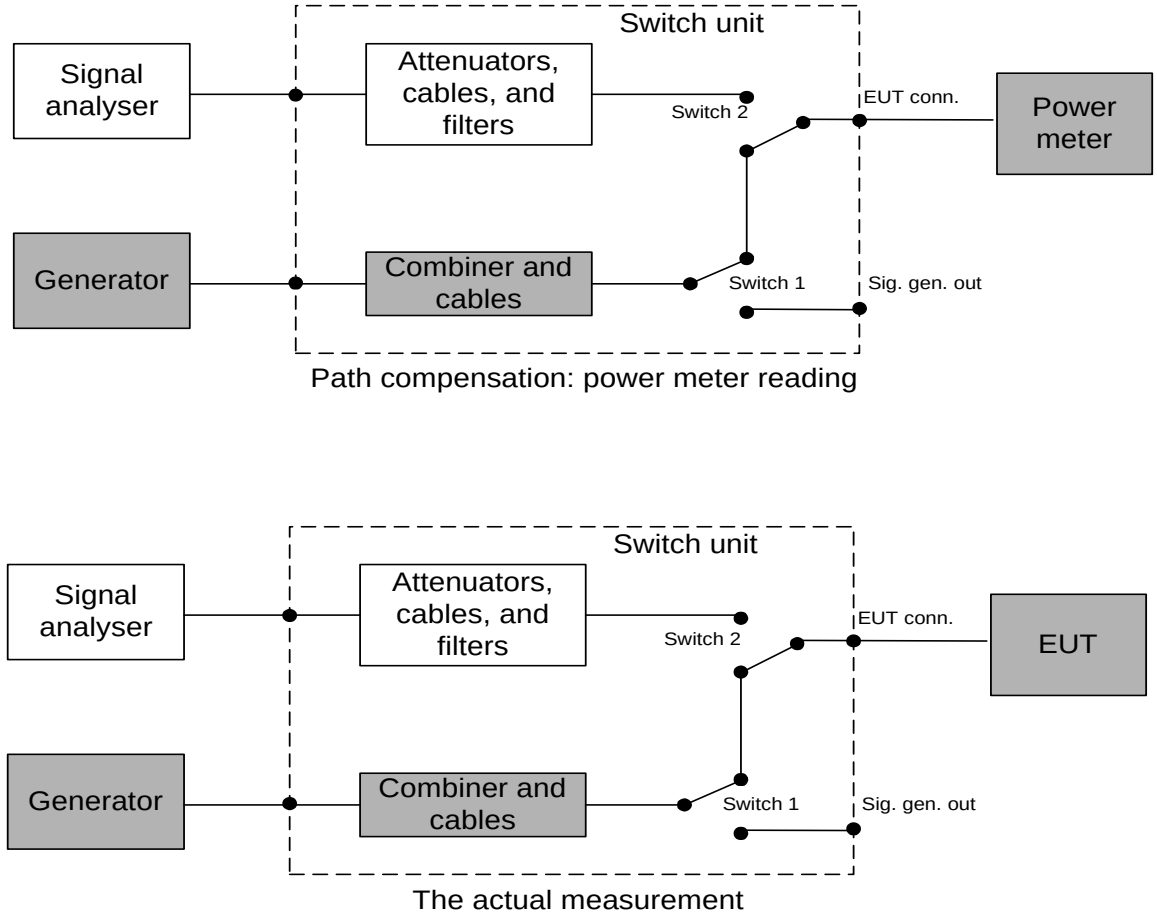

Figure 23: The two set-ups in a receiver measurement

As can be seen from figure 23, performing a similar analysis as with the transmitter measurement, the remaining mismatch uncertainty from the first measurement is the combination of all the mismatch uncertainties associated with the power meter, and from the actual measurement all the mismatch uncertainties associated with the EUT.

Again, based on this the calculation of the total mismatch uncertainty can be done in two ways.

If all VSWRs and insertion losses (or gains) of the individual components in the test system are known all the contributions can be calculated and combined.

But a more simple approach is to measure (or estimate by other methods) the reflection coefficient **Ro** of the EUT connector, measure (or take from the specification sheet) the reflection coefficient **Rp** of the power meter, and measure (or estimate) the reflection coefficient **Reut** of the EUT.

If these 3 reflection coefficients are known, the total uncertainty is the combination of

- **Ro*Rp/√2** (from the path compensation)
- **Reut*Rp//√2** (from the actual measurement)

Again exactly the same result as if the measurement had been done manually with a generator and power meter if the switch unit paths are considered as parts of the individual instruments.

For the "simple" test system it was not necessary to go through this lengthy analysis to get the uncertainty, because the analogy to the simple measurements can be directly seen. But the method is important to understand and to use, because it is needed for the analysis of more complex test systems where the similarity to simple measuring set-ups does not exist.

6.8.4 The "complex" test system

As the "simple" test system, the "complex" system consists of a set of measuring instruments and a switch unit.

And as with the "simple" test system the RF level traceability is provided by very accurate power meters rather than the other RF instruments.

The main difference between the "simple" and the "complex" test system is that the path compensation procedures and RF level setting procedures are more complex and involve reference and switch points inside the switch unit, which cannot be accessed from the outside.

The benefit is that most of the path compensation procedures can be done directly in connection with the actual measurements without need of test operator intervention. This reduces the potential stability errors which can be present in measurements with "simple" test systems due to the time between path compensation and measurements.

The error sources are generally the same for the two types of test systems, and the methods used to perform the analysis are the same, but the mismatch uncertainty is very complex, and can be difficult to estimate.

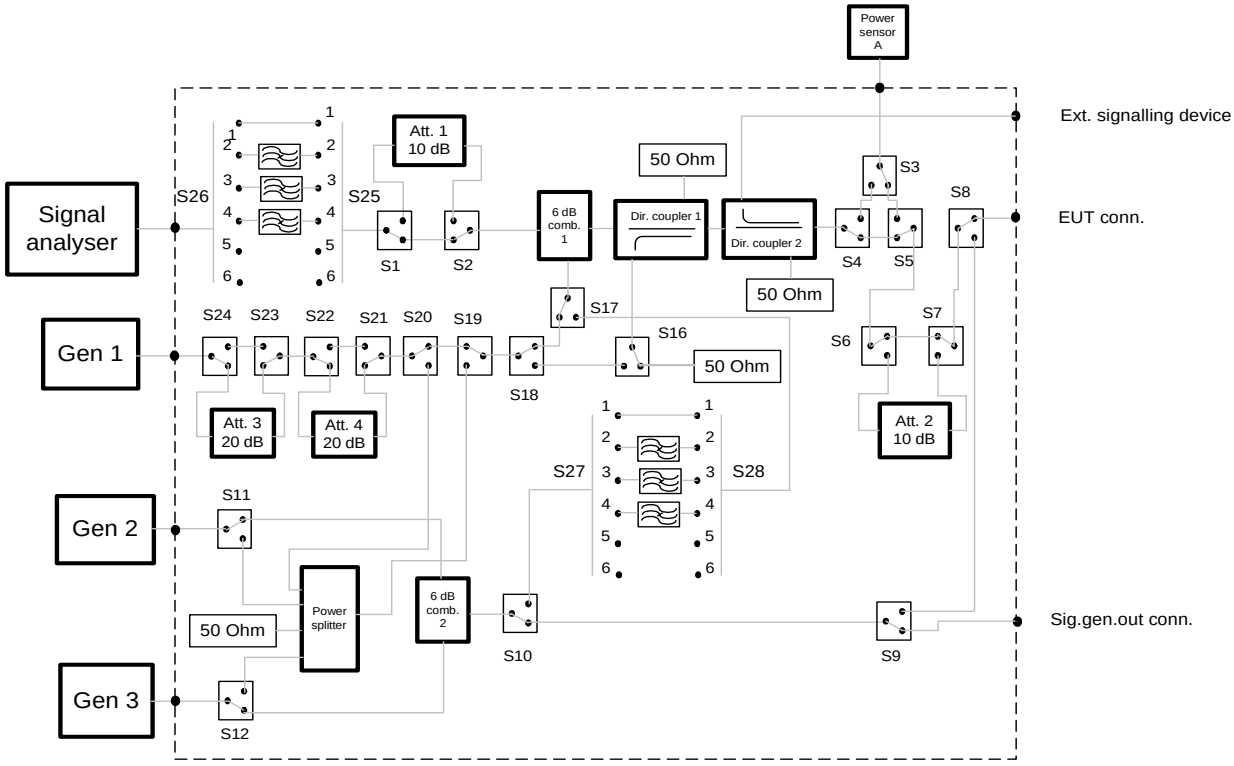

Figure 24: A complex test system

Figure 24 shows a "complex" type of test system which is capable of doing all normal RF measurements. More complicated test systems exist, but the following analysis will be similar for all of them.

The path compensation for this test system consists of two procedures: an external path compensation procedure which requires the test operator to connect cables and power meter to some external connectors and an internal path compensation procedure. This external path compensation characterizes a small part of the switch unit consisting of only cables, attenuators, and switches - in other words passive components which can be assumed to be stable over a relatively long time period. For transmitter measurements this part of the switch unit is the part from switch S5 to the EUT connector.

For receiver measurements it is the part between switch S4 and the EUT connector.

The rest of the switch unit and the instruments are covered by internal path compensation procedures which do not require test operators intervention, and they are run prior to the actual measurements as an integral part of each test. As with the "simple" test system the traceability is provided by an external power meter, which is the only instrument where the absolute uncertainty is important. Any systematic errors in the other instruments are compensated for.

The error sources are basically the same as with the "simple" test system:

- Absolute power meter uncertainty
- Instruments stability
- Instruments linearity
- Mismatch between the instruments and the individual components of the switch unit.
- Errors due to interpolation between correction factors at different frequencies

The difference compared to a "simple" test system is that the mismatch uncertainty is more complex because there are more procedures involved in the testing and path compensations and because some of the reflection coefficients of interest are inside the switch unit. To measure them, the switch unit would have to be disassembled.

6.8.4.1 Receiver measurements

For the purpose of analysing receiver measurements the "complex" test system can be simplified as shown in figure 25:

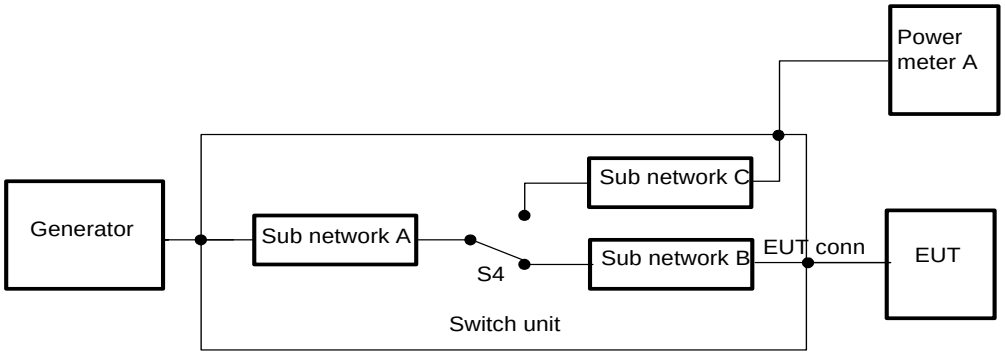

Figure 25: Model for analysis of receiver measurements

In figure 25:

Sub network A consists of everything between a generator and switch S4.

Sub network B consists of everything between switch S4 and the EUT connector.

Sub network C consists of everything between switch S4 and power meter A.

Each sub network contains cables, switches, attenuators, filters, and other components.

The external path compensation is performed as follows. This is not done in connection with every measurement, but may be done with for instance 3 month intervals.

Measurement 1:

A power meter (power meter B) is connected to the EUT connector. Switch S4 is set so the generator is connected to power meter B.

The RF generator is set to a level which gives a reading in the operational range of the power meter. When one generator is active the others are turned down, so they do not contribute to the measurement, but their output impedance is still 50 Ω. A series of measurements covering the frequency range of interest is done and for each frequency the reading are stored by the test system.

Measurement 2:

1) Then switch S4 is set so the generator is connected to power meter A.
2) For all the frequencies and generator level settings in measurement 1 step 2 the power level is measured by power meter A. The readings are stored by the test system.

3) For each frequency the correction factor is calculated as the difference (in dB) between the reading from power meter B and power meter A. These are the external correction factors (path compensation data) stored by the test system.

The internal path compensation is performed as follows. This is done immediately prior to every measurement as an integral part of the test case.

Measurement 3:

Switch S4 is set so the generator is connected to power meter A.

Then the RF generator is set to a level which gives a reading in the operational range of the power meter. When one generator is active the others are turned down, so they do not contribute to the measurement, but their output impedance is still 50 Ω. A series of power meter readings and generator level settings covering the frequency range of interest is done and for each frequency the reading and setting are stored by the test system.

For each frequency the correction factor is calculated as the difference (in dB) between the power meter reading and the generator level setting. These are the internal correction factors (path compensation data) stored by the test system.

The actual test is performed as follows. (For 2 or 3 signal measurements the following level setting procedure is done for each signal generator).

Measurement 4:

The EUT is connected to the EUT connector.

Switch S4 is set so the generator is connected to the EUT connector.

The generator is set to the wanted signal level (in dBm) minus the external and the internal correction factor at the appropriate frequency. (If a correction factor at the measuring frequency does not exist it is found by interpolation between the two correction factors at the nearest frequencies on each side).

Then the appropriate receiver measurement is done (BER or signal-to-noise ratio).

6.8.4.1.1 Error analysis

The combined path compensation procedure and the actual test consists of 4 individual measurements as shown in figure 26 to figure 28: two measurements in the external the path compensation part, one in the internal path compensation and one in the actual measurement.

In each of the 4 measurements a signal source is connected to a measuring instrument through a network consisting of several components and a level is measured.

In the following the total procedure is analysed.

The following assumptions apply for the analysis:

- The generator has a static error of **Egen1** dB in the measurement 1 (compared to the setting of the generator level)
- Between measurement 1 and measurement 2 there is a generator drift error **dEgen1** dB
- The generator has a static error of **Egen2** dB in the measurement 3 (compared to the setting of the generator level)
- Between measurement 3 and measurement 4 there is a generator drift and linearity error **dEgen2** dB (the generator level may not be the same in the path compensation and the measurement - therefore the linearity/log fidelity error)
- The attenuation between the generator and the switch S4 is **AttD** dB in measurement 1
- Between measurement 1 and measurement 2 there is an attenuation change in **AttD** of **dAttD** dB
- The attenuation between the input of switch S4 and the EUT connector is **AttB** dB in measurement 1
- Between measurement 1 and measurement 4 there is an attenuation change in **AttB** of **dAttB** dB

- The attenuation between the input of switch S4 and power meter A is **AttC** dB in measurement 2
- Between measurement 2 and measurement 3 there is an attenuation change in **AttC** of **dAttC** dB
- The attenuation between the generator and the switch S4 is **AttA** dB in measurement 3
- Between measurement 3 and measurement 4 there is an attenuation change in **AttA** of **dAttA** dB
- There is a static error of **EpowA** dB in the power meter A measurement in measurement 2
- Between measurement 2 and measurement 3 there is a change in **EpowA** of **dEpowA**
- The generator level is set to **Pgen1** dBm in measurement 1 and 2
- The generator level is set to **Pgen2** dBm in measurement 3
- The generator level is set to **Pgen3** dBm in measurement 4
- The wanted level at the EUT connector is **Pwanted** dBm in the actual measurement

In measurement 1 the reading from power meter B is:

P1 = Pgen1 + Egen1 - AttD - AttB + EpowB

In measurement 2 the reading from power meter A is:

P2 = Pgen1 + Egen1 + dEgen1 - AttD - dAttD - AttC + EpowA

The external correction factor

Ccorr1 = P1 - P2 =

(Pgen1+Egen1-AttD-AttB+EpowB) - (Pgen1+Egen1+dEgen1-AttD-dAttD-AttC+EpowA) =

-dEgen1 + dAttD + AttC - EpowA - AttB + EpowB

In measurement 3 the reading from power meter A is

P3 = Pgen2+Egen2-AttA-AttC-dAttC+EpowA+dEpowA

The internal correction factor

Ccorr2 = P3 - Pgen2 = Pgen2+Egen2-AttA-AttC-dAttC+EpowA+dEpowA - Pgen2 =

Egen2-AttA-AttC-dAttC+EpowA+dEpowA

In measurement 4 (the actual measurement) the generator level is set to:

Pgen3 = Pwanted - Ccorr1 - Ccorr2

The level at the EUT connector is:

P4 = Pgen3 + Egen2 + dEgen2 - AttA - dAttA - AttC - dAttC =

Pwanted - Ccorr1 - Ccorr2 + Egen2 + dEgen2 - AttA - dAttA - AttB - dAttB =

Pwanted - (-dEgen1 + dAttD + AttC - EpowA - AttB + EpowB) - (Egen2 - AttA - AttC - dAttC + EpowA + dEpowA) + Egen2 + dEgen2 - AttA - dAttA - AttB - dAttB =

Pwanted + dEgen1 - dAttD - EpowB +dAttC - dEpowA + dEgen2 - dAttA - dAttB

Again, as can be seen from the calculated result, again static errors in the combined measurement except the power meter B error have cancelled. Apart from that only the drift and linearity errors remain.

The remaining errors are:

- the absolute uncertainty of the power meter
- the linearity (or log fidelity) of the signal generator due to the fact that the level setting of the generator in actual measurement may be different from the level setting in the path compensation
- change of the insertion loss between the path compensation and the actual measurement including repeatability of the switches in the switch unit

Since the path compensation is performed at descrite frequencies there is an additional error

- error due to interpolation between correction factors at different frequencies

Finally, in addition to the uncertainties mentioned there is a mismatch uncertainty in each measurement.

The mismatch uncertainty is analysed in clause 6.8.4.1.2.

6.8.4.1.2 Mismatch uncertainties

For the analysis of the overall mismatch uncertainty, firstly the external path compensation is analysed. The settings are shown on figure 26. (The reason for introducing sub network D is that it is not necessarily the same sub network used in the actual measurement):

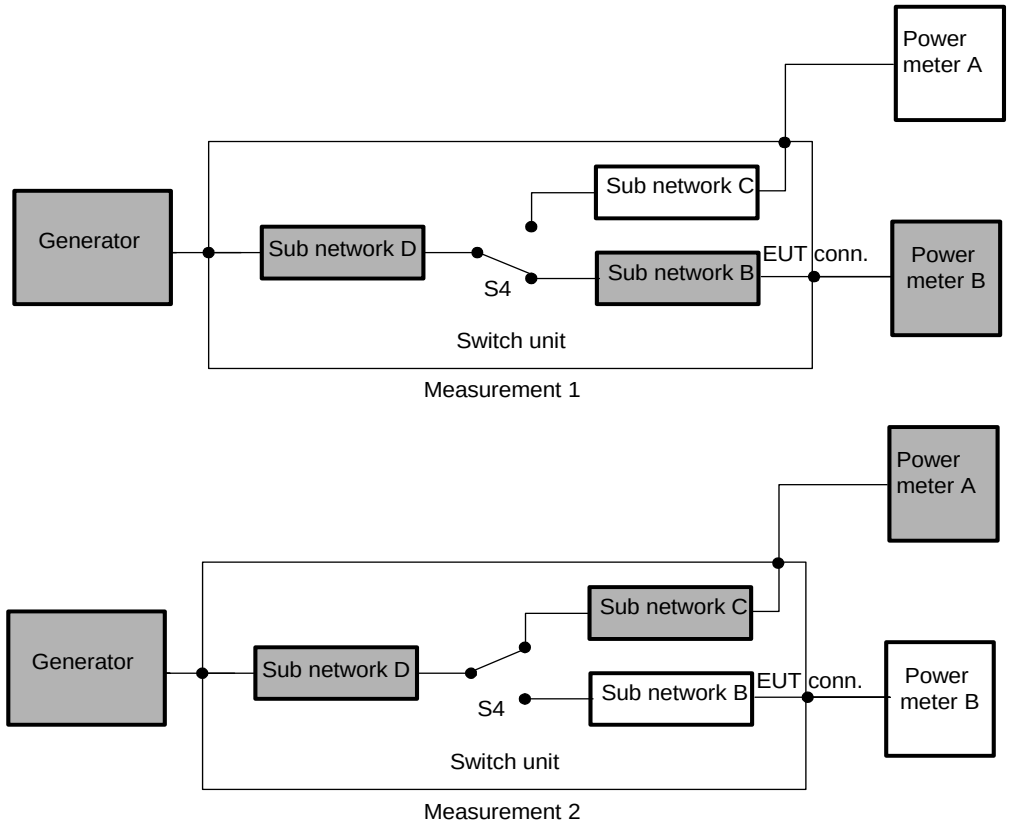

Figure 26: The external path compensation

In the power meter B reading (measurement 1) the following mismatch uncertainties contribute to the reading:

- Between Generator and sub network D
- Between sub network D and switch S4
- Between switch S4 and sub network B
- Between sub network B and power meter B

- Between **Generator** and **switch S4** (through sub network D)
- Between sub network D and sub network B
- Between switch S4 and power meter B
- Between **Generator** and **sub network B** (through sub network D)
- Between sub network D and power meter B
- Between **Generator** and **power meter B** (through sub network D)

In the power meter A reading (measurement 2) the following mismatch uncertainties contribute to the reading:

- Between Generator and sub network D
- Between sub network D and switch S4
- Between switch S4 and sub network C
- Between sub network C and power meter A
- Between **Generator** and **switch S4** (through sub network D)
- Between sub network D and sub network C
- Between switch S4 and power meter A
- Between **Generator** and **sub network C** (through sub network D)
- Between sub network D and power meter A
- Between **Generator** and **power meter A** (through sub network D)

As can be seen some of the mismatch uncertainties are part of both measurements (between Generator and switch S4), so they cancel. The following mismatch uncertainties remain:

- Between switch S4 and sub network B
- Between sub network B and power meter B
- Between sub network D and sub network B
- Between switch S4 and power meter B
- Between **Generator** and **sub network B** (through sub network D)
- Between sub network D and power meter B
- Between **Generator** and **power meter B** (through sub network D)
- Between switch S4 and sub network C
- Between sub network C and power meter A
- Between sub network D and sub network C
- Between switch S4 and power meter A
- Between **Generator** and **sub network C** (through sub network D)
- Between sub network D and power meter A
- Between **Generator** and **power meter A** (through sub network D)

Some of these uncertainties will cancel later in the process. Then the internal path compensation (with settings as shown in figure 27) is analysed:

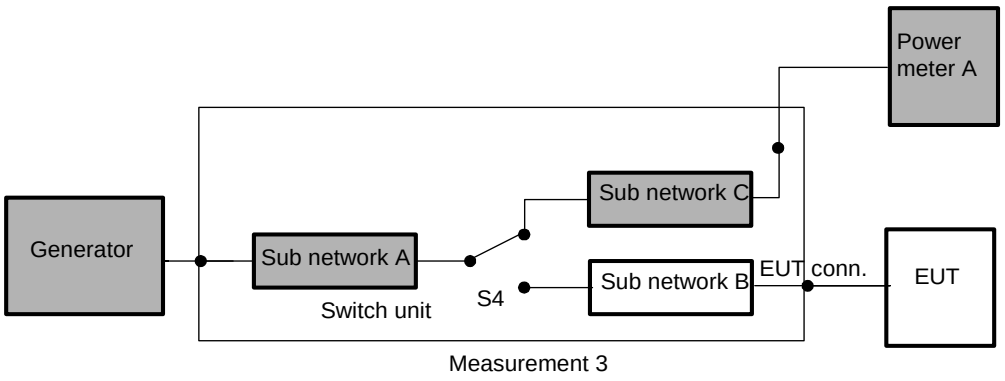

Figure 27: The internal path compensation

In the internal path compensation (measurement 3) the following mismatch uncertainties contribute to the reading:

- Between Generator and sub network A
- Between sub network A and switch S4
- Between switch S4 and sub network C
- Between sub network C and power meter A
- Between **Generator** and **switch S4** (through sub network A)
- Between sub network A and sub network C
- Between switch S4 and power meter A
- Between **Generator** and **sub network C** (through sub network A)
- Between sub network A and power meter A
- Between **Generator** and **power meter A** (through sub network A)

As can be seen, again, some of the mismatch uncertainties are part of both the internal and the external path compensation (between switch S4 and power meter A), so they cancel.

The following mismatch uncertainties remain from the total path compensation:

- Between switch S4 and sub network B
- Between sub network B and power meter B
- Between sub network D and sub network B
- Between switch S4 and power meter B
- Between **Generator** and **sub network B** (through sub network D)
- Between sub network D and power meter B
- Between **Generator** and **power meter B** (through sub network D)
- Between sub network D and sub network C
- Between switch S4 and power meter A
- Between **Generator** and **sub network C** (through sub network D)
- Between sub network D and power meter A

- Between **Generator** and **power meter A** (through sub network D)
- Between Generator and sub network A
- Between sub network A and switch S4
- Between **Generator** and **switch S4** (through sub network A)
- Between sub network A and sub network C
- Between switch S4 and power meter A
- Between **Generator** and **sub network C** (through sub network A)
- Between sub network A and power meter A
- Between **Generator** and **power meter A** (through sub network A)

Again, some of these uncertainties will cancel later in the process.

Then the actual measurement (with settings as shown in figure 28) is analysed:

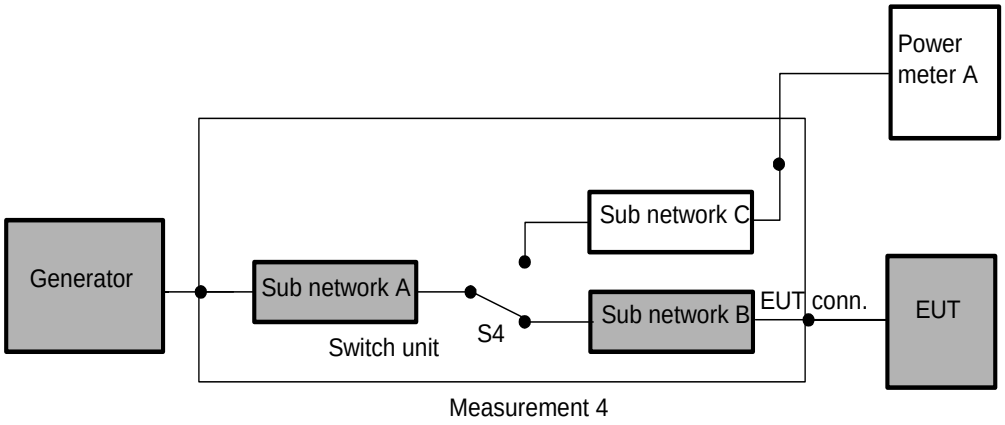

Figure 28: The actual measurement

In the actual measurement (measurement 4) the following mismatch uncertainties contribute:

- Between Generator and sub network A
- Between sub network A and switch S4
- Between switch S4 and sub network B
- Between sub network B and the EUT
- Between **Generator** and **switch S4** (through sub network A)
- Between sub network A and sub network B
- Between switch S4 and the EUT
- Between **Generator** and **sub network B** (through sub network A)
- Between sub network A and the EUT
- Between **Generator** and **the EUT** (through sub network A)

As can be seen, again, some of the mismatch uncertainties are part of both path compensation and the actual measurement (between switch S4 and sub network B), so they cancel.

The following mismatch uncertainties remain in the total measurement:

- Between sub network B and power meter B
- Between sub network D and sub network B
- Between switch S4 and power meter B
- Between **Generator** and **sub network B** (through sub network D)
- Between sub network D and power meter B
- Between **Generator** and **power meter B** (through sub network D)
- Between sub network D and sub network C
- Between switch S4 and power meter A
- Between **Generator** and **sub network C** (through sub network D)
- Between sub network D and power meter A
- Between **Generator** and **power meter A** (through sub network D)
- Between sub network A and sub network C
- Between switch S4 and power meter A
- Between **Generator** and **sub network C** (through sub network A)
- Between sub network A and power meter A
- Between **Generator** and **power meter A** (through sub network A)
- Between sub network B and the EUT
- Between sub network A and sub network B
- Between switch S4 and the EUT
- Between **Generator** and **sub network B** (through sub network A)
- Between sub network A and the EUT
- Between **Generator** and **the EUT** (through sub network A)

6.8.4.2 Transmitter measurements

For the purpose of analysing receiver measurements the test system can be simplified as showed in figure 29:

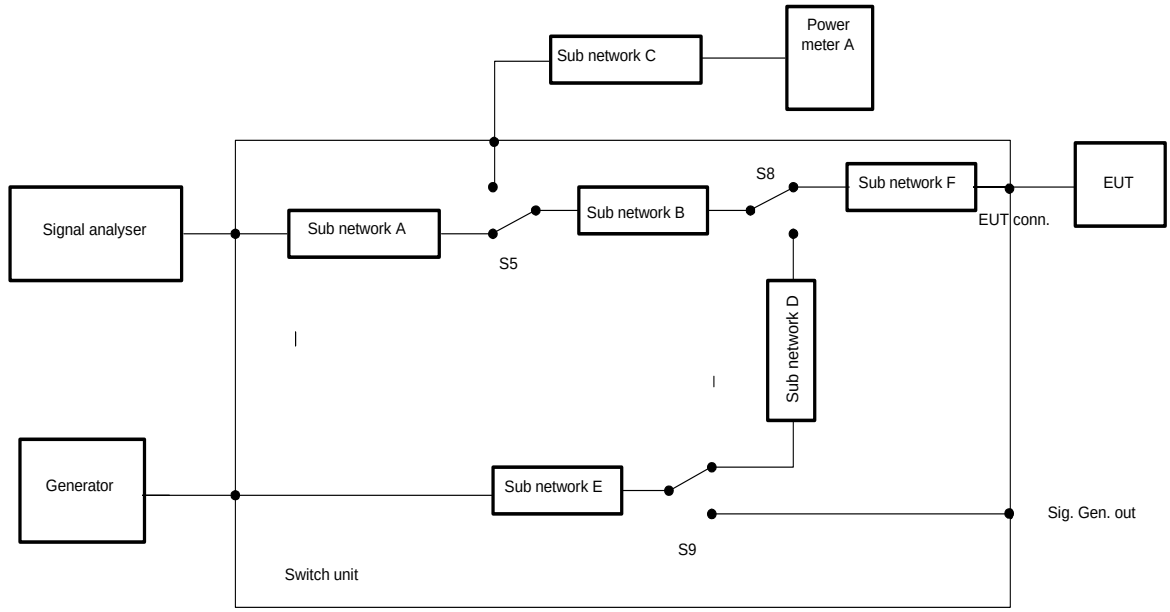

Figure 29: Model for analysis of transmitter measurements

In figure 29:

- Sub network A consists of all components and cables between the signal analyser and switch S5
- Sub network B consists of all components and cables between switch S5 and switch S8
- Sub network C consists of all components and cables between switch S5 and power meter A
- Sub network D consists of all components and cables between switch S9 and switch S8
- Sub network E consists of all components and cables between switch S9 and Generator
- Sub network F consists of all components and cables between switch S8 and the EUT connector
- Sub network G (not shown on this figure) consists of all components and cables between switch S9 and power meter B (including an external cable and a 10 dB attenuator)

The external path compensation is performed as follows. This is not done in connection with every measurement, but may be done with for instance 3 month intervals.

Measurement 1:

Power meter B is connected to the sig. gen. out connector through a cable and a 10 dB attenuator. Switch S9 is set so the generator is connected to the sig. gen. out connector.

Then the RF generator is set to a level which gives a reading in the operational range of the power meter. When one generator is active the others are turned down, so they do not contribute to the measurement, but their output impedance is still 50 Ω. A series of power meter readings and generator level settings covering the frequency range of interest is done and for each frequency the reading and setting are stored by the test system.

Measurement 2:

Then power meter B is removed and the 10 dB attenuator are connected to the EUT connector. Switch S5 and S8 are set so the generator is connected to power meter A through the 10 dB attenuator.

For all the frequencies and generator level settings in step 2 the power level is measured by power meter A. The readings are stored by the test system

For each frequency point the correction factor is calculated as the difference (in dB) between the reading from power meter A and power meter B. These are the external correction factors (path compensation data) stored by the test system.

The internal path compensation is performed as follows. This is done prior to every measurement as an integral part of the test case.

Measurement 3:

Switch S5, S8, and S9 are set so the generator is connected to power meter A through sub network D.

Then the RF generator is set to a level which gives a reading in the operational range of the power meter. When one generator is active the others are turned down, so they do not contribute to the measurement, but their output impedance is still 50 Ω. A series of power meter readings and generator level settings covering the frequency range of interest is done and for each frequency the reading and setting are stored by the test system.

Measurement 4:

Then switch S5 is set so the generator is connected to the signal analyser.

For all the frequencies and generator level settings in step 2 the power level is measured by the signal analyser. The readings are stored by the test system

For each frequency point the correction factor is calculated as the difference (in dB) between the reading from the signal analyser and power meter A. These are the internal correction factors (path compensation data) stored by the test system.

The actual test is performed as follows.

Measurement 5:

The EUT is connected to the EUT connector.

Switch S5 and S8 are set so the EUT is connected to the signal analyser.

The relevant power level generated by the EUT is measured, and the reading from the signal analyser is stored by the test system.

The final result is then calculated as the reading from step 3 (in dBm) minus the external and the internal correction factors at the appropriate frequency from step 3. (If a correction factor at the measuring frequency does not exist it is found by interpolation between the two correction factors at the nearest frequencies on each side).

6.8.4.2.1 Error analysis

The combined path compensation procedure and the actual test described consist of 5 individual measurements as shown in figure 30 to figure 32: two measurements in external the path compensation part, two in the internal path compensation and one in the actual measurement.

In each of the 5 measurements a signal source is connected to a measuring instrument through a network consisting of several components and a level is measured.

In the following the total procedure is analysed.

The following assumptions apply for the analysis:

- The generator has a static error of **Egen1** dB in measurement 1 (compared to the setting of the generator level).
- Between measurement 1 and measurement 2 there is a generator drift **dEgen1** dB.
- The generator has a static error of **Egen2** dB in measurement 3 (compared to the setting of the generator level).
- Between measurement 3 and measurement 4 there is a generator drift **dEgen2** dB.

- The attenuation between the generator and the switch S9 is **AttE1** dB in measurement 1.
- Between measurement 1 and measurement 2 there is an attenuation change in **AttE1** of **dAttE1** dB.
- The attenuation between the generator and the switch S9 is **AttE2** dB in measurement 3.
- Between measurement 3 and measurement 4 there is an attenuation change in **AttE2** of **dAttE2** dB.
- The attenuation of switch S9 and sub network G is **AttG** dB in measurement 1.
- Between measurement 1 and measurement 2 there is an attenuation change in **AttG** of **dAttG** dB.
- The attenuation of switch S8 and sub network F is **AttF** dB in measurement 2.
- Between measurement 2 and measurement 5 there is an attenuation change in **AttF** of **dAttF** dB.
- The attenuation of switch S8, switch S9 and sub network D is **AttD** dB in measurement 3.
- Between measurement 3 and measurement 4 there is an attenuation change in **AttD** of **dAttD** dB.
- The attenuation of sub network B is **AttB** dB in measurement 2.
- Between measurement 2 and measurement 3 there is an attenuation change in **AttB** of **dAttB1** dB.
- Between measurement 2 and measurement 4 there is an attenuation change in **AttB** of **dAttB2** dB.
- Between measurement 2 and measurement 5 there is an attenuation change in **AttB** of **dAttB3** dB.
- The attenuation between sub network B and power meter A is **AttC** dB in measurement 2.
- Between measurement 2 and measurement 3 there is an attenuation change in **AttC** of **dAttC** dB.
- The attenuation between sub network B and the signal analyser is **AttA** in measurement 4.
- Between measurement 4 and measurement 5 there is an attenuation change in **AttA** of **dAttA** dB.
- There is a static error of **EpowA** dB in power meter A in measurement 2.
- Between measurement 2 and measurement 3 there is a change in **EpowA** of **dEpowA**.
- There is a static error of **EpowB** dB in power meter B in measurement 1.
- The generator level is set to **Pgen1** dBm in measurement 1 and 2..
- The generator level is set to **Pgen2** dBm in measurement 3 and 4.
- The signal analyser error is **Esa** in measurement 4.
- Between measurement 4 and measurement 5 there is a drift and log fidelity error in **Esa** of **dEsa**.
- The EUT is generating a power level of **Peut** in the actual measurement.

In measurement 1 the reading from power meter B is:

P1 = Pgen1 + Egen1 - AttE1 - AttG + EpowB

In measurement 2 the reading from power meter A is:

P2 = Pgen1 + Egen1 + dEgen1 - AttE1 - dAttE1 - AttG - dAttG -AttF - AttB - AttC + EpowA

The external correction factor is:

Ccorr1 = P2 - P1 =

(Pgen1 + Egen1 + dEgen1 - AttE1 - dAttE1 - AttG -dAttG -AttF - AttB - AttC + EpowA) - (Pgen1 + Egen1 - AttE1 - AttG + EpowB) =

dEgen1 - dAttE1 - dAttG - AttF - AttB - AttC + EpowA - EpowB

In measurement 3 the reading from power meter A is

P3 = Pgen2+Egen2-AttE2-AttD-dAttB- dAttB1 - AttC - dAttC + EpowA + dEpowA

In measurement 4 the reading from the signal analyser is:

P4 = Pgen2+Egen2-AttE2-AttD-dAttB- dAttB2-AttA + Esa

The internal correction factor

Ccorr2 = P4 - P3 =

Pgen2+Egen2-AttE2-AttD-dAttB- dAttB2-AttA + Esa - (Pgen2+Egen2-AttE2-AttD-dAttB- dAttB1 - AttC - dAttC + EpowA + dEpowA) =

-dAttB - dAttB2 - AttA + Esa +dAttB- dAttB1 + AttC + dAttC - EpowA - dEpowA

In measurement 5 (the actual measurement) the reading from the signal analyser is:

P5 = Peut - AttF - dAttF - AttB - dAttB3 - AttA - dAttA + Esa + dEsa

The result of the measurement is:

P5 - Ccorr1 - Ccorr2 =

(Peut - AttF - dAttF - AttB - dAttB3 - AttA - dAttA + Esa + dEsa) - (dEgen1 - dAttE1 - dAttG -AttF - AttB - AttC + EpowA - EpowB) - (-dAttB- dAttB2-AttA + Esa +dAttB- dAttB1 + AttC + dAttC - EpowA - dEpowA) =

Peut - dAttF - dAttB3 - dAttA + dEsa - dEgen1 + dAttE1 + dAttG + EpowB + dAttB + dAttB2 -dAttB+ dAttB1 - dAttC + dEpowA

Again, as can be seen from the calculated result, again static errors in the combined measurement except the power meter B error have cancelled. Apart from that only the drift and linearity errors remain.

The remaining errors are:

- the absolute uncertainty of external power meter B;
- the drift and linearity (or log fidelity) errors of the signal generator, the internal power meter A and the signal analyser;
- change of the insertion loss between the various measurements including repeatability of the switches in the switch unit.

Since the path compensation is performed at discrete frequencies there is an additional error:

- error due to interpolation between correction factors at different frequencies.

Finally, in addition to the uncertainties mentioned there is a mismatch uncertainty in each measurement.

The mismatch uncertainty is analysed in clause 6.8.4.2.2.

6.8.4.2.2 Mismatch uncertainties

For the analysis of the mismatch uncertainty, firstly the external path compensation is analysed.

It consists of two measurements, and the settings are shown in figure 30:

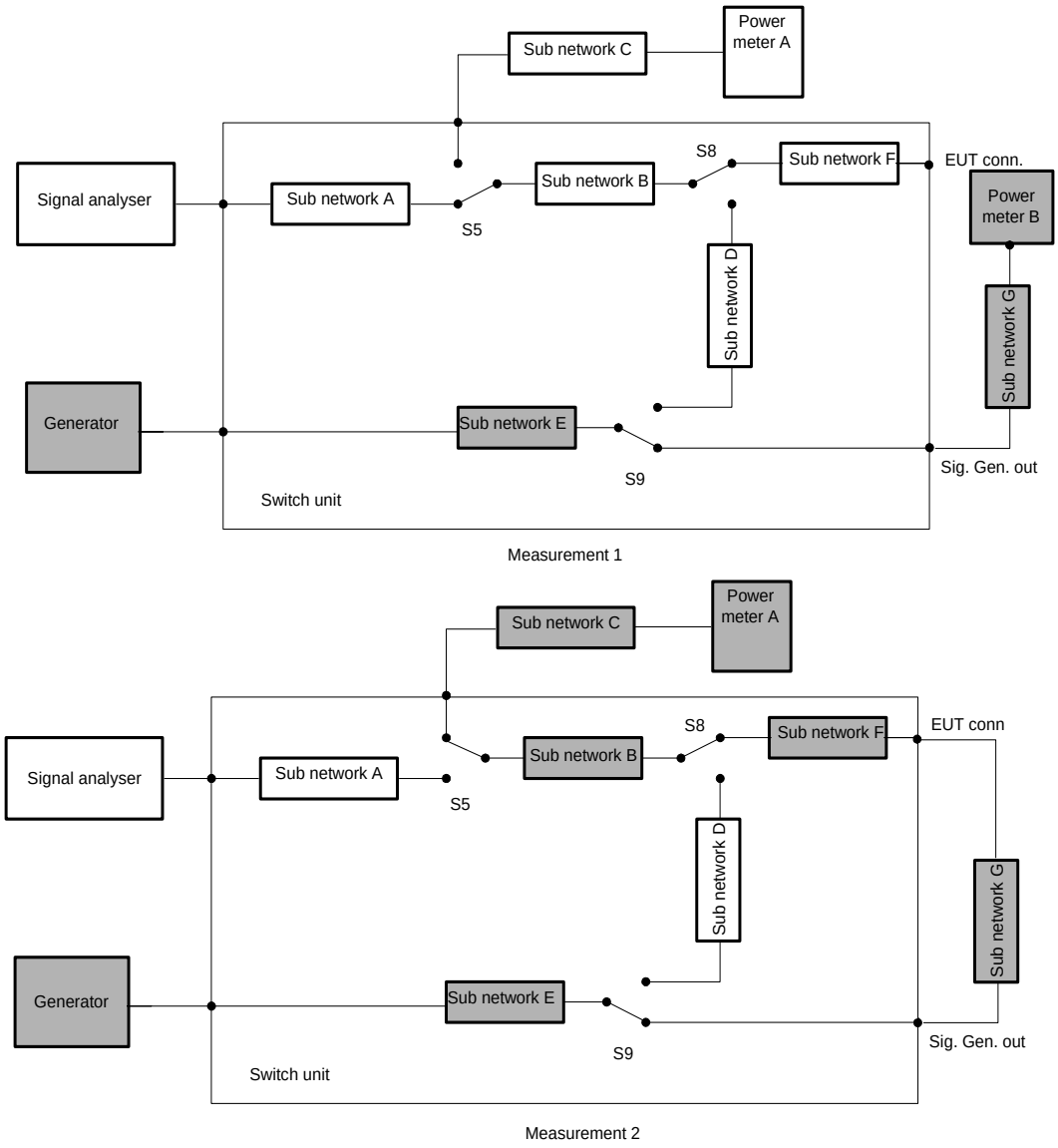

Figure 30: External path compensation

In the power meter B reading (measurement 1) the following mismatch uncertainties contribute:

- Between Generator and sub network E
- Between sub network E and switch S9
- Between switch S9 and sub network G
- Between sub network G and power meter B
- Between Generator and switch S9
- Between sub network E and sub network G
- Between switch S9 and power meter B
- Between **Generator** and **sub network G** (through sub network E)

- Between sub network E and power meter B
- Between Generator and power meter B

In the power meter A reading (measurement 2) the following mismatch uncertainties contribute:

- Between Generator and sub network E
- Between sub network E and switch S9
- Between switch S9 and sub network G
- Between sub network G and sub network F
- Between sub network F and switch S8
- Between switch S8 and sub network B
- Between sub network B and switch S5
- Between switch S5 and sub network C
- Between sub network C and power meter A
- Between Generator and switch S9
- Between sub network E and sub network G
- Between switch S9 and sub network F
- Between sub network G and switch S8
- Between sub network F and sub network B
- Between switch S8 and switch S5
- Between sub network B and sub network C
- Between switch S5 and power meter A
- Between Generator and sub network G
- Between sub network E and sub network F
- Between switch S9 and switch S8
- Between sub network G and sub network B
- Between sub network F and switch S5
- Between switch S8 and sub network C
- Between sub network B and power meter A
- Between Generator and sub network F
- Between sub network E and switch S8
- Between switch S9 and sub network B
- Between sub network G and switch S5
- Between sub network F and sub network C
- Between switch S8 and power meter A
- Between Generator and switch S8
- Between sub network E and sub network B

- Between switch S9 and switch S5
- Between sub network G and sub network C
- Between sub network F and power meter A
- Between Generator and sub network B
- Between sub network E and switch S5
- Between switch S9 and sub network C
- Between sub network G and power meter A
- Between Generator and switch S5
- Between sub network E and sub network C
- Between switch S9 and power meter A
- Between Generator and sub network C
- Between sub network E and power meter A
- Between Generator and power meter A

As can be seen some of the mismatch uncertainties are part of both measurements (between Generator and sub network G), so they cancel.

The following mismatch uncertainties remain:

- Between sub network G and power meter B
- Between switch S9 and power meter B
- Between sub network E and power meter B
- Between Generator and power meter B
- Between sub network G and sub network F
- Between sub network F and switch S8
- Between switch S8 and sub network B
- Between sub network B and switch S5
- Between switch S5 and sub network C
- Between sub network C and power meter A
- Between switch S9 and sub network F
- Between sub network G and switch S8
- Between sub network F and sub network B
- Between switch S8 and switch S5
- Between sub network B and sub network C
- Between switch S5 and power meter A
- Between sub network E and sub network F
- Between switch S9 and switch S8
- Between sub network G and sub network B

- Between sub network F and switch S5
- Between switch S8 and sub network C
- Between sub network B and power meter A
- Between Generator and sub network F
- Between sub network E and switch S8
- Between switch S9 and sub network B
- Between sub network G and switch S5
- Between sub network F and sub network C
- Between switch S8 and power meter A
- Between Generator and switch S8
- Between sub network E and sub network B
- Between switch S9 and switch S5
- Between sub network G and sub network C
- Between sub network F and power meter A
- Between Generator and sub network B
- Between sub network E and switch S5
- Between switch S9 and sub network C
- Between sub network G and power meter A
- Between Generator and switch S5
- Between sub network E and sub network C
- Between switch S9 and power meter A
- Between Generator and sub network C
- Between sub network E and power meter A
- Between Generator and power meter A

Then the analysis of the mismatch uncertainty from the internal path compensation is performed.

It also consists of two measurements, and the settings are shown in figure 31:

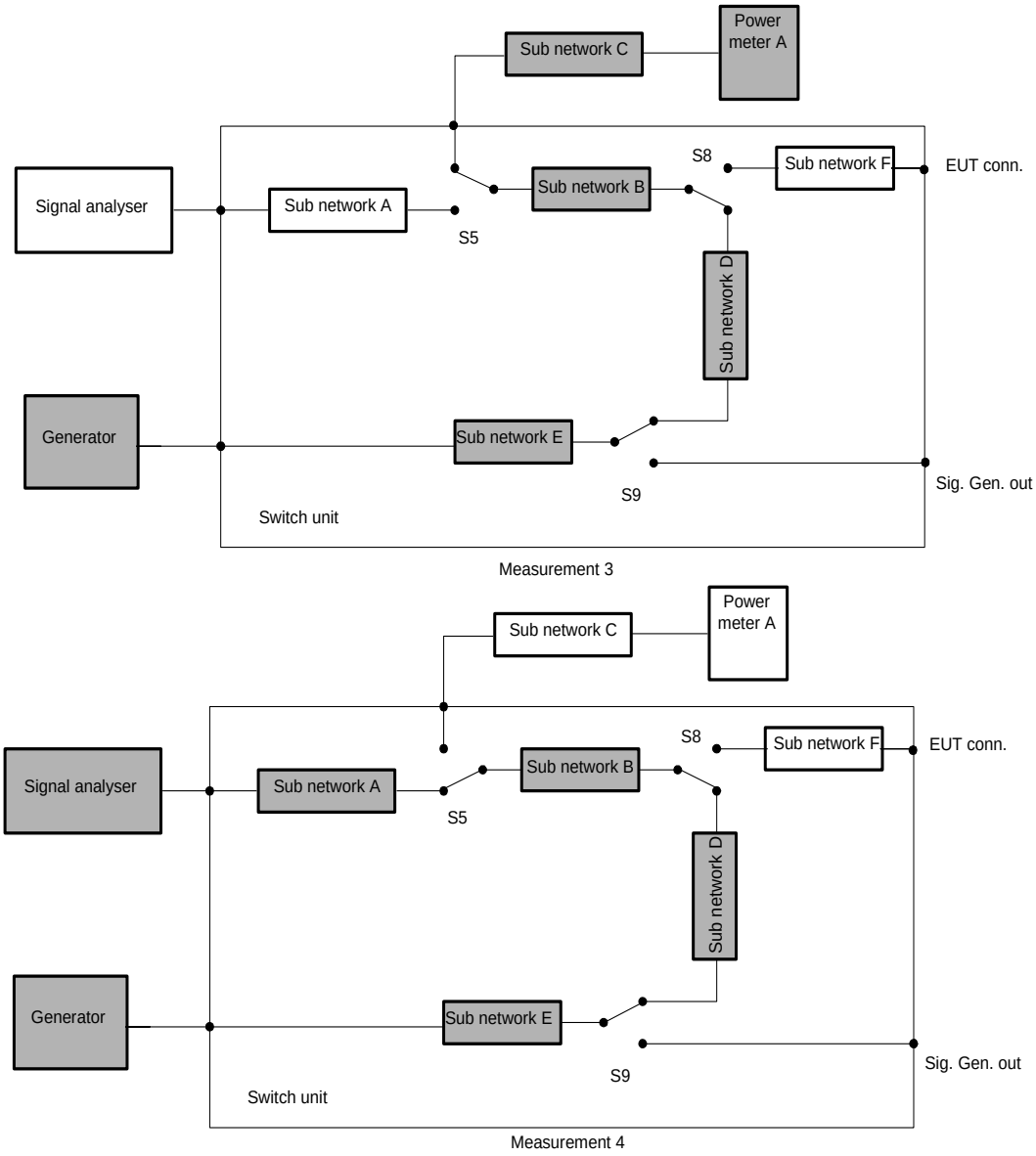

Figure 31: Internal path compensation

In the power meter A reading (measurement 3) the following mismatch uncertainties contribute:

- Between Generator and sub network E
- Between sub network E and switch S9
- Between switch S9 and sub network D
- Between sub network D and switch S8
- Between switch S8 and sub network B
- Between sub network B and switch S5
- Between switch S5 and sub network C
- Between sub network C and power meter A
- Between Generator and switch S9

- Between sub network E and sub network D
- Between switch S9 and switch S8
- Between sub network D and sub network B
- Between switch S8 and switch S5
- Between sub network B and sub network C
- Between switch S5 and power meter A
- Between Generator and sub network D
- Between sub network E and switch S8
- Between switch S9 and sub network B
- Between sub network D and switch S5
- Between switch S8 and sub network C
- Between sub network B and power meter A
- Between Generator and switch S8
- Between sub network E and sub network B
- Between switch S9 and switch S5
- Between sub network D and sub network C
- Between switch S8 and power meter A
- Between Generator and sub network B)
- Between sub network E and switch S5
- Between switch S9 and sub network C
- Between sub network D and power meter A
- Between Generator and switch S5
- Between sub network E and sub network C
- Between switch S9 and power meter A
- Between Generator and sub network C
- Between sub network E and power meter A
- Between Generator and power meter

In the signal analyser reading (measurement 4) the following mismatch uncertainties contribute:

- Between Generator and sub network E
- Between sub network E and switch S9
- Between switch S9 and sub network D
- Between sub network D and switch S8
- Between switch S8 and sub network B
- Between sub network B and switch S5
- Between switch S5 and sub network A

- Between sub network A and signal analyser
- Between Generator and switch S9
- Between sub network E and sub network D
- Between switch S9 and switch S8
- Between sub network D and sub network B
- Between switch S8 and switch S5
- Between sub network B and sub network A
- Between switch S5 and signal analyser
- Between Generator and sub network D
- Between sub network E and switch S8
- Between switch S9 and sub network B
- Between sub network D and switch S5
- Between switch S8 and sub network A
- Between sub network B and signal analyser
- Between Generator and switch S8
- Between sub network E and sub network B
- Between switch S9 and switch S5
- Between sub network D and sub network A
- Between switch S8 and signal analyser
- Between Generator and sub network B
- Between sub network E and switch S5
- Between switch S9 and sub network A
- Between sub network D and signal analyser
- Between Generator and switch S5
- Between sub network E and sub network A
- Between switch S9 and signal analyser
- Between Generator and sub network A
- Between sub network E and signal analyser
- Between Generator and signal analyser

As can be seen, again some of the mismatch uncertainties are part of both measurements (all of them except where the signal analyser, power meter A, sub network A, and sub network C is part), so they cancel.

The following mismatch uncertainties remain:

- Between switch S5 and sub network C
- Between sub network C and power meter A
- Between sub network B and sub network C

- Between switch S5 and power meter A
- Between switch S8 and sub network C
- Between sub network B and power meter A
- Between sub network D and sub network C
- Between switch S8 and power meter A
- Between switch S9 and sub network C
- Between sub network D and power meter A
- Between sub network E and sub network C
- Between switch S9 and power meter A
- Between Generator and sub network C
- Between sub network E and power meter A
- Between Generator and power meter A
- Between switch S5 and sub network A
- Between sub network A and signal analyser
- Between sub network B and sub network A
- Between switch S5 and signal analyser
- Between switch S8 and sub network A
- Between sub network B and signal analyser
- Between sub network D and sub network A
- Between switch S8 and signal analyser
- Between switch S9 and sub network A
- Between sub network D and signal analyser
- Between sub network E and sub network A
- Between switch S9 and signal analyser
- Between Generator and sub network A
- Between sub network E and signal analyser
- Between Generator and signal analyser

Some of the remaining mismatch uncertainties contribute to both the external and the internal path compensation (uncertainty components between switch S8 and power meter A)- therefore they also cancel. (When the two lists of mismatch uncertainties are combined it is necessary to mark some of them with extra information in order to distinguish between uncertainties which are between the same components, but with a different path between the two components. For instance between the generator and power meter A).

The remaining uncertainties are:

- Between sub network D and sub network C
- Between **switch S9** and **sub network C** (Through sub network D)
- Between sub network D and power meter A
- Between **sub network E** and **sub network C** (Through sub network D)

- Between **switch S9** and **power meter A** (Through sub network D)
- Between **Generator** and **sub network C** (Through sub network D)
- Between **sub network E** and **power meter A** (Through sub network D)
- Between **Generator** and **power meter A** (Through sub network D)
- Between switch S5 and sub network A
- Between sub network A and signal analyser
- Between sub network B and sub network A
- Between switch S5 and signal analyser
- Between switch S8 and sub network A
- Between sub network B and signal analyser
- Between sub network D and sub network A
- Between switch S8 and signal analyser
- Between switch S9 and sub network A
- Between sub network D and signal analyser
- Between sub network E and sub network A
- Between switch S9 and signal analyser
- Between Generator and sub network A
- Between sub network E and signal analyser
- Between Generator and signal analyser
- Between sub network G and power meter B
- Between switch S9 and power meter B
- Between sub network E and power meter B
- Between Generator and power meter B
- Between sub network G and sub network F
- Between sub network F and switch S8
- Between switch S8 and sub network B
- Between sub network B and switch S5
- Between switch S9 and sub network F
- Between sub network G and switch S8
- Between sub network F and sub network B
- Between switch S8 and switch S5
- Between sub network E and sub network F
- Between switch S9 and switch S8
- Between sub network G and sub network B
- Between sub network F and switch S5

- Between Generator and sub network F
- Between sub network E and switch S8
- Between switch S9 and sub network B
- Between sub network G and switch S5
- Between sub network F and sub network C
- Between Generator and switch S8
- Between sub network E and sub network B
- Between switch S9 and switch S5
- Between sub network G and sub network C
- Between sub network F and power meter A
- Between Generator and sub network B
- Between sub network E and switch S5
- Between **switch S9** and **sub network C** (Through sub network G)
- Between sub network G and power meter A
- Between Generator and switch S5
- Between **sub network E** and **sub network C** (Through sub network G)
- Between **switch S9** and **power meter A** (Through sub network G)
- Between **Generator** and **sub network C** (Through sub network G)
- Between **sub network E** and **power meter A** (Through sub network G)
- Between **Generator** and **power meter A** (Through sub network G)

Finally the analysis of the mismatch uncertainty from the actual measurement is performed.

The settings are shown in figure 32:

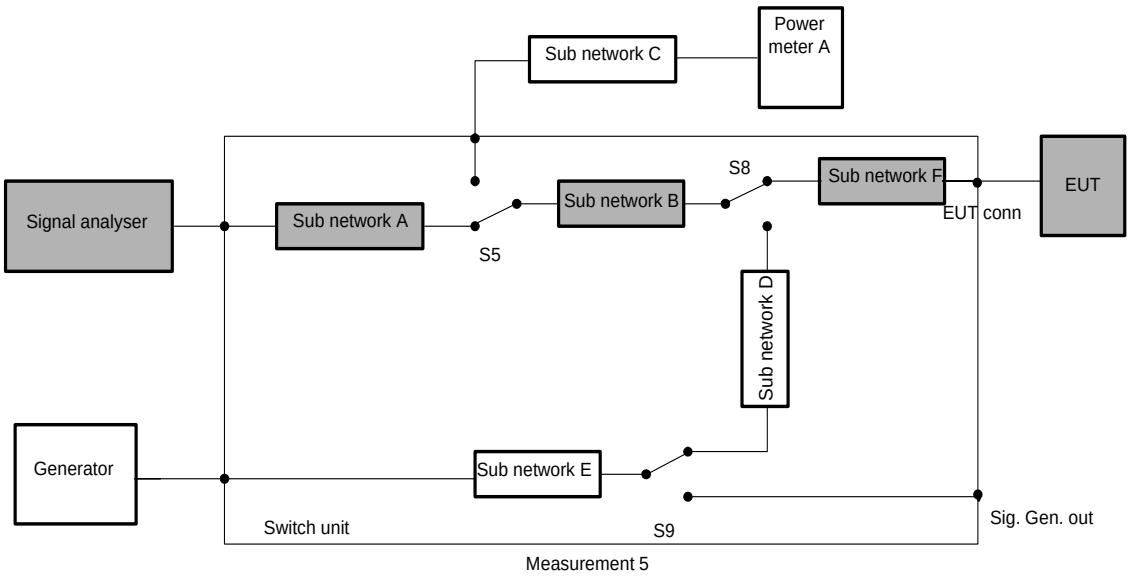

Figure 32: The actual measurement

In the actual measurement (measurement 5) the following mismatch uncertainties contribute:

- Between EUT and sub network F
- Between sub network F and switch S8
- Between switch S8 and sub network B
- Between sub network B and switch S5
- Between switch S5 and sub network A
- Between sub network A and signal analyser
- Between **EUT** and **switch S8**
- Between sub network F and sub network B
- Between switch S8 and switch S5
- Between sub network B and sub network A
- Between switch S5 and signal analyser
- Between EUT and sub network B
- Between sub network F and switch S5
- Between switch S8 and sub network A
- Between sub network B and signal analyser
- Between **EUT** and **switch S5**
- Between sub network F and sub network A
- Between switch S8 and signal analyser
- Between EUT and sub network A
- Between sub network F and signal analyser
- Between EUT and signal analyser

As can be seen, again some of the mismatch uncertainties are part of both the actual measurements and the path compensation (some components between switch S8 and the signal analyser), so they cancel.

The following mismatch uncertainties remain:

- Between sub network D and sub network C
- Between **switch S9** and **sub network C** (Through sub network D)
- Between sub network D and power meter A
- Between **sub network E** and **sub network C** (Through sub network D)
- Between **switch S9** and **power meter A** (Through sub network D)
- Between **Generator** and **sub network C** (Through sub network D)
- Between **sub network E** and **power meter A** (Through sub network D)
- Between **Generator** and **power meter A** (Through sub network D)
- Between sub network D and sub network A
- Between switch S9 and sub network A

- Between sub network D and signal analyser
- Between sub network E and sub network A
- Between switch S9 and signal analyser
- Between Generator and sub network A
- Between sub network E and signal analyser
- Between Generator and signal analyser
- Between sub network G and power meter B
- Between switch S9 and power meter B
- Between sub network E and power meter B
- Between Generator and power meter B
- Between sub network G and sub network F
- Between switch S9 and sub network F
- Between sub network G and switch S8
- Between sub network E and sub network F
- Between switch S9 and switch S8
- Between sub network G and sub network B
- Between Generator and sub network F
- Between sub network E and switch S8
- Between switch S9 and sub network B
- Between sub network G and switch S5
- Between sub network F and sub network C
- Between Generator and switch S8
- Between sub network E and sub network B
- Between switch S9 and switch S5
- Between sub network G and sub network C
- Between sub network F and power meter A
- Between Generator and sub network B
- Between sub network E and switch S5
- Between **switch S9** and **sub network C** (Through sub network G)
- Between sub network G and power meter A
- Between Generator and switch S5
- Between **sub network E** and **sub network C** (Through sub network G)
- Between **switch S9** and **power meter A** (Through sub network G)
- Between **Generator** and **sub network C** (Through sub network G)
- Between **sub network E** and **power meter A** (Through sub network G)

- Between **Generator** and **power meter A** (Through sub network G)
- Between EUT and sub network F
- Between **EUT** and **switch S8**
- Between EUT and sub network B
- Between **EUT** and **switch S5**
- Between sub network F and sub network A
- Between EUT and sub network A
- Between sub network F and signal analyser
- Between EUT and signal analyser

If there are for example 30 components involved in each measurement there are 5 times 435 = 2175 mismatch uncertainties involved before reduction. In some test systems there are even more components. This is the reason why there can be several thousand mismatch uncertainties in a single measurement.

6.8.5 Summary

As mentioned earlier the individual components can be calculated when their individual losses and reflection coefficients are known. The main problem is that some of the components are internal, so the relevant parameters cannot be measured directly without taking the switch unit apart.

The appropriate reflection coefficients may instead be assumed or calculated based on knowledge about the individual components of the sub network.

In addition to the mismatch uncertainties derived previously, there may be others. For example in some receiver tests it is necessary to switch attenuators in during the level settings because this gives a lower uncertainty than relying on the linearity of the generators. This, however, adds to both the mismatch uncertainty and may add new power meter linearity errors which must be taken into account.

As indicated the mismatch uncertainty calculation can be very complicated. Nevertheless it is necessary to perform the calculations of the overall measurement uncertainty for a test performed on such a test system.

One way to simplify it is to use software tools which can actually handle all the (sometimes more than 100) components in a test system. (Such a tool has actually been developed, but none are yet commercially available).

Such a tool must be capable of analysing networks with many components based on components data (s parameters), the component's location in the network, and which other components it is connected to.

To calculate the over all mismatch uncertainty (as done above) it must calculate the uncertainties from the different individual measurements and identify which uncertainties cancel.

Another simplified method could be to assume that cables and switches are loss-less when looking at mismatch uncertainties. This results in a lot of errors being identical. It gives a little more conservative figure for the uncertainty because the reduction in the mismatch due to loss between the two parts is not considered.

All of the listed uncertainties are between two sub networks, instruments or components which in some cases are separated by other sub networks. If so the mismatch uncertainties are reduced due to insertion loss between the two parts.

Further reductions can be accomplished by ignoring mismatch errors which are insignificant compared to the overall mismatch uncertainty. If for instance if the two parts are separated by more than 10 dB they will be reduced by at least a factor of 10. But care must be taken: some uncertainties may be caused by filters outside their pass bands causing their reflection coefficients to be close to 1. These should not automatically be ignored as they would be significant even with losses much greater than 10 dB involved.

The example in clause 6.8.5.1 shows how one of the mismatch uncertainties can be calculated if all the individual components are known.

A third approach could be to estimate the s-parameters for the different logical parts of the test system as they are shown on figure 29. This could be done by network analyser measurement on the switch unit connectors, by measurements on internal connectors or by assuming internal s-parameters based on external measurements or component data.

All the individual mismatch components (for instance the 55 components derived in clause 6.8.4.2.2) could be programmed in a spreadsheet program, so it would be easy to input new sets of s-parameters representing other frequencies or other switch unit settings.

6.8.5.1 Typical mismatch example

This example shows the calculation of the mismatch uncertainty between sub network C and sub network E through sub network G (from measurement 2, figure 30) in the external path compensation procedure related to a transmitter measurement.

Some details for the calculations must be assumed: Generator 2 is the generator, and the signal is connected through the 6 dB combiner and switch S10.

Furthermore it is assumed that attenuator 2 is by-passed between switches S6 and S7 during the path compensation and the actual measurement (see figure 24).

Then from figure 24 and figure 30 it can be seen that sub network C consists of a cable, switch S3, and a cable, and sub network E consists of the cable connecting the generator to the switch unit, a cable, switch S11, a cable, the combiner, a cable, switch S10, and a cable.

The loss separating these two sub networks consists of 3 switches and some cables, and a 10 dB attenuator.

In order to simplify the calculations it is assumed that the cables and the switches are loss-less. This will make the calculations slightly more conservative since there will be no reduction of the mismatch uncertainty due to the loss between the components, as loss between consists of only cables and switches.

The next assumption is that all cables are identical and all switches are identical.

Since a power combiner with 3 ports is involved, there will be a main path to be analysed, but in addition there will be components from the 3 port of the power combiner as well with the same set of components as between generator 2 and the combiner.

Figure 33 applies for the calculations:

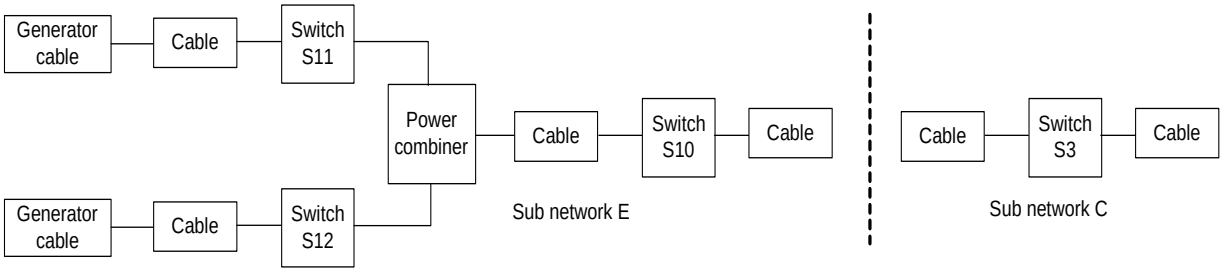

Figure 33: The two sub networks in the mismatch uncertainty calculation

Each mismatch uncertainty component has one part on each side of the dashed line.

Since there is a power combiner with a loss of 6 dB involved, there will be components separated by 10 dB and components separated by 16 dB as cables and switches are considered loss-less.

Since there are 10 components on the left side and 3 components on the right side there will be 30 mismatch contribution (of which some will be identical).

They are:

1) 4 mismatch components due to mismatch between a cable and a cable, separated by 10 dB

2) 1 mismatch component due to mismatch between a switch and a switch, separated by 10 dB

3) 4 mismatch components due to mismatch between a switch and a cable, separated by 10 dB
4) 2 mismatch components due to mismatch between a cable and the combiner, separated by 10 dB
5) 1 mismatch component due to mismatch between a switch and the combiner, separated by 10 dB
6) 4 mismatch components due to mismatch between a cable and a cable, separated by 16 dB
7) 2 mismatch component due to mismatch between a switch and a switch, separated by 16 dB
8) 6 mismatch components due to mismatch between a switch and a cable, separated by 16 dB
9) 2 mismatch components due to mismatch between a switch and a generator cable, separated by 16 dB
10) 4 mismatch components due to mismatch between a cable and a generator cable, separated by 16 dB

The following data are assumed for the mismatch uncertainty calculations:

- The reflection coefficient from a cable is 0,1
- The reflection coefficient from a switch is 0,15
- The reflection coefficient from the combiner is 0,08
- The reflection coefficient from the 10 dB attenuator is 0,05
- The reflection coefficient from a generator cable is 0,17
- 10 dB equals 0,3163 and 16 dB equals 0,1581

This gives the following standard deviation figures for the mismatch uncertainties:

1) $100 \times 0,1 \times 0,1/(0,3163 \times 0,3163 \times \sqrt{2})$ %= 0,070 % 4 times
2) $100 \times 0,15 \times 0,15/(0,3163 \times 0,3163 \times \sqrt{2})$ %= 0,159 % 1 time
3) $100 \times 0,15 \times 0,1/(0,3163 \times 0,3163 \times \sqrt{2})$ %= 0,106 % 4 times
4) $100 \times 0,1 \times 0,08/(0,3163 \times 0,3163 \times \sqrt{2})$ %= 0,057 % 2 times
5) $100 \times 0,15 \times 0,08/(0,3163 \times 0,3163 \times \sqrt{2})$ %= 0,085 % 1 time
6) $100 \times 0,1 \times 0,1/(0,1581 \times 0,1581 \times \sqrt{2})$ %= 0,018 % 4 times
7) $100 \times 0,15 \times 0,15/(0,1581 \times 0,1581 \times \sqrt{2})$ %= 0,040 % 2 times
8) $100 \times 0,15 \times 0,1/(0,1581 \times 0,1581 \times \sqrt{2})$ %= 0,027 % 6 times
9) $100 \times 0,15 \times 0,17/(0,1581 \times 0,1581 \times \sqrt{2})$ %= 0,045 % 2 times
10) $100 \times 0,1 \times 0,17/(0,1581 \times 0,1581 \times \sqrt{2})$ %= 0,030 % 4 times

This gives a total standard deviation = 0,34 % (≈ 0,03 dB) calculated by applying the RSS method to the 30 uncertainty components.

If only the components separated by more than 10 dB are considered, the result would be 0,32 % which is a little smaller, but since the approach was conservative from the beginning it would be justified to do so.

A suitable way to do the calculations is to use a spread sheet program calculations at different frequencies or with changed components data can easily be done if the components data are entered so each component only need to be modelled one time, which makes it much easier to re-do the analysis at different frequencies by just changing the models data in the spread sheet.

All the individual uncertainty components are as usual combined as standard deviations as the square root of the sum of the squares.

In a similar way the rest of the mismatch uncertainties can be analysed.

7 Theory of test sites

7.1 Introduction

The aim of this clause is to derive, starting from a basic theory of propagation, a theoretical model of an "ideal" test site i.e. a site completely devoid of all error sources. The model is then extended to different types of test site (e.g. Anechoic Chamber, Open Area Test Site, etc.) giving a theoretical baseline against which the measured performance of an actual test site can be compared.

This is approached by the following means:

- by covering the basic field theory as it applies to radiated measurements;
- by deriving the Friis transmission equation i.e. the equation which relates the power received to the power transmitted in terms of wavelength, distance, etc.;
- by incorporating into the theory the radiated fields of a dipole (having started with a consideration of ideal radiating sources);
- by extending and modifying the ideal-site model to derive individual models for different types of test site (i.e. Anechoic Chamber, Open Area Test Site, etc.).

Initially, however, an introduction to some of the basic concepts which feature in the relevant underlying theory is presented.

7.1.1 Basic concepts

In an alternating current circuit, the term impedance is used for the complex resistive and reactive attributes of a component. In the context of electromagnetic radiation, where energy is transferred in the form of a wave through a homogeneous medium, an equivalent term - intrinsic impedance - is used for that medium. Its value is given by the ratio of the electric field intensity to the magnetic field intensity. Its units are Ω, derived from V/m (electric field intensity) divided by A/m (magnetic field intensity). Intrinsic impedance is distinct from wave impedance which is defined as the ratio between the principal electric and magnetic field components from a radiating source. At a far enough distance away from a radiating source, the wave impedance becomes the same as the intrinsic impedance.

The term free Space infers a homogenous medium whose parameters i.e. permeability, permitivity, velocity of propagation, intrinsic impedance, etc. are those of a vacuum.

An isotropic radiator is a concept of an "ideal" radiating source with no physical size i.e. it is assumed to be an infinitesimally small "point source". It radiates with equal intensity in all directions and is completely loss-less.

7.2 Radiated fields

This clause essentially deals with the fields radiated by an isotropic radiator in free Space. After some discussion, directivity is then given to this radiating source and the implications discussed. Finally the Friis transmission formula is derived.

7.2.1 Fields radiated by an isotropic radiator

The starting point for the model of the ideal test site is to consider the nature of the amplitude and phase of the electromagnetic field generated by an isotropic radiator in free Space.

As stated in clause 7.1.1, the key characteristic of the isotropic radiator is that it radiates with equal intensity in all directions. This implies that at any point on a spherical surface, about the "point source" at its centre, both the magnitude and phase of the electric field will be constant.

The power radiated will be similarly distributed, so that, since the surface area of a sphere is:

$$4\pi \text{ r}^2 \text{ m}^2$$

where *r* is the radius of the sphere in m.

The radiated power density, W_0, at any point on the surface will be given by:

$$W_0 = \frac{P_t}{4\pi r^2} \text{ W/m}^2$$

where P_t is the transmitted power from the loss-less isotropic radiator in Watts.

To further develop the theory, the point source's nature of radiating energy equally in all directions, has to be changed since the concept cannot be realized physically - all practical radiating sources incorporate a measure of directivity. Consideration is now given to the implications of the source having some directivity.

7.2.2 Directivity implications on the ideal radiator

Directivity is a parameter which quantifies how directional the radiated fields from a source are.

In the spherical co-ordinates system (r,θ,ϕ), the source directivity can be represented by:

$D(\theta,\phi)$

in which case the power density equation now becomes:

$$W_o = \frac{P_t D(\theta,\phi)}{4\pi r^2} \text{ W/m}^2$$

Consequently, the introduction of the directivity function modifies the constant field strength on the spherical surface under consideration. However, given that the source is still in a homogeneous medium (in this case free Space) all radiated fields will still reach the spherical surface simultaneously, therefore retaining the constant phase characteristic. All electromagnetic radiation is characterized by this constant phase behaviour - the wave being said to propagate with a spherical phase front.

The main implication which arises from giving the source some directivity is that it possesses some physical size, and this is discussed in clause 7.2.3.

7.2.3 The nature of the fields around a source of finite size

All electromagnetic waves consist of two essential components: a magnetic field and an electric field. For transverse electromagnetic waves these two fields have only one component each. These are perpendicular to each other, and the direction of propagation is at right angles to the plane containing these two components. Close to a radiating source other field components usually exist and the relative magnitude between the magnetic (H) field and the electric (E) field depends on the distance from the source, and on the nature of the source itself. As stated in clause 7.1.1, the ratio of the principal field components is called the wave impedance. It is only sensible to calculate wave impedance for transverse electromagnetic waves since the additional electric and magnetic components present in the so called "near-field" are largely undefined.

In this near-field region it is more usual to describe the nature of the field as being either predominately magnetic or predominately electric. If the source has a high current flow relative to its potential, i.e. E/H ratio is low, it is known as a "low impedance source", and the near-field is referred to as being predominately magnetic. Where the inverse occurs and the source has a low current flow relative to its potential, i.e. E/H ratio is high, the source is known as a "high impedance source", and the near-field is referred to as being predominately electric.

As the distance from the source increases, the magnitude of the additional field components decrease. Eventually at some distance, irrespective of whether it is a high or low impedance source the wave becomes a truly transverse electromagnetic wave and the E/H ratio becomes equal to 377 Ω, the impedance of free Space. This distance is called the far-field distance and the wave is then said to be a plane wave. The polarization of the wave is determined by the change of amplitude and direction of the wave as it passes through a stationary point, and by convention is referred to the electric component of the field. Figure 34 shows graphically the transition of the electric and magnetic fields for electric and magnetic sources respectively.

For a rod or straight wire antenna, the source impedance is high, and the near-field is predominately electric. As the distance is increased, the electric field loses its intensity as some of its components attenuate at a rate of $1/r^3$ to $1/r^2$. Thus the wave impedance from a straight wire antenna decreases with distance and asymptotically approaches the impedance of free Space in the far-field.

For a predominantly magnetic field such as produced by a loop, the source impedance near the antenna is low, and as the distance from the source increases, some of the magnetic field components attenuate at a rate of $1/r^3$ to $1/r^2$. The wave impedance therefore increases with distance and again approaches that of free Space in the far-field.

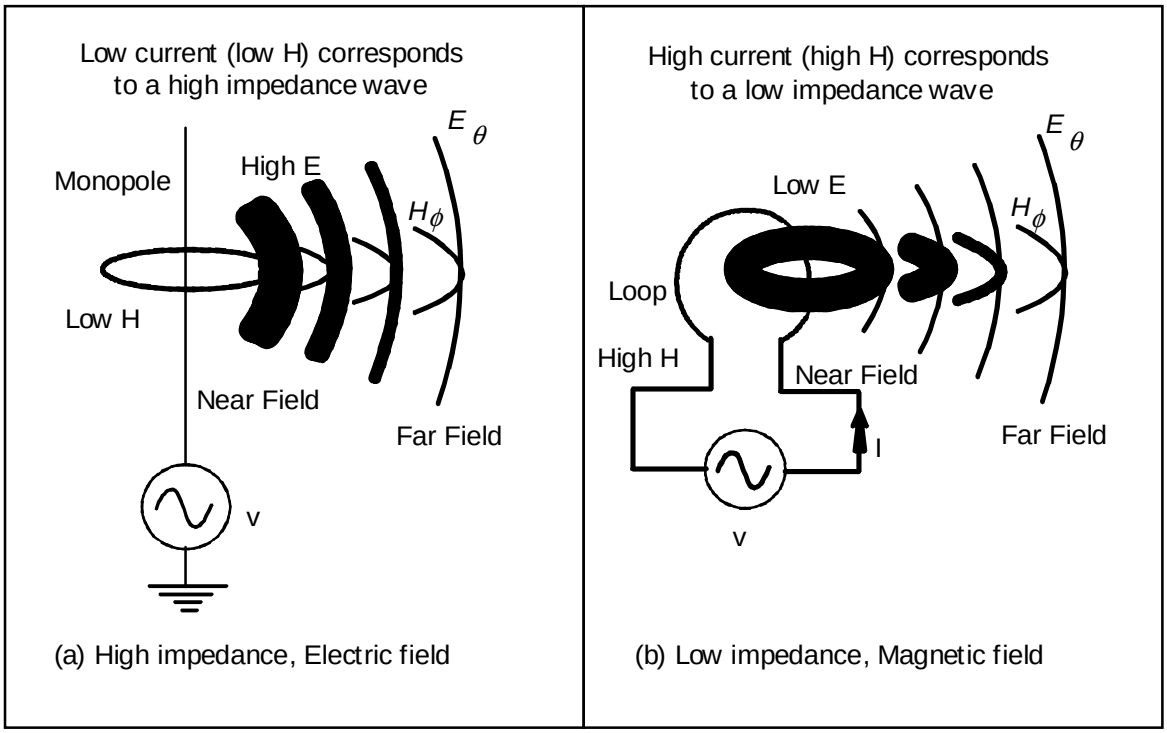

Figure 34: Transition of electric and magnetic fields intensities to far-fields values

In the far-field the electric and magnetic fields both possess only single components which attenuate at a rate of *1/r*.

Close to the source (in the region normally referred to as the reactive near-field) the electromagnetic field components are generally regarded as those associated with the transition between the physical components comprising the radiating source and its surrounding medium. Placing a receiving device in this region of close physical proximity can lead to measurement inaccuracies since energy can be coupled by induction as well as by radiation, with the possible result that the input impedance of both devices may change.

Also close to the source, but generally regarded as being beyond the reactive near-field, lies the radiating near-field, a region characterized by the distribution of the electromagnetic field becoming more uniform with increasing distance away from the source.

At greater distances away from the radiating source, some of the field components present in the near-field die away until, at a great enough distance from the radiating source, both electric (E) and magnetic (H) fields possess single components only, both of which exhibit simple *1/r* dependencies. (It is only when this *1/r* dependency exists that any of the formulas derived in clauses 7.2.1 and 7.2.2 for power density apply). The single components of the E and H fields will be orthogonal to each other and at right angles to the direction of propagation.

The boundaries of the three regions (the reactive near-field, the radiating near-field and the far-field) are not well defined although certain rules-of-thumb are in existence. For example, the generally accepted distance from the source to the boundary between the reactive and radiating near-fields is given in [5] as:

$$0{,}62\sqrt{\frac{d^3}{\lambda}} \text{ m}$$

whilst the far-field is generally reckoned to be a minimum distance away from the source of:

$$\frac{2d^2}{\lambda} \text{ m}$$

where:

λ is the wavelength in free-space;

d is the maximum size of the radiating source.

In the intervening space, i.e. when the separation between source and receiver is:

$$0{,}62\sqrt{\frac{d^3}{\lambda}} < \text{separation} < \frac{2d^2}{\lambda} \text{ m}$$

then the region is the radiating near-field (also referred to as the Fresnel zone). When the separation between the source and the receiver is:

$$\geq \frac{2d^2}{\lambda} \text{ m}$$

then the region is the far-field (also known as the Fraunhofer region).

The far-field formulation is a result of imposing a maximum curvature on the spherical phase front across the aperture d when placed in the field of a radiating **point** source. This is illustrated in figure 35.

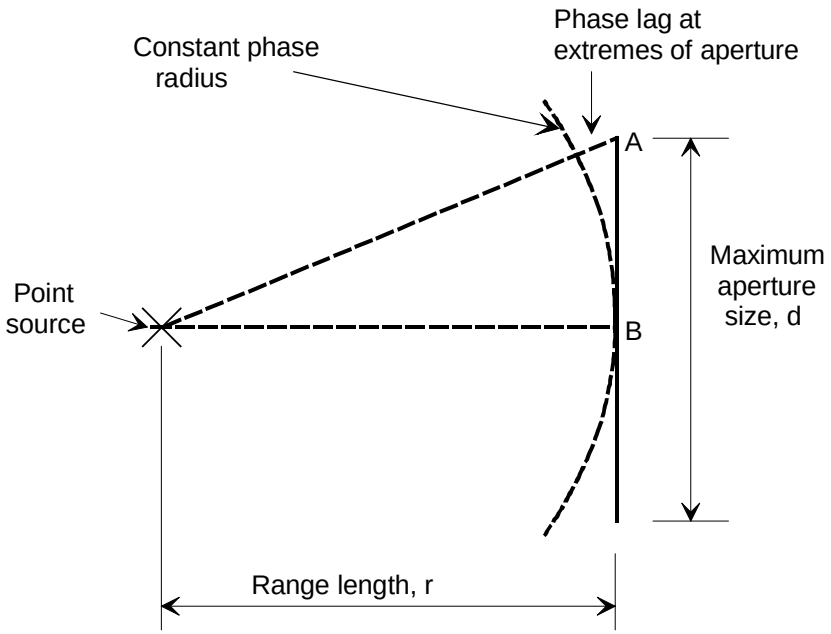

Figure 35: The constant phase radius and phase lag at an aperture's edges

At the formulated distance, this curvature will present $\lambda/16$ path length increase (i.e. 22,5° phase lag) at the extremities of the aperture relative to the path length at its centre. At separations equal to or exceeding the formulated distance, a measurement of the level of received power from the point source will reduce as $1/r^2$ since phase curvature of less than 22,5° will produce negligible error when compared to a perfect, uniformly illuminated aperture.

In practice, measurements of radiating sources can be made in any of the three regions. However, because the fields are fundamentally different, unless this is taken into consideration and corrected for, different results will be obtained from each of the regions.

7.2.3.1 Derivation of the far-field distance ($2d^2/\lambda$)

In figure 35, the difference in the path lengths from the point source to point A (the edge of the aperture) and the point source to point B (the centre of the aperture) is:

$$\sqrt{\left(r^2+\left(\frac{d}{2}\right)^2\right)}-r$$

The stipulation is that this path length difference should not exceed $\lambda/16$ (i.e. 22,5 ° phase). That is:

$$\sqrt{\left(r^2+\left(\frac{d}{2}\right)^2\right)}-r \le \frac{\lambda}{16}$$

Rewriting this equation as:

$$\left(r^2+\left(\frac{d}{2}\right)^2\right) \le \left(r+\frac{\lambda}{16}\right)^2$$

and squaring the right hand side gives, after collecting terms:

$$\frac{2}{\lambda}\left(d^2-\frac{\lambda^2}{64}\right) \le r$$

It is assumed that $d^2 >> \lambda^2/64$ for all practical testing and hence the formulation for the far-field distance becomes:

$$r \ge \frac{2d^2}{\lambda}$$

It should be noted that this formulation of far-field distance has been based on an aperture whose edges contribute fully to the received level i.e. the antenna's internal arrangements are assumed to ensure that every point in its aperture is fed with the same amplitude and phase. For any other distribution of the aperture illumination (e.g. sinusoidal as in the case of a dipole), it is arguably possible to employ a reduced far-field distance. However, any reduction would have to be proven, and not taken on trust, since the outermost segments of an aperture may affect performance simply by their physical presence and thereby contribute to the antenna's performance in that way. Furthermore, for the specific case of two half-wavelength dipoles, a spacing in excess of 5 wavelengths [5] (greatly in excess of the requirements of $2d^2/\lambda$) is strictly necessary to avoid all interaction effects. Whilst the half-wavelength dipole is an extreme case (it is highly tuned and has a reactive component of input impedance which can vary rapidly) it serves as a warning about assuming any reduction is possible without proof. Consequently, the above formulation is taken to apply generally.

7.2.4 Reception in the far-field ($2(d_1+d_2)^2/\lambda$)

A radiating device can equally well be used in a receiving mode to measure the radiated fields of another radiator. Introducing the term "antenna" to cover both radiating and receiving devices, we can now start to formulate a model for an ideal testing site. Such a model would include:

- a radiating antenna operating in free-space;
- a receiving antenna operating in free-space;
- both antennas aligned for the same polarization;
- both antennas are loss-free and perfectly matched to their respective circuits;

- they are a sufficient distance apart for both antennas to be in the far-field of the each other.

The last stipulation needs modification to take account of two factors. Firstly, the fact that neither antenna is now a point source (i.e. the far-field distance derived in clause 7.2.3.1 is no longer valid) and secondly that mutual coupling (i.e. changes in the input impedance, gain, radiation pattern, etc., of one antenna due simply to the physical presence of another) may exist.

With regard to the formulation for far-field distance, figure 36 illustrates the new situation:

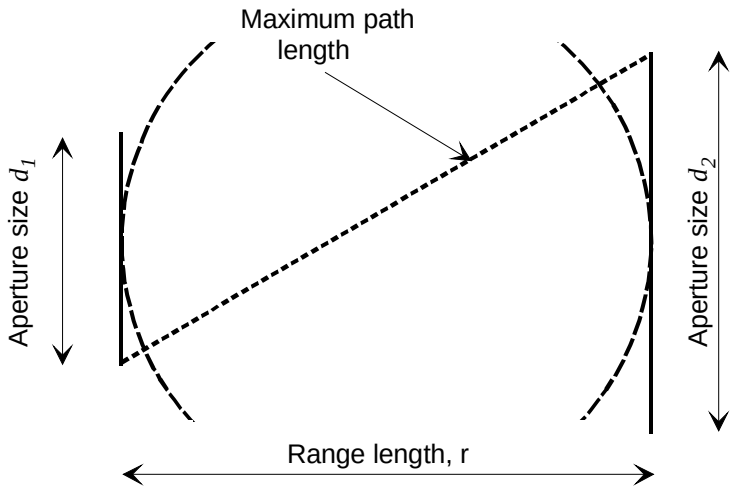

Figure 36: Maximum path length between two antennas of size d_1 and d_2

The derivation of the far-field distance in this case takes the identical form to that in clause 7.2.3.1 with the term (d_1+d_2) replacing d. This leads to the requirement that:

$$r \geq \frac{2}{\lambda}\left((d_1+d_2)^2 - \frac{\lambda^2}{64}\right)$$

So, provided $(d_1+d_2)^2 >> \frac{\lambda^2}{64}$ (an identical requirement to the point source case) this gives a far-field distance (i.e. the minimum range length for accurate testing of):

$$r \geq \frac{2(d_1+d_2)^2}{\lambda}$$

For the second qualification of the final stipulation for the ideal site, one major effect of mutual coupling is to mismatch the antennas to their otherwise matched feed lines producing power loss. Other more subtle effects can include changes to the current distribution on antennas with a resultant change in radiation patterns and gain. In the continuing development of our ideal model, these mutual coupling effects are assumed not to exist.

Generally, antennas are regarded as reciprocal devices in the sense that their radiation patterns apply equally whether used for receiving or for transmitting. This fact enables the power coupled from one antenna to another in a free-space environment under far-field conditions to be determined. This is the next stage in our theoretical development of an ideal test site.

Above, it has been shown that the power density, W_0, produced at a distance r by a source exhibiting a directivity function $D(\theta_t,\phi_t)$ is:

$$W_0 = \frac{P_t D(\theta_t,\phi_t)}{(4\pi r^2)} \text{ W/m}^2$$

where the suffix *t* has been introduced to refer to a transmitting antenna.

At this point, it is necessary to introduce the concept of "effective collecting area" of a receiving antenna at this point. This is a function which relates the power density of the field surrounding an antenna to the power produced by that antenna at its terminal, under impedance matched conditions. Effective collecting area is denoted here by the symbol A_e. The power, P_{rec}, from a receive antenna placed in the field, whose power density is as given above, can therefore be calculated from:

$$P_{rec} = \frac{P_t D(\theta_t, \phi_t) A_e}{4\pi r^2} \text{ W}$$

where the suffix $_{rec}$ refers to the receive antenna.

Further, since the directivity of an antenna and its effective collecting area can be shown [5] to be related by the following:

$$A_e = D(\theta,\phi)\left(\frac{\lambda^2}{4\pi}\right) \text{ m}^2$$

the received power can be rewritten as:

$$P_{rec} = P_t D(\theta_t, \phi_t) D(\theta_r, \phi_r)\left(\frac{\lambda}{4\pi r}\right)^2 \text{ W}$$

A refinement to this equation is now made by introducing the parameter of Gain. In a similar manner to directivity, Gain is used as a measure of directionality of an antenna. It is, however, distinguished from directivity by having included in its value, the dissipative losses within the antenna (i.e. those losses due to electrical resistance e.g. matching sections, etc.). Gain and directivity can therefore be related by the following formula [5] $G(\theta,\phi) = e_{ff} \times D(\theta,\phi)$

where e_{ff} is an efficiency factor which takes those losses into account. For the purpose of defining the ideal test site e_{ff} is considered to have a value equal to 1 i.e. no losses in the ideal case.

By substitution and some rearrangement, we obtain the following equation for the ratio of received power to transmitted power:

$$\frac{P_{rec}}{P_t} = G_t(\theta_t, \phi_t) G_r(\theta_r, \phi_r)\left(\frac{\lambda}{4\pi r}\right)^2$$

This is referred to as the "Friis Transmission Equation".

7.2.5 Choice of physical antenna for the "ideal" model

Before developing the model further, consideration is first given to other radiating sources.

7.3 Ideal radiating sources

There are several ideal radiating sources which, despite their idealistic nature have important roles to play in electromagnetic theory. For example the usage of the ideal isotropic radiator as a basis for the definition of antenna gain is one such role. As well as the isotropic radiator there are two other ideal sources, namely the electric current element and the magnetic current element. Both have their relevance as building blocks for the theory of radiated energy from, for example, the dipole for the electric current element and loops for the magnetic current element.

7.3.1 Electric current element

The electric current element is a fundamental theoretical concept, the analysis of which is applied to wire type antennas in general to calculate radiation patterns, radiation resistance, etc. The electromagnetic fields and other theoretical data are presented next.

Consider the infinitesimal electric current element shown in figure 37.

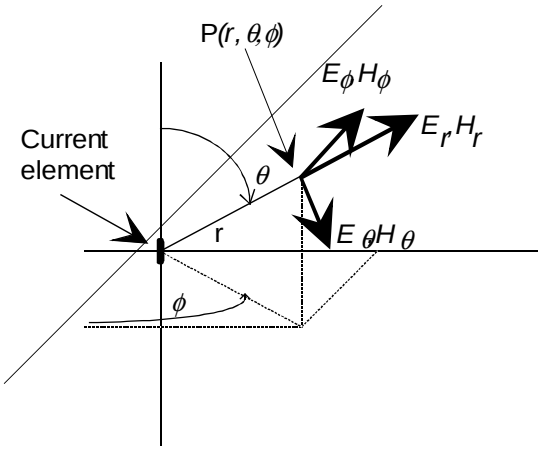

Figure 37: The infinitesimal current element at the centre of a spherical co-ordinate system

In spherical co-ordinates, the fields at point P can be shown [5] to be:

$$E_\theta = j\eta\frac{kI_o l\sin(\theta)}{4\pi r}\left[1+\frac{1}{jkr}-\frac{1}{(kr^2)}\right]e^{-jkr}$$

$$E_r = \eta\frac{I_o l\cos(\theta)}{2\pi r^2}\left[1+\frac{1}{jkr}\right]e^{-jkr}$$

$$E_\phi = 0$$

$$H_\theta = H_r = 0$$

$$H_\phi = j\frac{kI_o l\sin(q)}{4\pi r}\left[1+\frac{1}{jkr}\right]e^{-jkr}$$

where:

k = $2\pi/\lambda$, a constant;

η = $120\pi\ \Omega$ - the intrinsic impedance of free Space;

r = the distance to the field point (m);

I_0 = the (assumed constant) current (A);

l = the length of the infinitesimal dipole (m).

It can be seen from the field equations that some of the terms decrease as $1/r$, others more rapidly as $1/r^2$ and $1/r^3$. It should also be noted, that there is a radial component (E_r) of the electric field.

For $kr >> 1$ (i.e. $r >> \lambda/2\pi$) where far-field conditions exist, the above formulas simplify to:

$$E_\theta = j\eta\frac{kI_o le^{-jkr}}{4\pi r}\sin(\theta)$$

$$H_\phi = j\frac{kI_o le^{-jkr}}{4\pi r}\sin(\theta) = \frac{E_\theta}{\eta}$$

with $H_\theta = H_r = E_{\phi =} E_r \cong 0$ i.e. the radial component of the electric field has reduced to zero.

These two non-zero equations are the building blocks for the far-field radiation pattern analysis of wire type antennas in general. They are used as the basis for the analysis of the dipole in clause 7.4.

7.3.2 Magnetic current element

The magnetic current element occurs in the analysis of the loop antenna whose main usage, as far as testing is concerned, is in the frequency band of a few Hz to 30 MHz. They do find a use as the radiating element within body-worn devices such as pagers at frequencies up to 1 GHz but since they do not feature as antennas used on test sites above 30 MHz (the scope of the present document), and, as such, this clause is included for theoretical completeness rather than for its relevance to radiated tests.

Derivation of the electromagnetic field components arising from a small circular loop reveals field equations that are the exact "dual" of those for the electric current element i.e. all E-field components for the electric current element become H-fields for the loop and vice versa as long as all η's are changed to $1/\eta$'s. It is a result of this duality with the electric current element that the infinitesimally small loop is termed the magnetic current element.

7.4 Theoretical analysis of the dipole

Having given the ideal source some directivity (see clause 7.2.2) the next stage is to select a real physical antenna for inclusion into the "ideal" model. Amongst the various antennas used commonly on test sites (dipoles, bicones, log-periodic dipole arrays, waveguide horns, etc.) by far the most practical, most commonly used and easiest to model is the dipole. The dipole is therefore chosen as the source and receive antenna in the further development of the "ideal" model.

The results from the electric current element analysis in clause 7.3.1 are now used to derive the radiation patterns of the dipole.

In the derivation of the far-field radiation fields E_θ and H_ϕ, the current distribution was assumed to be constant. For the dipole, however, it has been shown [5] that as a result of centre-feeding and invoking the boundary condition that the current at the dipole ends is zero, a sinusoidal current distribution results. Therefore, I_0 in the relevant equations can be written as:

$$I_o = I_m \sin\left(\frac{L}{2} - l\right)$$

for current elements in the upper half of the dipole, and

$$I_o = I_m \sin\left(\frac{L}{2} + l\right)$$

for those in the lower half.

In these, I_m is the maximum current amplitude, L is the overall length of the dipole and l is the point on the dipole being considered.

Summing all the contributions from the individual current elements over the whole length of the dipole, the equations for E_θ and H_ϕ in clause 7.3.1 become:

$$E_\theta = j\eta \frac{I_o e^{-jkr}}{2\pi r}\left[\frac{\cos\left(\frac{kL}{2}\cos(\theta)\right) - \cos\left(\frac{kL}{2}\right)}{\sin(\theta)}\right]$$

$$H_\phi = j\frac{I_o e^{-jkr}}{2\pi r}\left[\frac{\cos\left(\frac{kL}{2}\cos(\theta)\right) - \cos\left(\frac{kL}{2}\right)}{\sin(\theta)}\right] = \frac{E_\theta}{\eta}$$

For a dipole of length $L=\lambda/2$, the electric field intensity reduces to:

$$E_\theta \propto \left(\frac{\cos\left(\frac{\pi}{2}\cos(\theta)\right)}{\sin(\theta)} \right)$$

which yields a 3 dB beamwidth of 78° in the *E*-plane, the pattern of which is shown in figure 38. In the *H*-plane the pattern is constant (i.e. omni-directional) because there is no dependence on ϕ.

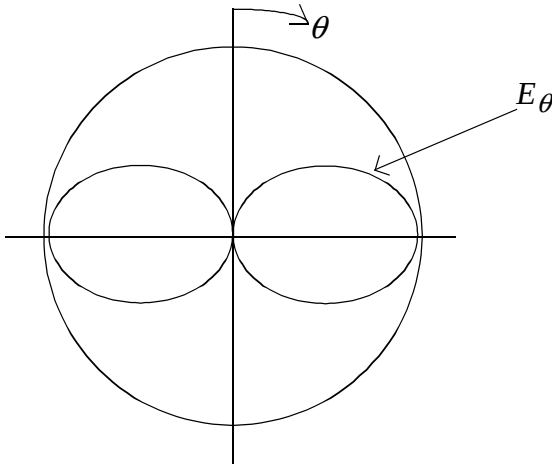

Figure 38: *E*-plane E_θ pattern of a λ/2 dipole

Again for the $\lambda/2$ dipole case, the directivity can be derived from the formulation of the E_θ pattern and can be shown [5] to be ≈ 1,643 (i.e. +2,15 dB).

The gain pattern $G(\theta,\phi)$ for the $\lambda/2$ dipole (assumed loss-free) is given by:

$$G(\theta,\phi) = 1{,}643 \left(\frac{\cos\left(\frac{\pi}{2}\cos(\theta)\right)}{\sin(\theta)} \right)^2$$

The effective collecting area is $0{,}13\lambda^2$ whilst its input impedance at resonance, in a free Space environment is 73,0 + j42,5 Ω [5].

7.5 Model of the ideal test site

This clause collates all the theory and concepts of the preceding clauses of clause 7 with the aim of defining the model of the "ideal" test site. A formula for the site attenuation (i.e. the magnitude of the loss of power between the terminals of the two dipoles) of that test site will then be determined.

Components to be added to the ideal model as stated in clause 7.2.4 are the inclusion of dipole antennas as both the radiating source and the receiving antennas with a stipulation of the range length plus the further requirement that no radiated interference from outside sources should exist.

To summarize, the ideal site comprises:

- a free Space environment;
- loss-free antennas perfectly matched to their circuits;
- both antennas to be tuned half-wavelength dipoles;

- both antennas possessing linear and parallel polarization;
- the distance between dipoles to be sufficiently great to ensure far-field conditions with no mutual coupling effects;
- absence of interference from outside sources (i.e. no ambient signals).

Any practical site will, in one or many ways, be a degradation of this ideal, but it will be against this ideal that the performance of that practical site will be assessed during the verification.

To formulate the power transmission for this ideal test range, the gain formula for the *λ/2* dipole is now incorporated into the Friis transmission formula:

By substitution, the formula becomes:

$$\frac{P_{rec}}{P_t} = 1{,}643\left(\frac{\cos\left(\frac{\pi}{2}\cos(\theta)\right)}{\sin(\theta)}\right)^2 1{,}643\left(\frac{\cos\left(\frac{\pi}{2}\cos(\theta)\right)}{\sin(\theta)}\right)^2\left(\frac{\lambda}{4\pi r}\right)^2$$

The ratio of P_{rec}/P_t represents the ratio of received to transmitted signal power level i.e. the loss through the overall system. In contrast "Site Attenuation" (regularly used in verification procedures) is a positive quantity and is the inverse of P_{rec}/P_t. Therefore, by inverting the above formula and converting into decibels, we achieve the following:

$$\textit{Site Attenuation} = 17{,}67 + 20\log_{10}\left(\frac{r}{\lambda}\right) + 20\log_{10}\left(\frac{\sin(\theta)}{\cos\left(\frac{\pi}{2}\cos(\theta)\right)}\right) + 20\log_{10}\left(\frac{\sin(\theta)}{\cos\left(\frac{\pi}{2}\cos(\theta)\right)}\right)\text{dB}$$

7.6 Ideal practical test sites

In this clause, ideal practical sites are examined. All types of practical test site (i.e. Anechoic Chamber, Anechoic Chamber with a Ground Plane, Open Area Test Site and stripline) are considered and an ideal, lossless formula for the site attenuation is given for each case. Additionally, Test Fixtures and salty man/salty-lite are discussed, although these are not test sites in themselves - they can only be used in conjunction with one of the four previously mentioned sites.

7.6.1 Anechoic Chamber

An Anechoic Chamber is an enclosure, usually shielded, whose internal surfaces are covered with radio absorbing material. It is intended to simulate a free Space environment by absorption of all the RF energy incident on the absorbing panels.

The truly ideal Anechoic Chamber should behave as an infinite empty space i.e. for a fixed transmitting and receiving antenna system (i.e. where the antennas, the spacing between them and their relative orientations remain the same) the received signal level should remain constant for any orientation of that system (in the three dimensions, x, y and z) within the "working volume" of the chamber. This performance is referred to as the "primary characteristic" for this type of test facility and is shown schematically in figure 39.

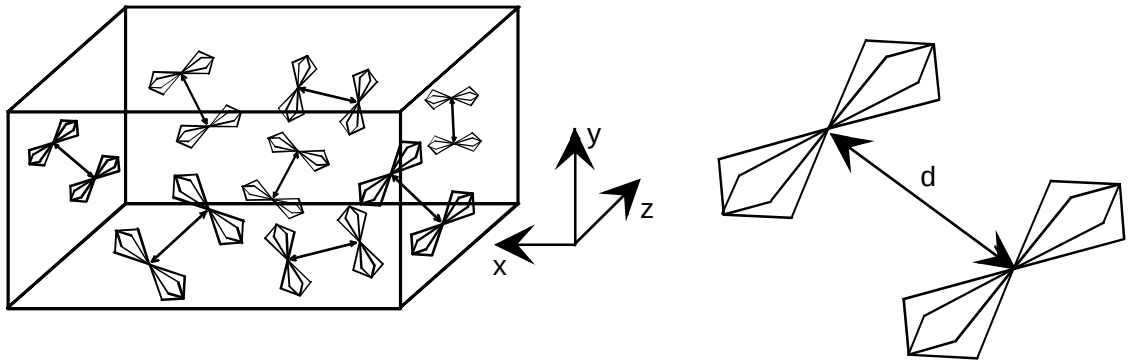

Figure 39: Fixed antenna system at various orientations in an Anechoic Chamber

The ideal Anechoic Chamber emulates free Space and as such should not possess the usual performance limitations imposed by boundaries, reflecting surfaces and impedance "zones". In other words, the boundaries and reflection surfaces should be so well covered by absorbing material that they do not exist in an electrical sense (i.e. they should not act as interference sources or allow either room resonances or the propagation of waveguide modes), whilst, within the working volume of the chamber, the impedance should be unvarying and equate to the intrinsic impedance of free-space.

For shielding from ambient transmissions, the walls, ceiling and floor of a practical Anechoic Chamber should comprise a continuous metal shield whose presence needs to be masked in order to satisfy the minimal boundary and reflection surfaces conditions. The ceiling and walls of such a test site are usually covered with pyramidal urethane foam absorbers whose thickness is chosen according to the lowest frequency to be used. The floor is covered with special absorbers usually capable of supporting the weight of test personnel and equipment in transit. Ideally the characteristics of all the radio absorbing materials used should be the absorption of all the radiated power incident upon it - independent of both incident angle and frequency. A typical Anechoic Chamber is shown in figures 40 and 41.

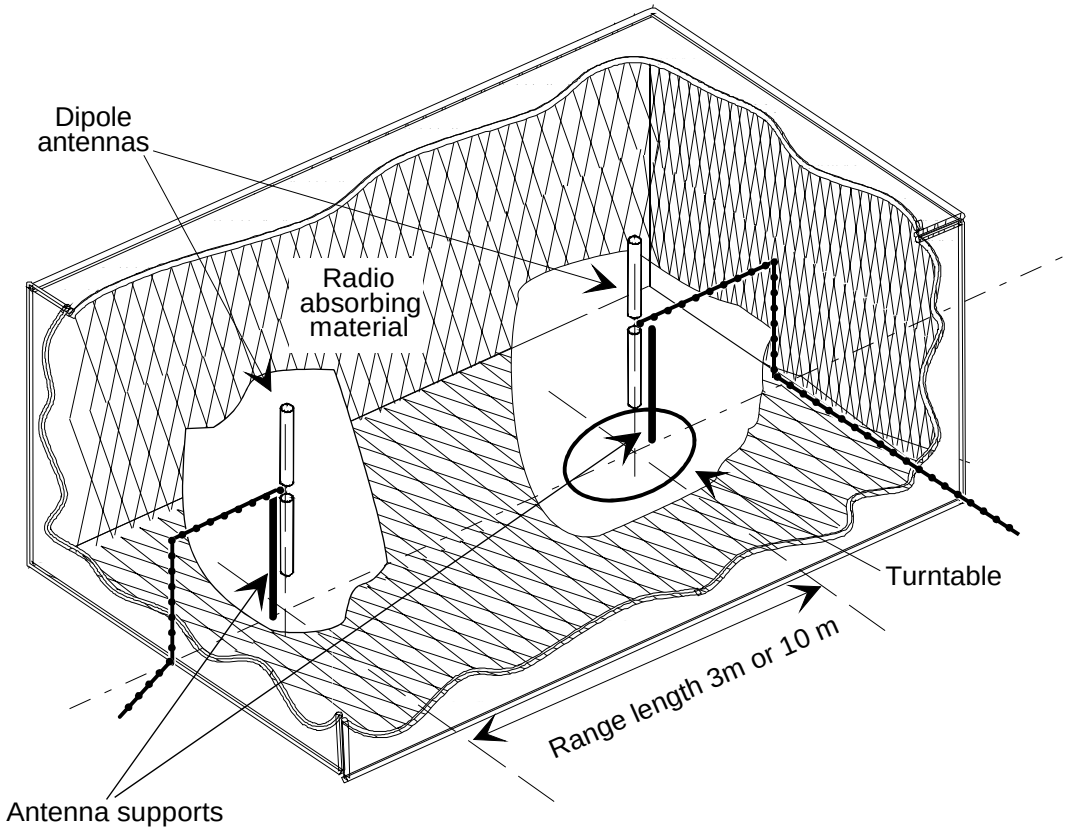

Figure 40: A typical Anechoic Chamber

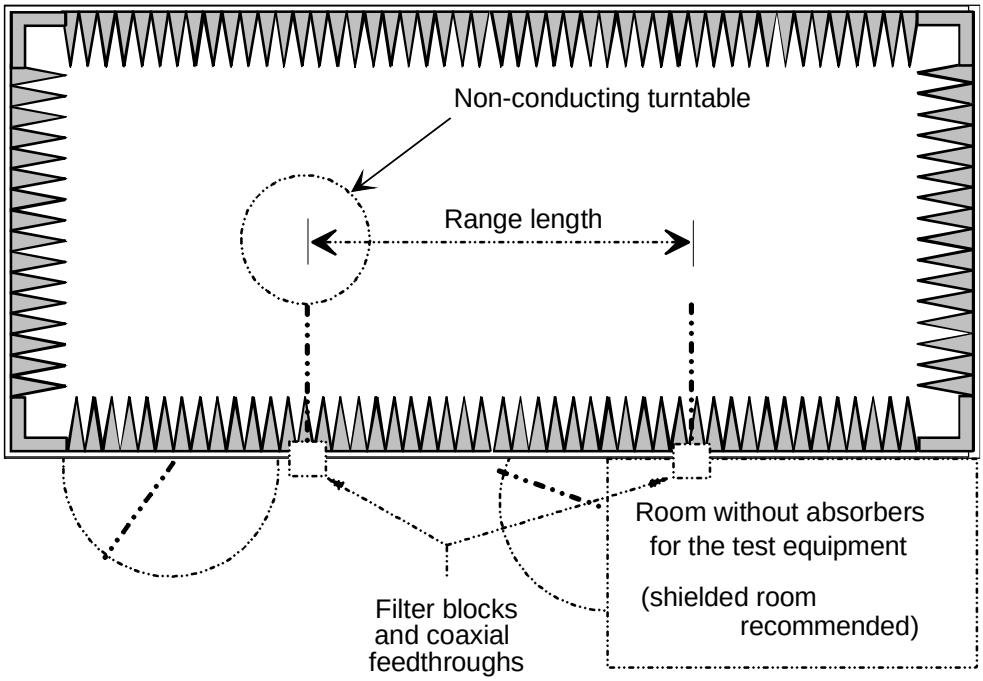

Figure 41: A typical Anechoic Chamber (plan view)

The axis of measurement (i.e. the straight line joining the phase centre of the transmitting antenna to the phase centre of the receiving antenna) is usually coincident with the central axis of the chamber. Unlike test sites which incorporate a reflecting ground plane (i.e. Open Area Test Sites and Anechoic Chambers with Ground Planes), the lack of a reflected signal from the floor means that the measurement axis can remain unchanged during all tests since the height of the test antenna does not need to be optimized.

The physical size of the practical chamber has a limiting effect on the performance obtainable. The primary requirement of absorption of all incident energy relies partially on the adequate transformation of the incident impedance of 377 Ω at the surface of the absorbing panels to a low impedance at their base (metal shield). For pyramidal absorbers to be effective (here the word "effective" is used qualitatively) they should be at least a quarter of a wavelength in thickness. At 30 MHz, the thickness required is 2,5 m which is too large to be accommodated in most practical facilities. The size of the chamber and the thickness of the absorber panels has an additional impact on the facility's performance, since the closer the antennas approach the absorber panels, the greater the mutual coupling that can take place between them. Generally 1 m is taken in the present document as the minimum spacing necessary between antennas and absorbing panels to avoid this mutual coupling effect.

To reduce these size problems at the lower frequencies, some facilities use ferrite tiles under the radio absorbing material. Whilst it is true that in some frequency bands improved performance can result, such a scheme can also produce unwanted resonances and impedance mismatches (leading to increased reflection levels) at certain frequencies as a result of the impedance of the boundaries differing from those assumed in the design of both absorber types.

For an ideal Anechoic Chamber, the specification would comprise:

- a free Space environment;
- loss-free antennas perfectly matched to their circuits;
- both antennas aligned for the same polarization;
- both antennas possessing linear and parallel polarization;
- both antennas to be tuned half-wavelength dipoles;
- the distance between dipoles to be sufficiently great to ensure far field conditions with no mutual coupling effects;
- the distance between the dipoles and chamber walls to be sufficiently great to avoid mutual coupling effects;
- no interference from localized ambient signals.

Any practical Anechoic Chamber will, in one or more ways, be a degradation of this ideal, but it will be a comparison against this ideal that the performance of the Anechoic Chamber will be assessed.

The transmission loss (path loss) of the ideal site, using dipole antennas, is (see clause 7.2.4):

$$\frac{P_{rec}}{P_t} = 1{,}643\left(\frac{\cos\left(\frac{\pi}{2}\cos(\theta)\right)}{\sin(\theta)}\right)^2 1{,}643\left(\frac{\cos\left(\frac{\pi}{2}\cos(\theta)\right)}{\sin(\theta)}\right)^2\left(\frac{\lambda}{4\pi r}\right)^2$$

This can be simplified for the perfectly aligned case, since $\left(\frac{\cos\left(\frac{\pi}{2}\cos(\theta)\right)}{\sin(\theta)}\right)^2 = 1$

Also, by using $\lambda = \frac{c}{f}$, the formula becomes:

$$\frac{P_{rec}}{P_t} = 1{,}643^2\frac{c^2}{16 f^2 \pi^2 r^2}$$

which can be rewritten as:

$$\frac{P_{rec}}{P_t} = \left(\frac{c1{,}643}{4 f \pi r}\right)^2 = \left(\frac{3{,}920\times10^7}{f r}\right)^2$$

Site attenuation (in dB) for this ideal Anechoic Chamber can then be deduced as the inverse of this equation:

$$Site\,Attenuation = 10\log_{10}\left(\frac{P_t}{P_{rec}}\right) = 20\log_{10}\left(\frac{f r}{3{,}920\times10^7}\right)$$

from which it is apparent that the site attenuation, for a fixed frequency, is directly proportional to *r*. Equally, for a fixed distance, site attenuation is directly proportional to *f*.

7.6.2 Anechoic Chamber with a Ground Plane

A variation on the design of the Anechoic Chamber (see clause 7.6.1) is the inclusion of a ground plane, in an attempt to emulate the Open Area Test Site (historically, the reference site upon which the majority of the specification limits have been set). The ideal Anechoic Chamber with a Ground Plane is, conceptually, the same as the ideal Anechoic Chamber except that the infinite empty space is bounded on one side by an infinite, perfectly conducting ground plane.

The introduction of this ground plane creates a modification to the primary characteristic behaviour of a fixed transmit and receive system as described in clause 7.6.1. The ground plane creates a reflection path which will supply, at the receiving antenna, a signal which will add to or subtract from (depending on its relative phasing) the direct signal from the transmitting antenna. This creates a unique received signal level for each height of the transmitting and receiving antennas above the ground plane. The primary characteristic behaviour that the chamber should emulate is, therefore, that for a fixed (in height, separation and antenna alignment) transmitting and receiving antenna system, the received signal level should remain constant for any orientation of that system (in two dimensions, x and z) within the working area of the chamber (see figure 42).

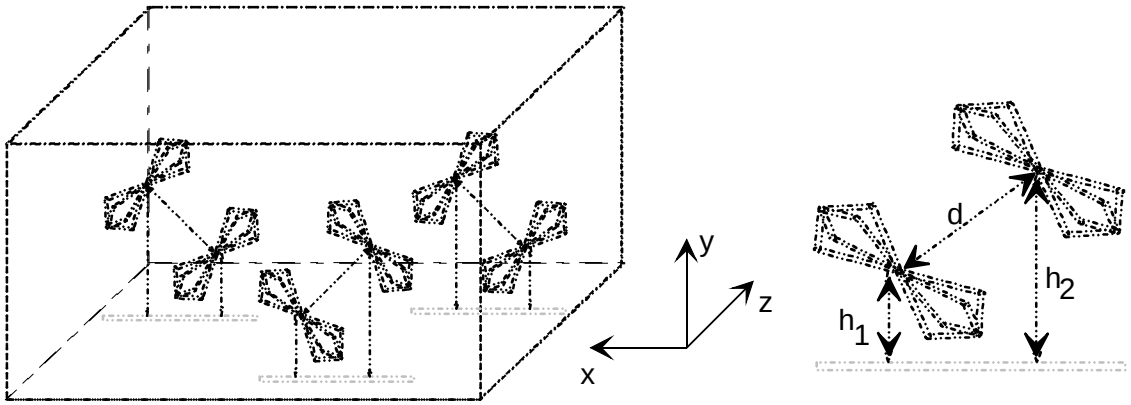

Figure 42: Illustration of the primary characteristic of an Anechoic Chamber with a Ground Plane

Another way in which the ground plane can modify the performance of the chamber is by mutually coupling to the antennas. This effect can change the current distributions on the antennas, resulting in changes to their input impedance, radiation patterns and gain figures. These changes can be severe for the case of tuned half-wavelength dipoles, particularly when used in horizontal polarization. Both the highly resonant nature of the half-wavelength dipole and its zero reactance are easily changed by these mutual coupling effects especially when the ground plane is illuminated beneath it (horizontal polarization). Conversely, the mechanical simplicity of the tuned half-wavelength dipole and the degree to which it lends itself for computer modelling (in marked contrast to other antenna types), have resulted in the dipole being adopted as the standard antenna in the ideal models, despite their apparent drawbacks. For the ideal Anechoic Chamber with a Ground Plane, however, no mutual coupling interaction is considered to take place.

The ideal Anechoic Chamber with a Ground Plane should still emulate free Space on the remaining five sides (side walls, ends and ceiling), but as in the case of the basic Anechoic Chamber, physical size plays a significant part in limiting the available performance from this test facility (see clause 7.6.1). Figure 43 shows a typical Anechoic Chamber with a Ground Plane.

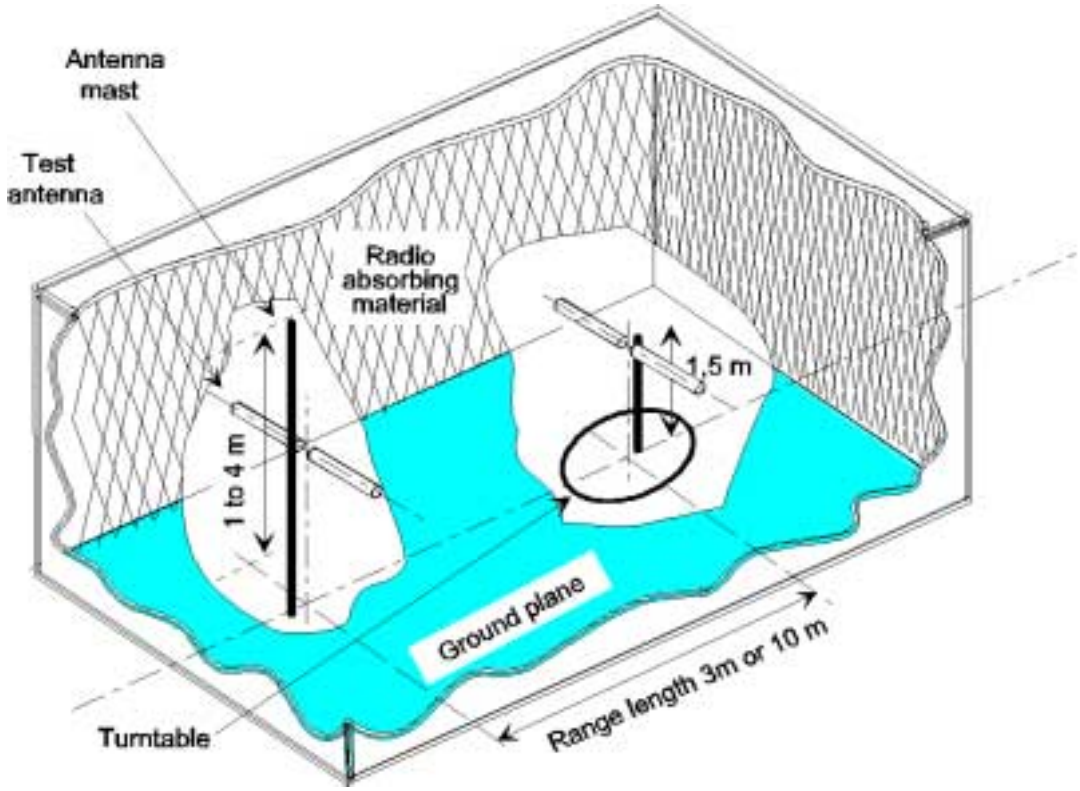

Figure 43: Anechoic Chamber with a Ground Plane

The ideal Anechoic Chamber with a Ground Plane comprises:

- a free Space environment bounded on one side by a perfectly conducting ground plane of infinite extent;
- loss-free antennas perfectly matched to their circuits;
- both antennas aligned for the same polarization;
- both antennas possessing linear and parallel polarization;
- both antennas to be tuned half-wavelength dipoles;
- the distance between dipoles to be sufficiently great to ensure far field conditions with no mutual coupling effects;
- the distance between the dipoles and chamber walls to be sufficiently great to avoid mutual coupling effects;
- no mutual coupling between the dipoles and the ground plane;
- no interference from localized ambient signals.

The mathematical formulation for the site attenuation of an ideal Anechoic Chamber with a Ground Plane is more complicated than for the fully anechoic version, since there are now two signals (the direct and the reflected) to take into account. Also, the signals are not necessarily transmitted or received on the elevation boresights of the antennas; where dipoles are used in vertical polarization, this can result in the signal strength falling off as a result of the directivity in this plane. Figure 44 illustrates the two signal paths involved as well as the elevation plane radiation pattern of a dipole (when used in vertically polarized tests).

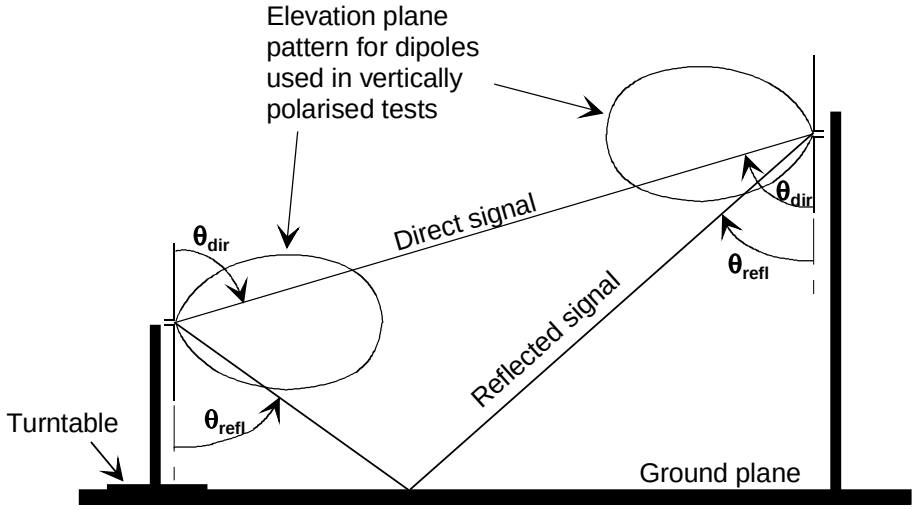

Figure 44: Direct and reflected signal paths over a ground plane

The formula for the power coupled in a direct path between two dipoles was derived in clause 7.5 as:

$$\frac{P_{rec}}{P_t} = 1{,}643 \times \left(\frac{\cos\left(\frac{\pi}{2}\cos(\theta)\right)}{\sin(\theta)} \right)^2 \times 1{,}643 \times \left(\frac{\cos\left(\frac{\pi}{2}\cos(\theta)\right)}{\sin(\theta)} \right)^2 \times \left(\frac{\lambda}{4\pi r} \right)^2$$

To use this formula in the derivation of the model for an Anechoic Chamber with a Ground Plane, several changes need to be made. Firstly, the formula needs to be converted into field strength, since only voltage (and not power) can be used for the addition of signals. This conversion is easily carried out as follows:

$$\frac{E_{rec}}{E_t} = \sqrt{\frac{P_{rec}}{P_t}} = 1{,}643 \times \left(\frac{\cos\left(\frac{\pi}{2}\cos(\theta)\right)}{\sin(\theta)} \right)^2 \times \left(\frac{\lambda}{4\pi r} \right)$$

where E_{rec} and E_t are the received and transmitted electric fields strengths respectively. Next, for both the direct and the reflected signals, the formula needs to be modified to take into account the different path lengths and elevation angles.

For the direct signal:

$$E_{recdir} = E_t \times 1{,}643 \times \left(\frac{\cos\left(\frac{\pi}{2}\cos(\theta_{dir})\right)}{\sin(\theta_{dir})} \right)^2 \times \left(\frac{\lambda}{4\pi r_{dir}} \right)$$

where:

dir suffix refers to the direct signal.

And for the reflected signal:

$$E_{rrefl} = E_t \times 1{,}643 \times \left(\frac{\cos\left(\frac{\pi}{2}\cos(\theta_{refl})\right)}{\sin(\theta_{refl})} \right)^2 \times \left(\frac{\lambda}{4\pi r_{refl}} \right)$$

where:

refl suffix refers to the reflected signal.

Before being able to add these two signals however, their relative phasing, ϕ, needs to be taken into account. The phasing of the reflected signal relative to the direct signal is derived from the difference in their path lengths:

$\phi = \left(\frac{r_{refl} - r_{dir}}{\lambda} \right) 2\pi$ radians for vertically polarized signals.

NOTE: For horizontally polarized signals, the ground reflection adds 180° (π radians).

Adding the two signals for vertical polarization gives:

$$E_r = E_{rec\,dir} + E_{rec\,refl} =$$

$$E_t \times 1{,}643 \times \left(\frac{\lambda}{4 \times \pi} \right) \sqrt{\left(\left(\frac{\cos\left(\frac{\pi}{2}\cos(\theta_{dir})\right)}{\sin(\theta_{dir})} \right)^2 \times \left(\frac{1}{r_{dir}} \right) + \left(\frac{\cos\left(\frac{\pi}{2}\cos(\theta_{refl})\right)}{\sin(\theta_{refl})} \right)^2 \times \left(\frac{1}{r_{refl}} \right) \times \cos\phi \right)^2 + \left(\left(\frac{\cos\left(\frac{\pi}{2}\cos(\theta_{refl})\right)}{\sin(\theta_{refl})} \right)^2 \times \left(\frac{1}{r_{refl}} \right) \times \sin\phi \right)^2}$$

and converting back to power gives:

$$\frac{P_{rec}}{P_t} = \left(\frac{E_r}{E_t}\right)^2 =$$

$$\left(1{,}643 \times \left(\frac{l}{4 \times \pi}\right)\right)^2 \times \left(\left(\left(\frac{\cos\left(\frac{\pi}{2}\cos(\theta_{dir})\right)}{\sin(\theta_{dir})}\right)^2 \times \left(\frac{1}{r_{dir}}\right) + \left(\frac{\cos\left(\frac{\pi}{2}\cos(\theta_{refl})\right)}{\sin(\theta_{refl})}\right)^2 \times \left(\frac{1}{r_{refl}}\right) \times \cos\phi\right)^2 + \left(\left(\frac{\cos\left(\frac{\pi}{2}\cos(\theta_{refl})\right)}{\sin(\theta_{refl})}\right)^2 \times \left(\frac{1}{r_{refl}}\right) \times \sin\phi\right)^2\right)$$

This simplifies to:

$$\frac{P_{rec}}{P_t} = \left(1{,}643 \times \left(\frac{l}{4\pi}\right)\right)^2 \left(\left(\left(\frac{\cos\frac{\pi}{2}\cos(\theta_{dir})}{\sin(\theta_{dir})}\right)^4 \times \left(\frac{1}{r_{dir}^2}\right)\right) + \left(\left(\frac{\cos\frac{\pi}{2}\cos(\theta_{refl})}{\sin(\theta_{refl})}\right)^4 \times \left(\frac{1}{r_{refl}^2}\right)\right) + \left(\frac{2\cos\theta}{(r_{dir} r_{refl})}\left(\left(\frac{\cos\frac{\pi}{2}\cos(\theta_{dir})}{\sin(\theta_{dir})}\right)^2 \left(\frac{\cos\frac{\pi}{2}\cos(\theta_{refl})}{\sin(\theta_{refl})}\right)^2\right)\right)$$

These equations apply for dipoles used in vertically polarized tests only. For horizontal polarization, the terms for the directivity pattern are all equal to 1 (the dipole is omni-directional in the vertical plane) and, after inclusion of the π radian phase shift of the ground reflection, the formula reduces to:

$$\frac{P_{rec}}{P_t} = \left(\frac{E_r}{E_t}\right)^2 = \left(1{,}643 \times \left(\frac{\lambda}{4\pi}\right)\right)^2 \times \left(\left(\left(\frac{1}{r_{dir}}\right) + \left(\frac{1}{r_{refl}}\right) \times \cos(\phi + \pi)\right)^2 + \left(\left(\frac{1}{r_{refl}}\right) \times \sin(\phi + \pi)\right)^2\right)$$

and

$$\frac{P_{rec}}{P_t} = \left(\frac{E_r}{E_t}\right)^2 = \left(1{,}643 \times \left(\frac{\lambda}{4\pi}\right)\right)^2 \times \left(\left(\frac{1}{r_{dir}}\right)^2 + \left(\frac{1}{r_{refl}}\right)^2 - \left(\frac{2}{r_{dir} * r_{refl}}\right) \times \cos\phi\right)$$

The final formulas for both vertically and horizontally polarized tests can be converted into site attenuation formulas by inverting and converting to dB. The resulting formula is therefore:

$$S.A.(vertical) = 17{,}67 + 20\log(\lambda) + 10\log\left(\frac{D_{dir}^4}{r_{dir}^2} + \frac{D_{refl}^4}{r_{refl}^2} + \frac{2\cos\phi\left(D_{dir}^2 \times D_{refl}^2\right)}{r_{dir} \times r_{refl}}\right) \text{dB}$$

where:

$$\text{D}_{\text{dir}} = \left(\frac{\cos\left(\frac{\pi}{2}\cos(\theta_{dir})\right)}{\sin(\theta_{dir})}\right)$$

$$\text{D}_{\text{refl}} = \left(\frac{\cos\left(\frac{\pi}{2}\cos(\theta_{refl})\right)}{\sin(\theta_{refl})}\right)$$

$$S.A.(horizontal) = 17{,}67 + 20\log(\lambda) + 10\log\left(\left(\frac{1}{r_{dir}}\right) + \left(\frac{1}{r_{refl}}\right) - \frac{2\cos\phi}{r_{dir} \times r_{refl}}\right) \text{dB}$$

7.6.3 Open Area Test Site

An Open Area Test Site is usually constructed in an outdoors, unprotected environment. An ideal Open Area Test Site should be situated in an area that is completely devoid of buildings, electric lines, fences, trees etc., is perfectly level and does not suffer from ambient transmissions. The reflecting ground plane should provide the equivalent characteristics of an infinite, perfectly conducting ground plane, see figure 45.

The primary characteristic for the Open Area Test Site is the same as for the Anechoic Chamber with a Ground Plane (see clause 7.6.2). A similar correspondence with clause 7.6.2 applies regarding the performance limitations imposed on a practical facility by the presence of the ground plane. Again the ideal version of the Open Area Test Site assumes no mutual coupling between dipole antennas and the ground plane.

The ideal Open Area Test Site comprises:

- a free Space environment bounded on one side by a perfectly conducting ground plane of infinite extent;
- loss-free antennas perfectly matched to their circuits;
- both antennas aligned for the same polarization;
- both antennas possessing linear and parallel polarization;
- both antennas to be tuned half-wavelength dipoles;
- the distance between dipoles to be sufficiently great to ensure far field conditions with no mutual coupling effects;
- no mutual coupling between the dipoles and the ground plane;
- no interference from localized ambient signals.

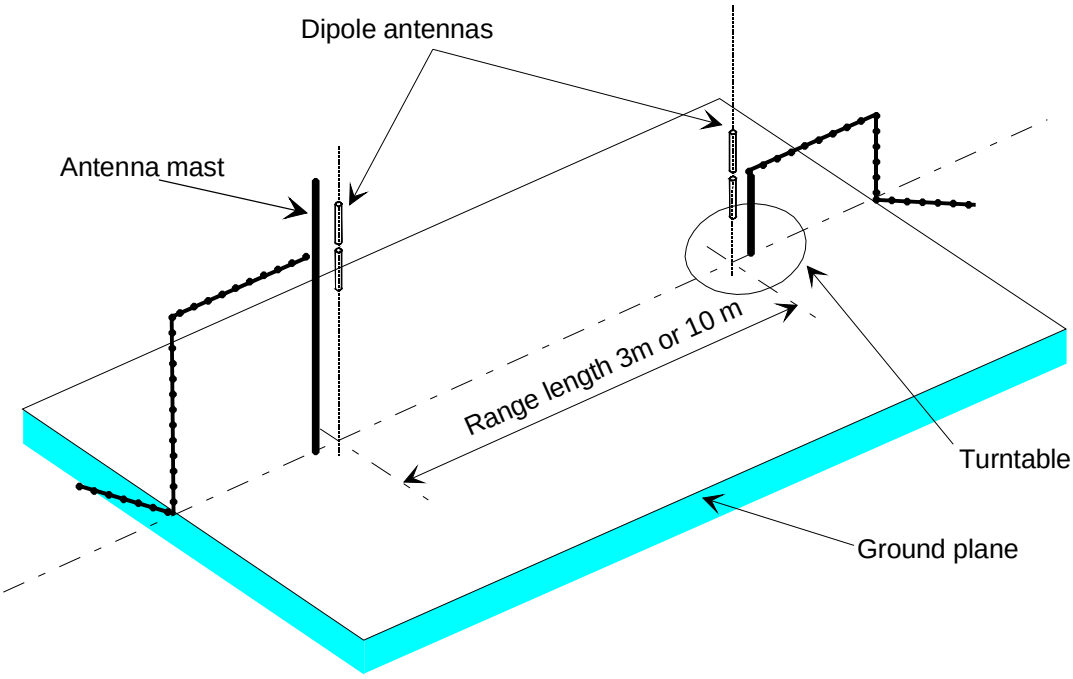

Figure 45: Open Area Test Site arrangement

The theoretical analysis of the performance of the ideal Open Area Test Site is identical to that for the ideal Anechoic Chamber with a Ground Plane (see clause 7.6.2) and will not be repeated here. In particular, the final formulas for site attenuation are identical to the case of the ideal Anechoic Chamber with a Ground Plane.

7.6.4 striplines

A stripline is essentially a transmission line (i.e. similar to coaxial cable, waveguide, etc.) in which RF energy is assumed to propagate with the properties of a Transverse ElectroMagnetic (TEM) wave i.e. the wave is assumed to comprise single electric and magnetic components only and, further, that these components are assumed to be orthogonal to each other and to the direction of propagation. In a truly ideal stripline, these assumptions would be realities and the characteristic impedance of the line (i.e. the ratio of the electric to the magnetic components) would be equivalent to that of free-space (377 Ω).

The ideal stripline would have its plates spaced an adequate distance apart to allow for insertion of a test item whose presence would not disturb the internal fields, create any propagation modes other than the assumed TEM mode and would not suffer mutual coupling/imaging problems. In a practical stripline, the tapered matching sections can be sources of unwanted mode generation as can the termination. For the perfect stripline, therefore, the termination is assumed to be perfectly matched as also is the input section to the line. With perfect matching at both ends of the ideal line, standing waves within the facility should not be present.

The electric field lines run from one plate to the other in a two-plate stripline and in a practical facility, these field lines can fringe which, if conditions are suitable, can lead to radiation from the line. In an ideal facility there would be no loss due to radiation. Equally, an ideal facility would not be susceptible to outside sources of radiation (ambient signals).

The ideal stripline would therefore comprise:

- a perfect termination;
- no losses due to radiated energy;
- perfectly matched input connector;
- no frequency dependency;
- a linear field strength throughout its entire volume;
- no ambient interference;
- no disturbance of the internal field by the insertion of a test item;
- no ambient coupling;
- no internal standing waves;
- no higher order mode generation.

The site attenuation analysis of this test site is carried out assuming a monopole is mounted centrally on the lower plate. The analysis is too complicated to be performed by derivation, so the stripline and monopole have been modelled by practical measurements taken in several accredited test houses. It should be noted that only two-plate striplines are covered by the present document and, even more specifically, only one design - EN 55020 [9]. The site attenuation values are not given here: they are presented in clause 6 of the TR 102 273-5 [13].

The EN 55020 [9] two-plate open cell, illustrated in figure 46, possesses a bottom plate somewhat wider than the upper. This has both practical and electrical advantages. Practically, the width of the plate demands that test equipment, people, etc., are kept a certain minimum distance away, whilst electrically, the effect of having one plate wider than the other is to prevent concentration and bowing of the fields at the plate edges, the ideal field generation is illustrated in figure 47.

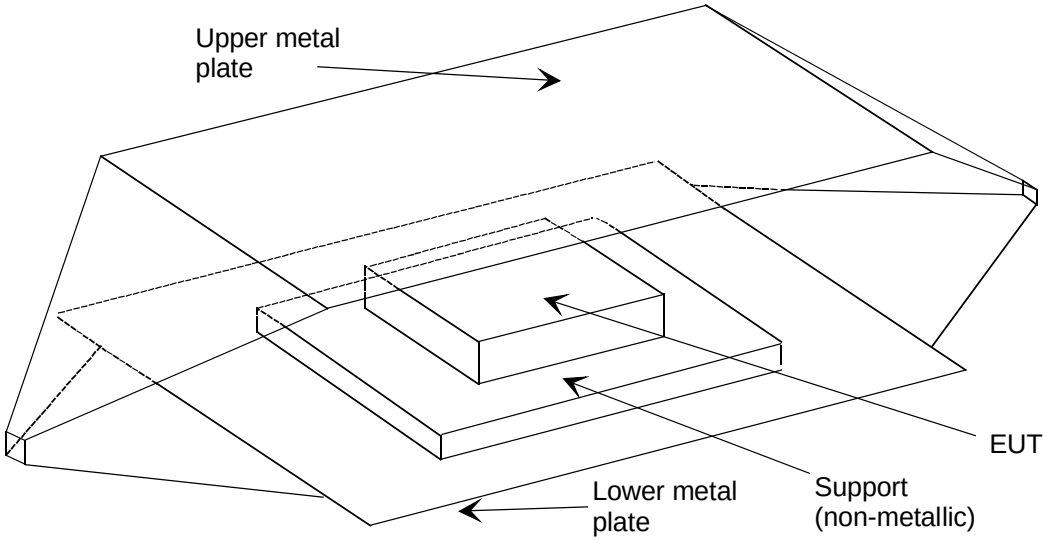

Figure 46: Typical 2 layer open stripline test facility

The EN 55020 [9] stripline measures 2,76 m in length with a height of 0,8 m. It has a lower plate of width 0,9 m and an upper plate width of 0,6 m. For this cell, the characteristic impedance is 150 Ω and this high impedance therefore needs careful matching to the 50 Ω feed lines. This can be achieved either by varying the width of the conductors within the feed taper, or by a matching network.

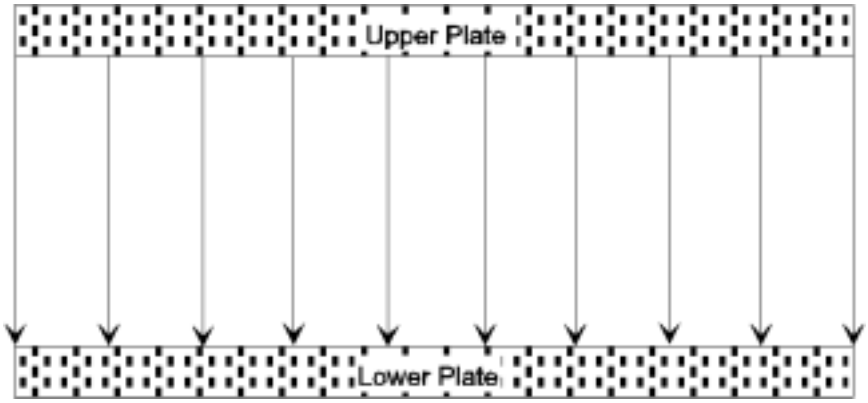

Figure 47: An ideal stripline exhibits no fringing fields

In use, the EUT is placed on a pedestal which is made of a low dielectric constant material and centred in the horizontal plane.

7.7 Verification

7.7.1 Introduction

The verification procedure is a process carried out on all Open Area Test Sites, anechoic facilities (both with and without a ground plane) and striplines to prove their suitability as free field test sites.

A verification procedure is also applied to Test Fixtures and the saltwater column/salty man. In these cases, however, the process is a calibration rather than a true verification procedure since neither of these two devices can be used independently as a free field test site. In the case of the Test Fixture the performance measured during the procedure has to be correlated directly to results from a free field test site, whilst the saltwater column/salty man is verified indirectly by measuring the conductivity of its saline solution.

Anechoic facilities and Open Area Test Sites

For both types of anechoic facility and Open Area Test Sites the procedure involves the transmission of a known signal level from one calibrated antenna (usually a dipole) and the measurement of the received signal level in a second calibrated antenna (also usually a dipole).

By comparison of the transmitted and received signal levels, an "insertion loss" can be deduced. After inclusion of any correction factors to the measurement, the figure of loss which results from the verification procedure, gives the site attenuation.

Site attenuation is defined in "Control of errors on Open Area Test Sites" [8]: as: "The ratio of the power input of a matched, balanced, lossless, tuned dipole radiator to that at the output of a similarly matched, balanced, lossless, tuned dipole receiving antenna for specified polarization, separation and heights above a flat reflecting surface. It is a measure of the transmission path loss between two antennas".

As the definition states ".... above a flat reflecting surface", it is usual for the verification procedure to involve one antenna (the transmitting antenna) remaining fixed in height whilst a second antenna (the receiving antenna) is scanned through a specified height range looking for a peak in the received signal level.

The parameter of site attenuation originated for Open Area Test Sites, hence the reference to a reflective ground plane in the definition. The term is, however, also used in the present document in association with anechoic facilities without a ground plane. The measurement of site attenuation in such an anechoic facility provides an equally good measure of the facility's quality as it does for an Open Area Test Site. Without a ground plane, an ideal anechoic facility has no ground reflection and hence a vertical height scan is unnecessary.

The determination of site attenuation involves two different measurements of received signal level. The first is with all the items of test equipment connected directly together via an adapter, whilst the second involves the coaxial cables being connected to the antennas. The difference in received levels (after allowance for any correction factors which may be appropriate), for the same signal generator output level, gives the site attenuation.

Normalized site attenuation (NSA)

NSA is determined from the value of site attenuation by subtraction of the antenna factors and mutual coupling effects. The subtraction of the antenna factors makes NSA independent of antenna type.

NOTE: The uncertainty of the resulting value for NSA depends directly on the uncertainty with which the antenna factors are known.

Symbolically,

Normalized Site Attenuation = $V_{direct} - V_{site} - AF_T - AF_R - AF_{TOT}$

where:

V_{direct} = received voltage for cables connected via an adapter;

V_{site} = received voltage for cables connected to the antennas;

AF_T = antenna factor of the transmit antenna;

AF_R = antenna factor of the receive antenna;

AF_{TOT} = mutual coupling correction factor.

It is particularly for the verification of Open Area Test Sites that normalized site attenuation has historically found use. However, the same approach has also been adopted in the verification procedures which follow for fully Anechoic Chambers and Anechoic Chambers with Ground Planes.

The verification procedure compares the measured normalized site attenuation (after any appropriate corrections) against the theoretical figure calculated for an ideal site. The difference between the two figures, when taken over the full range of frequencies for which the site is to be used, is a measure of the quality of the test facility.

In general, ANSI and CISPR consider a test site suitable for making measurements (both relative and absolute) if the measured normalized site attenuation differs by less than ±4 dB (throughout the entire frequency range) from the theoretical values. However, for any absolute field strength measurements carried out on that test site, this magnitude of the difference would be automatically added to the uncertainties of the measurement.

7.7.1.1 Anechoic Chamber

In an ideal Anechoic Chamber where there are:

- no unwanted reflections (ground reflected or others);
- no interaction between transmit and receive dipoles;
- no coupling of the dipoles to the absorbing material;
- and where perfectly aligned, loss-less, matched tuned dipoles are used.

the coupling between the dipoles (which are assumed to be half wavelength) is given by the Friis transmission equation (as derived in clause 7):

$$P_{rec} = \left(\frac{\lambda}{4\pi d}\right)^2 1{,}643^2 \left(\frac{\cos\left(\frac{\pi}{2}\cos\theta\right)}{\sin\theta}\right)^2 \left(\frac{\cos\left(\frac{\pi}{2}\cos\theta\right)}{\sin\theta}\right)^2 P_t$$

where:

P_t = power transmitted (W);

P_{rec} = power received (W);

λ = wavelength (m);

d = distance between dipoles (m),

and θ is a spherical co-ordinate, as shown in figure 48.

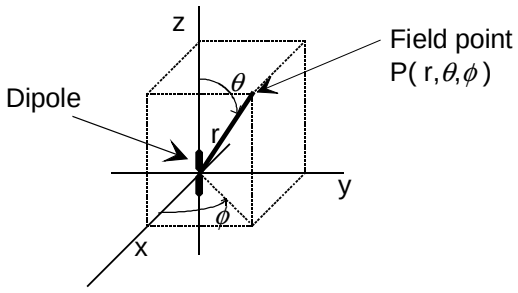

Figure 48: Spherical co-ordinates

For this ideal site, the site attenuation is given by:

$$\frac{P_t}{P_{rec}} = \left(\frac{4\pi d}{\lambda}\right)^2 \frac{1}{1{,}643^2} \left(\frac{\sin\theta}{\cos\left(\frac{\pi}{2}\cos\theta\right)}\right)^2 \left(\frac{\sin\theta}{\cos\left(\frac{\pi}{2}\cos\theta\right)}\right)^2$$

More usually, this formula is given in logarithmic (dB) terms as follows:

$$\textit{Site Attenuation} = 17{,}67 + 20\log\left(\frac{d}{\lambda}\right) + 20\log\left(\frac{\sin\theta}{\cos\left(\frac{\pi}{2}\cos\theta\right)}\right) + 20\log\left(\frac{\sin\theta}{\cos\left(\frac{\pi}{2}\cos\theta\right)}\right) \text{ dB}$$

Since both transmit and receive antennas are assumed to be at the same height, $\theta = \pi/2$ and the formula reduces to:

$$\text{Site Attenuation} = 17{,}67 + 20 \log (d/\lambda) \text{ dB}$$

NOTE 1: In an actual measurement, the value of site attenuation is likely to be greater than given by this formula due to mismatch and resistive losses, mutual coupling effects, etc.

An alternative formulation for site attenuation, based on field strength (V/m) and antenna factors has been derived in [8]. The resulting formulas are for use with ground reflection sites but they are easily adapted for the fully Anechoic Chamber.

The general formula given in [8] for site attenuation, *A*, is:

$$A = \frac{279{,}1\, AF_T\, AF_R}{f_m E_{D(H\ or\ V)}^{\max}}$$

where:

AF_T = antenna factor of the transmitting antenna (m^{-1});

AF_R = antenna factor of the receiving antenna (m^{-1});

f_m = frequency (MHz); and

$E_{D(H\ or\ V)}^{\max}$ = calculated maximum electric field strength (μV/m) in the receiving antenna height scan from a half wavelength dipole with 1 pW of radiated power.

$E_{D(H\ or\ V)}^{\max}$ takes the form $E_{DH}^{\max}$ for horizontal polarization and $E_{DV}^{\max}$ for vertical polarization.

NOTE 2: The stipulations of a half wavelength dipole and 1 pW of radiated power in $E_{D\ (H\ or\ V)}^{max.}$ do not limit the use of the site attenuation equation to those conditions. The definition of $E_{D\ (H\ or\ V)}^{max.}$ in the text of [8] is for convenience only and the stipulated conditions cancel out in the final formulas for site attenuation and normalized site attenuation, both of which apply generally.

For the fully Anechoic Chamber, $E_{D(H\ or\ V)}^{\max}$ (a term whose amplitude is generally peaked on a ground reflection range by height scanning on a mast) is simply replaced by $E_{D(H\ or\ V)}$ since no maximization is involved and both polarizations behave similarly. $E_{D(H\ or\ V)}$ can be shown to be:

$$E_{DH} = E_{DV} = 7{,}01/d$$

In decibel terms, the site attenuation formula becomes:

$$A = 48{,}92 + 20 \log (AF_T) + 20 \log (AF_R) - 20 \log f_m - 20 \log (7{,}01/d) \text{ dB}$$

The formula for NSA then follows as:

$$NSA = A - 20 \log (AF_T) - 20 \log (AF_R) \text{ dB}$$

$$\text{i.e. } NSA = 48{,}92 - 20 \log f_m - 20 \log (7{,}01/d) \text{ dB}$$

For commonality of approach with ground reflection test sites, it is this formulation of normalized site attenuation which has been adopted in the verification processes for fully Anechoic Chambers given in clause 7.7.2.

7.7.1.2 Anechoic Chamber with a Ground Plane and Open Area Test Site

The formula for $E_{D(H\ or\ V)}$ in the site attenuation equation for the fully Anechoic Chamber, given above, is only applicable if no reflections (ground or otherwise) are present. In the case of an Anechoic Chamber with a Ground Plane or the Open Area Test Site, where a ground reflection is present, the formula is modified to take the reflections into account. However, this situation is further complicated by:

- the ground reflected ray suffering a phase reversal at the metal/air boundary for the horizontally polarized case (vertically polarized signals suffer no phase change); and
- the radiation pattern of the dipole, (which is omni-directional in the H-plane and directional in the E-plane), resulting in received amplitudes which change with off-boresight angles in the E-plane for vertical polarization. This does not occur in the horizontally polarized case.

As a result different formulas apply for horizontal and vertical polarizations and these are now derived. For both polarizations however, the basic formula for site attenuation remains as:

$$A = \frac{279{,}1\, AF_T\ AF_R}{f_m\ E_{D(H\ or\ V)}{}^{\max}}$$

For the horizontal polarized case of this formula, the term $E_{D(H\ or\ V)}{}^{\max}$ in an ideal Anechoic Chamber with a Ground Plane using dipoles and optimized over the height scan range, is [8]:

$$E_{DH}{}^{\max} = \frac{7{,}01}{d_{dir}\, d_{refl}} \sqrt{d_{refl}{}^2 + |\rho_H|^2\, d_{dir}{}^2 + 2 d_{dir}\, d_{refl} |\rho_H| \cos\left(\phi_H - \beta\left(d_{refl} - d_{dir}\right)\right)}$$

where:

$$\rho_H = \frac{\sin\gamma - \left(K - j60\lambda\sigma - \cos^2\gamma\right)^{\frac{1}{2}}}{\sin\gamma + \left(K - j60\lambda\sigma - \cos^2\gamma\right)^{\frac{1}{2}}} = |\rho_H| e^{j\phi_H}\ ;$$

d_{dir} = path length of the direct signal (m); d_{refl} = path length of the reflected signal (m);

β = $2\pi/\lambda$ (radians/m); K = relative dielectric constant;

σ = conductivity (Siemens/m); ϕ_H = phase angle of reflection coefficient

γ = incidence angle with ground plane

For a perfectly reflecting metallic ground plane, $|\rho_H| = 1{,}0$ and $|\phi_H| = 180$ °. As a result, the formula for $E_{DH}{}^{\max}$ reduces to:

$$E_{DH}{}^{\max} = \frac{7{,}01\sqrt{d_{refl}{}^2 + d_{dir}{}^2 - 2 d_{dir}\, d_{refl} \cos\beta\left(d_{refl} - d_{dir}\right)}}{d_{dir}\, d_{refl}}$$

Figure 49 shows the geometry for horizontally polarized tests using dipoles above a reflecting surface.

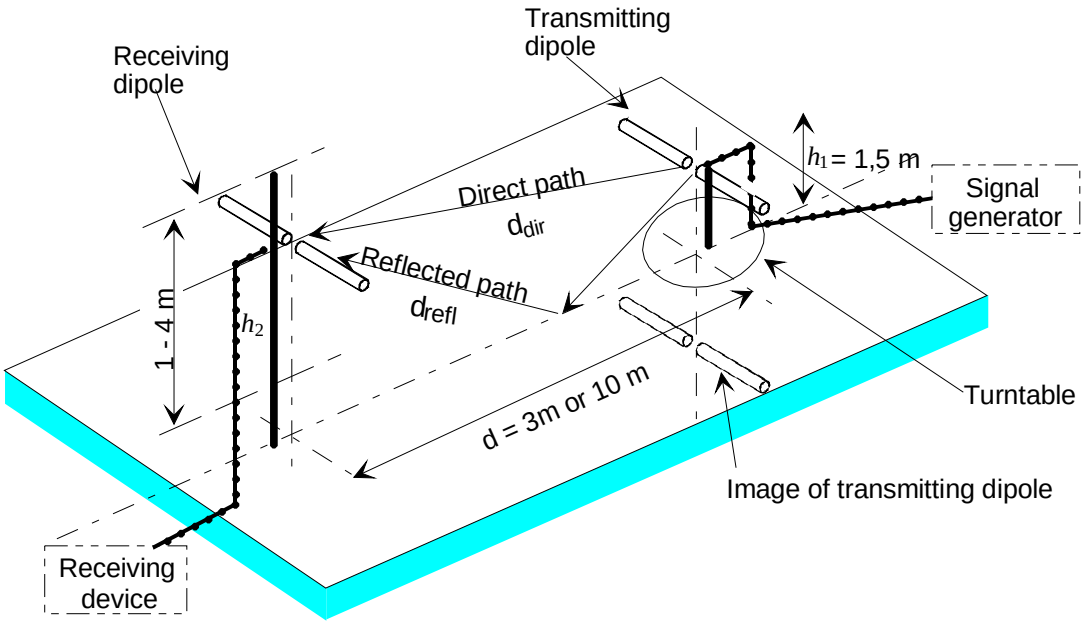

Figure 49: Ground reflection test site layout for horizontally polarized verification using dipoles

From figure 49 it can be seen that:

$$d_{dir} = \sqrt{(h_2 - h_1)^2 + d^2} \text{ and } d_{refl} = \sqrt{(h_1 + h_2)^2 + d^2}$$

For vertical polarization, a similar procedure is used to find $E_{DV}{}^{max}$. However, in the vertical case, off boresight angles of incidence, shown in figure 50 introduce additional terms.

This off boresight angle effect is accounted for in [8] by giving the dipoles a "sin θ" pattern in the E-plane (the vertical plane as shown in figure 50).

Geometrically,

$$\sin\theta_1 = \frac{d}{d_{dir}} \text{ and } \sin\theta_2 = \frac{d}{d_{refl}}$$

and incorporating these into the calculation of $E_{DV}{}^{\max}$, optimized over the height scan range, produces:

$$E_{DV}{}^{\max} = \frac{7{,}01\,d^2}{d_{dir}{}^3 d_{refl}{}^3}\sqrt{d_{refl}{}^6 + d_{dir}{}^6|\rho_V|^2 + 2d_{dir}{}^3 d_{refl}{}^3|\rho_V|\cos\left(\phi_V - \beta\left(d_{refl} - d_{dir}\right)\right)}$$

where:

$$\rho_V = \frac{(K - j60\sigma)\sin\gamma - \left(K - j60\lambda\sigma - \cos^2\gamma\right)^{\frac{1}{2}}}{(K - j60\sigma)\sin\gamma + \left(K - j60\lambda\sigma - \cos^2\gamma\right)^{\frac{1}{2}}} = |\rho_V| e^{j\phi_V}$$

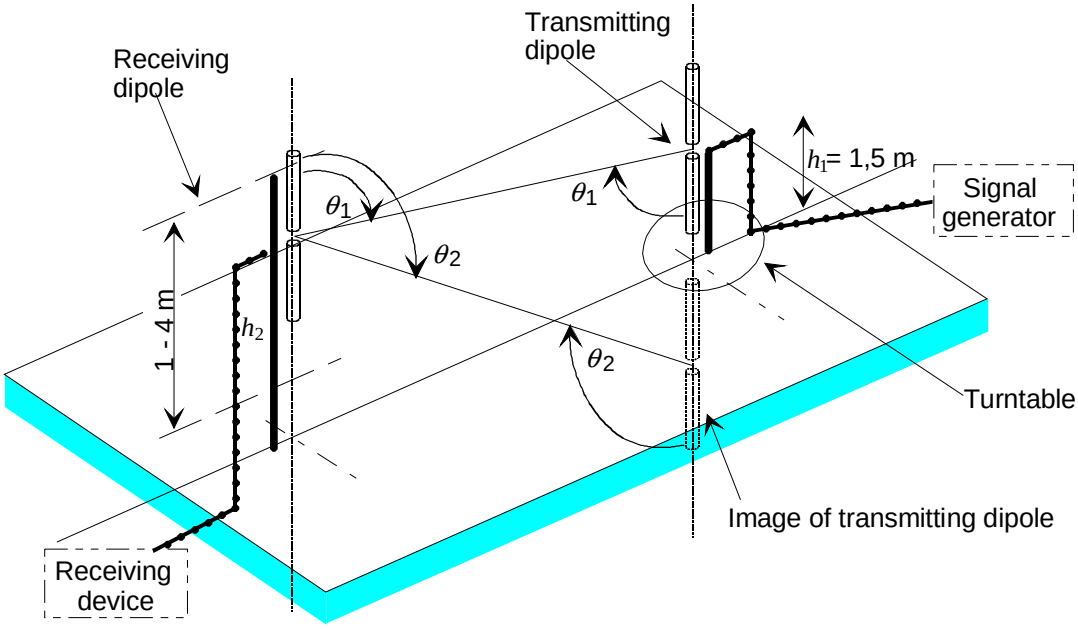

Figure 50: Off-boresight angles involved in verification using vertical polarization

For a perfectly reflecting metallic ground plane, $|\rho_V|$=1,0 and ϕ_V = 0°. As a result, the formula for $E_{DV}{}^{\max}$ reduces to:

$$E_{DV}{}^{\max} = \frac{7{,}01 d^2}{{d_{dir}}^3 {d_{refl}}^3} \sqrt{{d_{refl}}^6 + {d_{dir}}^6 + 2{d_{dir}}^3 {d_{refl}}^3 \cos\beta\left(d_{refl} - d_{dir}\right)}$$

It is important, on ground reflection sites, to state again that the received signal level needs to be peaked by varying the height of the receive antenna on the antenna mast (usually from 1 to 4 m) for these formulas to be used correctly.

7.7.1.3 Improvements to the formulas for $E_{DH}{}^{\max}$ and $E_{DV}{}^{\max}$

In the verification procedures for Anechoic Chambers with Ground Planes and Open Area Test Sites (see clauses 7.7.3 and 7.7.4 respectively), the performance of a facility is measured for a number of transmitting dipole positions within a specified volume. This results in several positions for which off-boresight angles of incidence occur, for both polarizations. As a consequence, the formula for $E_{DH}{}^{max}$ has to be modified. However, so too does $E_{DV}{}^{max}$ since the angles involved are no longer simple as considered above but are compound.

Further modifications to the formulas for $E_{DH}{}^{max}$ and $E_{DV}{}^{max}$ have also been made to more accurately represent the patterns of the dipoles. A better approximation to the nearly half wavelength dipoles of

$$\frac{\cos\left(\frac{\pi}{2}\cos(\theta)\right)}{\sin\theta}$$

has been used, resulting in the following formulas.

For horizontal polarization:

$$E_{DH}{}^{\max} = \frac{7{,}01}{YZ} \sqrt{{d_{dir}}^2 Z^2 \cos^4\alpha_1 + {d_{refl}}^2 Y^2 \cos^4\alpha_2 - 2 d_{dir} d_{refl} YZ \cos^2\alpha_1 \cos^2\alpha_2 \cos\beta\left(d_{refl} - d_{dir}\right)}$$

where:

$\alpha_1 = \frac{\pi}{2}\frac{y_{offset}}{d_{dir}}$ (radians), where y_{offset} is given in figure 51;

$$\alpha_2 = \frac{\pi}{2}\frac{y_{offset}}{d_{refl}} \text{ (radians);}$$

$$Y = {d_{dir}}^2 - {y_{offset}}^2 \text{ (m}^2\text{);}$$

$$Z = {d_{refl}}^2 - {y_{offset}}^2 \text{ (m}^2\text{).}$$

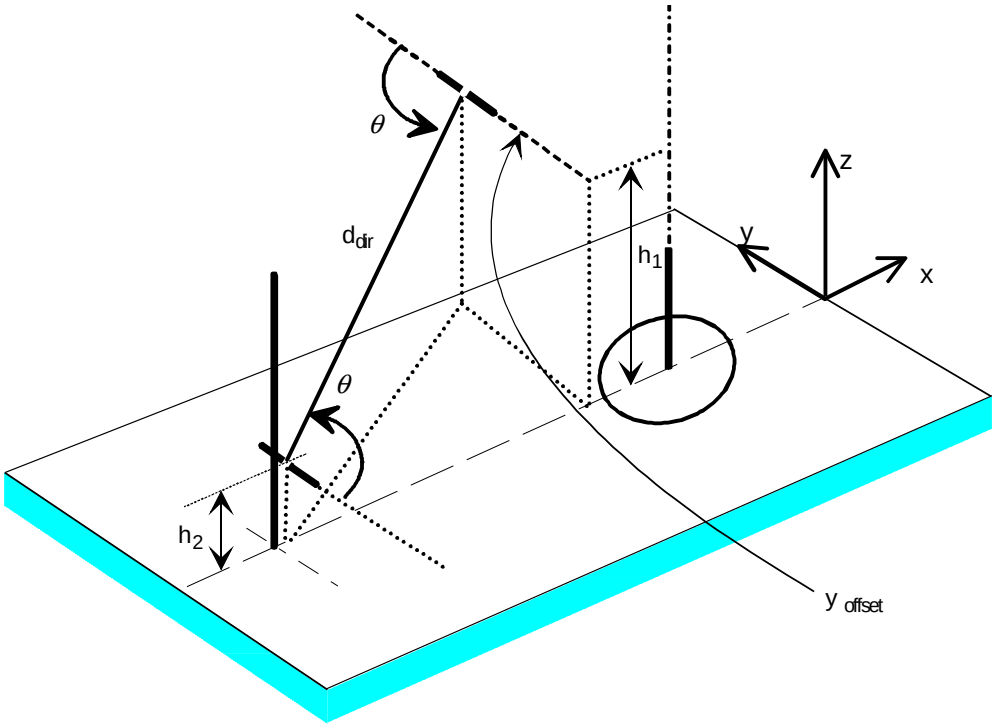

Figure 51: Geometry of the verification set-up for horizontal polarization

For vertical polarization, a similar procedure results in:

$$E_{DV}{}^{\max} = \frac{7{,}01}{D}\sqrt{{d_{dir}}^2 \cos^4\delta_1 + {d_{refl}}^2 \cos^4\delta_2 + 2 d_{dir} d_{refl} \cos^2\delta_1 \cos^2\delta_2 \cos\beta\left(d_{refl} - d_{dir}\right)}$$

where:

$$\delta_1 = \frac{\pi}{2}\frac{\left(h_2 - h_1\right)}{d_{dir}} \text{ (radians);}$$

$$\delta_2 = \frac{\pi}{2}\frac{\left(h_2 + h_1\right)}{d_{refl}} \text{ (radians);}$$

$$D = d^2 + {y_{offset}}^2 \text{ (m}^2\text{).}$$

To derive NSA, these figures (maximized within the height scan limits) are inserted into:

$$NSA = 20\ \log\left(\frac{279{,}1}{f_m E_{D(H\,or\,V)}{}^{\max}}\right) \text{dB}$$

i.e.: $NSA = 48{,}92 - 20 \log f_m - 20\ \log E_{D(H\,or\,V)}{}^{\max}$ dB

These formulas given above for normalized site attenuation apply equally for both Anechoic Chambers with a ground plane and Open Area Test Sites. The major differences between these two types of facility are not therefore in their fundamental electromagnetic behaviour, they are more concerned with shielding from ambients, a potentially longer range on an Open Area Test Site (to 30 m) and potential height limitations within an Anechoic Chamber with a Ground Plane.

7.7.1.4 Mutual coupling

For both types of anechoic facilities (i.e. with and without a ground plane) as well for Open Area Test Sites there may be mutual coupling (see clause 7.2.3) between the antennas (see figure 52). This will serve to modify the results since mutual coupling changes both antenna input impedance/voltage standing wave ratio and gain/antenna factor.

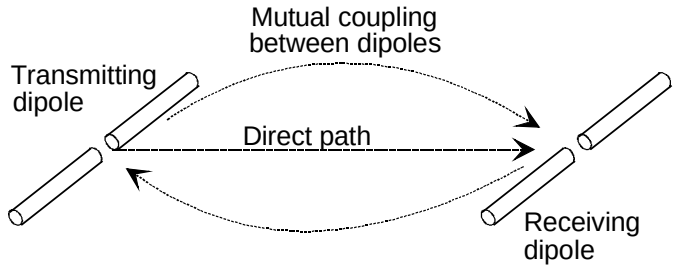

Figure 52: Direct path and mutual coupling

Figure 52 shows schematically mutual coupling as it occurs between dipoles in a reflection-free environment (i.e. an ideal Anechoic Chamber).

The situation is more complex for those test site facilities incorporating a reflecting surface, since the ground plane acts like a mirror, imaging each dipole in the ground. Because of this imaging there are, in effect, four dipoles to be considered. The transmitting dipole "sees" its own image in the ground as well as the real receiving dipole and its image. The receiving dipole "sees" its own image in the ground along with the transmitting dipole and its image. Mutual coupling can exist between all these dipoles, whether real or images. This is shown in figure 53b alongside the ideal model in figure 53a.

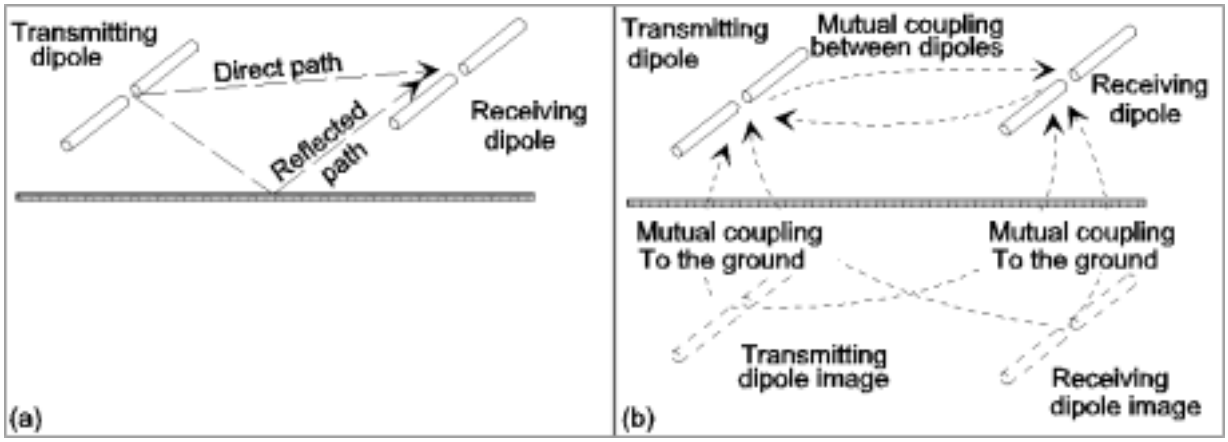

Figure 53: (a) Ideal model of an Open Area Test Site and (b) mutual coupling effects on a real site

A further complication is that for fixed geometries the mutual coupling effects vary with frequency. The actual situation when horizontally polarized NSA is measured is shown schematically in figure 54.

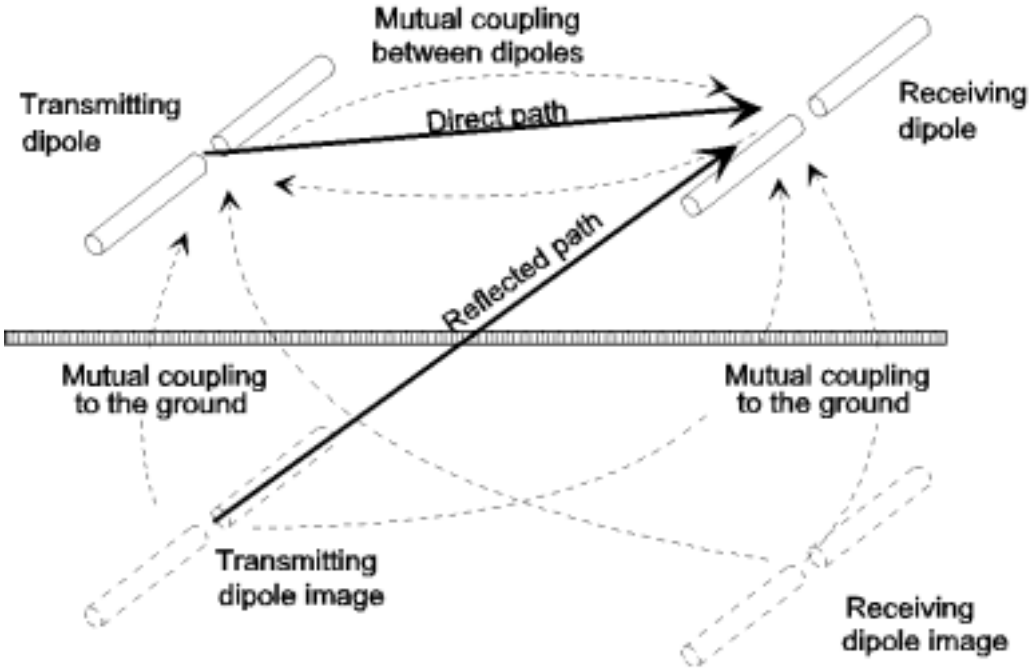

Figure 54: Measuring site attenuation

For accurate determination of NSA these additional effects needs to be taken into consideration and correction factors should be applied to the measured results to compensate.

In the verification procedure that follows, tables of correction factors are provided for mutual coupling between dipoles, where relevant, for 3 mand 10 m range lengths.

7.8 The nature of the testing field on free field test sites

7.8.1 Fields in an Anechoic Chamber

Since the far-field formula ($2(d_1+d_2)^2/\lambda$) contains a wavelength term, the frequency has a major impact on the available volume in which testing can be carried out. For a fixed separation (range length), assuming a point source for the transmitter, the length of the side of an approximate cube within which 22,5° maximum phase curvature exists can be calculated from:

$$d_1 + d_2 = \sqrt{\frac{\lambda \times r}{2}}$$

i.e. the size of the cube reduces with increasing frequency. This is illustrated in figure 55.

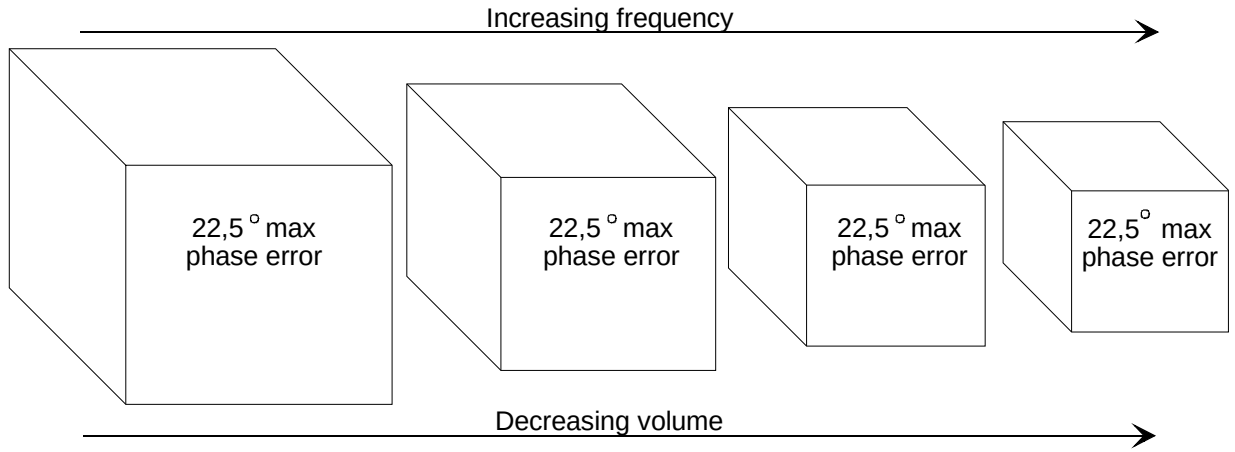

Figure 55: Initial formulation

If, however, for a given frequency a relaxation of the 22,5° maximum phase curvature across the aperture is allowed, then the length of the side, and hence the volume of the approximate cube, can be increased. This will be at the expense of increased uncertainty arising from the additional phase variation across the aperture. This is illustrated in figure 56.

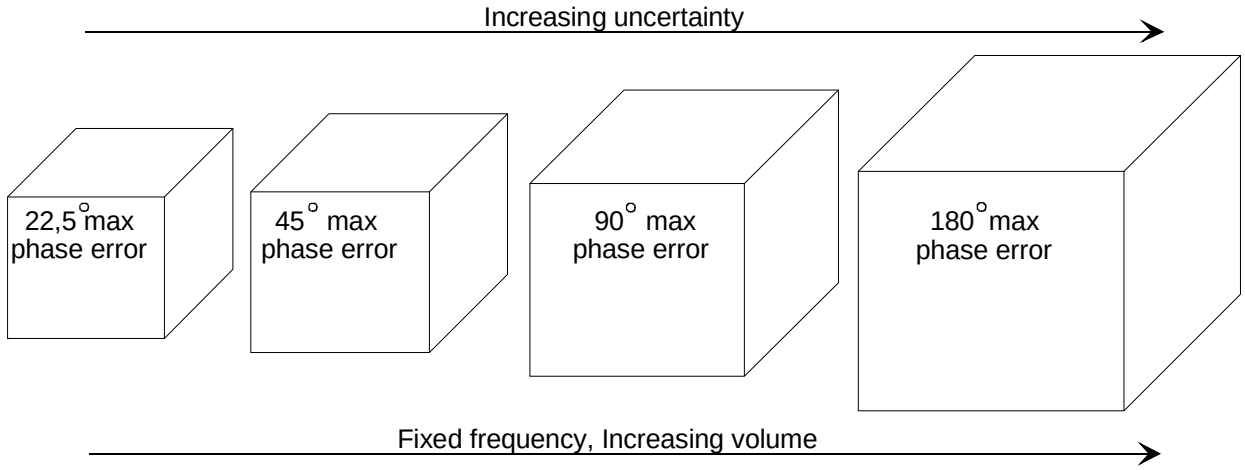

Figure 56: Effect of increasing the volume, keeping the range length constant

7.8.1.1 Practical uniform field testing

The practical situation however is illustrated in figure 57 where the volume of the cube is fixed i.e. there are specific dimensions associated with the EUT and source antenna.

In some cases it is not possible to have a separation distance $\geq 2(d_1+d_2)^2/\lambda$ and as a result more than $22{,}5°$ phase variation exists over the measuring aperture of the receiving equipment (EUT or receiving antenna).

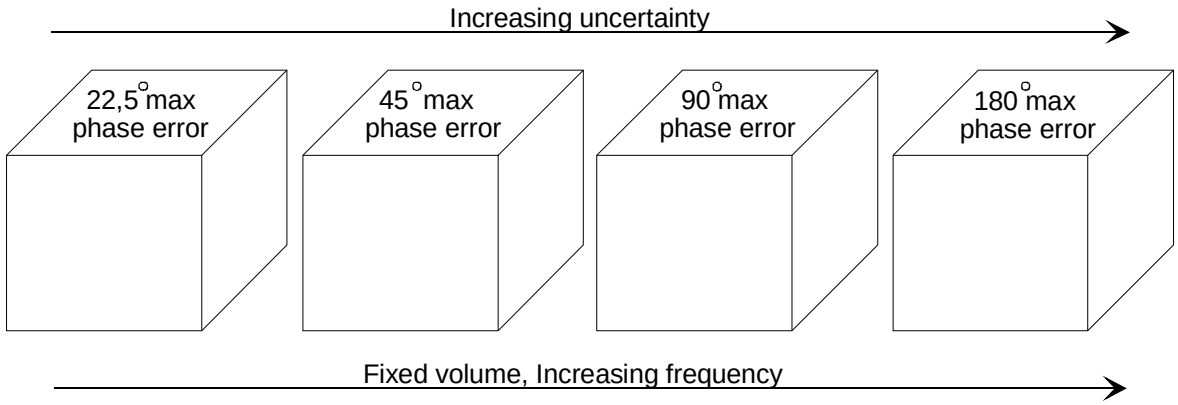

Figure 57: Constant volume, fixed range length

For set values of range length, frequency, and sizes of source antenna and EUT, the maximum phase curvature can be calculated from:

$$Maximum\ phase\ curvature = \frac{\sqrt{r^2 + \left(\frac{d_1 + d_2}{2}\right)^2} - r}{\lambda} 360^\circ$$

The present document strongly recommends that, in all tests, the phase variation does not exceed 22,5°. However, uncertainty values (given in annex A) are given for phase curvatures up to approximately 180°.

The limits of uncertainty for 180° phase curvature across the aperture are illustrated in figure 58. The resulting range of uncertainties depends on the required amplitude and phase across the EUT/antenna (which may be an array whose elements have a non uniform phase requirement). Taking initially the case of an EUT/antenna requiring uniform phase and uniform amplitude (illustrated in figure 58b), 180° phase curvature will result in a received signal level about 4,1 dB BELOW that of the far-field level. This case is shown in figure 58a. The alternative extreme case, in terms of received level error, would be that for an EUT/antenna whose array elements or aperture are actually fed with a phase distribution which exactly matches that of the incident 180° curvature. In this case, the EUT/antenna will actually receive a signal about 4,1 dB ABOVE that of the far-field case. This is illustrated in figure 58c. The uncertainty resulting from phase curvature is therefore distributed symmetrically about zero.

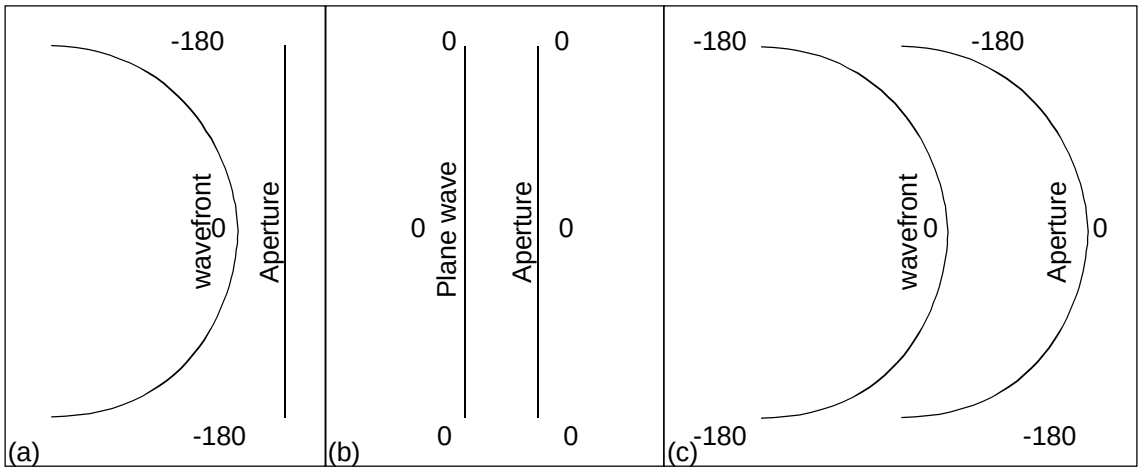

Figure 58: Extreme cases of wavefront and aperture compared to the ideal case

It is assumed in practice that the extreme cases are unlikely and that as a consequence the distribution of this uncertainty is normal, hence the worst case uncertainties are actually the 99,9 % confidence values. The standard uncertainties corresponding to various phase errors are given in table 3 and have been found by dividing the uncertainty limits by 3,209 4.

Table 3: Additional measurement uncertainty due to proximity of the EUT

Maximum phase curvature	Range length	Standard uncertainty
22,5 °	$2(d_1 + d_2)^2 / \lambda$	0,00 dB
45 °	$(d_1 + d_2)^2 / \lambda$	0,10 dB
90 °	$(d_1 + d_2)^2 / 2\lambda$	0,30 dB
180 °	$(d_1 + d_2)^2 / 4\lambda$	1,26 dB
NOTE: This table has been calculated on the basis of gain loss from an aperture uniformly illuminated in amplitude (the worst case figures).		

7.8.1.2 Sensitivity considerations

As discussed in clause 10.6.3, the sensitivity of the measuring receiver becomes a significant limiting factor in a measurement at high frequencies. For a given size of EUT, as the frequency increases, so does the far-field distance. Consequently the path loss will also increase.

To make accurate measurements on, say, a 6 m EUT at 12,75 GHz, it is necessary to be 3,06 km distant from the source (a calculated path loss of more than 124 dB!) and a compromise has to be made between practicality of measurement and measurement uncertainty.

7.8.1.3 Appreciable size source

This situation is more complicated, since the source is almost certainly of appreciable size. In this case the phase variation, as seen across the receiving aperture, is larger since longer path lengths are involved (see clause 7.2). To maintain a maximum phase variation of 22,5 ° across the receive aperture, the far-field range length should be:

$$\text{far-field range length} = 2(d_1+d_2)^2 / \lambda \qquad (7.1)$$

The formulation of the far-field range length is used to determine the distance required between the antenna and the EUT for negligible measurement errors. For a variety of reasons, however, it is not always practical to maintain this distance.

7.8.1.4 Minimum separation distance

Measurements at reduced separations from the EUT will result in larger uncertainties in the measurement until, at very close distances, the mutual interaction between source and receive apertures mean the measurement no longer has any validity.

The separation at which the measurement becomes meaningless occurs when the inductive near field of either the EUT or the test antenna is entered. This is considered to be at a distance of [5]:

$$0{,}62\sqrt{\frac{d^3}{\lambda}} \qquad (7.2)$$

Between an EUT and test antenna of aperture size d_1 and d_2, this formula can be modified as follows:

$$0{,}62\sqrt{\frac{(d_1 + d_2)^3}{\lambda}}$$

7.8.1.5 Summary

Many test engineers think of far-field problems as low frequency concerns only. Provision of the far-field distance is often overlooked therefore, at the top end of the frequency band. This problem is not limited to "in situ" or "on site" testing that may be carried out at remote premises, it also applies to test sites in general.

When a test site undergoes the verification procedure, the response of the facility throughout a "volume" is measured. If no significant problems are detected the facility is regarded as satisfactory. Clauses 7.8.1 and 7.8.1.1 however, identify various sizes of "volume" for different phase variations. Provided these volumes fall within the "verification proven volume", testing can be carried out with calculable error (see table 3).

It should be noted that the phase variation across a test aperture or volume is purely a result of the geometry involved and cannot be avoided. This geometric phase variation would be apparent if a test volume was scanned with a field probe connected to a phase sensitive receiver.

There is a limit to how close a transmit aperture can be approached by a receiving aperture, namely when the two inductively couple. Therefore between the two values defined by equations (7.1) and (7.2), there is a progressive degradation of measurement uncertainty.

7.8.2 Fields over a ground plane

In clause 7.8.1 we considered a spherically spreading wavefront. The wavefront is spherical in the *x* and *y* directions travelling along the *z* direction as illustrated in figure 59.

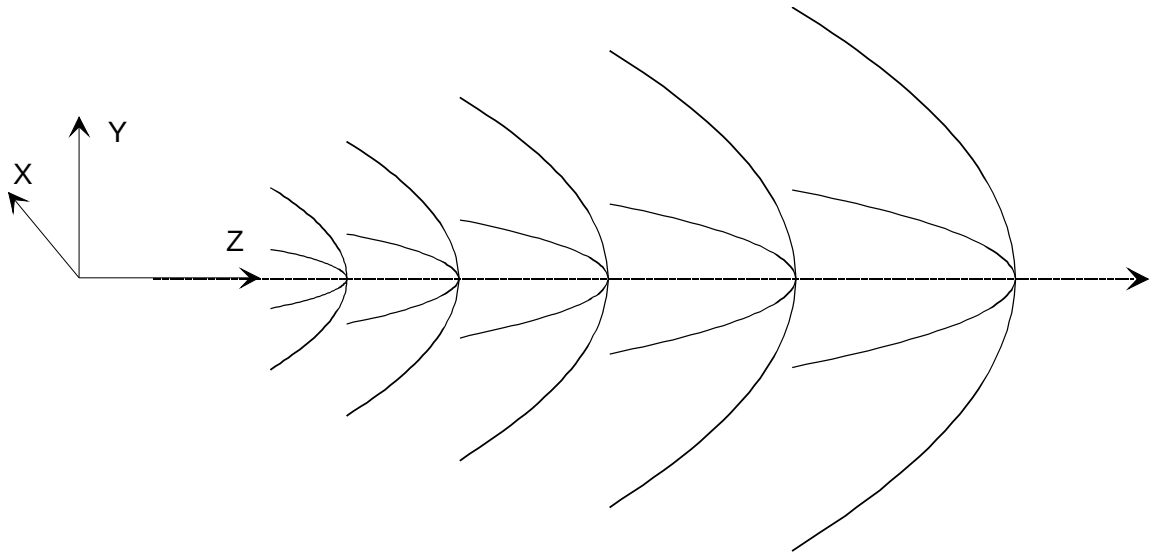

Figure 59: Spherically spreading wavefront

This model enables us to determine the appropriate value for a given phase error across the test volume and some general rules of thumb regarding measuring distances. These apply only in the free Space environment provided by a good Anechoic Chamber. For an Anechoic Chamber with a Ground Plane or an Open Area Test Site, this simple model is no longer valid. The more complex situation over a ground plane is illustrated in figure 60 where a ground reflected wave combines with the direct wave and travels through the test volume.

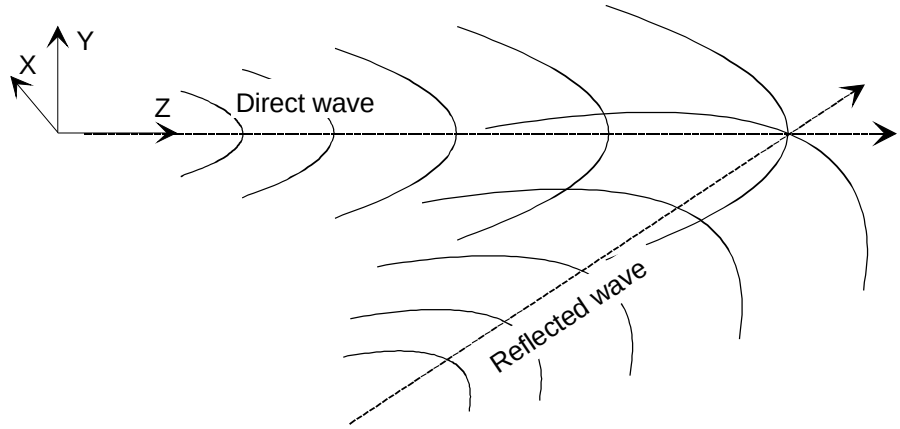

Figure 60: Spherically spreading wavefront from two directions

In this case the phase variation through the receive volume is the resultant interaction of the two waves.

If the direct and reflected waves are traced out in a fixed *z* direction, as shown in figure 61, the phase change is more rapid in the *y* direction than in the *x* direction due to the more rapidly changing ratio of the direct and reflected path lengths. This results in an EUT height limitation when an Open Area Test Site or Anechoic Chamber with a Ground Plane is used. This implies a more severe range length requirement than $2\,(d_1+d_2)^2/\lambda$, although, due to the slower changing direct and reflected path lengths in the *x* direction, $2\,(d_1+d_2)^2/\lambda$, is still a good rule in this direction.

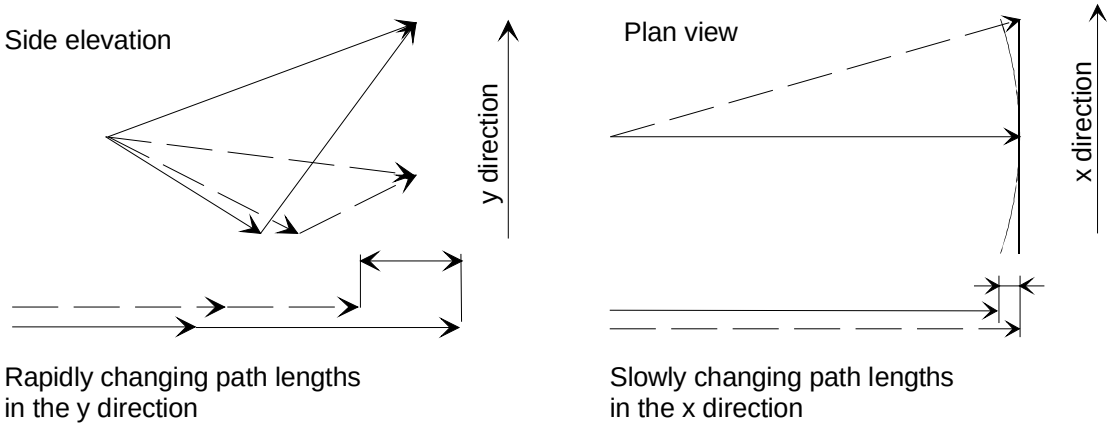

Figure 61: Path length differences for x and y directions

The following diagrams, (see figures 62 and 63) illustrate graphically this problem. The shaded "plates" indicate the points in space around the test volume at which the direct and reflected signals (assumed to be of equal amplitude for this illustration) are 90 ° to each other i.e. they add to a signal level of 3 dB below the level when they are exactly in phase. In both figures, the lower "plate" has been positioned to pass through a height of 1,5 m (the surface height of the turntable) at a range length of 3,0 m. Figure 62 illustrates the situation for 100 MHz, figure 63 corresponds to 1 000 MHz.

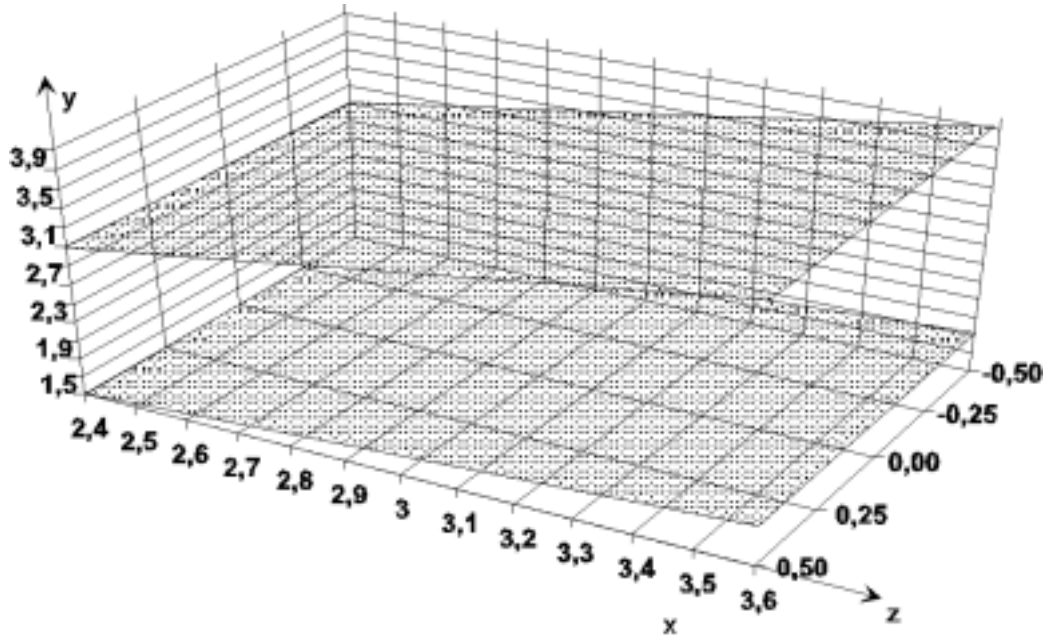

Figure 62: Upper and lower -3 dB amplitude "plates" over a ground plane at 100 MHz

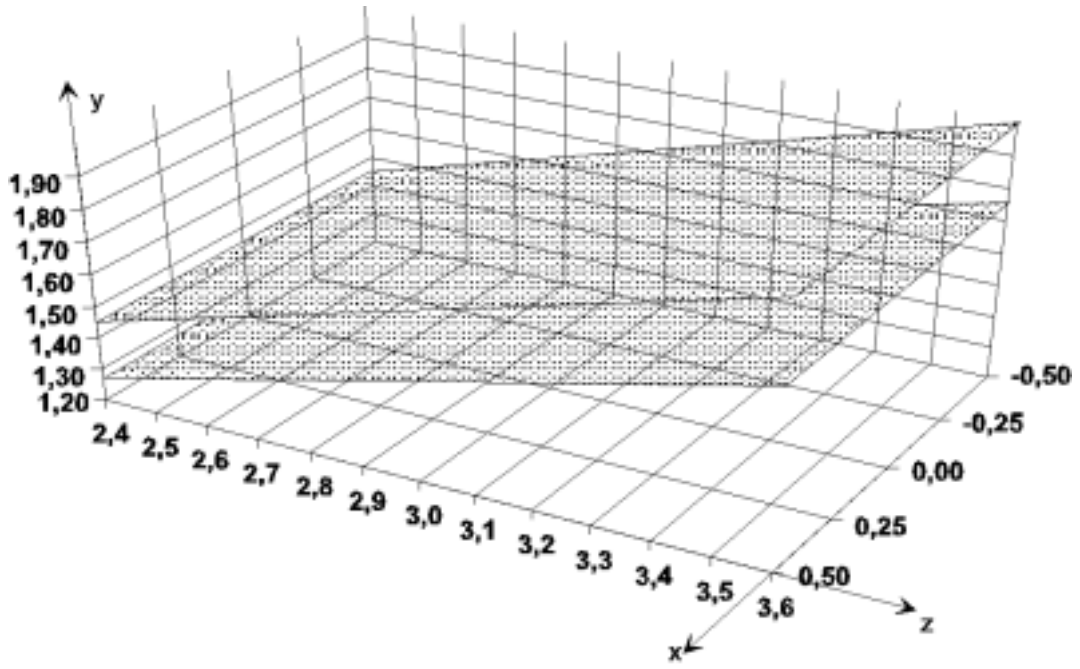

Figure 63: Upper and lower -3 dB amplitude "plates" over a ground plane at 1 000 MHz

Comparison between figures 62 and 63 shows the diminishing height with frequency that is available for reasonably accurate testing over a ground plane. For the example cases given, an EUT with a maximum height of about 0,6 wavelengths can be tested with an amplitude taper of less than 3 dB across it. This is a serious limitation for this type of test facility and is a limitation based on amplitude taper rather than on phase taper as in the case of an Anechoic Chamber. It should be borne in mind that figures 62 and 63 are only examples for a specific geometry considered. In practise, the spatial separation of the "90° plates" depends not only of frequency, but also on the height of the antenna on the mast, which is always optimized.

8 Practical test sites

8.1 Introduction

Practical test sites are often far from the ideal sites described in clause 7. The deviations from the ideal are due to many factors such as test site construction, materials used, test methodology employed, operation quality procedures, etc. To quantify the amount of deviation from the ideal site, verification is carried out.

The verification procedure involves the transmission of a known signal level from one calibrated antenna (usually a dipole) and the measurement of the received signal level in a second calibrated antenna (also usually a dipole). By comparison of the transmitted and received signal levels, an "insertion loss" can be deduced. After inclusion of any correction factors for the measurement, the figure of loss which results from the verification procedure gives the site attenuation. When a site has been deemed suitable for use by the verification process (i.e. the measured site attenuation a stipulated number of dB of the theoretical expectation), some confidence can begin to be placed on the testing carried out on the site.

8.1.1 Test types

Normally, two types of radiated tests are carried out. Transmitter tests (maximum carrier power, spurious emissions, cabinet radiation, etc.) and receiver tests (average or maximum usable sensitivity, spurious emissions, cabinet radiation, spurious response immunity, etc.).

These tests are carried out with the EUT in one of the following modes: transmitting, in transmitter standby mode, receiving or in receiver standby mode.

NOTE 1: When a standby mode is not available, the EUT either transmits or receives.

Spurious emissions are unwanted sources of radiation from the EUT. The level of the spurious emissions are measured by the substitution technique as the effective radiated power of the cabinet and integral antenna together. These emissions are at frequencies other than those of the carrier and sidebands associated with normal modulation and by definition, their radiating mechanisms and locations within the equipment, as well as their directivities, polarizations and directions are unknown. If the EUT is large in terms of wavelength, it may possess highly directive (i.e. narrow beam) spurious, particularly at high frequencies, which could radiate at angles that are difficult to detect. These unknowns complicate the measurement process.

For sensitivity and immunity testing the EUT is normally in the receive mode.

The sensitivity test requirement is to measure the minimum (or average) field strength to which the receiver responds in a specified manner. The tests involve measuring the transform factor (i.e. the relationship between the signal generator output power and the resulting field strength) of the test site. The actual receiver sensitivity can then be assessed by rotating the receiver through eight fixed positions 45° apart and taking either the minimum signal generator output value or a calculated average of the signal generator output level for the eight positions.

Immunity tests e.g. spurious response rejection, adjacent channel selectivity, blocking, etc. concern the performance degradation of an EUT in the presence of various interfering radiation. These characteristics of the EUT are tested by generating a field at the nominal frequency of the EUT as well as at the frequency (possibly a swept range) of the interference and subsequently determining the ratio of wanted to unwanted signal level for a given degradation in EUT performance.

NOTE 2: If the frequency is swept, the sweep needs to progress slowly as a device often malfunctions in only a few narrow frequency bands. For instance, a data receiver might operate flawlessly until a particular frequency is encountered. At the problem frequency, data errors may occur or the data may be totally corrupted. When the signal generator is tuned higher, normal operation returns.

Radiated sensitivity or immunity tests involving two or more signals are best carried out in shielded enclosures that are lined with anechoic material since testing over a ground plane makes it difficult to sweep the frequency and maintain a constant field strength at the EUT. This is due to the relative phasing of the direct and reflected signals.

NOTE 3: There are a number of solutions to this problem. One is to monitor and control the field strength with a field strength probe providing feedback to the amplifier, another is to spread radio absorbent material on the ground plane to minimize or eliminate the ground reflection. Both solutions however incur additional and often dominant uncertainties.

Performing sensitivity or immunity tests in an unshielded environment is not recommended, since on the one hand, large fields may be generated, possibly causing interference to others, whilst on the other, ambient signals may be present that will give erroneous results.

8.2 Test sites

The very brief overview of the type of tests to be carried out using the various test sites (given in clause 8.1) is intended as a reminder of the practical testing problems. The following clauses give an overview of practical test sites and the variations caused by their individual characteristics compared to the other test sites described.

8.2.1 Description of an Anechoic Chamber

As stated in clause 7.6.1 an Anechoic Chamber is an enclosure, usually shielded, whose internal walls, floor and ceiling are covered with radio absorbing material, normally of the pyramidal urethane foam type. The chamber usually contains an antenna support at one end and a turntable at the other. A typical Anechoic Chamber is shown in figure 64.

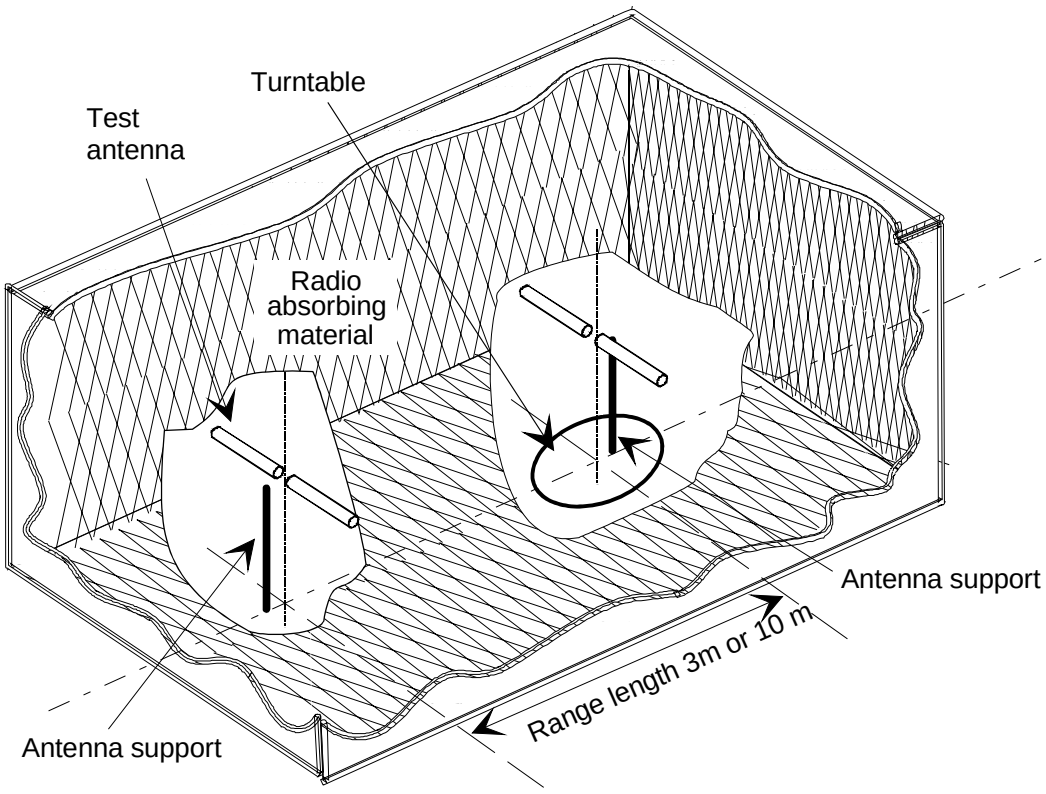

Figure 64: A typical Anechoic Chamber

The chamber shielding and radio absorbing material work together to provide a controlled environment for testing purposes. This type of test chamber attempts to simulate free Space conditions.

The shielding provides a test space, with reduced levels of interference from ambient signals and other outside effects, whilst the radio absorbing material minimizes unwanted reflections from the walls and ceiling which can influence the measurements. In practice it is relatively easy for shielding to provide high levels (80 dB to 140 dB) of ambient interference rejection, normally making ambient interference negligible.

No design of radio absorbing material, however, satisfies the requirement of complete absorption of all the incident power (it cannot be perfectly manufactured and installed) and its return loss (a measure of its efficiency) varies with frequency, angle of incidence and in some cases, is influenced by high power levels of incident radio energy. To improve the return loss over a broader frequency range, ferrite tiles, ferrite grids and hybrids of urethane foam and ferrite tiles are used with varying degrees of success.

Field uniformity in an Anechoic Chamber resulting from constructive and destructive interference of the direct and any residual reflected fields can be minimal, but will still vary, depending on the quality of the absorber, in amplitude, phase, impedance and polarization from one measurement point to another and from one frequency to another within the test volume or test area.

The Anechoic Chamber generally has several advantages over other test facilities. There is minimal ambient interference, minimal floor, ceiling and wall reflections and it is independent of the weather. It does however have some disadvantages which include limited measuring distance and limited lower frequency usage due to the size of the pyramidal absorbers.

Both absolute and relative measurements can be performed in an Anechoic Chamber. Where absolute measurements are to be carried out, or where the test facility is to be used for accredited measurements, the chamber should be verified.

8.2.2 Description of an Anechoic Chamber with a Ground Plane

As stated in clause 7.6.2 an Anechoic Chamber with a Ground Plane is an enclosure, usually shielded, whose internal walls and ceiling are covered with radio absorbing material, normally of the pyramidal urethane foam type. The floor, which is metallic, is not covered and forms the ground plane. The chamber usually contains an antenna mast at one end and a turntable at the other. A typical Anechoic Chamber with a Ground Plane is shown in figure 65.

This type of test chamber attempts to simulate an ideal Open Area Test Site (historically, the reference site upon which the majority, if not all, of the specification limits have been set) whose primary characteristic is a perfectly conducting ground plane of infinite extent.

The chamber shielding and radio absorbing material work together to provide a controlled environment for testing purposes. The shielding provides a test space, with reduced levels of interference from ambient signals and other outside effects, whilst the radio absorbing material minimizes unwanted reflections from the walls and ceiling which can influence the measurements. In practice it is relatively easy for shielding to provide high levels (80 dB to 140 dB) of ambient interference rejection, normally making ambient interference negligible.

No design of radio absorbing material, however, satisfies the requirement of complete absorption of all the incident power (it cannot be perfectly manufactured and installed) and its return loss (a measure of its efficiency) varies with frequency, angle of incidence and in some cases, is influenced by high power levels of incident radio energy. To improve the return loss over a broader frequency range, ferrite tiles, ferrite grids and hybrids of urethane foam and ferrite tiles are used with varying degrees of success.

Both absolute and relative measurements can be performed in an Anechoic Chamber with a Ground Plane. Where absolute measurements are to be carried out, or where the test facility is to be used for accredited measurements, the chamber should be verified.

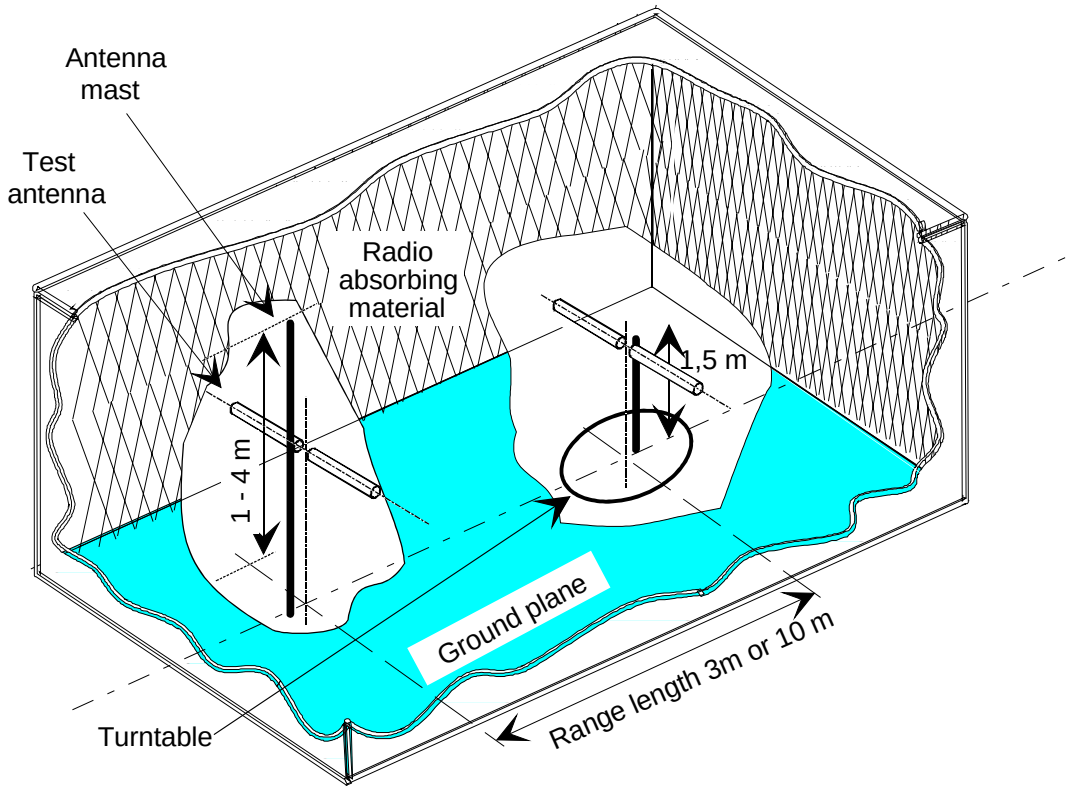

Figure 65: A typical Anechoic Chamber with a Ground Plane

In this facility the ground plane creates the wanted reflection path, such that the signal received by the receiving antenna is the sum of the signals received from the direct and reflected transmission paths. This creates a unique received signal level for each height of the transmitting antenna (or EUT) and the receiving antenna above the ground plane.

The electric field resulting from constructive and destructive interference between the direct and reflected fields, may vary considerably in amplitude, phase, impedance and polarization from one measurement point to another and from one frequency to another within the test volume.

In use, the antenna mast provides a variable height facility so that the elevation height of the test antenna can be optimized for maximum coupled signal between antennas, or, in conjunction with the turntable for azimuth angle, between an EUT and test antenna.

Under these conditions, spurious emission testing involves firstly "peaking" the field strength from the EUT by raising and lowering the receiving test antenna on the mast to obtain the maximum constructive interference of the direct and reflected signals from the EUT and then rotating the turntable for a "peak" in the azimuth angle. At this height of the test antenna on the mast, the amplitude of the received signal is noted. Subsequently the EUT is replaced by a substitution antenna, positioned at the EUT's volume centre, and connected to a signal generator. The signal is again "peaked" and the signal generator output level is then adjusted until the level, noted in stage one, is again measured on the receiving device.

Radiated sensitivity tests over a ground plane also involve "peaking" the field strength by raising and lowering the test antenna on the mast to obtain the maximum constructive interference of the direct and reflected signals, this time using a measuring antenna. The test antenna is fixed at this height for stage two. A Transform Factor is derived. For stage two the measuring antenna is replaced by the EUT, and the amplitude of the transmitted signal is adjusted to determine the level at which a specified response is obtained on the receiver.

Immunity tests involving two or more signals at different frequencies should not be carried out in an Anechoic Chamber with a Ground Plane since the ground plane makes it is difficult to sweep the frequency and maintain a constant field strength at the EUT. This is due to the relative phasing of the direct and reflected signals.

8.2.3 Description of an Open Area Test Site

An Open Area Test Site comprises a turntable at one end and an antenna mast of variable height at the other set above a ground plane which, in the ideal case, is perfectly conducting and of infinite extent. In practice, whilst good conductivity can be achieved, the ground plane size has to be limited. A typical Open Area Test Site is shown in figure 66.

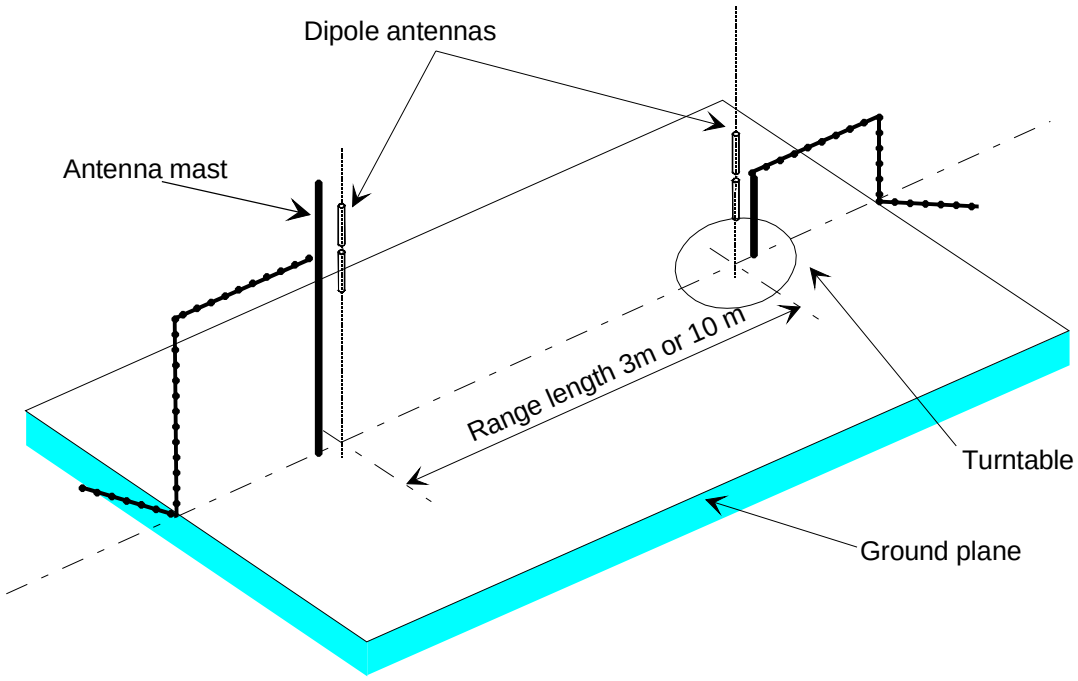

Figure 66: A typical Open Area Test Site

The ground plane creates a wanted reflection path, such that the signal received by the receiving antenna is the sum of the signals received from the direct and reflected transmission paths. The phasing of these two signals creates a unique received level for each height of the transmitting antenna (or EUT) and the receiving antenna above the ground plane.

In practice, the antenna mast provides a variable height facility so that the position of the test antenna can be optimized for maximum coupled signal between antennas, or, in conjunction with the turntable for azimuth angle, between an EUT and test antenna.

Both absolute and relative measurements can be performed on an Open Area Test Site. Where absolute measurements are to be carried out, or where the test facility is to be used for accredited measurements, the Open Area Test Site should be verified.

For spurious emission, radiated sensitivity and immunity testing discussion refer to the Anechoic Chamber with a Ground Plane.

The Open Area Test Site has been, historically, the reference site upon which the majority, if not all, of the specification limits have been set. The ground plane was introduced for uniformity of ground conditions for all test sites.

8.2.4 Description of striplines

As stated in clause 7.6.4 a stripline is essentially a transmission line in the same sense as a coaxial cable (see clause 10.2). It sets up an electromagnetic field between the plates in a similar way that a coaxial cable sets up fields between inner and outer conductors. In both cases, the basic mode of propagation is in the form of a Transverse ElectroMagnetic (TEM) wave i.e. a wave which possesses single electric and magnetic field components, transverse to the direction of propagation, as in the case of propagation in free-space. stripline test facilities, therefore, are transmission lines constructed with their plates separated sufficiently for an EUT to be inserted between them.

There are various types of stripline test facilities, mainly comprising either two or three plates. The three plate designs are available as either open or closed i.e. the fields can either extend into the region surrounding the line or they can be totally enclosed by metal side plates.

Typical two and three-plate open striplines are shown in figure 67. For the three-plate open cell, the middle plate can be either symmetrically spaced between the outer two (as shown in figure 67), or offset more towards the bottom or top plate.

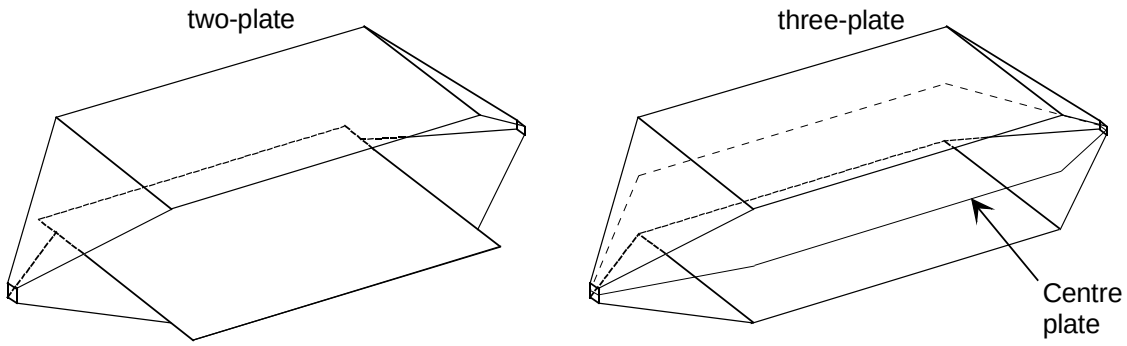

Figure 67: Typical open two-plate and three-plate stripline test facilities

A typical closed stripline (alternatively termed TEM cell) is shown in figure 68.

For all versions of the open stripline, some portion of the electromagnetic field extends beyond the physical extent of the line since the sides are not enclosed by metal. As a direct consequence, the performance of an open cell is dependent not only on its construction but also on its immediate environment - the cell interacting with physical objects which may be present e.g. test equipment, people, etc., as well as suffering from the influences of external electrical effects such as local ambient signals and resonances of the room in which the cell is located. Shielding the room has the benefit of eliminating ambient signals but can seriously increase the magnitude of the room resonance effects (the room acting like a large resonant waveguide cavity). Where a shielded room is used to locate the open stripline, strategic use of absorbing panels (for damping resonance effects and generally reducing other interactions) is regarded as essential. Use of an open stripline in a non-shielded room may cause interference to others.

The closed TEM cell is constructed using five plates, the central conductor in addition to the four sides. Benefits, resulting from the enclosure of all four sides, include the elimination of effects due to external reflections, local ambient signals and room resonances suffered by the open stripline. Drawbacks include internally generated resonances and a dramatic cost increase relative to the equivalent open version. The available designs of closed cell include the so-called GTEM cell (a broadband version of the TEM cell).

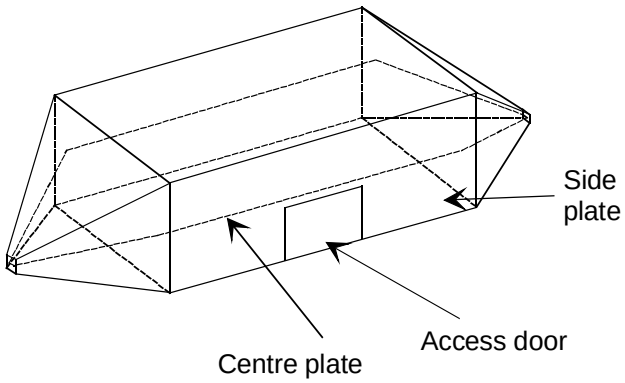

Figure 68: A typical closed stripline test facility

A stripline test facility needs a large room in which to be installed. Room resonances can be encountered in rooms of rectangular cross-section at all frequencies satisfying the following formula:

$$f = 150\sqrt{\left(\frac{x}{l}\right)^2 + \left(\frac{y}{b}\right)^2 + \left(\frac{z}{h}\right)^2} \text{ MHz}$$

Here *l*, *b* and *h* are the length, breadth and height of the room in metres and *x*, *y* and *z* are mode numbers. The only condition limiting the use of this formula is that only one of *x*, *y* or *z* can be zero at any one time.

For a room measuring 8 m by 8 m by 4 m, there are 25 resonant frequencies within the band 26,5 MHz to 120,1 MHz. This shows that, in principle, room resonances can pose major problems. Their effects are worse for rooms which are metal lined for shielding from ambient signals. In this condition, the room acts like a waveguide and will possess high Q-factors for some or all resonant frequencies. Their effects are to put sharp spikes into the field strength variation with frequency within the cells. In general, these can only be damped by the use of absorbing material placed around the cell.

Other factors which can contribute to disturbance in the field within the stripline include cabling (in terms of reflections and its possible parasitic effect) and local ambient effects. In general, to keep cabling problems to a minimum, these should be as short as possible within the stripline, gain access to the test area via small holes in the bottom plate and be heavily loaded with ferrite beads. To completely nullify ambient signals, a shielded room is required but it should be borne in mind that such a room can provide extremely sharp resonances.

8.3 Facility components and their effects

For the facilities outlined in clause 8.2 the following comprise the major components:

- a metallic shield lined with radio absorbing material for the Anechoic Chamber;
- a metallic shield, radio absorbing material and a highly reflective ground plane for the Anechoic Chamber with a Ground Plane;
- a highly reflective ground plane for the Open Area Test Site.

Whilst these components are included to improve the quality of the testing environment, each has negative effects as well. These effects are now discussed.

8.3.1 Effects of the metal shielding

The benefits of shielding a testing area can be seen by considering the situation on a typical Open Area Test Site where ambient RF interference can add considerable uncertainty to measurements. Such RF ambient signals can be continuous sources e.g. commercial radio and television, link services, navigation etc. or intermittent ones e.g. CB, emergency services, DECT, GSM, paging systems, machinery and a variety of other sources. The interference can be either narrowband or broadband. The Anechoic Chamber (with and without a ground plane) overcomes these problems by the provision of a shielded enclosure.

A shielded enclosure is defined as any structure that protects its interior from the effects of an exterior electric or magnetic field, or conversely, protects the surrounding environment from the effects of an interior electric or magnetic field. The shielding is normally provided by metal panels with continuous electrical contact between adjoining panels and around any doors.

Further advantages of the shield are protection from the weather and the general degradation effects it can have.

8.3.1.1 Resonances

Any metal shield will act as a reflecting surface and grouping six of them together to form a metal box makes it possible for the chamber to act like a resonant waveguide cavity, if excited. Whilst these resonance effects tend to be narrowband, their peak magnitudes can be high resulting in a significant disruption of the desired field distribution.

A resonant waveguide cavity mode can, in theory, be excited at any frequency which satisfies the following formula:

$$f = 150\sqrt{\left(\frac{x}{l}\right)^2 + \left(\frac{y}{b}\right)^2 + \left(\frac{z}{h}\right)^2} \text{ MHz}$$

where l, b and h are respectively the length, breadth and height of the chamber in m and x, y and z are mode numbers of which only one is allowed to be zero at any time. As an example, the lowest frequency at which a resonance could occur in a facility which measures 5 m by 5 m by 7 m long is 36,87 MHz.

Caution should be exercised whenever measurements are attempted close to any frequency predicted by this formula, particularly for the lowest values at which the absorber might offer only poor performance. To improve confidence in the chamber, these lower calculated frequencies could be included in the verification procedure.

8.3.1.2 Imaging of antennas (or an EUT)

The shield can have a significant impact on the overall performance of the chamber if the absorbing material has inadequate absorption characteristics.

In the limiting case of 0 dB return loss (i.e. zero absorption/perfect reflection) an antenna or EUT will "see" an image of itself in the end wall close behind, the two side walls, the ceiling and, to a lesser extent, in the far end wall, see figure 69. For the fully Anechoic Chamber, there is an additional image in the floor absorbers whilst, for the Anechoic Chamber with a Ground Plane, the image in the ground plane is "wanted" as it is a direct consequence of the presence of the ground plane.

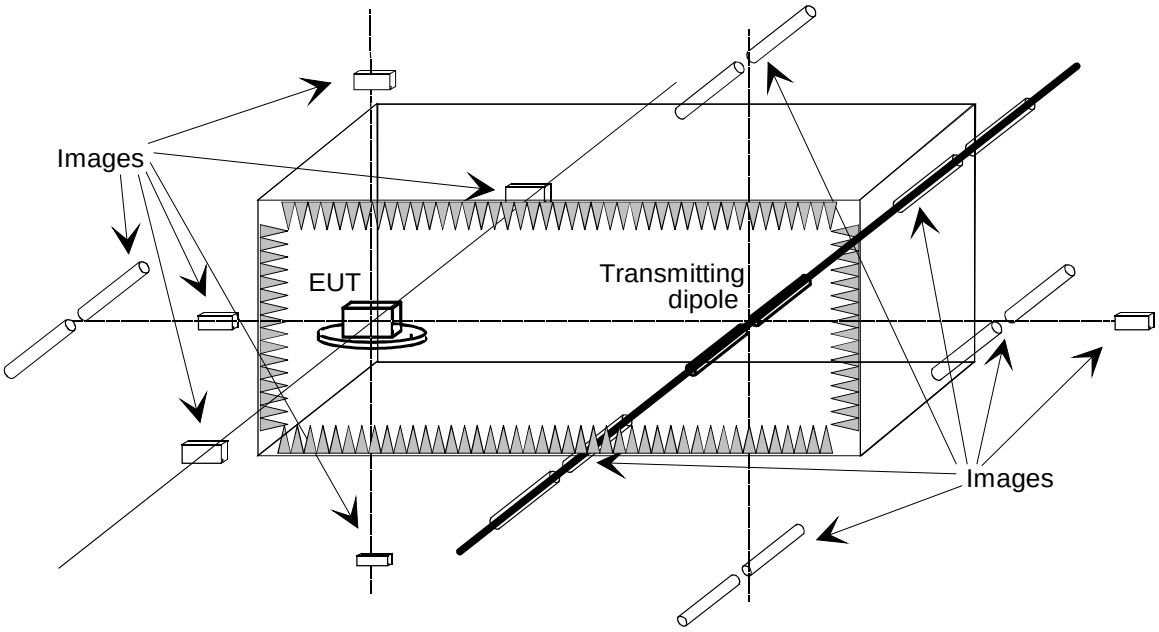

Figure 69: Imaging in the shielded enclosure

In this multi-image environment, the one driven (real) antenna is, in effect, powering a seven element array (of which it is one), instead of just itself (Anechoic Chamber) or of a two element array (itself and its image in the ground plane for an Anechoic Chamber with a Ground Plane). Major changes result to all of the antenna's electrical characteristics such as input impedance, gain and radiation pattern.

No chamber should be used at any frequency for which the absorbing material would perform so poorly as to appear "invisible" as in this example, but any finite value of reflectivity will produce this imaging to an extent.

Good absorption (low reflectivity) will prevent reflections from any surface in an Anechoic Chamber, and it will prevent ceiling, side and end wall reflections in an Anechoic Chamber with a Ground Plane. Poor absorption (high reflectivity) will not only produce unwanted imaging of the antennas, and/or the EUT, (in addition to those in the ground plane if applicable), but can also contribute numerous high amplitude reflections. Thus the absorbing materials can also play a critical role in the chamber's performance.

8.3.2 Effects of the radio absorbing materials

8.3.2.1 Introduction

Absorption is the irreversible conversion of the energy of an electromagnetic wave into another form of energy as a result of wave interaction with matter "The new IEEE standard dictionary of electrical and electronic terms" [16] (i.e. it gets hot!). The efficiency with which the material absorbs energy is determined by the absorption coefficient. This is defined as the ratio of the energy absorbed by the surface to the energy incident upon it [1]. It is more usual, however, for the reflectivity (i.e. return loss) of an absorbing material to be quoted rather than its absorption, the assumption being that any incident power not reflected is absorbed.

Different types of absorbers are available, see figure 70. They all absorb radiated energy to a greater or lesser extent, but possess different mechanical and electrical properties making certain types more suitable for some applications than others.

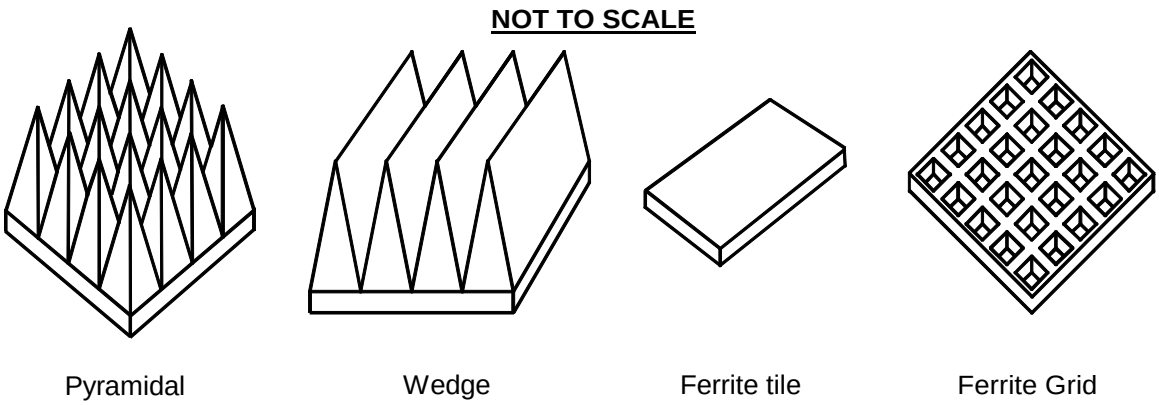

Figure 70: Typical RF absorbers

A review of commonly available types is now given.

8.3.2.2 Pyramidal absorbers

This type of absorber is manufactured from polyurethane foam impregnated with carbon, and moulded into a pyramidal shape, see figure 70. This shape has inherently wide bandwidth, small polarization dependence and gives reasonably wide angular coverage.

Pyramidal absorbers behave as lossy, tapered transitions, ranging from low impedance at the base to 377 Ω at the tip to match the impedance of free Space. They work on the principle that if all of the energy is converted to heat before the base is reached, there is nothing to reflect from the shield.

A line, drawn from the centre of the base through the centre of the tip of the pyramid is termed the normal angle of incidence (0°) and the pyramidal shape maximizes the absorber performance at this angle of incidence. As the angle of incidence increases, however, the return loss degrades, as illustrated in figure 71 for 50°, 60° and 70° angles against absorber thickness.

This absorption characteristic leads to large reflection coefficients at large angles of incidence where the incident radio energy approaches broadside to the side faces of the pyramids. The reflection is primarily due to impedance mismatch between the incident wave and the absorber impedance taper.

The actual performance varies according to the degree of carbon loading and the shape and size of the cones. At low frequencies its effectiveness in suppressing surface reflections is mainly a function of the cone height to wavelength ratio, the absorption improving as this ratio increases, see figure 72.

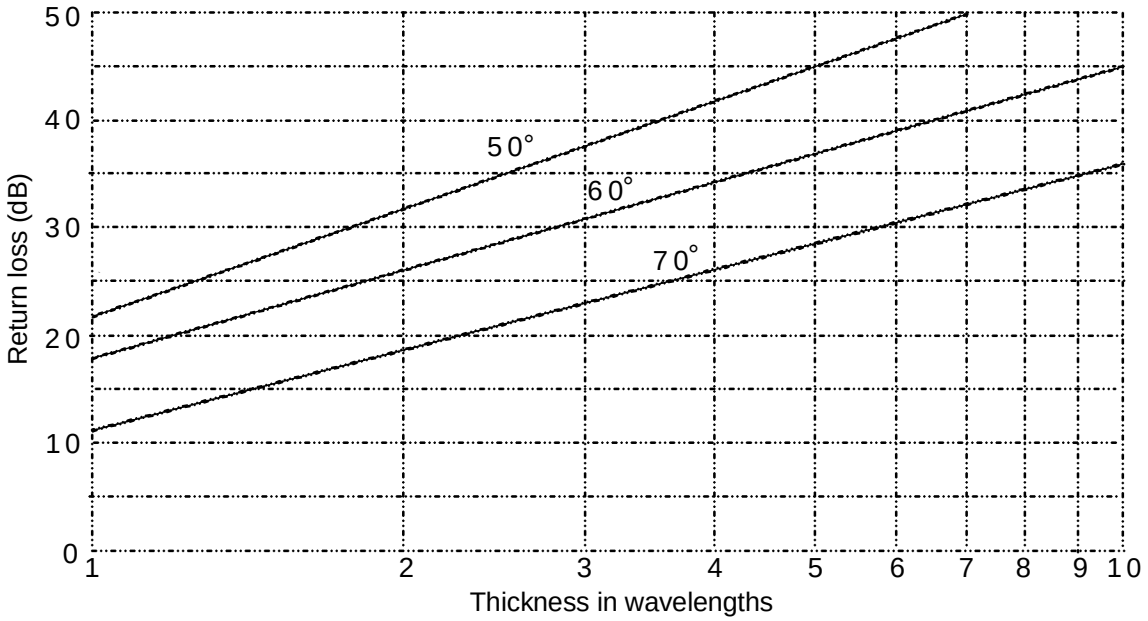

Figure 71: Typical return loss of pyramidal absorber at various incidence angles

Longer cones therefore, have better low frequency performance e.g. 0,6 m length cones can only be used effectively down to about 120 MHz, whereas, for comparable performance, 1,778 m cones can be used effectively down to about 40 MHz. This improved performance can, however, only be attained at significantly increased cost and reduction in space efficiency (see table 4).

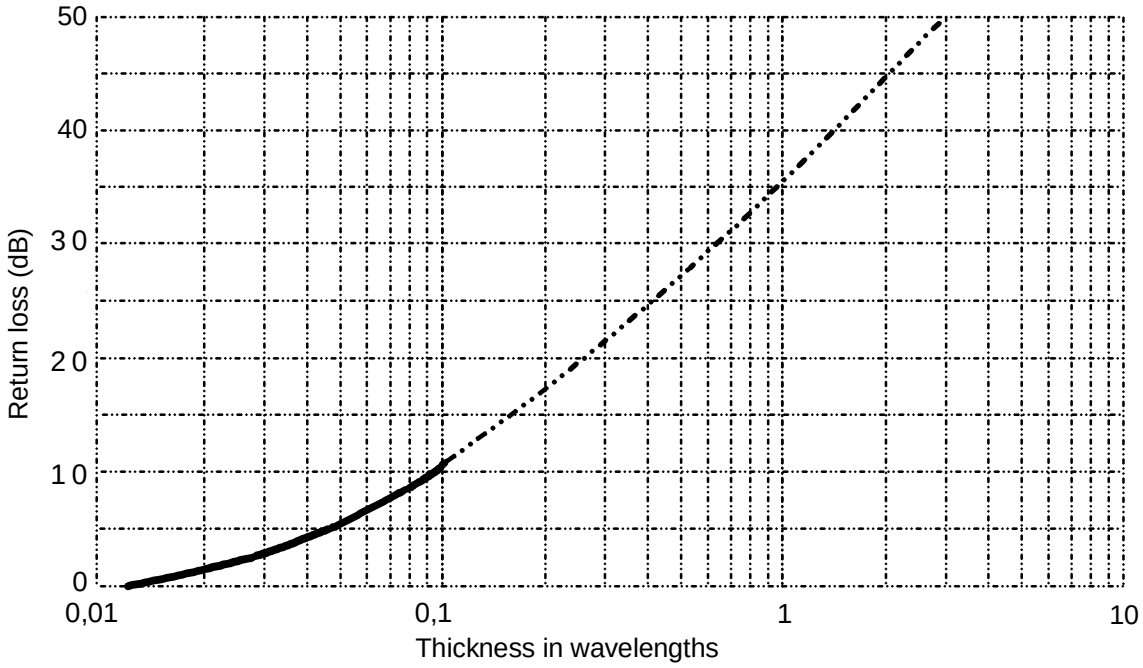

Figure 72: Typical return loss of pyramidal absorber at normal incidence

The high frequency performance of the pyramidal absorbers seems unlimited, see figure 72, but this is not the case. In practice, it is limited by resonant effects of the spacing between the peaks of the pyramids, absorber layout pattern and surface finish of the absorber. In some chambers, mixed size pyramids are used to randomize the absorber pattern to improve its high frequency performance with only minimum degradation at the lower frequencies.

Flammability, space inefficiency and performance degradation over time (caused by drooping under their own weight) and the breaking of the absorber tips and rounding of the valleys are major disadvantages of this type of absorber. However, a hollow cone version is available which reduces the overall weight and improves the mechanical stability. Flame retarding types are also available, but space inefficiency and "fragility" remain major problems with this type of absorber.

8.3.2.3 Wedge absorbers

Wedge absorbers (see figure 70), are a variation of the polyurethane pyramidal foam type, which tend to overcome the degradation of reflectivity with increasing angle of incidence suffered by pyramidal cones, but at some performance cost.

This improvement is only for cases where the incident wave direction is parallel to the ridge of the wedge as no broadside presents itself at off normal angles as is the case with pyramidal absorbers.

Disadvantages of this type of absorber are degraded performance compared to pyramidal types for both normal angles of incidence and (if used with the ridge perpendicular to the incident wave) when a complete face is broadside to the incident wave.

These effects make wedge absorbers more suitable for use in chambers with range lengths of 10 m or more where they are used to good advantage in the middle sections of the ceilings and side walls.

8.3.2.4 Ferrite tiles

Ferrite is a ferromagnetic ceramic material. Its susceptibility and permeability are dependant on the field strength and magnetization curves (which have hysterisis). Its magnetic characteristics can be affected by pressure, temperature, field strength, frequency and time. Its mechanical and electromagnetic characteristics depend heavily on the sintering process used to form the ferrite. It is hard (physically), brittle (as are all ceramics) and will chip and break if handled roughly.

Ferrite tiles are thin, flat, ceramic blocks typically 15 cm by 8 cm by 1 cm thick (see figure 70). Both thickness and composition of the ferrite material affect their absorption performance. In practice, their layout is also very critical since small air gaps between adjacent tiles can considerably degrade performance at the lowest frequencies (30 MHz to 100 MHz). However, when properly installed this is the frequency range for which they give the most benefit over pyramidal foam absorbers. They are generally manufactured to give about 15 dB to 20 dB return loss at 30 MHz (see figure 73).

Their main advantages are that they are thin (typically 1 cm) so the shielded enclosure outside dimensions are relatively small compared to pyramidal foam for the same internal volume (see table 4). Ferrite tiles also have a durable surface and have stable performance with time.

Disadvantages are cost, the strong dependence of the reflectivity performance on both polarization and angle of incidence and possible non linear performance due to saturation at high field strengths.

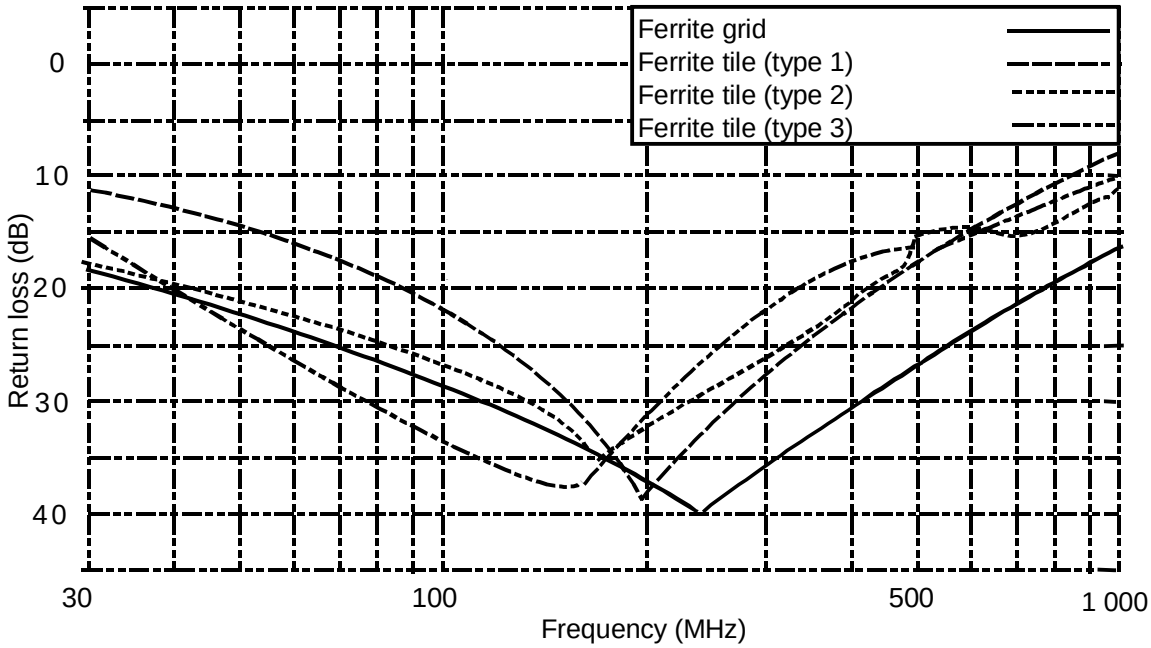

Figure 73: Normal incidence return loss variation of a ferrite grid and three different designs of ferrite tile against frequency

Due to their relatively high cost ferrite tiles are mainly built up into 1 m or 2 m square blocks which are placed strategically in the chamber under pyramidal foam absorbers in the middle sections of the side walls and ceiling - the main reflection paths between antennas (or between an antenna and EUT). They are also used on the end walls to improve absorption and to reduce image coupling.

This combination of ferrite tiles and pyramidal foam absorbers is more cost effective in performance terms than a fully ferrited room.

8.3.2.5 Ferrite grids

Ferrite grids are typically 10 cm by 10 cm by 2,5 cm thick. They provide absorption from 30 MHz to 1 000 MHz. The grid structure provides better power handling characteristics and avoids the installation problems associated with plain tiles. Their absorption characteristics are basically the same as for ferrite tiles (see figure 73).

8.3.2.6 Urethane/ferrite hybrids

Urethane/ferrite hybrid absorbers (as introduced in clause 8.3.2.4) consist of pyramidal foam absorber bonded to a ferrite tile backing. They are designed in such a way that the ferrite tiles are active at the low frequencies, where the pyramidal foam absorbers are not very efficient, whilst the pyramidal absorbers take over at higher frequencies.

A disadvantage is the impedance mismatch between the ferrite base and the dielectric pyramids which results in performance degradation in some frequency ranges.

In a similar manner to the ferrite tile, the hybrid absorber is used in the middle sections of the side walls and ceiling - the main reflection paths between antennas (or between an antenna and EUT). They are also used on the end walls to improve absorption and to reduce image coupling.

8.3.2.7 Floor absorbers

Anechoic materials (except ferrite tiles and grids) cannot, in general, support loads. Normally, therefore, a false floor of RF transparent material is built above the anechoic materials, to enable access to the test antenna and turntable. It is, however, very difficult to obtain a floor that is truly RF transparent and the floor is often "visible". This tends to be revealed when the performance of the chamber is being verified and has been known to lead to constructional modifications.

Special types of floor absorbers can be used. These are constructed of normal pyramidal absorbers whose external profiled section has been filled with a low loss rigid foam so as to form a solid block. This is usually capable of supporting the weight of a man, but with usage, degradation in performance occurs.

The most common solution is not to have a floor for access, but to arrange access to the antenna support, either with another access door (degrades chamber performance) or by making the antenna mount such that it can be easily moved to the turntable end to facilitate antenna changes etc.

8.3.2.8 Performance comparison

Table 4 and table 5 detail numerous relative parameters for the different absorber types discussed above. Table 4 gives the physical parameters relating to an Anechoic Chamber of internal testing dimensions of 8 m by 3 m by 3 m. Table 5 details the return loss (at 0° angle of incidence) for the various absorber types considered in table 4. The same data is shown graphically in figure 74.

Table 4: Typical parameters of an 8 m by 3 m by 3 m Anechoic Chamber for various absorbers

Features	Pyramidal 0,66 m	Pyramidal 1,778 m	Ferrite tiles	Ferrite Grid	Hybrid
Inside dimensions	8 m by 3 m by 3 m	8 m by 3 m by 3 m	8 m by 3 m by 3 m	8 m by 3 m by 3 m	8 m by 3 m by 3 m
Outside dimensions (approx.)	9,3 m by 4,3 m by 4,3 m	11,6 m by 6,6 m by 6,6 m	8,2 m by 3,2 m by 3,2 m	8,3 m by 3,3 m by 3,3 m	9,9 m by 4,9 m by 4,9 m
Overall volume	174 m^3	497 m^3	84 m^3	90 m^3	240 m^3
Flammable	yes	yes	no	no	yes
Risk of damage	high	high	low	low	high
Floor absorbers	moveable	fixed	fixed	fixed	fixed
Frequency range (MHz)	80 to > 1 000	30 to > 1 000	30 to > 500	30 to > 1 000	30 to > 1 000

Table 5: Typically return loss at 0° incidence for various absorbers against frequency

Frequency	Pyramidal 0,66 m	Pyramidal 1,778 m	Ferrite tiles	Ferrite grid	Hybrid
30 MHz	7 dB	15 dB	17 dB	17 dB	16 dB
80 MHz	15 dB	25 dB	25 dB	20 dB	18 dB
120 MHz	19 dB	30 dB	26 dB	20 dB	20 dB
200 MHz	25 dB	35 dB	25 dB	37 dB	20 dB
300 MHz	30 dB	40 dB	23 dB	25 dB	20 dB
500 MHz	35 dB	45 dB	18 dB	23 dB	20 dB
800 MHz	40 dB	50 dB	14 dB	18 dB	25 dB
1 GHz	50 dB	50 dB	12 dB	15 dB	25 dB
3 GHz	50 dB	50 dB	6 dB	10 dB	30 dB
10 GHz	50 dB	50 dB	-	-	30 dB
18 GHz	50 dB	50 dB	-	-	35 dB

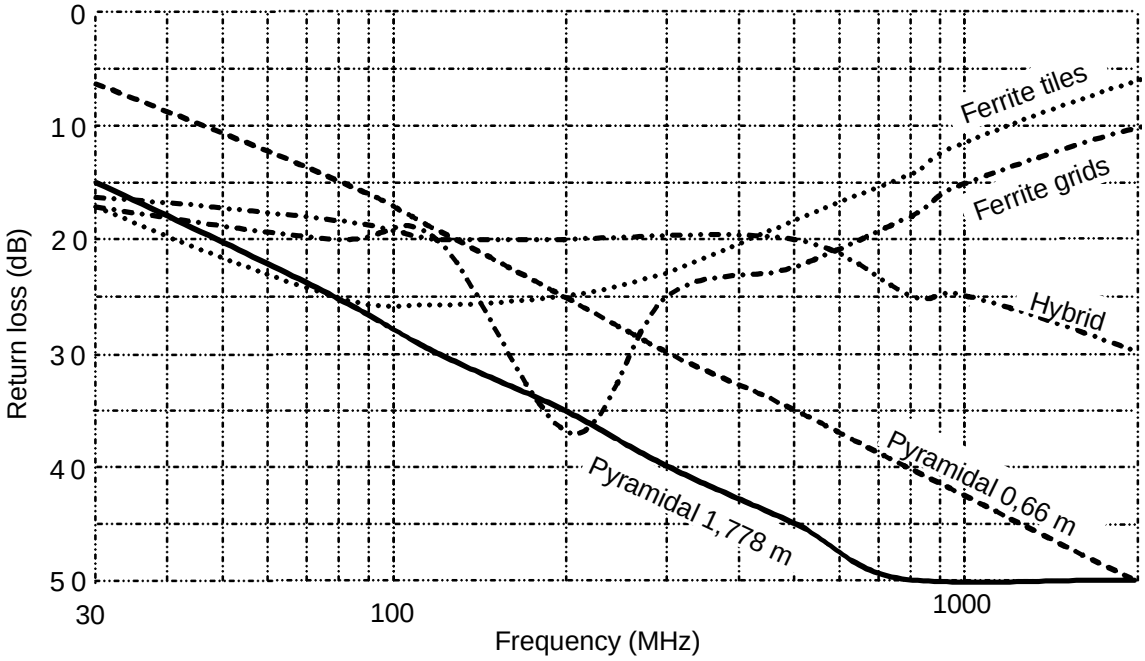

Figure 74: Return loss variation with frequency of the absorbers listed in table 5

All of these types of absorber dissipate the energy incident on their surfaces in the form of heat. When in the presence of high value fields, the power absorbed in the foam variety can exceed its ability to dissipate the heat, and the resulting increase in temperature degrades its performance. This is not normally a problem with ferrite types.

8.3.2.9 Reflection in an Anechoic Chamber

As has been stated, the absorbing materials used and their layout play a critical role in the chamber's performance. A plan view of an Anechoic Chamber with its end and side walls covered in pyramidal foam absorbers is shown in figure 75. Mounted in the chamber are two dipoles (shown for illustration purposes only, although this being a common arrangement found in test methods and the verification procedure). Various single and double bounce reflection paths are also illustrated.

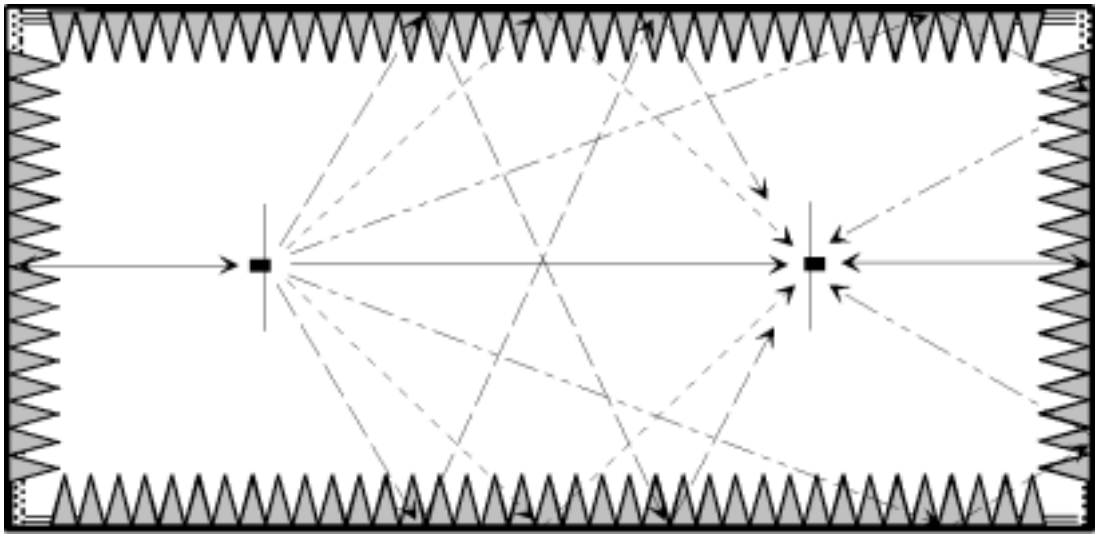

Figure 75: Plan view of an Anechoic Chamber which uses pyramidal absorber

The single bounce reflection paths via the end walls are at normal incidence to the absorbers, and since the absorbers are at maximum efficiency at normal incidence the reflections are of a low amplitude. However, the amplitude of the worst case reflections, the single bounce paths between the antennas via the side walls, are dependant on the angles of incidence, which themselves are dependent on the geometry (cross section and range length) of the chamber. The ceiling and floor provide other single bounce reflection paths.

The direct path between the antennas is the only wanted signal and all other signals, whether the result of reflections from the absorber or from extraneous sources (see clause 8.5.11) interfere with the required field and result in measurement uncertainty. The situation is further complicated by the directional nature of the dipoles, reflections in the E-plane of the dipole being reduced in amplitude when compared to the case for the orthogonal polarization, as a result of the dipole's radiation pattern.

As an example of the magnitude of the problem, the following is calculated for illustrative purposes. A typical chamber of 5 m by 5 m by 7 m long, employing 0,66 m pyramidal foam absorbers is used over a 3 m range length. The angles of incidence on the side walls, floor and ceiling of the main single bounce reflection paths are:

$$\tan^{-1}(1,5 / 2,5) = 31,0°$$

Assuming a frequency of 80 MHz, the reflectivity at this angle of incidence is approximately 15 dB. If the polarization of the transmitting dipole is taken as horizontal, then its directivity in the horizontal plane reduces the magnitude of the side wall reflections by 1,9 dB which, in addition to the extra path length loss (relative to the direct ray) of 5,8 dB, leads to the amplitudes of the four main one-bounce reflections being -22,7 dB, -22,7 dB, -20,8 dB and -20,8 dB for the two side walls, floor and ceiling respectively (these levels being relative to the amplitude of the direct path).

NOTE 1: In a facility of identical cross section but offering a 10 m range length, these three main interfering rays have greater amplitudes of approximately -13,4 dB, -13,4 dB, 12,0 dB and -12,0 dB as a result of increased reflectivity from the absorbing materials (grazing angle of incidence), less relative path loss (the path lengths are more nearly equal) and less benefit from the directivity of the dipole pattern.

Whilst the addition of these rays is rather more complex than just a straightforward addition (and for a full analysis one should also include multiple bounce reflections), their amplitudes serve to illustrate the potential problem of signal level uncertainty since, again for illustrative purposes only, a single -20 dB interfering signal can, at its maximum relative phasing, enhance or reduce the received signal strength by +0,83 or -0,92 dB respectively. Table 6 illustrates the uncertainty caused by a single unwanted interfering signal.

Table 6: Uncertainty in field strength due to a single unwanted interfering signal

Ratio of unwanted to wanted signal level	Received level uncertainty		Ratio of unwanted to wanted signal level	Received level uncertainty
-30,0 dB	+0,27 -0,28 dB		-9,0 dB	+2,64 -3,81 dB
-25,0 dB	+0,48 -0,50 dB		-8,0 dB	+2,91 -4,41 dB
-20,0 dB	+0,83 -0,92 dB		-7,0 dB	+3,21 -5,14 dB
-17,5 dB	+1,09 -1,24 dB		-6,0 dB	+3,53 -6,04 dB
-15,0 dB	+1,42 -1,70 dB		-5,0 dB	+3,88 -7,18 dB
-14,0 dB	+1,58 -1,93 dB		-4,0 dB	+4,25 -8,66 dB
-13,0 dB	+1,75 -2,20 dB		-3,0 dB	+4,65 -10,69 dB
-12,0 dB	+1,95 -2,51 dB		-2,0 dB	+5,08 -13,74 dB
-11,0 dB	+2,16 -2,88 dB		-1,0 dB	+5,53 -19,27 dB
-10,0 dB	+2,39 -3,30 dB		0,0 dB	+6,04 -∞ dB

For optimized chamber performance therefore, the middle sections of the ceiling, floor and side walls of Anechoic Chambers should be carefully constructed to provide the highest values of absorption in the chamber, especially for range lengths greater than 3 m. From a measurement viewpoint, inside the chamber, the amount of reflection from the walls has a direct effect on the "quality" of the measurement.

Experience has shown that in chambers which have 0,66 m pyramidal absorbers the overall performance has three distinct stages:

- below about 150 MHz or so the amplitude of reflections from the walls, floor and ceiling can be observed to degrade the operation of the facility. The shielded enclosure may act as a large cavity resonator, although all possible modes may not be excited as they are dependant on the configurations of the test equipment and EUT;

- from about 150 MHz up to a few hundred MHz most of the components (e.g. absorber dimensions) return to full specification and the chamber tends to "behave" quite well;

- at very high frequencies, arbitrarily hundreds of MHz to well above 1 000 MHz resonances can be set up by the physical dimensions of the absorber material which can negate the fact that the absorber materials themselves have good performance characteristics at these frequencies.

In the present document, the uncertainty contributions due to reflectivity of the absorbers are estimated in annex A of TR 102 273-1-2 [12] and given representative symbols as follows:

u_{j01} is used throughout all parts of the present document for the contribution associated with the reflectivity of the absorbing material between the EUT and the test antenna in test methods.

NOTE 2: This uncertainty contributes to test methods in anechoic facilities, both with and without a ground plane. It is the uncertainty due to reflections from the absorbing material. In stage one of a substitution measurement the standard uncertainty is 0,00 dB, otherwise the relevant value from table 7 should be used in all uncertainty calculations.

u_{j02} is used throughout all parts of the present document for the contribution associated with the reflectivity of the absorbing material between the substitution or measuring antenna and the test antenna in test methods.

NOTE 3: This uncertainty contributes to test methods in anechoic facilities, both with and without a ground plane. It is the uncertainty due to reflections from the absorbing material. The standard uncertainty is 0,5 dB.

u_{j03} is used throughout all parts of the present document for the contribution associated with the reflectivity of the absorbing material between transmitting antenna and receiving antenna in verification procedures.

NOTE 4: This uncertainty contributes to test methods in anechoic facilities, both with and without a ground plane. It is the uncertainty due to reflections from the absorbing material. As the verification process is not one of substitution, the relevant value from table 7 should be used in all uncertainty calculations.

Table 7: Uncertainty contribution: reflectivity of absorbing material: EUT to the test antenna

Reflectivity of the absorbing material	Standard uncertainty of the contribution
reflectivity < 10 dB	4,76 dB
10 ≤ reflectivity < 15 dB	3,92 dB
15 ≤ reflectivity < 20 dB	2,56 dB
20 ≤ reflectivity < 30 dB	1,24 dB
reflectivity ≥ 30 dB	0,74 dB

8.3.2.10 Reflections in an Anechoic Chamber with a Ground Plane

The discussion given in clause 8.3.2.9 for the fully Anechoic Chamber is fully applicable to the case of an Anechoic Chamber with a Ground Plane with the exception that the floor reflection becomes a wanted signal and is of higher magnitude.

8.3.2.11 Mutual coupling due to imaging in the absorbing material

Mutual coupling is the mechanism which produces changes in the electrical behaviour of an EUT or antenna when placed close to a conducting surface, another antenna, etc. The changes can include, amongst others, de-tuning, gain variation and changes to the radiation pattern. Whilst the absorbing materials help to reduce these effects, it does not remove them completely. To avoid the major effects of any such performance changes, it is a stipulation in all tests that no part of any antenna, or EUT, should at any time approach to within less than 1 m of any absorbing material. Where this condition cannot be satisfied, testing should not be carried out.

The magnitude of the effects on the electrical characteristics due to the degree of imaging in the absorber/shield of the chamber are estimated in annex A of TR 102 273-1-2 [12] and the uncertainty contributions due to the mutual coupling effects to the absorber materials are given representative symbols as follows:

u_{j04} is used throughout all parts of the present document for the uncertainty contribution associated with the mutual coupling of the EUT to its images in the absorbing material in test methods;

NOTE 1: The uncertainty contributes to test methods in anechoic facilities, both with and without a ground plane. It is the uncertainty which results from the degree of imaging in the absorber/shield of the chamber and the resulting effect on the input impedance and gain of the integral antenna of the EUT.

u_{j05} is used throughout all parts of the present document for the uncertainty contribution associated with the de-tuning effect of the absorbing material on the EUT in test methods;

u_{j06} is used throughout all parts of the present document for the uncertainty contribution associated with the substitution, measuring or test antenna and its images in the absorbing material in test methods;

NOTE 2: The uncertainty contributes to test methods in anechoic facilities, both with and without a ground plane. It is the uncertainty which results from the degree of imaging in the absorber/shield of the chamber and the resulting effect on the antenna's input impedance and gain.

u_{j07} is used throughout all parts of the present document for the uncertainty contribution associated with the transmitting or receiving antenna and its images in the absorbing material in verification procedures.

NOTE 3: The uncertainty only contributes to verification procedures in anechoic facilities, both with and without a ground plane. It is the uncertainty which results from the degree of imaging in the absorber/shield of the chamber and the resulting effect on the antenna's input impedance and gain.

8.3.2.12 Extraneous reflections

Within the chamber, reflecting objects such as internal lighting, cameras and safety circuits (which are normally used in chambers where high power fields are generated) should be avoided (or their effects minimized) as they will have a direct effect on the quality of the measurement at that site. Similarly, the materials from which the antenna mount and turntable are constructed should be of low relative dielectric constant.

8.3.3 Effects of the ground plane

A conducting ground plane should be made from metals preferably of a non ferrous nature such as copper or aluminium. It does not have to be constructed of solid sheet but can be perforated metal, welded mesh, metal gratings, etc. Wherever a gap or a void occurs within the screen, it should not measure more than $\lambda/10$ at the highest frequency of operation in any dimension. This maximum dimension applies equally to joints and seams between metal sheets/panels where these have been used to make the ground plane.

The main reflection comes from the ray which makes equal incident and reflected angles on the ground plane surface, although other areas within the plane contribute to the overall interference signal level coming from the ground. This is a result of diffraction. The resulting size of the ground plane for reliable measurements is subject to both calculation and practical experience and can vary depending on the profile of ground plane chosen i.e. there are different recommendations for elliptical and rectangular planes.

The size of the ground plane should be large enough to cover the entire area from which reflections will arise. ANSI use Fresnel ellipses on the reflecting surface (see figure 76) as a basis for determining the size, where the ellipse is defined by the locus of equal reflected path lengths from the EUT to the test antenna.

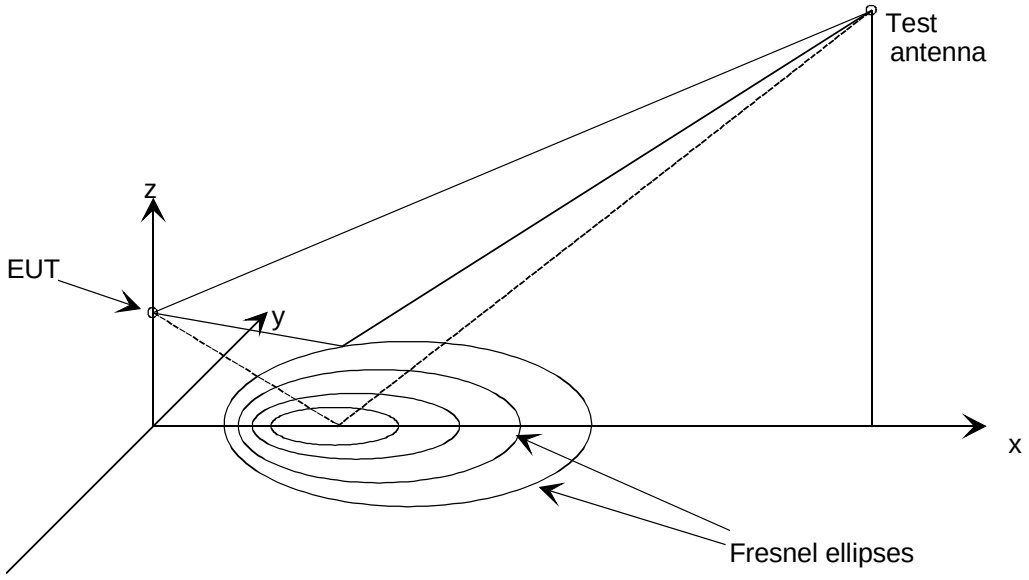

Figure 76: Fresnel ellipses drawn on the reflecting surface

The ellipse corresponding to the first Fresnel zone i.e. the one which gives a path length change of half a wavelength at the lowest frequency of operation, is the minimum size of ground plane recommended by ANSI. This is dependent on the test site geometry (i.e. measurement distance, source height, receive antenna height variation) and the wavelength of the lowest frequency.

It has been reported "Control of errors on Open Area Test Sites" [8] that simply increasing the ground plane size, in an attempt to improve its approximation to an infinite plane, may not always be beneficial. When the edge of the ground plane is not well terminated, the edge effects (i.e. the difference between theoretical and measured results for vertical polarization) can actually increase as the ground plane gets larger.

The smoothness of the reflecting surface is of importance and as a general rule of thumb, the surface roughness is taken to be less than $\lambda/10$ at the shortest wavelength of usage. For all tests under consideration here (where 12,75 GHz is the uppermost frequency of interest), this implies that the surface should be smoother than 2,35 mm.

8.3.3.1 Coatings

Where thick dielectric coatings have been applied to a metal ground plane e.g. asphalt, gravel, concrete, etc., or where a layer of snow has fallen, the nature of the reflection can be significantly changed, particularly for vertical polarization. This effect is illustrated in figure 77 where the patterns above ground of a vertical dipole are presented. The solid line represents the performance above a perfectly reflecting surface, whereas the dashed line is for the same antenna above a dielectric covered, reasonably conductive ground plane. The received signal levels consequently can show an enormous variation in level depending on the state of the reflecting surface when vertically polarized tests are being performed. The change in reflectivity for horizontal polarization is relatively minor in comparison.

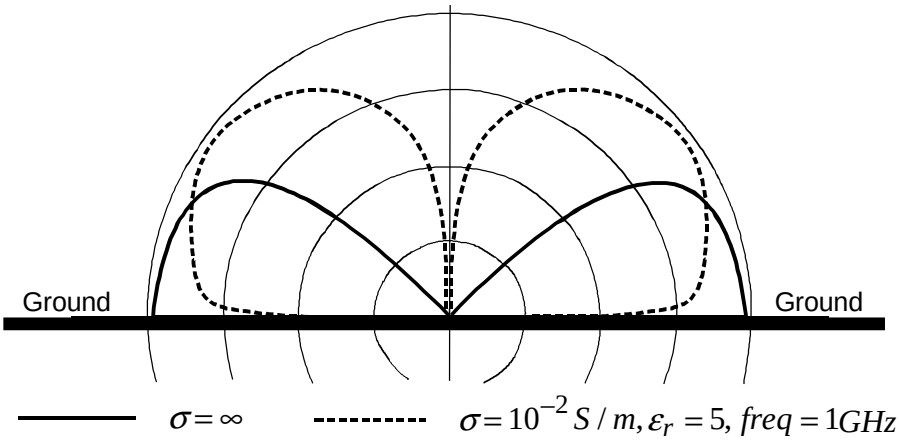

Figure 77: Patterns for vertical dipole above different ground planes

When comparing results from different sites, the reflection coefficient variations from one ground plane medium to another, even when measurement geometry remains the same, can produce significant differences in the measured results.

To minimize these uncertainties, the ground plane should be a highly conductive, relatively non ferrous metal with no coating.

8.3.3.2 Reflections from the ground plane

Far from a perfectly conducting ground plane, at a distance sufficient to make the difference between the direct and reflected path lengths negligible and the direct and reflected waves appear parallel to each other, the amplitude of the reflected wave is equal to the amplitude of the direct wave. When these two waves add "in phase" the electric field strength doubles (6 dB gain) whereas, at another point the two waves are "out of phase" and cancel entirely resulting in no net electric field. Therefore, over a perfectly conducting ground plane at infinite distance it is possible to obtain field strengths varying from +6 dB to - ∞ dB relative to the free Space field strength (see figure 78a).

In practice, the distance between the EUT and the test antenna is not infinite, the direct and reflected waves are not parallel and their path lengths can differ substantially. In this condition the field measured by the test antenna can alternate between peaks and nulls many times as the test antenna is raised and lowered through the available height range. The difference in path lengths, along with any directivity of the test antenna in the vertical plane result in the direct and reflected waves not being equal in amplitude. As a result, when they add "in phase" the peak will be less than +6 dB and when they are out of phase their amplitudes do not fully cancel, resulting in an electric field greater than - ∞ dB (null filling) (see figure 78b).

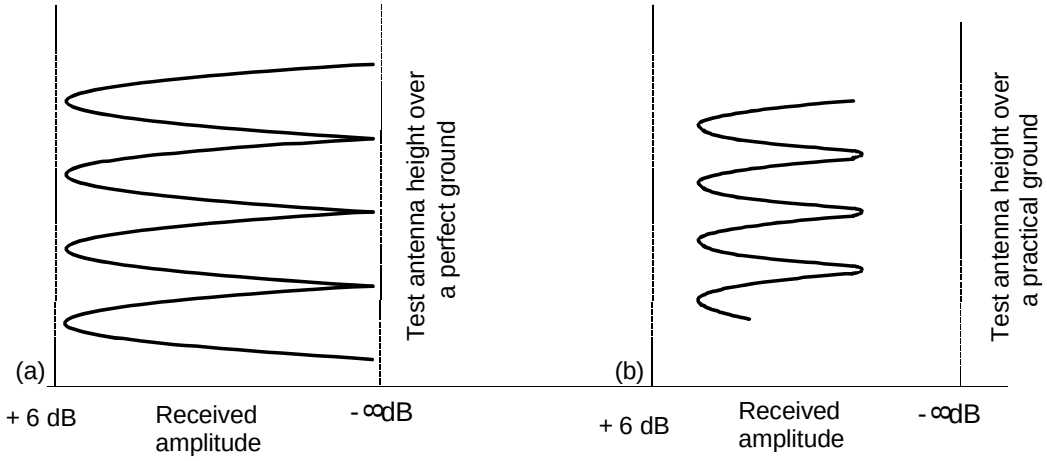

Figure 78: Comparison of the received amplitude for an ideal site against a practical site

For testing purposes, when it is necessary to generate a uniform field in, for example, immunity measurements, the region of interest is either a particular volume or area into which the EUT will be placed. The degree of uniformity of the fields within this volume is affected by many factors, such as the relative positions of the radiating antenna and the EUT, the radiation patterns, the size and construction of the EUT, etc.

The interaction of the direct and ground reflected waves produce regular sharp amplitude nulls in the volume occupied by the EUT or receiving/measuring antenna (see figure 79).

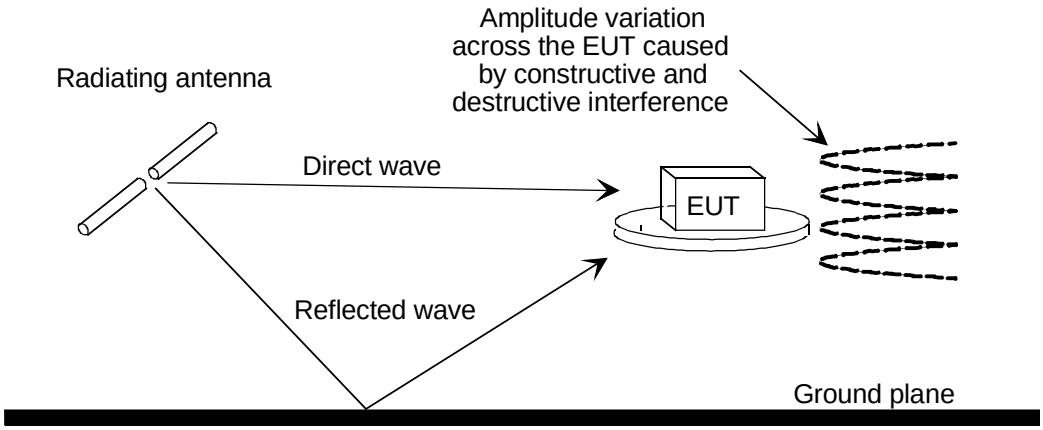

Figure 79: Amplitude variation in the test volume

The smaller the EUT the more uniform the field across it. As a general rule, for minimum measurement uncertainty during tests, its size should be significantly smaller than the distance between the nulls. The nulling effect is more severe in the vertical plane than the horizontal plane of the volume occupied by the EUT, and it is worst when the transmitting antenna is at its maximum height (4 m) and horizontally polarized (since the ground plane is fully illuminated by the omni-directional pattern of the dipole in this polarization). In this worst case, the maximum vertical dimension an EUT or receiving/measuring antenna can have on a 3 m test range is between 0,4 to 0,6 wavelengths (depending on the frequency, height on the mast, mutual coupling effects etc.) for the amplitude of the field across it to vary by no more than -3 dB at its edges (relative to its centre).

The phase variation is not curved as in the case of a point source in free Space (see clause 6), but tends to be more linear with a tilt, relative to vertical, which is roughly equivalent to the angle at which a single source, placed midway between the real antenna on the mast and its image, would impinge on the receive aperture. If one were to impose, say, a phase variation across the receive aperture of no greater than 22,5°, the maximum size of an EUT would be much reduced (typically by a factor of at least 2) from the 0,4 to 0,6 wavelengths quoted, to a point where the test site would be virtually unusable at some frequencies.

8.3.3.3 Mutual coupling to the ground plane

Mutual coupling, as stated in clause 8.3.2.11, is the mechanism which produces changes in the electrical behaviour of an EUT (or antenna) when placed close to a conducting surface, another antenna, etc. The changes can include detuning, gain variation and distortion of the radiation pattern.

To illustrate the effects of mutual coupling to the ground plane it is useful to start by considering the interaction between two closely spaced resonant dipoles in free Space i.e. without a ground reflection. Some texts [5] show that in this condition, noticeable changes to a dipole's input impedance result for dipole to dipole spacing of up to 10 wavelengths (assuming side by side orientation).

In a transmit/receive system between two resonant dipoles the input impedance of the driven dipole (Z_{in1}) can be calculated as a combination of its own self impedance (Z_{11}), the self impedance of the other dipole (Z_{22}) and a contribution from the mutual interaction between them. The mutual interaction comprises both resistive (R_{12}) and reactive (X_{12}) components and the relationship between them can be shown to be:

$$Z_{in1} = Z_{11} - \frac{(R_{12} + jX_{12})^2}{Z_{22}}$$

The variations with separation distance of the mutual resistance and reactance for two half wavelength dipoles are shown in figure 80.

EXAMPLE 1: If the range length is 3 m and the frequency is 30 MHz, from figure 80, R_{12} = 29,11 Ω and X_{12} = -34,36 Ω. As a result, Z_{in1} = 88,32 + j 60,98 Ω whereas with no coupling it would be 73 + j 42,5 Ω.

EXAMPLE 2: The input impedance of the transmitting antenna for two half wavelength dipoles spaced half a wavelength apart, becomes 70 + j 30,5 Ω as a result of the mutual coupling.

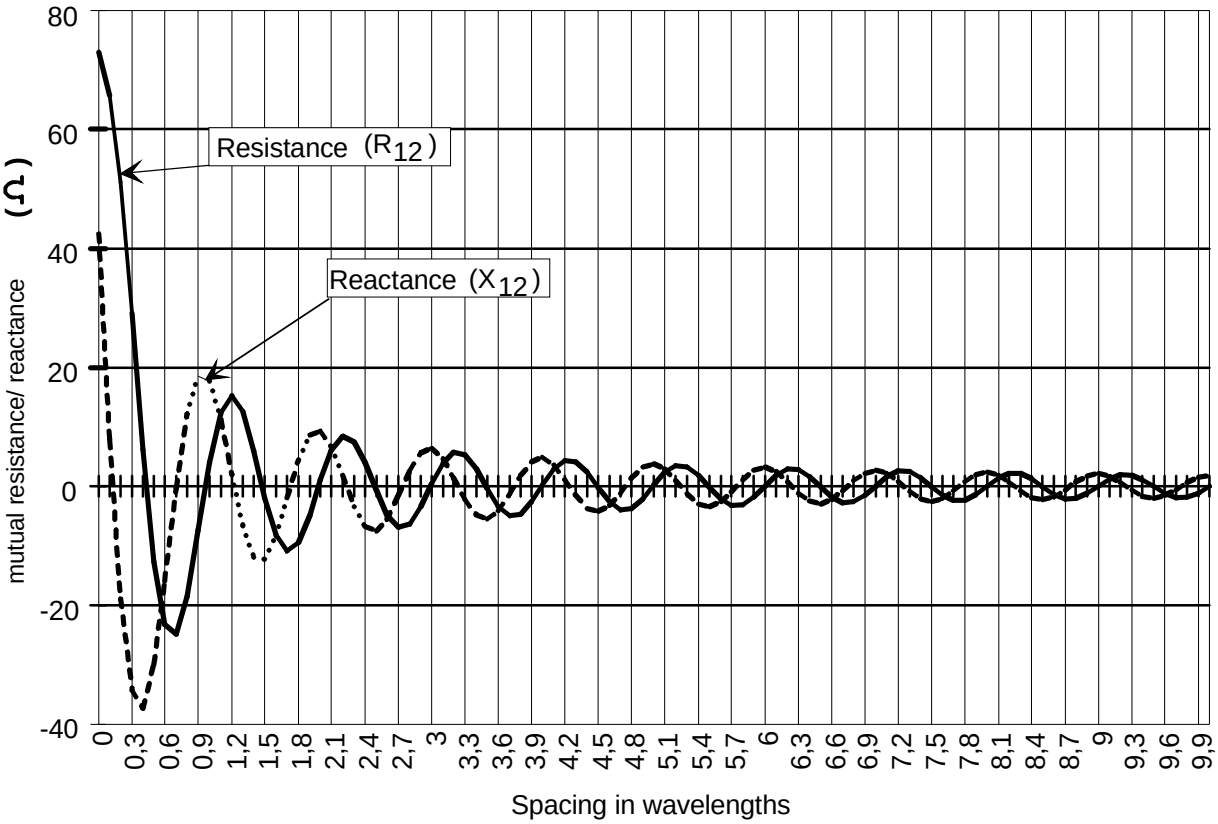

Figure 80: The mutual resistance and reactance of two side-by-side dipoles, each λ/2

ΩAlong with the change in input impedance arising from mutual coupling, there will be a signal strength loss due to the associated mismatch to the line. However, it is not only the dipole impedance that changes as a result of its proximity to another. The radiation pattern and gain (or antenna factor) will also change. Indeed, the gain change has been shown (see [2] to have an unexpected relationship with the radiation resistance - namely that their product remains constant no matter how much either quantity may vary. Specifically:

Gain = 120 /Radiation resistance

As a result, for the first example above (30 MHz dipoles spaced 3 m apart) a gain loss of 0,83 dB occurs whilst for the second example of two dipoles half a wavelength apart an increase of 0,19 dB in the gain results. Simply increasing the range length to minimize mutual coupling, requires a receiver with sufficient sensitivity to cope with the increased path loss.

In this case the input resistance to the antenna and the radiation resistance is assumed to be the same. If a matching network i.e. a balun or attenuator is inserted this is not the case.

The magnitude of the effects on the electrical characteristics of the EUT or antenna due to the degree of mutual coupling between them are estimated in annex A of TR 102 273-1-2 [12] and the uncertainty contributions which result are given representative symbols as follows:

u_{j08} is used throughout all parts of the present document for the uncertainty contribution associated with the mutual coupling amplitude effect of the test antenna on the EUT in test methods.

NOTE 1: It is the uncertainty which results from the interaction (impedance changes, etc.) between the EUT and the test antenna when placed close together.

u_{j09} is used throughout all parts of the present document for the uncertainty contribution associated with the de-tuning effect of the test antenna on the EUT in test methods.

NOTE 2: It is the uncertainty of any de-tuning effect due to mutual coupling between the EUT and the test antenna.

u_{j10} is used throughout all parts of the present document for the uncertainty contribution associated with the mutual coupling between the transmitting antenna and the receiving antenna in the verification procedures.

NOTE 3: It is the uncertainty which results from the change in coupled signal level between the transmitting and receiving antenna when placed close together. For ANSI dipoles the value of this uncertainty is 0,00 dB as it is included, where significant, in the mutual coupling and mismatch loss correction factors. For non-ANSI dipoles the standard uncertainty for frequencies can be taken from table 8.

Table 8: Uncertainty contribution: Mutual coupling: transmitting antenna to receiving antenna

Frequency	Standard uncertainty of the contribution (3 m range)	Standard uncertainty of the contribution (10 m range)
30 MHz ≤ frequency < 80 MHz	1,73 dB	0,60 dB
80 MHz ≤ frequency < 180 MHz	0,6 dB	0,00 dB
frequency ≥ 180 MHz	0,00 dB	0,00 dB

u_{j11} is used throughout all parts of the present document for the uncertainty contribution associated with the mutual coupling between substitution or measuring antenna and the test antenna in test methods.

NOTE 4: For ANSI dipoles the value of this uncertainty is 0,00 dB as it is included, where significant, in the mutual coupling and mismatch loss correction factors. For non-ANSI dipoles the standard uncertainty for frequencies can be taken from table 8.

Over a ground plane, this mutual coupling situation becomes further complicated by the creation of images of both antennas. Without giving a full analysis, it is indicative to look at the case of a single dipole and the effect its image (i.e. the presence of the ground plane) has on its performance. For this configuration, the orientation of the dipole is important. For a horizontal dipole, the input impedance can be shown to be:

$$Z_{in} = Z_{11} - Z_{12}$$

whereas for a vertical one,

$$Z_{in} = Z_{11} + Z_{12}$$

where $Z_{12} = R_{12} + jX_{12}$. Again, the gain of the dipole will change in line with its input resistance and for the worst case of a horizontal dipole, the variation in gain against height above the ground plane is given in figure 81. Even for a spacing above the ground plane of more than two wavelengths, the figure shows that the dipole's gain can vary by ±0,5 dB with the ripple being slow to diminish even at spacing of five wavelengths.

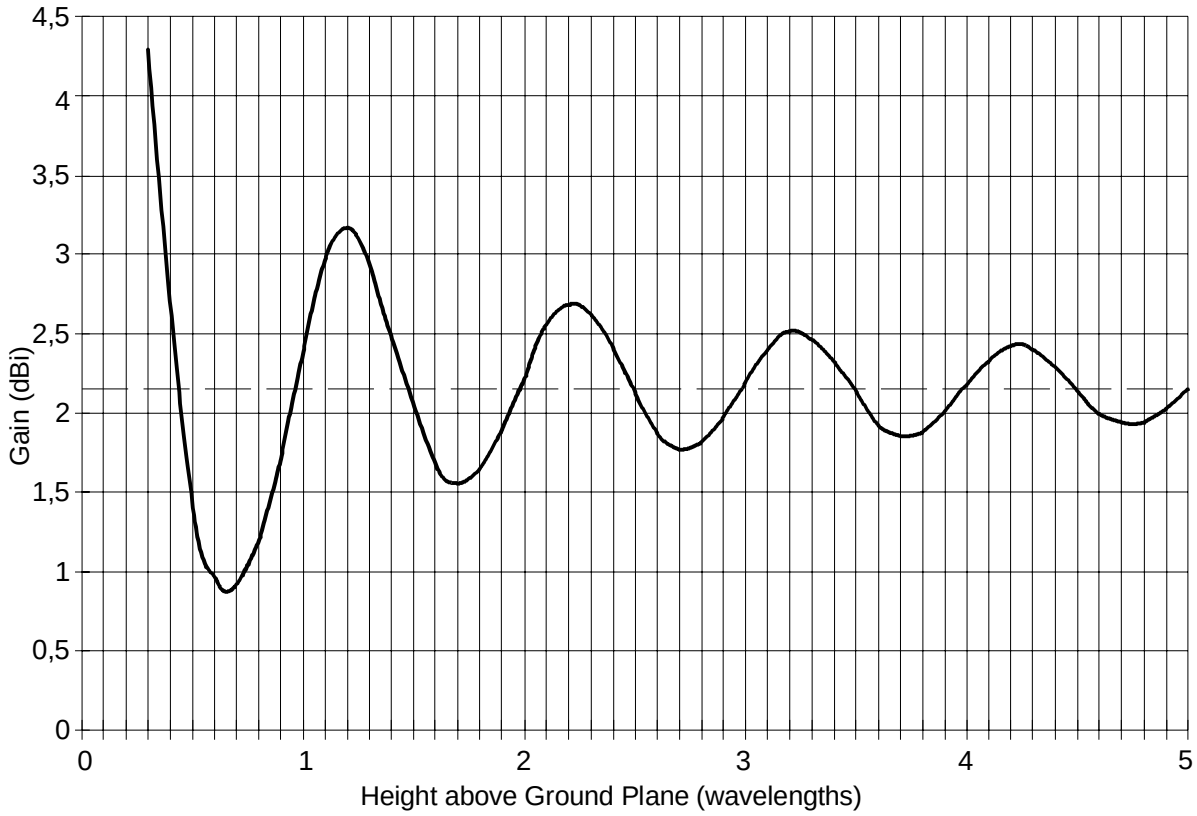

Figure 81: Gain variation of a horizontal half wavelength dipole above a ground plane

This real life testing situation is very much more involved than the theoretical coupled dipole examples given above since there is interaction not only between the transmitting and receiving devices and their own images (whether an EUT and antenna or two antennas) but also between each device and the image of the other and between images.

NOTE 5: The overall mutual coupling effect between two ANSI dipoles over a ground plane have been modelled and figures are provided as "Mutual coupling and mismatch loss" correction factors in the individual test procedures.

Furthermore, for an EUT, the magnitude of the overall effect will be dependant on its size, polarization, frequency, etc.

Mutual coupling to the ground plane for a typical test is illustrated in figure 82.

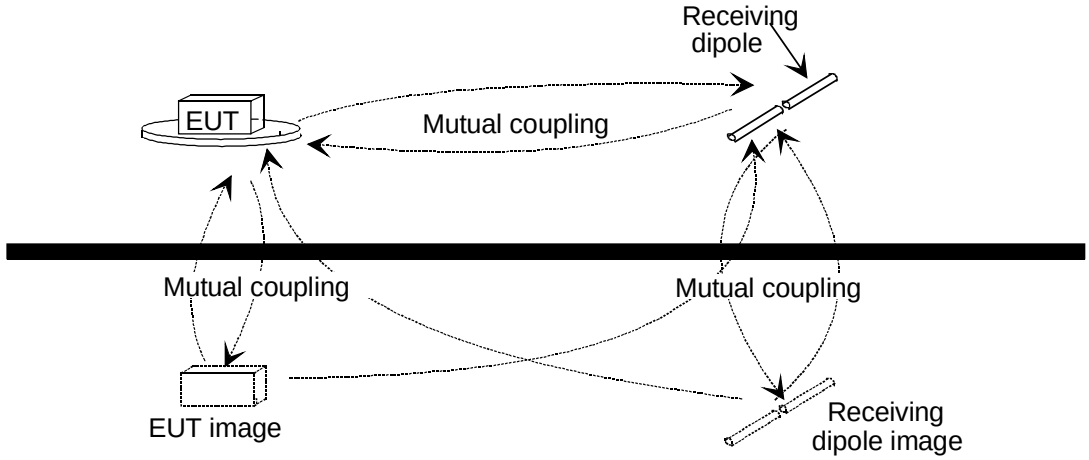

Figure 82: Mutual coupling in the ground plane

The magnitude of the effects on the electrical characteristics of an EUT or antenna due to the mutual coupling between them and/or the ground plane are estimated in annex A of TR 102 273-1-2 [12] and the uncertainty contributions which result are given representative symbols as follows:

u_{j12} is used throughout all parts of the present document for the uncertainty contribution associated with the interpolation of mutual coupling and mismatch loss correction factors (factors to allow for coupling between ANSI dipoles only).

NOTE 6: The standard uncertainty which results from interpolation between two values of mutual coupling is given in table 9.

Table 9: Uncertainty contribution: mutual coupling: interpolation of mutual coupling and mismatch loss correction factors

Frequency (MHz)	Standard uncertainty of the contribution
for a spot frequency given in the table	0,00 dB
30 MHz ≤ frequency < 80 MHz	0,58 dB
80 MHz ≤ frequency < 180 MHz	0,17 dB
frequency ≥ 180 MHz	0,00 dB

u_{j13} is used throughout all parts of the present document for the uncertainty contribution associated with change in the gain/sensitivity of an EUT due to mutual coupling to its image in the ground plane in test methods.

NOTE 7: When the mutual coupling of the EUT to the ground plane affects the measurement, the standard uncertainty of the contribution should be taken from table 10.

Table 10: Uncertainty contribution: mutual coupling: EUT to its image in the ground plane

Spacing between the EUT or antenna and the ground plane	Standard uncertainty of the contribution
For a vertically polarized EUT	
spacing ≤1,25 λ	0,15 dB
spacing >1,25 λ	0,06 dB
For a horizontally polarized EUT	
spacing < $\lambda/2$	1,15 dB
$\lambda/2$ ≤ spacing < $3\lambda/2$	0,58 dB
$3\lambda/2$ ≤ spacing < 3λ	0,29 dB
spacing ≥ 3λ	0,15 dB

u_{j14} is used throughout all parts of the present document for the uncertainty contribution associated with the change in gain/sensitivity of the substitution, measuring or test antenna to its image in the ground plane in test methods.

NOTE 8: It is the uncertainty which results from the change in gain/sensitivity of the substitution, measuring or test antenna when placed close to a ground plane. The standard uncertainty of the contribution is taken from table 10.

u_{j15} is used throughout all parts of the present document for the uncertainty contribution associated with the mutual coupling between the transmitting or receiving antenna and its image in the ground plane in verification procedures.

NOTE 9: It is the uncertainty which results from the change in gain of the transmitting or receiving antenna when placed close to a ground plane. For ANSI dipoles the value of this uncertainty is 0,00 dB as it is included, where significant, in the mutual coupling and mismatch loss correction factors. For other dipoles the value can be obtained from table 10.

8.3.4 Other effects

8.3.4.1 Range length and measurement distance

Range length is defined as the horizontal distance between the phase centres (or volume centres) of the EUT and test antenna or between antennas. Measurement distance, on the other hand, is defined as the actual distance between the phase centres (or volume centres) of the EUT and test antenna. The distinction between the two parameters is illustrated in figure 83 where the test antenna is at 4 m.

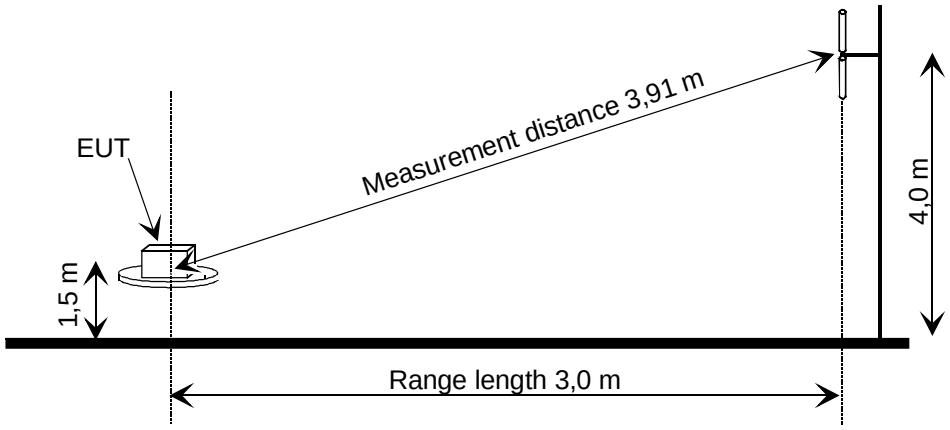

Figure 83: Range length and measurement distance

Measurement uncertainties are always encountered when measurements of any kind are made in the near-field. One of the main difficulties in testing is being able to define for an unknown emission, where the near-field conditions end and the far-field conditions start. There is a general zone, referred to as the transition zone, within which near-field or far-field conditions may exist, depending on the characteristics of the source.

In the near-field the electric and magnetic fields should be considered separately as the ratio of the two is not constant and, as a result, the wave impedance is not constant. In the far-field, however, they comprise a plane wave having an impedance of 377 Ω. Therefore, when plane waves are discussed they are assumed to be in the far-field.

Various near-field/far-field boundary formulas are in frequent usage on test sites. Table 11 lists these for various frequencies. Table 12 lists the far-field distances for a typical range of pyramidal waveguide horn antennas (1 GHz to 12,75 GHz).

Table 11: Distance from source for various far-field formulations

(30 MHz to 200 MHz)			
	λ/2π	λ/2	5λ
30 MHz	1,6 m	5 m	50 m
200 MHz	0,24 m	0,75 m	7,5 m
(200 MHz to 1 000 MHz)			
	λ/2π	λ/2	5λ
200 MHz	0,24 m	0,75 m	7,5 m
1 000 MHz	0,0478 m	0,15 m	1,5 m
(1 000 MHz to 12,75 GHz)			
	λ/2π	λ/2	5λ
1 000 MHz	0,0478 m	0,15 m	1,5 m
12,75 GHz	0,00375 m	0,0118 m	0,1176 m

Commonly used range lengths of 3 m and 10 m yield measurement distances which can fall within the near-field in the frequency range 30 MHz to 200 MHz. In an attempt to avoid this, a lower measurement distance of $\lambda/2$ is quoted in current (I)-ETSs and ENs. However, the present document recommends the far-field formulation of $2(d_1+d_2)^2/\lambda$ (see clause 6) where d_1 and d_2 are the aperture sizes of the devices at the two ends of the test site.

In the frequency range 200 MHz to 1 000 MHz, the near-field/far-field boundary is typically less than 3 m, hence a plane wave should have developed within the space between the EUT and the antenna. In the frequency range above 1 000 MHz most measurements will be made in the far-field.

Table 12: Far-field for a typical range of pyramidal waveguide horn antennas (1 GHz to 12,75 GHz)

Far-field distances for typical waveguide horn antennas	$2d^2/\lambda$ (m)	
Frequency range (GHz)	at minimum frequency	at maximum frequency
0,96 to 1,46	2,506 m	3,812 m
1,14 to 1,79	2,120 m	3,329 m
1,70 to 2,60	1,310 m	2,004 m
2,60 to 3,95	0,957 m	1,454 m
3,95 to 5,85	0,649 m	0,961 m
5,85 to 8,20	0,525 m	0,736 m
8,20 to 12,40	0,316 m	0,478 m
12,40 to 18,00	0,213 m	0,310 m

8.3.4.2 Minimum far-field distance

The recommended minimum conditions for a plane wave to exist, for testing purposes, is when the separation is equal to or greater than $2(d_1+d_2)^2/\lambda$. Generally this gives less than 0,06 dB of amplitude loss in either received or transmitted signal level for the apertures involved.

8.3.4.2.1 Measurement distances

Clause 3.3.1.1 of the original edition of TR 100 027 [10] stated: "Measuring distances of 3 m, 5 m, 10 m, and 30 m are in common use. The EUT size (excluding the antenna) shall be less than 20 % of the measuring distance". This allowed EUT sizes of up to 0,6 m maximum dimension on a 3 m site, 1 m on a 5 m site, 2 m on a 10 m site and 6 m on a 30 m site and pays no regard to the most important aspect of the EUT, namely the antenna.

Allowing these sizes of EUT to exist on any test site has several implications for measurement uncertainty since they are not based on the "far-field" criterion of $2 (d_1+d_2)^2/\lambda$ (see clauses 7.2.3 and 7.2.4).

Table 13 indicates the comparison between the TR 100 027 [10] statement and the far-field criteria of $2d_1+d_2)^2/\lambda$, at 12,75 GHz, where a point source is assumed at the other end.

Table 13: Far-field distance from source (dependant on EUT size)

Equipment size 20 % of separation (m)	Range length (m)	Far field at 12,75 GHz (m)	Site length short by (%)
0,6	3,0	30,6	1 020
1,0	5,0	85,0	1 700
2,0	10,0	340	3 400
6,0	30,0	3 060	10 200

The range length over which any radiated test is carried out should always be adequate to enable far-field testing of the EUT i.e. range length should always be greater than or equal to:

$$\frac{2(d_1 + d_2)^2}{\lambda}$$

where:

d_1 is the largest dimension of the EUT/dipole after substitution (m);

d_2 is the largest dimension of the test antenna (m);

λ is the test frequency wavelength (m).

Table 14 illustrates EUT sizes for different range lengths using the $2(d_1+d_2)^2/\lambda$ formula assuming a point source at the other end.

Table 14: Maximum EUT dimensions at 3 m, 5 m, 10 m and 30 m

Range length (m)	Frequency (MHz)	Maximum dimension of EUT (m)	Maximum dimension of EUT (λ's)
3	30	3,87	0,387
3	100	2,12	0,707
3	1 000	0,671	2,24
3	12 750	0,188	7,99
5	30	5,000	0,500
5	100	2,739	0,913
5	1 000	0,866	2,887
5	12 750	0,242	10,31
10	30	7,07	0,707
10	100	3,87	1,29
10	1 000	1,225	4,08
10	12 750	0,343	14,58
30	30	12,247	1,225
30	100	6,708	2,236
30	1 000	2,121	7,071
30	12 750	0,594	25,25

Figure 84 graphically illustrates the $2(d_1+d_2)^2/\lambda$ formula for various sizes of EUT, again assuming a point source at the other end. The lines show the variation of frequency against wavelength. For example, an EUT with a maximum dimension of 0,6 m (this is 20 % of the measuring distance of a 3 m site) just meets the far-field conditions at 1,1 GHz on a 3 m site. On a 5 m site it can be tested to 2 GHz, or 4 GHz on a 10 m site, but full frequency range testing (30 MHz to 12,75 GHz) can only be carried out with a separation of 30,6 m. Full frequency testing on a 30 m range will only produce a small additional uncertainty ("ONLY" for this particular example being of the order of < 0,05 dB) and this only at frequencies above 12,5 GHz.

To test over the full frequency range, 30 MHz to 12,75 GHz, on a 3 m site the maximum dimension of the EUT cannot exceed 0,188 m, see point (A) in figure 84.

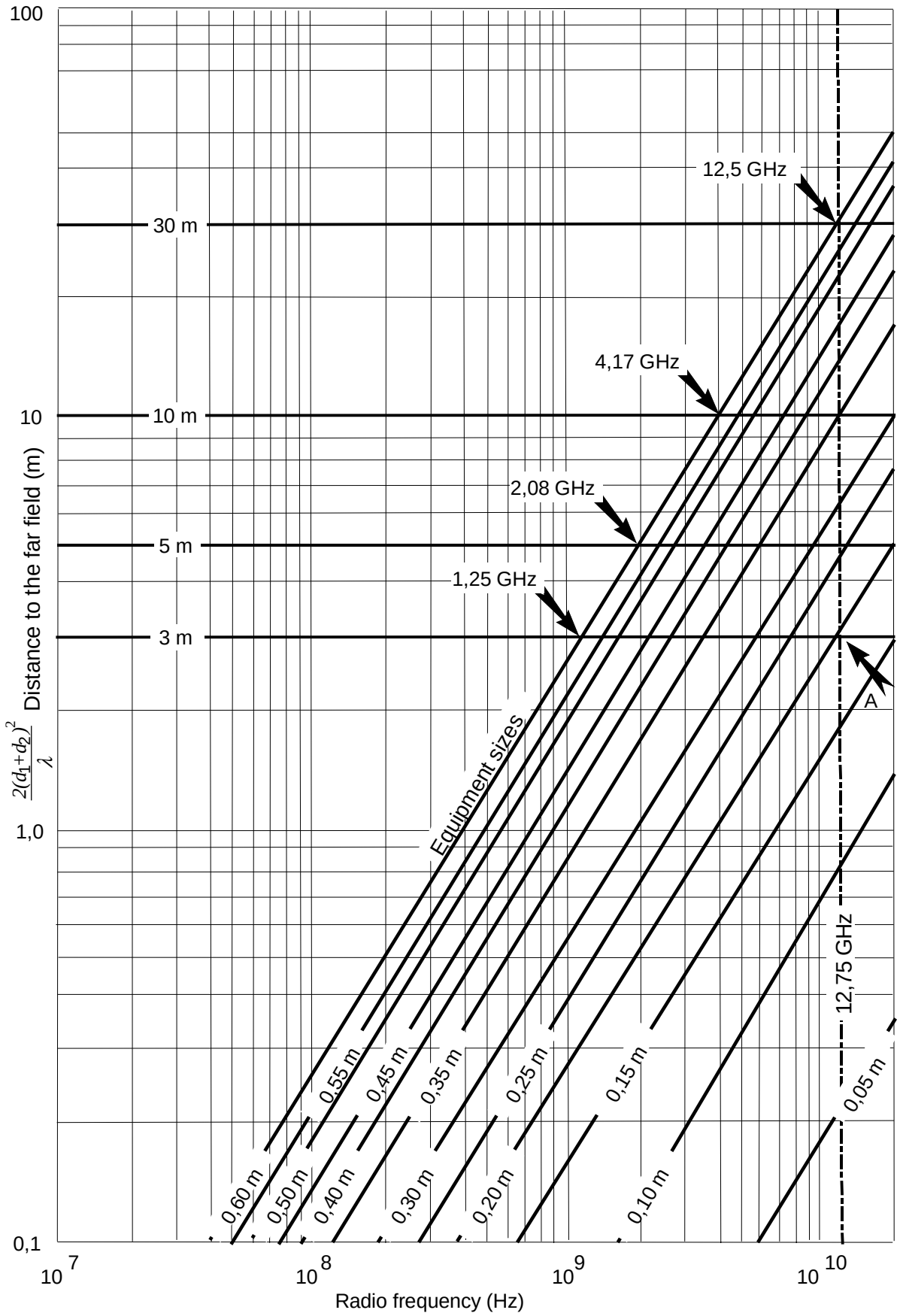

Figure 84: Maximum frequency of test for a given equipment size and measurement separation

The uncertainty contribution which arises from the range length not satisfying the far-field range length is estimated in annex A of TR 102 273-1-2 [12] and is given the representative symbol as follows:

u_{j16} is designated throughout all parts of the present document as the uncertainty contribution associated with the range length (when it does not meet the far-field requirement).

NOTE 1: The uncertainty contribution that results can be found in table 15. For distances equal to or less than $(d_1+d_2)^2/4\lambda$ the magnitude of the contribution is unspecified, since measurements should not be carried out at these separations (the uncertainty is too large).

Table 15: Uncertainty contribution: range length

Range length (i.e. the horizontal distance between phase centres)	Standard uncertainty of the contribution
$(d_1 + d_2)^2/4\lambda \leq$ range length $< (d_1 + d_2)^2/2\lambda$	1,26 dB
$(d_1 + d_2)^2/2\lambda \leq$ range length $< (d_1 + d_2)^2/\lambda$	0,30 dB
$(d_1 + d_2)^2/\lambda \leq$ range length $< 2(d_1 + d_2)^2/\lambda$	0,10 dB
range length $\geq 2(d_1 + d_2)^2/\lambda$	0,00 dB

NOTE 2: In table 15, d_1 and d_2 are either the sizes of the EUT and the test antenna or the sizes of the two antennas.

The radiated test methods in the present document all involve a substitution measurement. A substitution measurement always involves two stages. One stage is the measurement on the EUT, the other stage involves a similar measurement using a reference (normally a dipole) against which the first result can be compared and evaluated.

Complications arise when the radiated test is carried out over a reflective ground plane, since this requires the raising and lowering of the test antenna to maximize the received signal. Two uncertainties are introduced by this action.

The first uncertainty concerns the radiation pattern of the test antenna in the vertical plane. For a vertically polarized dipole, the directivity in the vertical plane means that the higher on the mast that the test antenna peaks, the larger the angle subtended to the device at the other end and hence the further down the side of the beam the illumination falls.

EXAMPLE 1: For a peak height of 1,5 m, the direct signal to the test device comes from the boresight of the beam, whereas for a peak height of 4 m, an angle of 39,8° is subtended over a 3 m range length. This corresponds to a fall off of 3,1 dB for a half wavelength dipole (see figure 85).

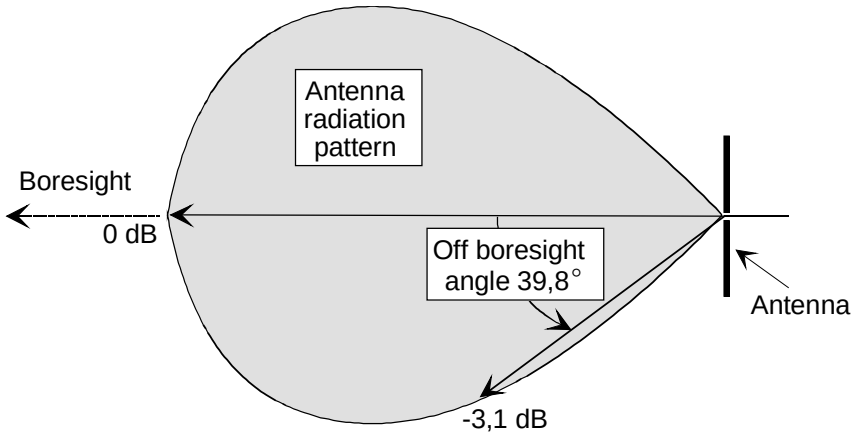

Figure 85: Signal loss due to off boresight angle

Whilst this is an over simplification of the case (no account has been paid to the reflected signal) nonetheless it illustrates the potential magnitude of the effect. It should be noted that this effect does not occur when dipoles or bicones are used in horizontal polarization. Corrections can be obtained for signal loss due to off boresight angles in the elevation plane (see figure 86). There is, however, an uncertainty associated with this correction factor:

u_{j17} is used throughout all parts of the present document for the uncertainty contribution associated with the correction factor for off boresight angle in the elevation plane due to signal attenuation with increasing elevation offset angle.

NOTE 3: Where the optimized height of the antenna on the mast is the same in the two stages of the test, this value is 0,00 dB. Where the optimized height of the antenna on the mast is different in the two stages of the test, the standard uncertainty of the contribution is 0,10 dB.

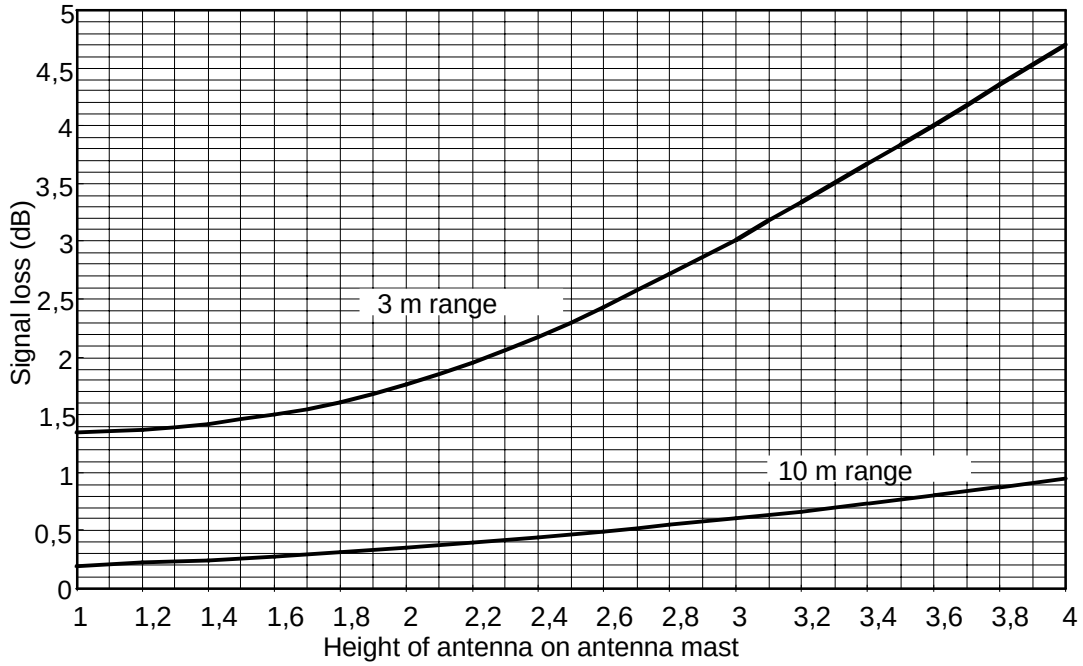

Figure 86: Signal attenuation with increasing elevation offset angle

The second uncertainty is that a measurement distance error occurs when the peak position found on the mast during the substitution is at a different height to that for the measurement on the EUT.

EXAMPLE 2: Suppose a peak is found on the top of the mast (4,0 m) when measuring the EUT, (see figure 83), giving a measurement distance of 3,91 m. For the substitution measurement however the test antenna peaks at 1,5 m giving a measurement distance of 3,0 m. A graph is provided (see figure 87) for obtaining the correction to be applied.

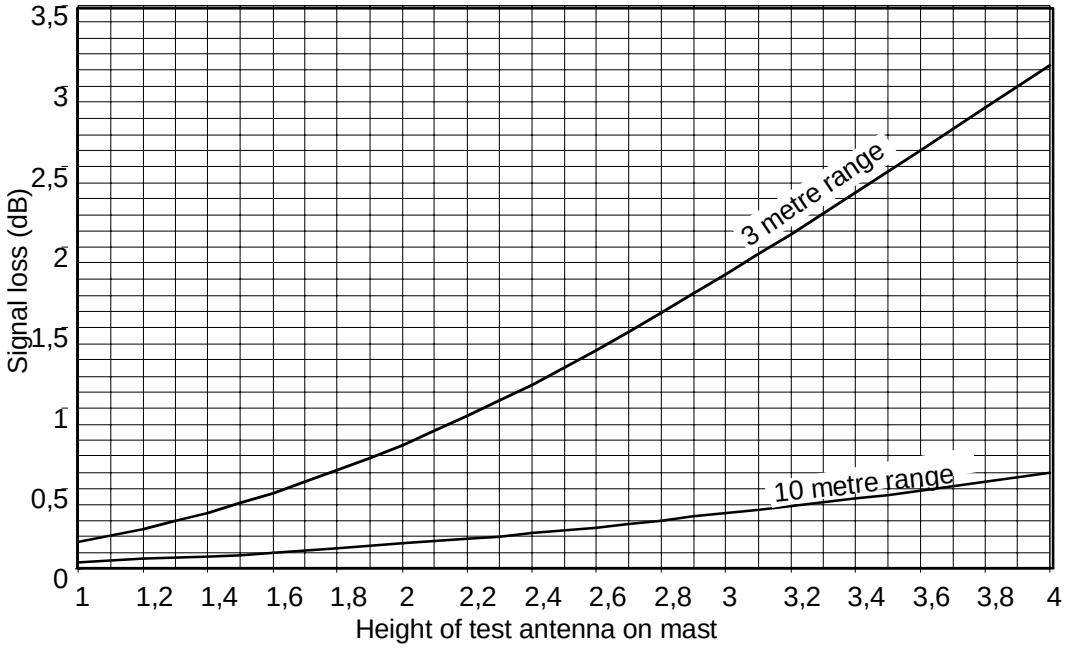

Figure 87: Signal attenuation for antenna height on mast

There is, however, an uncertainty associated with this correction factor:

u_{j18} is used throughout all parts of the present document for the uncertainty contribution associated with the calculated correction factor for measurement distance.

NOTE 4: Where the optimized height of the antenna on the mast is the same in the two stages of the test, this value is 0,00 dB. Where the optimized height of the antenna on the mast is different in the two stages of the test, the standard uncertainty of the value is 0,10 dB.

8.3.4.3 Antenna mast, turntable and mounting fixtures

As the turntable and mounting fixtures are in close proximity to the EUT/antenna they can significantly change its performance. The antenna mast likewise for the test antenna. The antenna mast, turntable and mounting fixtures should, therefore, be constructed from non conducting, low relative dielectric constant plastics or wood to reduce reflections and interactions. Where wood is used, nails should not be used to join the sections - they should be jointed and glued. Table 16 gives examples of popularly used construction materials. It is recommended that materials with dielectric constants of less than 1,5 be used for all supporting structures.

Table 16: Dielectric data of constructional materials

Material	Dielectric constant	Frequency
Fibre Glass	4,8	100 MHz
Dry Oak	4,2	1 MHz
Douglas Fir	1,82	3 000 MHz
Balsawood	1,22	3 000 MHz
Polystyrene Foam	1,03	3 000 MHz
PTFE	2,1	3 000 MHz
Nylon	2,73	3 000 MHz

Wooden constructions need to be protected, by some surface coating from absorbing moisture. Either varnish or paint finishes can be used, but care should be exercised in selection so that low dielectric constant, low conductivity types are applied in order to minimize reflections.

On ground reflection sites, masts should be strong enough to raise and lower the antenna, its mount and feed cable. Its stability is an important aspect, particularly when the antenna is raised and lowered since it should do so in a straight vertical line. The rigidity of the antenna mast needs to be sufficient to prevent any angular errors in the pointing direction of the mounted antenna, in either horizontal or vertical planes, whatever load is placed on it. This is particularly important when tests are carried out on unprotected outdoor sites on windy days. Should the mast twist and the antenna's boresight be directed away from the EUT, then, unless the antenna's pattern is omni-directional in the horizontal plane, there will be an uncertainty in signal level. Similarly, should the antenna be deflected in the vertical plane, unless the pattern is omni-directional in that plane, the beam will either nod towards the ground (thereby increasing the ground illumination), or tilt upwards reducing the signal level directed at the EUT. This deflection will also change the measurement distance and additionally change the relative phasing of the direct and reflected signals (see figure 88).

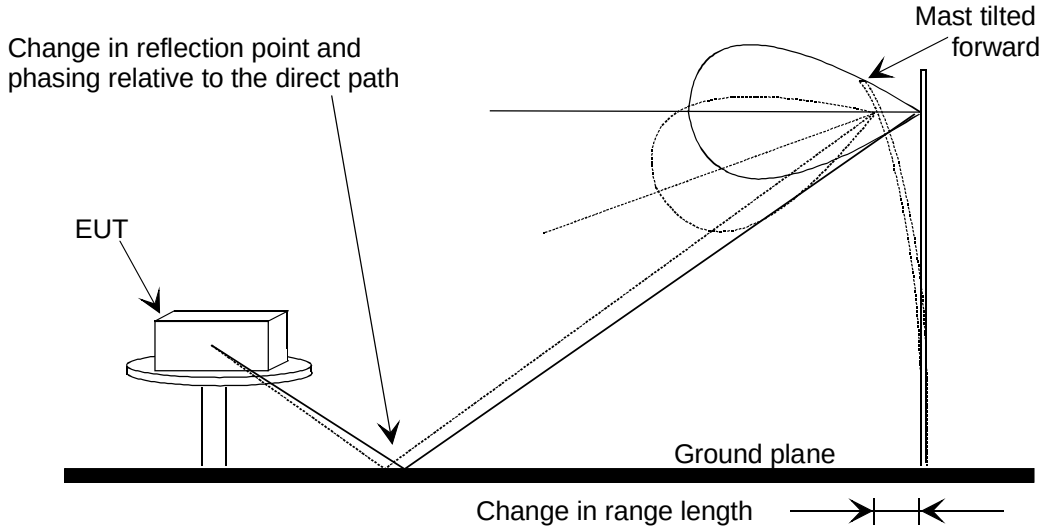

Figure 88: Mast stability

Similarly, if the antenna is allowed to rotate "off axis" due to a poorly anchored mast the signal level may also be reduced, see figure 89.

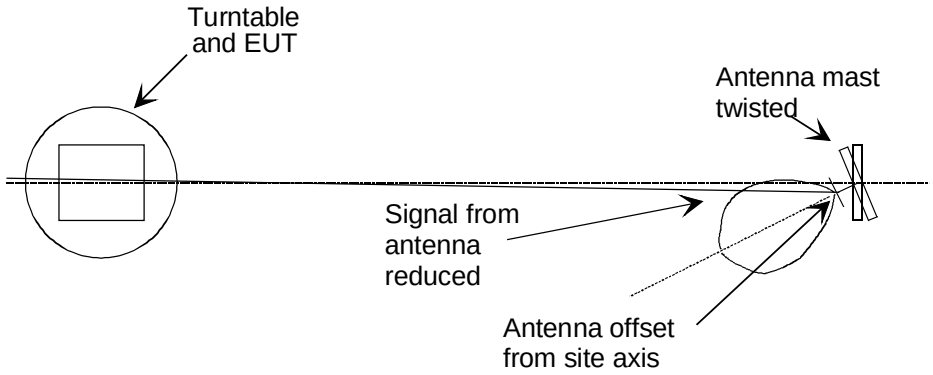

Figure 89: Signal reduction due to a twisted mast (plan view)

Accurate vertical positioning of the antenna is also important. The antenna supports should provide repeatable positioning and the limits of the weight capacities should not be exceeded. The stability of the turntable is important since an unstable, or non uniform turntable will also affect the measurement distance.

Controllers for both the mast and turntable should be carefully considered to avoid measurement uncertainties. For example, rapid changes in height or speed of rotation can lead to missing peak values. Settling times are important for measuring equipment. The controllers should, therefore, be designed with fixed, acceptable speeds which avoid these problems.

8.3.4.4 Test antenna height limitations

All tests on ground reflection sites are carried out so that the peak signal level is detected by varying the height of the antenna on the mast. For an EUT with an omni-directional pattern in the vertical plane above a perfectly conducting ground, theoretically, this peak for vertical polarization occurs on the surface of the ground plane. It is difficult to measure this precise peak with an antenna of any finite size although a fixed monopole mounted on the ground plane could be used. Practically, this is not a viable solution and the antenna therefore has to be moved up the mast until the next peak in the vertical plane is located. With an upper limit of 4 m, the lowest frequency at which this next peak will appear on the mast is only achieved when the length of the reflected path is one wavelength longer than the direct path.

The situation regarding tests involving horizontal polarization is different since the phase of the ground reflection dictates a null appearing on the surface of the ground plane. To achieve a first peak on the mast for horizontal polarization therefore, the path difference between direct and reflected rays has only to be half a wavelength. Table 17 shows the lowest frequencies for different range lengths at which the difference in path lengths produces a peak on a mast offering a 1 m to 4 m height scan.

Table 17: The lowest frequency at which a peak appears against range length

Range length (m)	Lowest frequency at which a peak appears on the 4 m mast (Vertical polarization)	Lowest frequency at which a peak appears on the 4 m mast (Horizontal polarization)
3,0	127,1 MHz	63,6 MHz
5,0	162,8 MHz	81,4 MHz
10,0	271,5 MHz	135,8 MHz
30,0	757,5 MHz	378,8 MHz
NOTE: The frequencies given are, to an extent, dependant on the directivity of the antennas, but they are valid for the general case over a perfectly conducting ground plane. If the ground plane is not a perfect conductor these frequencies will differ.		

Taking the other extreme, when the source has high directivity (e.g. waveguide horn) and the angle of its first null (in the vertical plane) coincides with the angle of the reflected ray, the height of the maximum peak on the mast will be at the height of the source itself (usually 1,5 m) irrespective of polarization.

8.3.4.5 Test antenna cabling

There are radiating mechanisms by which RF cables can introduce uncertainties into radiated measurements:

- leakage;
- acting as a parasitic element to the test antenna;
- introducing common mode current to the balun of the test antenna.

Leakage allows electromagnetic coupling into the cables. Because the electromagnetic wave contains both electric and magnetic fields, mixed coupling can occur and the voltage induced is very dependant on the orientation, with respect to the cable, of the electric and magnetic fields. This coupling can have different effects depending on the length of the cable and where it is in the system. Cables are usually the longest part of the test equipment configuration and as such leakage can make them act as efficient receiving or transmitting antenna's, thereby contributing significantly to the uncertainty of a measurement.

The parasitic effect of the cable can potentially be the most significant of the three effects and can cause major changes to the antenna's radiation pattern, gain and input impedance. The common mode current problem has similar effects on the antenna's performance.

All three effects can be largely eliminated by routing and loading the cables with ferrite beads as detailed in the test methods given in parts 2 to 7 of the present document. A cable for which no precautions have been taken to prevent these effects can cause different results to be obtained simply by being repositioned.

u_{j19} is used throughout all parts of the present document for the uncertainty contribution associated with cable factor (the combined uncertainty which results from interaction between any antenna and its cable).

NOTE 1: In the direct attenuation stage of a verification procedure (a conducted measurement) all fields are enclosed and hence the contribution is assumed to be zero. However in the radiated attenuation stages the standard uncertainty for each cable is 0,5 dB provided the precautions detailed in the procedure have been observed. If the precautions have not been observed the contribution for each cable has a standard uncertainty of 4,0 dB.

NOTE 2: Exceptionally, where a cable and antenna combination has not been repositioned between the two stages of the test method (as in the case of the test antenna in an Anechoic Chamber during the substitution part of an emission test) and the precautions detailed in the procedure have been observed, the contribution is assumed to be zero. If the combination has not been repositioned but the precautions have not been observed the contribution is 0,5 dB.

NOTE 3: Repositioning means any change in the positions of either the cable or the antenna in stage two of the measurement relative to stage one. e.g. height optimization over a ground plane.

8.3.4.6 EUT supply and control cabling

EUT cable layout can contribute significantly to the uncertainty of the measurement. Large variations can occur when measuring spurious emissions for example, as a result of the positions of the supply and control cables.

These cables can act as parasitic elements and can receive radiated fields. The effects vary with cable type, the configuration and use, but they may strongly influence the outcome of a measurement. A number of schemes can be used to reduce these problems, amongst which is a total replacement by fibre optic cables, twisting wires together and loading them with ferrite beads.

u_{j55} is used throughout all parts of the present document for the uncertainty contribution which results from interaction between the EUT and the power leads.

8.3.4.7 Positioning of the EUT and antennas

The phase centre of an EUT or an antenna is the point within the EUT or antenna from which it radiates. If the EUT or antenna was rotated about this point, the phase of the received/transmitted signal would not change. For some test procedures, especially those which require an accurate knowledge of the measurement distance, it is vital to be able to identify the phase centre.

Where an EUT is being tested the uncertainty in the position of the phase centre of the source within the equipment volume can lead to signal level uncertainties since all calculations deriving emission levels will be based on the precise measurement distance.

u_{j20} is used throughout all parts of the present document for the uncertainty contribution associated with not knowing the exact position of the phase centre within the EUT volume in test methods.

NOTE 1: It is only applicable in the stage of the procedure in which the EUT is measured. If the precise phase centre is unknown it is assumed it can be anywhere inside the EUT and therefore the uncertainty is assumed to be rectangularly distributed.

The positioning, on the turntable, of the phase centre of the EUT's radiating source, can lead to uncertainties if it is offset from the tables axis of rotation. Any offset will cause the source to describe a circle about the axis as the EUT is rotated. Variations in path lengths (both direct and reflected) are thereby introduced leading directly to changes in the received/transmitted field strength.

u_{j21} is used throughout all parts of the present document for the uncertainty contribution associated with the positioning of the phase centre within the EUT over the axis of rotation of the turntable in test methods.

NOTE 2: It is only applicable in the stage of the procedure in which the EUT is measured. If the precise phase centre is unknown it is assumed it can be anywhere inside the EUT and therefore the uncertainty is assumed to be rectangularly distributed.

Dipoles and bicones have phase centres at their feed points, whilst that for a waveguide horn is in the centre of its open mouth. The phase centres do not change with frequency for these antennas.

u_{j22} is used throughout all parts of the present document for the uncertainty contribution associated with the position of the phase centre of the measuring, substitution, receiving, transmitting or test antenna.

NOTE 3: It is the uncertainty with which this phase centre of the antenna can be positioned.

Certain antennas, most notably the LPDA, possess a phase centre which is difficult to pin point at any particular frequency. Further, for this type of antenna the phase centre moves along the array with changing frequency resulting in a measurement distance uncertainty (e.g. an LPDA with a 0,3 m length contributes a standard uncertainty level due to range length uncertainty of u_j = 1,0 dB). To use such an antenna for site calibration, for example, could introduces large uncertainties.

u_{j23} is used throughout all parts of the present document for the uncertainty contribution associated with the position of the phase centre for LPDAs.

NOTE 4: It is the uncertainty associated with the changing position of the LPDA phase centre with frequency.

8.3.5 Effects of the stripline

Several different types of stripline test facilities are discussed in part 5 of the present document but of these, only one has been found to be in regular use in European test houses. This is the open two-plate stripline as detailed in EN 55020 [9]. The following review of uncertainties specific to stripline test facilities is, therefore, strictly limited to that particular two-plate design although most of the uncertainties will be present in other types.

8.3.5.1 Mutual coupling

The close proximity of the stripline's metal plates can produce de-tuning effects and imaging of the device placed within the line. These effects are generally termed mutual coupling effects. Imaging can be particularly serious since it can result in changes to the radiation pattern, gain and input impedance of the test device. Essentially these effects concern only an EUT and a three-axis probe (used to measure field strength within the line). The only other device inserted into the line during either the verification procedure or any of the test methods is a monopole. Since this deliberately uses the lower metal plate as a ground plane, the mutual coupling effects on this device are considered negligible.

The effects on the electrical characteristics of the EUT and antennas due to the degree of mutual coupling are estimated in annex A of TR 102 273-1-2 [12] and the uncertainty contributions which result are given representative symbols as follows:

u_{j24} is used throughout all parts of the present document for the uncertainty contribution associated with the mutual coupling of the EUT to its image in the plates of the stripline.

NOTE: The magnitude is dependent on the size of the EUT (assumed to be placed midway between plates). The standard uncertainty can be obtained from table 18.

Table 18: Uncertainty contribution: mutual coupling of the EUT to its images in the stripline plates

Size of the EUT relative to the plate separation	Standard uncertainty of the contribution
size/separation < 33 %	1,15 dB
33 % ≤ size/separation < 50 %	1,73 dB
50 % ≤ size/separation < 70 %	2,89 dB
70 % ≤ size/separation ≤ 87,5 % (max.)	5,77 dB

u_{j25} is used throughout all parts of the present document for the uncertainty contribution associated with the mutual coupling of the three-axis probe to its image in the plates of the stripline.

8.3.5.2 Characteristic impedance of the line

Virtually all test devices, whether an EUT, antenna, field probe, etc., are designed to operate in free-space i.e. their radiating structures are matched to the intrinsic impedance of 377 Ω. Therefore when used in environments which have different impedances e.g. stripline test facilities, the matching schemes employed within these devices will see a changed load impedance. This gives rise to uncertainties in radiated/detected levels. Symbolically:

u_{j26} is used throughout all parts of the present document for the uncertainty contribution associated with the characteristic impedance of the stripline.

NOTE: This uncertainty results from immersing the EUT in a medium whose characteristic impedance is not that of free Space.

8.3.5.3 Non-planar nature of the field distribution

Ideally, all EUTs should be tested in plane wave far-field conditions i.e. fields which are uniform in both phase and amplitude. Various effects disturb the required field distribution in a stripline, amongst which are non-TEM (also termed higher order) modes, reflections, room resonances, etc.

u_{j27} is used throughout all parts of the present document for the uncertainty contribution associated with the non-planar nature of the field distribution in the stripline resulting from all the disturbing sources.

8.3.5.4 Field strength measurement

A three-axis probe or a monopole can be optionally used in test methods to measure the field strength within the stripline during, for example, sensitivity measurements. Alternatively, the value of the stripline's transform factor (i.e. the relationship between power in dBm input into the stripline and the resulting field strength in dBμV/m derived in the verification procedure) can be used to calculate its value.

For the case of the three-axis probe, the field strength reading is subject to an uncertainty which is usually declared by the manufacturer.

u_{j28} is used throughout all parts of the present document for the uncertainty contribution associated with the field strength measurement as determined by the three-axis probe.

The stripline's transform factor is derived during the verification procedure, so for cases in which it is used to determine the field strength, the associated uncertainty contribution is the combined standard uncertainty, u_c, with which the verification was carried out.

u_{j29} is used throughout all parts of the present document for the uncertainty contribution associated with the derivation of the transform factor for the stripline during the verification procedure.

NOTE 1: It is the uncertainty with which the transfer factor (i.e. the relationship between the input voltage to the stripline and the resulting electric field strength between the plates) is determined.

For test methods in which the transform factor is used, the exact transform factor value can be used when the test frequency corresponds to a spot frequency in the verification procedure. However, in the majority of cases, the value will need to be interpolated from the spot frequency values.

u_{j30} is used throughout all parts of the present document for the uncertainty contribution associated with the interpolation of values for the transform factor of the stripline.

NOTE 2: It is the uncertainty associated with interpolating between two adjacent transfer factors for the stripline. Where the frequency of test corresponds to a set frequency in the verification procedure, this contribution to the combined uncertainty is 0,00 dB. For any other frequency, the value of the standard uncertainty is taken as 0,29 dB.

For the case of the monopole, the antenna factor of the monopole needs to be known in order to convert the received signal level into field strength. There is an uncertainty associated with the knowledge of the value of the antenna factor.

u_{j31} is used throughout all parts of the present document for the uncertainty contribution associated with the antenna factor of the monopole.

8.3.5.5 Correction factor for the size of EUT

The height of the EUT within the stripline is known to distort field strength levels. In EN 55020 [9], correction figures are given to allow for this effect. These figures are, however, subject to uncertainty.

u_{j32} is used throughout all parts of the present document for the uncertainty contribution associated with the correction factor for the size of the EUT in the stripline.

NOTE: It is the uncertainty due to the EUT being mounted in the stripline where the height of the EUT is significant in the E-plane compared to the plate separation. For EUT mounted centrally in the stripline, values can be obtained from table 19.

Table 19: Uncertainty contribution: stripline: correction factor for the size of the EUT

Height of the EUT (in the E-plane) is:	Standard uncertainty of the contribution
height < 0,2 m	0,30 dB
0,2 m ≤ height < 0,4 m	0,60 dB
0,4 m ≤ height ≤ 0,7 m	1,20 dB

8.3.5.6 Influence of site effects

A considerable amount of energy is radiated by the EN 55020 [9] stripline from its open sides. This not only represents a power loss from the facility but also serves as an interference source, by giving rise to possible outside reflections. As a consequence, external objects can influence the results of measurements.

u_{j33} is used throughout all parts of the present document for the uncertainty contribution associated with the influence of site effects on the stripline.

NOTE: For any method of field strength measurement, it is assumed that, provided none of the absorbing panels placed around the stripline or the stripline itself are moved either between the verification procedure and the test or between the measurement on the EUT and the field measurement parts of the test (for monopole or three-axis probe), the uncertainty remains the same throughout the test and hence cancels in the uncertainty calculation. Its value is therefore assumed to be 0,00 dB. If, however, the arrangement has been changed, the standard uncertainty is 3,00 dB.

9 Constructional aspects

This clause concerns all types of test sites i.e. free field test sites and striplines. It discusses the performance implications of key aspects of their construction starting with a major consideration of whether or not to shield against radiated local ambient signals. An individual review of each type of facility is then given, followed by a general section in which long term aspects, power supply details, auxiliary equipment, etc., are discussed.

Before constructing any type of test site the following points should be considered:

- type of site; Anechoic Chamber (with or without a ground plane) or an Open Area Test Site;
- will the site be used for "internal only customer" confidence testing;
- will the site be used for internal and external customer confidence testing;
- will the site be used for accredited measurements;
  - what range of specifications need to be covered;
  - what are the requirements of these specifications regarding the test site;
- will there be future expansion of the capability of the site (i.e. provision of a 400 Hz generator);
- where should the site be located.

9.1 Introduction

For any test site, a key aspect is to determine whether or not a shield against local ambient signals is required. The provision or otherwise of a shield can have a major impact on both the overall performance of the site as well as the cost. For example, high ambient signal levels may dictate against the construction of an Open Area Test Site which is usually considered to be the most cost effective type of facility.

Ambient RF interference can add considerable uncertainty to radiated measurements. Such RF ambient signals can be continuous sources e.g. commercial radio and television, link services, navigation etc. or intermittent ones e.g. CB, emergency services, DECT, GSM, paging systems, machinery and a variety of other sources, see figure 90.

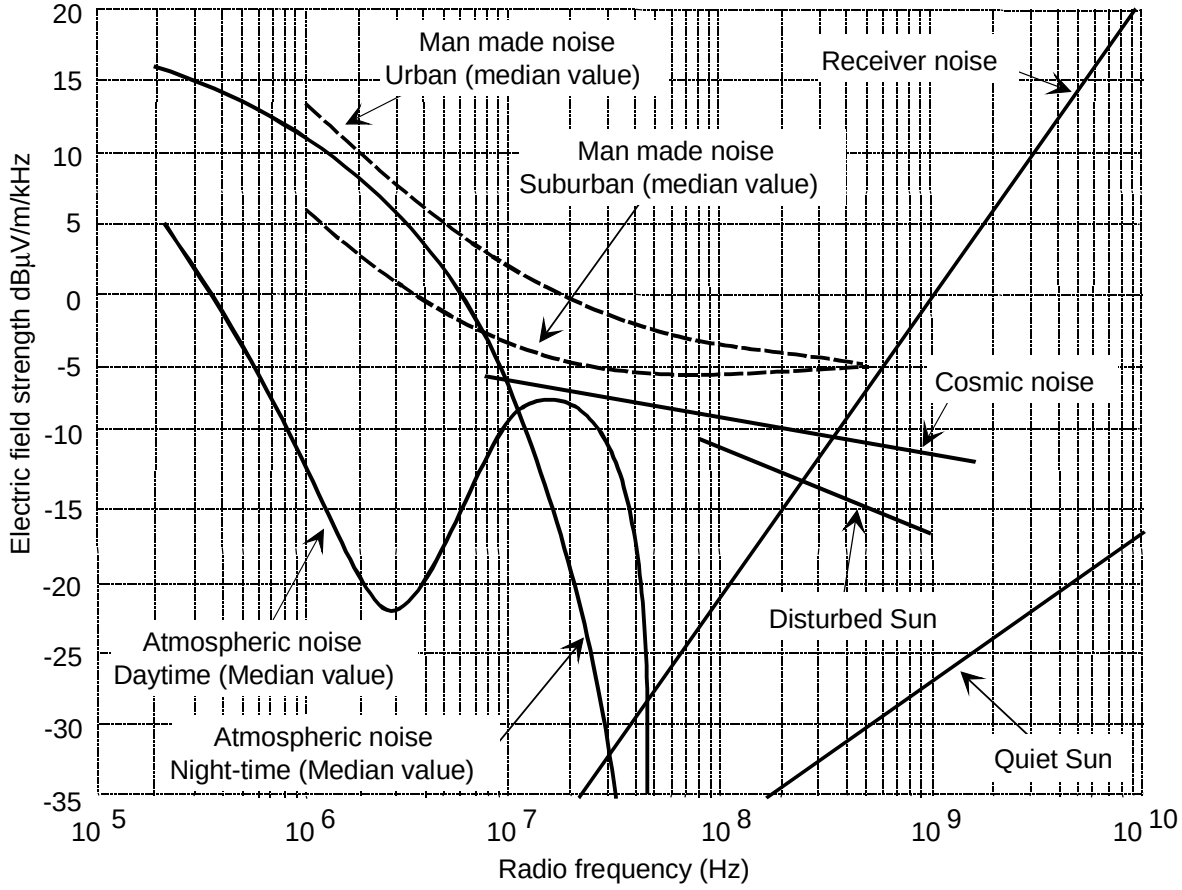

Figure 90: Electromagnetic noise sources and approximate levels

The interference can be either narrowband or broadband. Power and telephone lines can produce radiated noise, as can large machinery (e.g. lathes, etc.) in nearby premises. Nearby railway tracks (particularly electric) are other sources. All these noise sources add to the general background levels which can disturb measurements.

On a test site with high levels of these interference sources, it may be possible to choose a time slot for testing when the overall RF environment does meet the requirement as a result of the sources not being continuously active for 24 hours a day. Another solution could be to provide an electromagnetic shield, as in an Anechoic Chamber (with or without a ground plane).

A site survey can prove helpful in determining whether shielding is required. Details of how to carry out a site survey are given in clause 9.2.

9.2 Open Area Test Site

Where possible, for minimum interference, an Open Area Test Site should be located in an area having low levels of ambient signals and for minimum uncertainty, tests on an EUT should be carried out when the level of ambient signals do not exceed certain specified levels. For conformance testing, the ambient signals should be at least 6 dB below any limits specified in the relevant standard.

9.2.1 Site surveys and site location

The site survey is one of the most important aspects before the construction of an unshielded Open Area Test Site. There are three main objectives to a site survey:

- identify (visually) any obvious obstructions within the area which would prohibit its use;
- identify (by measurement) which of the available locations have the lowest ambient levels in both horizontal and vertical polarizations (site location); and
- identify (by measurement) the azimuth angle of the quietest measurement axis at each location.

9.2.1.1 Detection system sensitivity

A site survey determines the detection system sensitivity, i.e. the lowest level of signal that can be distinguished from the background noise (ambient signals). The detection system sensitivity can be affected by many factors such as:

- ambient levels;
- measurement bandwidth;
- type of detection;
- distance between receive antenna and source;
- "in line" amplification;
- sweep speed/settling time.

The setting these of parameters will play a major part in determining if a particular site may be suitable for measurements. For conformance assessment only three conditions need to be considered:

- If the detection system sensitivity is above the specification levels, no signals can be detected below this level. It is not possible therefore to determine if an EUT meets the specification requirement or not, see figure 91a. This site would not be suitable for accredited measurements against this specification level.
- If the detection system sensitivity is well below the specification levels then it is possible to determine if an EUT meets the specification requirement at any frequency in the band, see figure 91b. This site should be considered a suitable site for possible accreditation against this specification level.
- If the detection system sensitivity varies about the specification level across the frequency band it is only possible to determine if an EUT meets the specification requirement in those frequency bands where the detection system sensitivity is below the specification limit by an agreed amount. Other parts of the frequency spectrum cannot be verified, see figure 91c. This site would not be suitable for accredited measurements against this specification level.

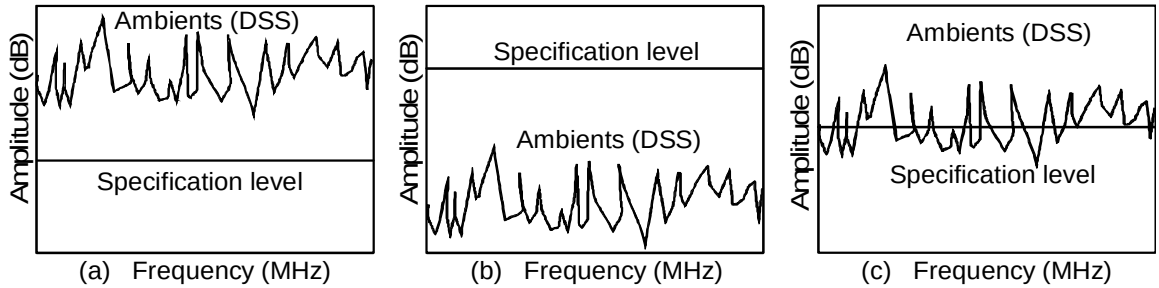

Figure 91: Ambient signals and specification limits

Performance testing, in contrast to conformance testing, provides a slightly different problem as there is no specified level. All that is required is the level of, for example, a spurious emission without reference to a specification limit. In this case spurious emissions are either measured or they are below the detection system sensitivity (there may be an emission there, you just cannot see it and the detection system sensitivity should be quoted).

These ambient signals contribute to test methods and verification procedures on unshielded free field test sites and in striplines. They contribute an uncertainty to all measurements by raising the noise floor at the measurement/substitution frequency. For their contribution to any measurement:

u_{j34} is used throughout all parts of the present document for the uncertainty contribution which results from local ambient signals raising the noise floor at the test frequency.

NOTE: Whenever ambient signals affect the measurements the standard uncertainty of the contribution is taken from table 20.

Table 20: Uncertainty contribution: ambient effect

Receiving device noise floor (with signal generator OFF) is within:	Standard uncertainty of the contribution
3 dB of measurement	1,57 dB
3 dB to 6 dB of measurement	0,80 dB
6 dB to 10 dB of measurement	0,30 dB
10 dB to 20 dB of measurement	0,10 dB
20 dB or more of the measurement	0,00 dB

9.2.1.2 Site survey procedure

A site survey may be carried out using, for example, a biconic and log periodic dipole antenna (LPDA) covering the frequency range 30 MHz to 200 MHz and 200 MHz to 1 000 MHz respectively, a spectrum analyser covering the same frequency range, a tripod placed on the earth and a coaxial cable as shown in figure 92. A typical site survey test procedure is detailed below:

NOTE: There is a high probability that the signals monitored by the antenna/spectrum analyser combination during the site survey satisfy far-field conditions.

1) With the biconic antenna horizontally polarized and at an arbitrary 0° of rotation, carry out a single scan from 30 MHz to 200 MHz using the spectrum analyser in the peak hold mode. Note any peaks. Save this trace in store B.

2) Rotate the test antenna by 30° and clear trace A.

3) Carry out a single scan from 30 MHz to 200 MHz and compare this trace with the one stored in B. Any differences should be obvious.

4) Note the "general" noise floor level.

5) Repeat steps 2, 3 and 4.

6) Repeat steps 2, 3, 4 and 5 until the procedure has been carried out at 330°.

7) With the biconic antenna vertically polarized, scan from 30 MHz to 200 MHz using the spectrum analyser in the peak hold mode. Note any peaks.

8) Repeat steps 2 to 6 for the LPDA horizontally polarized (frequency range 200 MHz to 1 000 MHz).

9) Repeat steps 2 to 6 for the LPDA vertically polarized (frequency range 200 MHz to 1 000 MHz).

The results of the site survey provide the engineer with a comprehensive overview of the electrical conditions of a particular area, and when repeated at other sites of interest, will enable comparisons between sites to be made.

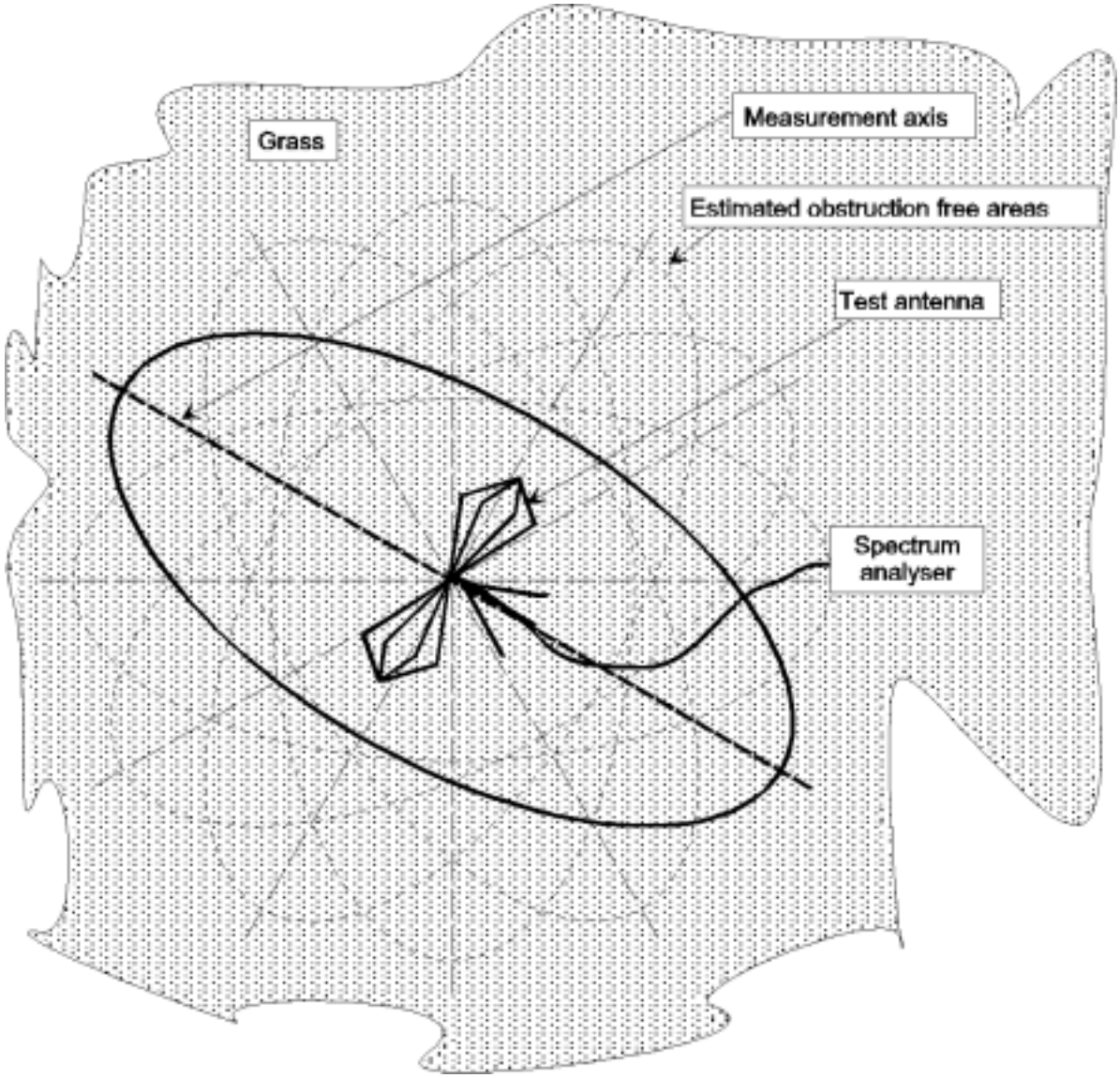

Figure 92: Measuring arrangement for a site survey

9.2.1.3 Example of a site survey

Figure 93 shows the positions of an imaginary site survey.

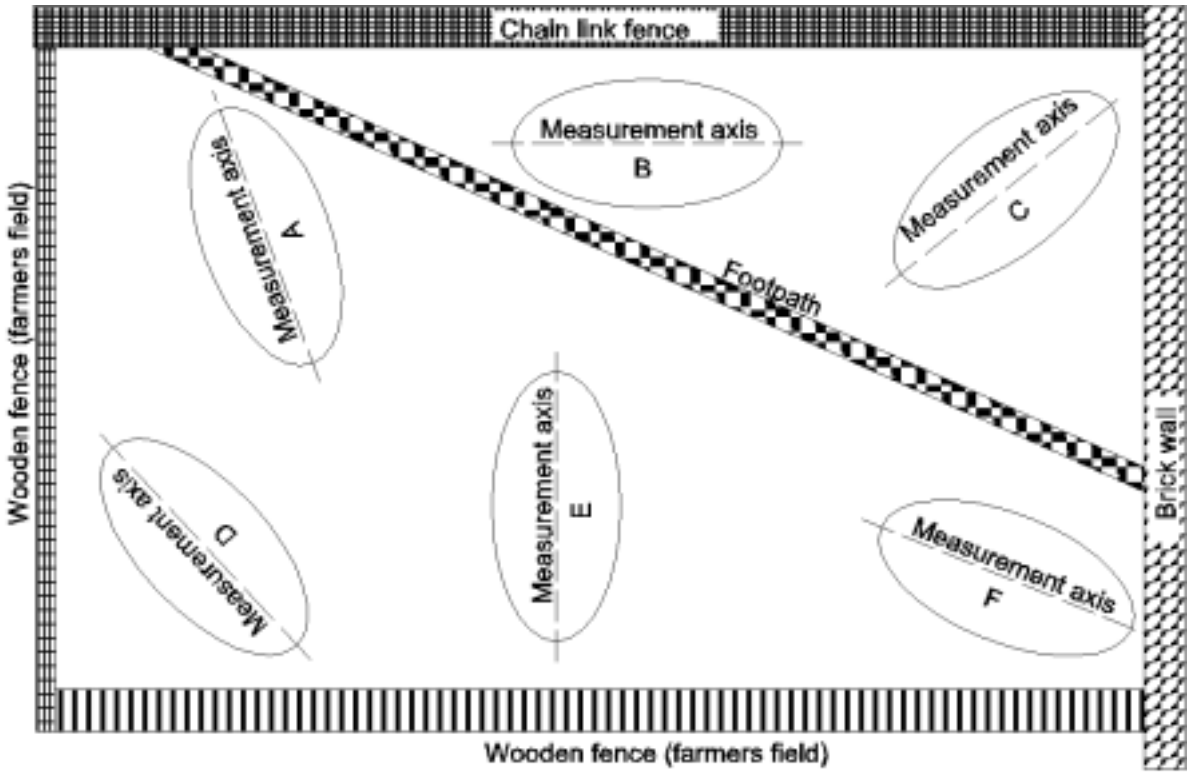

Figure 93: Site surveys

There are decisions that need to be made before the engineer can proceed with a site survey. For the testing parameters he needs to know:

- what range of measurement bandwidths will be used on the site;
- can one typical bandwidth be used or will several bandwidths be required;
- what constitutes an unacceptable ambient level;
- which ambient signals are continuous or intermittent;
- are there intermittent signals that are not "on line" when the survey is carried out (not receiving anything from an antenna mast for example);
- how the site survey information should be recorded and reported;
- if the site is to be used for accredited measurements, what requirements the specifications lay down regarding the test site (the specification may actually define a specific type of site);
- if there will be future expansion of the capability of the site (provision of a 400 Hz generator for example).

For the practicalities of carrying out the survey he needs to know:

- the site location;
- what test equipment is required (cables, connectors, antennas, antenna mounts, receiver, etc.);
- if the test equipment can be transported there safely;
- if there will be power for the equipment at the site, or will a generator be needed;
- if the test equipment will be available for the survey which may take several days.

When these have been resolved the engineer will be able to carry out the task.

A site survey is carried out in the area shown in figure 93. Sets of measurements have been made over the desired frequency range using the procedure detailed in clause 9.2.1.2, with a polarized directional antenna (a biconic for low frequencies and a log periodic for higher frequencies).

In this site survey ellipses A to F of figure 93 represent 6 different surveys. In practice the distance between sites may be any distance from a few metres to, for example, tens of kilometres.

NOTE: A few metres may not seem very advantageous, but in cases where the geographical site location may be fixed i.e. the test site needs to be built in a particular location, the selection is between which measurement axis gives the quietest ambient levels and is least affected by reflections from surrounding objects.

Suppose the results indicate measurement axis E is the quietest, axis B the noisiest, whilst A, B, D and F are somewhere in-between.

Verification procedures are then carried out over a temporary ground plane (e.g. wire mesh). Comparisons are made of the deviations from the ideal and it is found that measurement axis E is the worst, axis D is closest to the ideal, whilst A, B, C and F are somewhere in-between.

Further decisions have to be made (in the form of compromises) for the best test site location;

- is it too remote;
- is it too close to a new or planned development site (yet to be built) etc.;
- it may not have easy access to local amenities (drainage, telephones, power etc.);
- it may be that the ambient levels at all sites are too high to enable the Open Area Test Site to be constructed and other solutions (for example, Anechoic Chambers) may need to be found.

But assuming all the above requirements have been met, the sites can be listed in some sort of order of preference and in the above example, measurement site D would be chosen, although it is not the quietest it does have the best site attenuation figures and its operation will not be adversely affected by ambient signals.

9.2.2 Extraneous reflections

Whilst the ideal Open Area Test Site should be completely clear of any possible reflecting objects, this is not very realistic in practice and items such as trees, buildings, movements of people, etc. will always be in and around the area. Care should therefore be taken to ensure that the effects of such objects do not disturb the uniformity of the transmitted fields. Table 21 shows how much the received signal level can vary as a result of a single reflected signal.

Since the magnitude of the field scattered from an object depends on many factors such as the object's size, its distance from the EUT, conductivity, permeability, permitivity, frequency, etc., it is not possible to specify a minimum obstruction-free area that is appropriate for all applications. The size and shape of the obstruction-free area is also dependant on whether or not the EUT will be rotated.

In practice, the creation of a stipulated obstruction-free zone has the benefit of preventing any possible interference from people, cars, stored objects etc. This area should also be kept clear of accumulated litter and other objects capable of disturbing the generated fields. A past recommendation of the IEC was for a circular obstruction-free zone of diameter equal to eight times the range length on the basis that if all the energy were reflected back coherently from the boundary, the path loss involved would not allow the measurement uncertainty to exceed ± 1 dB. This size of clear area is only practical in a few cases.

An alternative scheme, proposed by ANSI, is to make the obstruction free area large enough so that the path length of a ray which hits a reflecting object on the boundary and is then received should be twice the direct path length. This ensures the magnitude of the reflection is attenuated by 6 dB compared to the direct ray.

Generally, actual obstructions only intercept a small portion of the energy and tend to scatter only a part of that back to the receiver. At low frequencies, therefore, small objects will have negligible effects. Above 1 GHz, and particularly towards the top end of the frequency band (12,75 GHz), even small objects can cause problems, however. Site verification procedures should be able to identify these and result in their removal.

Table 21: Uncertainty in received signal level due to a single unwanted interfering signal

Ratio of unwanted to wanted signal level	Received level uncertainty		Ratio of unwanted to wanted signal level	Received level uncertainty
-30,0 dB	+0,27 -0,28 dB		-9,0 dB	+2,64 -3,81 dB
-25,0 dB	+0,48 -0,50 dB		-8,0 dB	+2,91 -4,41 dB
-20,0 dB	+0,83 -0,92 dB		-7,0 dB	+3,21 -5,14 dB
-17,5 dB	+1,09 -1,24 dB		-6,0 dB	+3,53 -6,04 dB
-15,0 dB	+1,42 -1,70 dB		-5,0 dB	+3,88 -7,18 dB
-14,0 dB	+1,58 -1,93 dB		-4,0 dB	+4,25 -8,66 dB
-13,0 dB	+1,75 -2,20 dB		-3,0 dB	+4,65 -10,69 dB
-12,0 dB	+1,95 -2,51 dB		-2,0 dB	+5,08 -13,74 dB
-11,0 dB	+2,16 -2,88 dB		-1,0 dB	+5,53 -19,27 dB
-10,0 dB	+2,39 -3,30 dB		0,0 dB	+6,04 -∞ dB

In figure 93 obvious problem areas are the chain link fence, which on the one hand may help shield the site from ambient signals originating behind it, but on the other hand causes a major reflection uncertainty. The brick wall is slightly different in that it is unlikely to shield the site and its reflectivity will vary between a hot sunny day (when the wall is dry) and after a rain shower. The footpath is unlikely to cause problems, likewise the wooden fence (which is on two sides of the location), unless it has metal uprights supporting it. The farmer's field is flat open grassland.

The effects of trees have been looked at, [8], and the results indicate that vertical polarization is affected more than horizontal. The tests were limited to a band of 30 MHz to 200 MHz and indicate that for trees 10 m away from the receiver, virtually no effects are observable. Site verification procedures should again prove helpful in determining tree effects at other frequencies, particularly those above 1 GHz.

A shielded room can be used for housing the test equipment and recording the test results and, from the point of view of cable loss and convenience, it is advisable to have this facility close to the test site. To prevent this room being a reflection source, it should be under the ground plane. If the site cannot be constructed in this fashion, the metallised room will cause reflection uncertainties to be present during measurements. Alternatively a wooden or plastic hut could be used to reduce the reflection problems but it may allow radiated fields to permeate the test gear. Equally radiated signals generated by the test equipment could produce additional ambient signals. Either way, an increase in measurement uncertainties is likely to result.

The presence of overhead power and telephone lines can cause reflections, particularly for horizontal polarization. Where these lines are services to the site they should be buried under the ground plane. External lines (national grids and national telephone lines) however, cannot be dealt with in this fashion. Railway lines are a slightly different problem in that, whilst the lines themselves are probably only minor sources of reflection, the passage of the trains and carriages can significantly disturb the test fields if they pass close to the test site. The effects of car and lorry traffic on roads running nearby test sites will be similar. Aircraft, particularly low flying military ones, can produce a momentary reflection, but in general, the path lengths involved will attenuate the magnitude to a very low level. The main problem with aircraft is the emissions from the "on board" avionics systems.

The Open Area Test Site may have to have a weather protective enclosure if it is to be used throughout the year in areas which experience unsettled weather. The protective enclosure may be constructed over part, or all of, the site. The RF transparency of the materials being considered for permanent structures should be evaluated and the use of metal (for fixtures and fittings) above the ground plane should be avoided. In general, should metal objects be necessary, they should have dimensions of less than a tenth of a wavelength at the highest frequency of operation. The structure should additionally be shaped to allow for the easy removal of snow, ice or water. Such test sites employing "reflection-free" skins need routine cleaning of the outer skin to prevent a build up of dirt, dust, etc., which could, if allowed to accumulate, become a reflection source.

9.3 Anechoic Chamber (with and without a Ground Plane)

Site surveys are not usually carried out for the Anechoic Chamber (with or without a Ground Plane), as it is normally a measurement of the ambient signal levels at a proposed unprotected (or open) test site. The effects of the metal walls should provide adequate shielding, unless it is built close to a power transmitter or other radiating structure.

9.3.1 Basic shielded enclosure parameters

An Anechoic Chamber (with or without a Ground Plane) is usually based on a shielded enclosure, see figure 94.

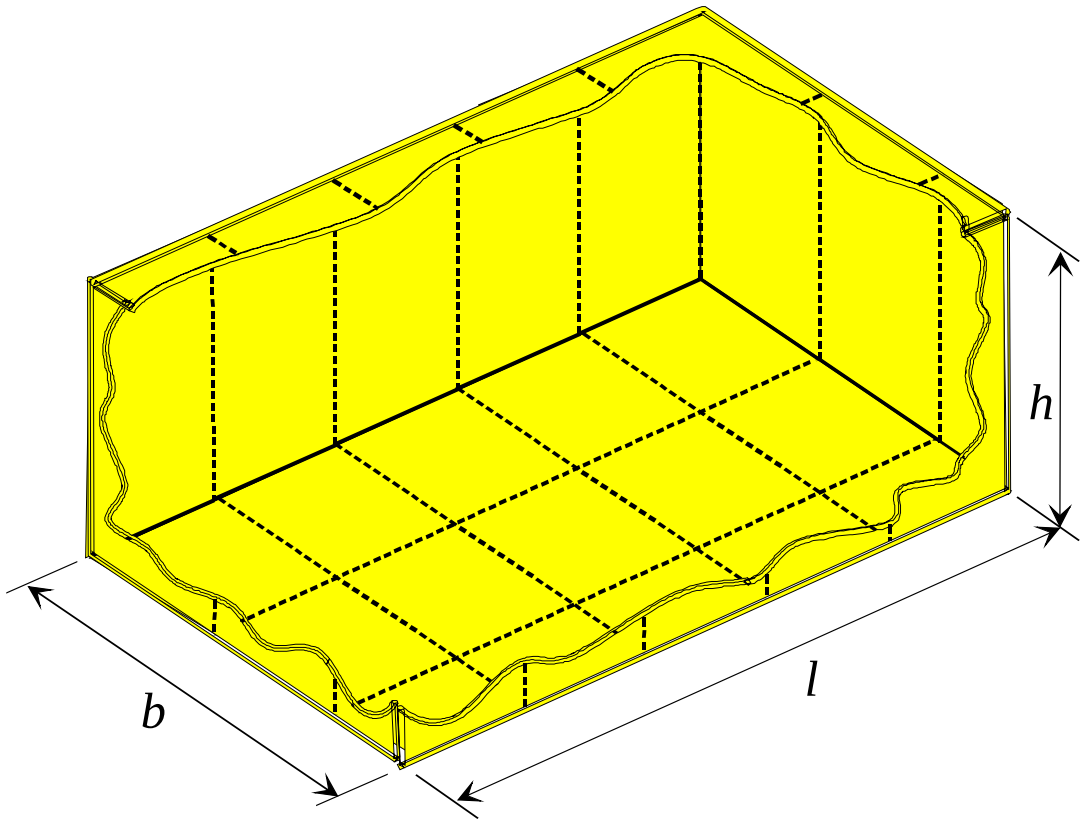

Figure 94: Basic shielded enclosure

A shielded enclosure is defined as any structure that protects its interior from the effect of an exterior electric or magnetic field, or conversely, protects the surrounding environment from the effect of an interior electric or magnetic field. A high performance shielded enclosure is generally capable of reducing the effects of both electric and magnetic field strengths by between 80 dB to 140 dB depending upon the frequency. Such an enclosure is normally constructed of metal with provisions for continuous electrical contact between adjoining panels, including doors. There are several basic chamber parameters that can affect the performance of an Anechoic Chamber (with or without a Ground Plane), amongst these are basic shielded enclosure resonances, waveguide type propagation modes and earthing arrangements.

9.3.2 Basic shielded enclosure resonances

The approximate frequencies of the basic shielded enclosure resonances can be calculated (in MHz) by using the following formula: see [18].

$$f = 150\sqrt{\left(\frac{x}{l}\right)^2 + \left(\frac{y}{b}\right)^2 + \left(\frac{z}{h}\right)^2} \text{ MHz}$$

Where l, b and h are the length, breadth, and height (in m) respectively (see figure 94) and x, y and z are mode numbers of which only one may be zero. The lowest frequency at which a resonance can occur will be given by inserting the two largest dimensions only into this formula and equating their mode numbers to 1. For example, in a shielded enclosure of dimensions 10 m by 5 m by 5 m, the lowest resonant frequency will be:

$$f = 150\sqrt{\left(\frac{1}{5}\right)^2 + \left(\frac{1}{10}\right)^2} = 33{,}54 \text{ MHz}$$

These resonances will only exist, however, if the mechanisms exist for their generation.

9.3.3 Waveguide type propagation modes

The propagation of transverse electric and transverse magnetic modes are also possible within the shielded enclosure. These modes can only be supported when the cross sectional dimensions of the shielded enclosure exceed half a wavelength. As the shielded enclosure is rectangular in cross section with side lengths of either *l* and *b*, *h* and *l* or *b* and *h*, the lowest frequency at which these modes can propagate is given by [2]:

$$f = \frac{c}{2\sqrt{m_r e_r}} \sqrt{\left(\frac{m}{a}\right)^2 + \left(\frac{n}{b}\right)^2}$$

which simplifies to:

$$f = 150 \sqrt{\left(\frac{m}{a}\right)^2 + \left(\frac{n}{b}\right)^2} \text{ MHz}$$

where *m* and *n* are the mode numbers and *a* and *b* can take mutually exclusive values of *l*, *b* and *h*.

For the transverse magnetic modes the lowest frequency possible requires both mode numbers to be equal to 1, but for the transverse electric case, the lowest mode only requires one to be equal to 1 with the other zero. This latter case gives, for the largest dimension in a 10 m by 5 m by 5 m enclosure:

$$f = 150 \sqrt{\left(\frac{1}{10}\right)^2} = 15{,}0 \text{ MHz}$$

These modes can theoretically exist in any plane within the shielded enclosure that has a rectangular cross section. They will only be generated, however, if the mechanisms exist for their excitation.

9.3.4 Earthing arrangements

The shielding effectiveness is critically dependant on the earthing arrangements of the chamber. A typical good earth consists of a number of square metal plates (i.e. galvanized steel) arranged vertically in a row at about 1 m to 3 m depth and all connected via a bond strap. The bond straps are made of good conductivity copper bars, braids or thick flexible cables. A good earth should be located sufficiently close to where it is needed, in soil with adequate depth and constant water content to maintain its quality. A bad earth is generally one where there is insufficient depth of top soil possibly due to dry sand, or rock just below the surface. Soil consisting largely of chalk or clay can dry out in hot weather conditions and change the earthing characteristics accordingly.

Bonding strap dimensions are critical for avoidance of electromagnetic interference effects. They should not be longer than $\lambda/5$ (where λ is the wavelength of the highest frequency) otherwise they may become radiators. The width of the bonding strap should be a minimum of $\lambda/5$ to $\lambda/10$. The thickness of the strap will depend upon the safety ground current requirements (normally several tens of Amps).

9.3.5 Skin depth

At high frequencies for a bonding strap or coaxial cable, currents due to external fields are restricted to the outside surface of the conductor. This is a result of skin depth.

For copper the skin depth is 6,6 mm at a frequency of 100 Hz, falling to 66 μm at 1 MHz, the changeover from a uniform current distribution to the skin effect distribution occurs in the audio frequency range.

As the frequency increases the current moves away from the centre of the strap (or cable) towards the outer edges. In doing so it effectively makes the cross sectional area of the conductor smaller, thus increasing its impedance. This is because, at high frequencies, electromagnetic forces tend to restrict the flow of current in a conductor to the surface layer. The current density falls off exponentially with distance from the surface and the skin depth δ (the distance over which the current density falls to *1/e* (or $\frac{1}{2{,}178}$, of its initial value) is given by the following expression which is for materials with high conductivities [3]:

$$Skin\ depth = \delta = \frac{1}{\sqrt{f\mu\pi\sigma}}\ \text{m}$$

where:

f = frequency (Hz);

μ = permeability (H/m);

σ = the conductivity (Siemens/m).

Conductivities of various materials are given in table 22.

Within a distance of 4,6 δ the current density falls to 1 % of its initial value, and so for most practical purposes the current is confined within a few skin depths of the surface.

For frequencies at 1 MHz and above, the skin effect is well established. Due to the skin effect, the energy losses in the conductor occur approximately within the cross sectional area formed by the surface perimeter and one skin depth.

Under these conditions an equivalent surface resistance for the conductor R_S is defined as:

$$R_S = 1/\ \delta\sigma\ \Omega/m^2$$

where R_S is the equivalent resistance per unit length of surface for unit width. Therefore at high frequency the resistance for a conductor is not controlled by its whole cross sectional area, but by an area equal to the total length of the perimeter times a few skin depths. Consequently, whereas for low frequencies minimum resistance is provided by a conductor of circular cross section, at high frequencies it is provided by a thin strip conductor. Figure 95 illustrates skin effect. As can be seen straps provide a proportionately larger cross sectional area than cables, this reduces the effect and the straps can be used at higher frequencies.

The skin effect also alters the inductance of a conductor. At dc the current is distributed uniformly throughout the cross section. The conductor contains a magnetic field and the internal inductance is independent of the radius of the conductor. For non-magnetic wire (i.e. $\mu_r = 1$) the magnitude is:

$$\frac{4\pi\times10^{-7}}{8\pi} = 0{,}5\times10^{-7}\ \ H/m\ or\ 50\ nH/m$$

Table 22: Conductivities of various materials

Material	Conductivity Siemens/m at 20 °C		Material	Conductivity Siemens/m at 20 °C
Aluminium, (soft)	$3{,}65 \times 10^7$		Lead	$4{,}58 \times 10^6$
Aluminium, (Tempered)	$2{,}32 \times 10^7$		Magnesium	$2{,}54 \times 10^7$
Aluminium, (Household foil)	$3{,}07 \times 10^7$		Molybdenum	$2{,}00 \times 10^7$ (0 °C)
Aluminium, (Flame sprayed)	$2{,}09 \times 10^6$		Monel (67 % Ni, 30 % Cu, 2 % Fe, 1 % Mn)	$2{,}38 \times 10^6$
Aluminium, (commercial hard-drawn)	$3{,}54 \times 10^7$		Nickel	$1{,}28 \times 10^7$
Beryllium	$3{,}57 \times 10^7$ (0 °C)		Palladium	$1{,}02 \times 10^7$ (0 °C)
Brass (91 % Cu, 9 % Zn)	$2{,}73 \times 10^7$		Platinum	$9{,}86 \times 10^6$
Brass (66 % Cu, 34 % Zn)	$2{,}03 \times 10^7$		Rhodium	$2{,}33 \times 10^7$ (0 °C)
Brass, yellow	$1{,}56 \times 10^7$		Steel (Carbon)	$4{,}31 \times 10^6$ (0 °C)
Bronze	$7{,}35 \times 10^6$ (0 °C)		Steel (Ni-Cr)	$2{,}97 \times 10^6$ (0 °C)
Cadmium	$1{,}35 \times 10^7$		Steel (Silicon)	$2{,}13 \times 10^6$ (0 °C)
Chromium	$7{,}87 \times 10^6$ (0 °C)		Steel (Stainless)	$1{,}58 \times 10^6$ (0 °C)
Cobalt	$1{,}79 \times 10^7$ (0 °C)		Steel (Others)	1,0 to 10×10^6
Copper, annealed	$5{,}80 \times 10^7$		Silver, 99,98 %	$6{,}14 \times 10^7$
Copper, beryllium	$1{,}72 \times 10^7$		Tin	$8{,}69 \times 10^6$
Gold, pure drawn	$4{,}10 \times 10^7$		Titanium	$2{,}56 \times 10^6$ (0 °C)
Graphite	3,33 to $16{,}7 \times 10^5$ (0 °C)		Tungsten, cold worked	$1{,}81 \times 10^7$
Iron, 99,98 %	$1{,}0\ 0 \times 10^7$		Zinc	$1{,}74 \times 10^7$
Iron, grey cast	0,05 to $0{,}20 \times 10^7$			

On the other hand, at high frequencies the current is restricted to the surface of the conductor and the internal magnetic field has zero magnitude. Under these conditions the internal inductance for the conductor tends towards zero.

NOTE: This can be likened to the case of the magnet over a super conductor. As the temperature is decreased and the material becomes super-conducting the magnet levitates above the surface. Under these conditions the skin depth is zero, the conductivity infinite, and as the magnetic field cannot penetrate the surface the magnetic force supports the weight of the magnet. Under these conditions the material has no inductance as no current penetrates the surface.

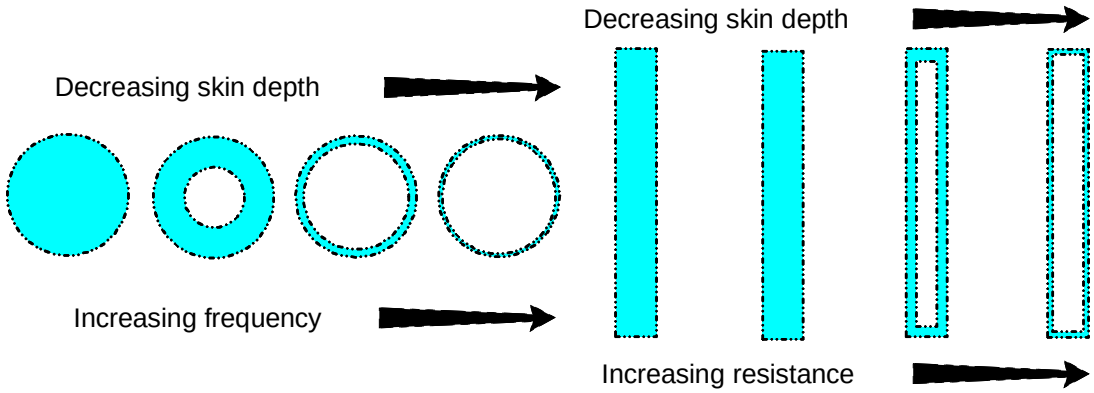

Figure 95: Skin effect in cables and straps

For earth bonding, the objective of the bond strap is to provide a low inductance path to ground. Bond straps are always connected onto other metals with the use of bolts, nuts and washers drilled through both the strap and metal. The order of use of bond straps is (with increasing inductance):

- copper or aluminium strap;
- silver or plated copper braid (100 A or 50 A rating);
- multi-strand copper wires (2,5 mm^2 cross section or greater);
- single strand copper wire (2,5 mm^2 cross section or greater).

Flat braided bond straps are particularly useful as they provide a considerable amount of flexibility. However, when used in the presence of high RF power they are prone to suffer from inter-strand arcing. This may be overcome by flood soldering the braid, but this can cause a potential corrosion problem. Flood soldered braided straps should therefore also have anti-corrosive treatment applied and a regular servicing policy.

Bond straps are only useful when their inductance is low. Bond straps thinner than 1,6 mm are not good enough for most applications.

9.3.6 Shielding effectiveness

The effectiveness of the shield is easier to measure than it is to calculate analytically. Effectiveness depends on many factors such as:

- the distance of the source from the shield and the receiver;
- the frequency of the radiation;
- the material used;
- the type of field;
- the nature of any discontinuities in the shield.

Shielding can be specified in terms of the reduction in magnetic and/or electric field strength caused by the shield. It is convenient to express this shielding effectiveness in units of decibels (dB). Use of dB permits the shielding produced by various effects to be added to obtain the total shielding.

In the design of a shielded enclosure, there are two primary considerations:

- the shielding effectiveness of the shield material itself, and;
- the shielding effectiveness due to discontinuities and holes in the shield.

The shielding effectiveness of the shield material can be limited by the distance of the source from the shield. If the source is close to the shield its wave impedance is of primary concern. The importance of wave impedance is best illustrated when the wave comes into contact with a metal object e.g. a screened room wall. When an electromagnetic wave encounters a discontinuity in the medium through which it is travelling, a proportion of the energy within the wave will be reflected. This proportion is determined by the difference between the characteristic impedances of the wave and the discontinuity. When a wave travelling through free Space encounters a metal, the magnitude of the reflection from the metal surface will be very high due to the very low characteristic impedance of the metal.

Some of the energy however will enter the metal, induce currents and generate heat (ohmic loss) which causes the wave to be further attenuated. The currents pass through the metal and re-radiate on the other side. The degree to which this occurs is obviously a measure of the shielding effectiveness of the metal. In general this is an extremely efficient method of providing good shielding from external ambient signals, especially electric fields.

In the near-field there is a fundamental difference between the screening effectiveness of metals. For an electric source, the electric field dominates and the wave is of high impedance as shown in figure 96. Therefore it is reflected more efficiently by the metal. Conversely for a magnetic source where the magnetic field dominates, the wave is of low impedance and is therefore reflected less efficiently. More of the energy couples into the metal and because of this improved coupling, it is more difficult to screen against magnetic than electric waves.

A gap or slot in any shield will allow electromagnetic fields to radiate through the shield unless the current-carrying capability can be preserved. That is the responsibility and function of an electromagnetic interference gasket. If the gasket can be manufactured from the identical material of the shield, then the current distribution within that gasket will be the same as for the shield. If the gasket material is lower in conductivity than the prime shielding material, then the current decay within the gasket will be less, enabling more current to flow on the opposite side of the shield. This in turn produces a leakage field around the area of the gasket. This "leakage" needs to be kept to an absolute minimum. A second source of leakage can occur at the interface between the gasket and the shield if an air-gap exists or the mating surface of the shield has been painted or anodized, thereby reducing the current flow through the shield/gasket interface. This also changes the current distribution within the shield and the gasket. These all help to render the gasket ineffective.

For shielded enclosures which have cable ports and penetration panels these should be adequately bonded to earth, have the right impedance and sufficient filtering such that only those signals that are required are allowed to pass through the shield.

It is of little value to make a well designed shield and then allow electromagnetic energy to enter (or exit) the enclosure by an alternative path such as cable penetrations. Cables can pick up noise on one side of the shield and conduct it to the other side where it will be re-radiated.

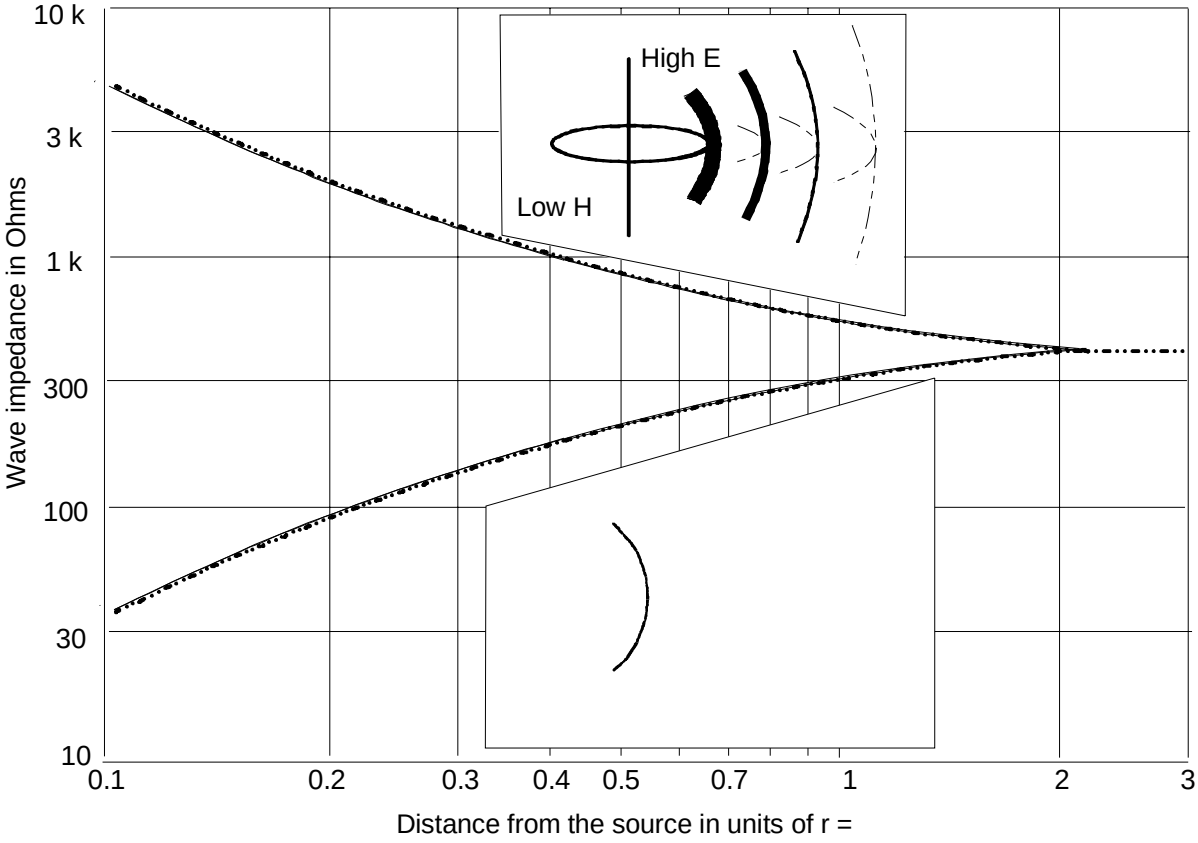

Figure 96: Wave impedance as a function of distance from the source

The following points should be taken into account when considering shielded enclosures:

- adequate attention should be given to holes and joints (a high-resistance joint can effectively destroy shield capabilities);
- cable shield requirements should be considered in view of other electromagnetic interference control methods, particularly RF interference filters;
- cable shields work best when applied to the attenuation of electric fields or the electric components of an electromagnetic field;
- discount reflection losses at frequencies where the shield is electrically thin (i.e. less than one skin depth);

- it is better to design for adequate attenuation of magnetic fields (usually low impedance sources), because shields are less effective than with respect to electric fields (usually high impedance sources). Exceptions can be made at very high frequencies and in cases where the noise source is known to be of high impedance;

- twisting the power or signal line with its own return usually provides adequate protection against all but the very highest amplitude magnetic fields.

For shielded enclosures which employ a rack or metal frame approach, care should be taken to provide good "bonding" between panels and frame members. Good bonds are ones that make direct metal to metal contact under pressure from a fastener. These fasteners needs to be conductive (not greasy or oily), bolts, washers and nuts. Once a good metal to metal contact bond has been made, it may then be coated to protect it from attack. The best bonds are made by welding, brazing, sweating and soldering (in that order).

Other fasteners, such as captive nuts, spring clasps or self tapping screws are not recommended. Many fasteners now consist of plastic components, or anodized metal surfaces these should be identified and discarded.

9.4 striplines

An open stripline (e.g. that specified in EN 55020 [9]) is susceptible to local ambient radiated signals in the same way as an Open Area Test Site. Consideration should therefore be given to provision of a shielded room in which to use the facility. Room resonances and waveguide type transmission modes could however be set up as described in clauses 9.3.2 and 9.3.3.

Whether shielded or not the room housing the stripline should be large enough to comply with any instructions regarding layout and minimum spacing away from walls, floor and ceiling. For example, EN 55020 [9] specifies that the lower plate be at least 0,8 m above the floor and the upper one at least 0,8 m from the ceiling.

Constructionally, both open and closed striplines have tapered sections at either one or both ends, although it is more usual for open striplines to taper at both ends. With tapers at both ends, one will be loaded with a terminating resistor whereas, if only one end is tapered, the non-tapered end is usually terminated with an evenly distributed resistive load and RF absorbing material(s). The terminating resistor/absorber reduces the magnitudes of internal standing waves and resonances and absorbs unwanted propagation modes.

9.4.1 Open 2-plate stripline test cell

A specific example of the open 2-plate stripline is that described in EN 55020 [9]. As shown in the outline drawing (see figure 97), the EN 55020 [9] stripline measures 2,76 m in overall length with a height of 0,8 m, a lower plate width of 0,9 m and an upper plate width of 0,6 m.

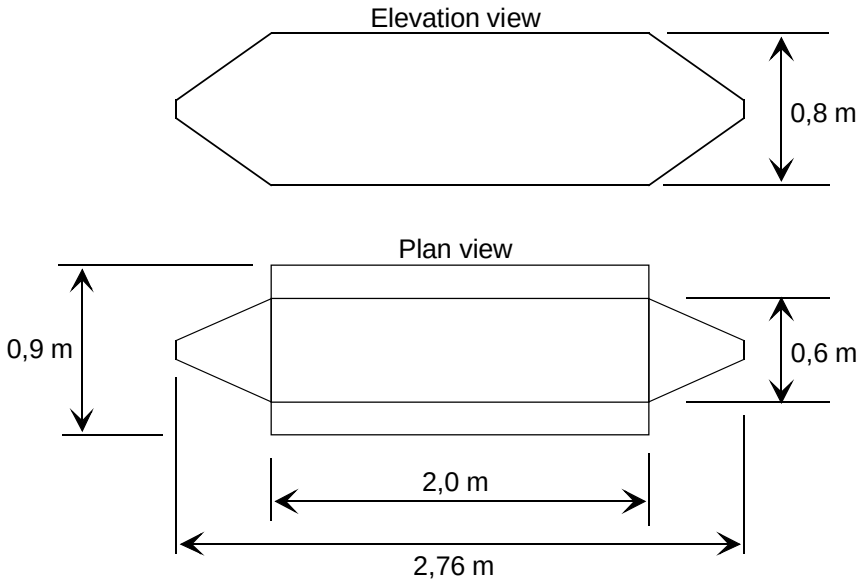

Figure 97: Outside dimensions of EN 55020 stripline

For this EN 55020 [9] stripline cell, the characteristic impedance is 150 Ω and this high impedance therefore needs careful matching to the 50 Ω lines which make up the associated items of test equipment. This is achieved by use of a resistive matching network. The operating frequency band for this cell is up to 150 MHz.

striplines are subject to numerous uncertainties (uniformity of field strength, room resonances, etc.,) plus limited bandwidth/EUT size in addition to providing a test environment that lacks correspondence with either real-life or other test sites, striplines are not, in general, a recommended means of making radiated measurements on radio equipment.

9.5 Miscellaneous

9.5.1 Long term stability

There are a variety of ways in which a test site, when built can degrade with age and whilst a number of the ageing mechanisms will be present at all sites, the actual effect on performance will differ from site to site. Abrupt changes in the performance of a test site are easier to detect than slow, evolutionary changes, which result from ageing of components, corrosion, etc.

For long term reliability and performance, it is essential to assess the different metals that will be used in the construction in terms of their suitability of mating together. Certain dissimilar metals, under action of an electrolyte such as salt water or spray, give rise to corrosion. To assess if metals may be bonded with minimum galvanic action being set up (i.e. a dc potential difference), table 23 should be referred to.

Galvanic action can occur when two dissimilar metals come into contact with one another. The process is caused by potential differences between the metals. Gold and silver are cathodic and will not easily corrode when placed in contact with other metals, whereas zinc and magnesium are anodic and will corrode when placed in contact with other metals.

If dissimilar metals need to be in close contact with one another, the best solution is to join dissimilar metals that are as close to each other in the galvanic series as possible (see table 23). Contact between small anodes and large cathodes should be avoided, as should contact between any dissimilar metals in a corrosive environment. Another possibility is to use an intermediate layer of a third metal that is neutral or as near neutral as possible to the two metals being separated.

Weathering, on an unprotected site can be a problem, particularly in regions of frequent precipitation. In general, site personnel do not necessarily protect all items of test equipment every time rain, hail, sleet or snow falls. Antennas, cables, connectors, etc., may then suffer from the effects of penetration of moisture, which can result in the contacts being coated with particles carried by the water, making them intermittent until they are cleaned. Without adequate cleaning (and general maintenance), over a period of time the deposited particles will cause increased signal losses and degradation of the VSWR at all connection interfaces that have been affected.

PolyVinyl Chloride (PVC) covered braided cables can deteriorate with time by experiencing cracking of the plastic coating after prolonged exposure to sunlight. This will permit the ingress of moisture and the consequent degradation of the shielding properties. Moisture can also, by capillary action, be drawn into the connection interfaces at the cable ends.

Frequently used flexible cables can slowly degrade as a result of continual flexing and connecting. Flexing can result in degradation of the contact between the connector body and the shield, whilst continual connecting and disconnecting can result in the spreading out of the centre pin receptor of the female connector. Continual use can also result in metal shavings being embedded on the mating dielectric faces of both connectors. These and other effects will degrade the performance of the cable and connector over the course of time.

Semi-rigid cables suffer similar degradation in performance and can be seriously impaired by minor bending - the resulting pull on the centre conductor being sufficient, in some cases, to break its solder joint to the connector centre pin. Excessive bending the cable can also fracture the outer sheath making a complete replacement necessary.

Ambient temperature is important for "seasonal" sites where perhaps on a clear winter's day it might fall below 0°C, whereas, on a summer's day, it might climb above 40°C and under direct sunlight the EUT might even rise to 60 or 70 °C. Differential expansion due to these temperature swings can, over time, cause fracturing of joints. Where metal is used in sheet form (ground planes, etc.), this can be a major problem. Additionally, expansion and contraction can result in buckling.

Table 23: Galvanic series of metals

Most Cathodic (Protected)				Most Anodic (Corroded)	
Gold	Cobalt	Beryllium	Aluminium Alloys (some)	Aluminium	Magnesium
Gold/Platinum Alloys	Cobalt Alloys	Brass	Brass Leaded	Aluminium Alloys (All)	Tin
Graphite	Graphite	Brass Leaded	Bronze	Beryllium	
Palladium	Monel	Bronze	Carbon Steel	Cadmium	
Platinum	Nickel	Chromium Plate	Chromium Plate	Chromium Plate	
Rhodium	Nickel Copper Alloys	Cobalt	Lead	Lead	
Silver	Palladium	Cobalt Alloys	Molybdenum	Molybdenum	
Silver Alloys	Rhodium	Copper	Steels (Some)	Steel	
Titanium	Silver	Copper Alloys	Tin-Indium	Tin-Indium	
	Silver Alloys	Monel	Tin Lead Solder	Tin Lead Solder	
	Steel (some)	Molybdenum	Tungsten	Tungsten	
	Titanium	Nickel		Zinc (Galvanized)	
		Nickel Alloys		Zinc Base Castings	
		Silver Solder			
		Stainless Steel			
		Titanium			
		Tungsten			

Oxidation of the metals used should also be considered, coating any bonds with a water repellent after mating may be imperative for sub-terrainen use. Ground planes constructed from metal mesh (e.g. chicken wire) should be coated, otherwise broken cells might result within the mesh due to corrosion. This will degrade the reflectivity at higher frequencies.

Where a ground plane comprises a combination of metal sheets and metal mesh, there is a possibility that joints between dissimilar metals will corrode.

Further long term problems for outdoor ground planes in general are the accumulation of surface layers of dielectric materials (which can change the phase of the reflected energy and the reflection coefficient of the ground plane), e.g. dust, dirt, etc. Metal mesh ground planes laid on grass or bare soil can suffer from the underground burrowing activity of life forms such as moles which can distort the flatness of the surface. Also, the grass has to be cut frequently to ensure minimal day to day variations. Trees, however, are more of a long term problem in that, if they are allowed to grow unchecked, the increasing reflections can slowly change the distribution of incident fields.

Oxidation is obviously a greater problem on exposed outdoor sites than on those protected from the weather. Ageing can, however, also be a problem for shielded anechoic facilities (with and without a ground plane), where the integrity of the shields around, for example, access doors and cable inlets can degrade simply as a result of use or vibration. Similarly, the jointing between the flat metal panels comprising the shield can deteriorate particularly on edges and corners, whilst the efficiency of the earth connection (vital to the integrity of the shield) might slowly degrade through corrosion around the joints between the earthing plates and bond straps.

A problem associated with Anechoic Chambers is the accumulation of miscellaneous objects in the dark corners of pyramidal absorbing materials. These objects tend to be nuts and bolts (used for mounting the various test items and antennas) which are inadvertently dropped from the mounting platforms and lodge in places which are not easily accessible. Over a period of time, there is a potential for the combined effect of these objects to result in performance degradation.

Personnel using the sites can also be responsible for a gradual reduction in the site performance. Obvious examples for anechoic facilities (with and without a ground plane) are the accidental breaking of the tips of pyramidal absorber panels and the compression with time of the absorbing panels which can be walked on. General complacency with a site known to provide accurate results and over-familiarity with a particular test procedure can also be problematic since less concentration is applied by the operator and it is at these times that procedural errors can occur.

In general, a lot of site ageing problems can be reduced or eliminated by a regular, systematic approach to preventative maintenance, for example, the cleaning of ground planes and connector interfaces, inspection of metal to metal junctions, testing of cables, the cutting back of vegetative growth, removal of clutter from within the Anechoic Chamber (with and without a ground plane) etc.

Whilst corrosion is difficult to prevent in the long term, sudden changes in performance are relatively easy to detect and correct. A systematic approach, aided by a programme of regular site inspection and verification is required to reveal the more subtle evolutionary changes.

9.5.2 Power supplies

Electrically clean supplies are very important. Signals conducted on the ac power mains may interfere with the correct operation of the test site. For example, test equipment may give spurious readings, computer equipment may "glitch", and equipment being tested may respond inappropriately. The interfering signals may be either common mode or differential mode or both, and can be further subdivided into "continuous" and "transient" interference. Site test equipment may be particularly vulnerable to transients, even those of short duration, because they can exhibit peaks as high as several kiloVolts.

Isolating transformers using one or more shield layers between the primary and secondary windings reduces the conducted interference. For common mode interference, the shield should be connected to ground. For differential mode interference, it is best to return the transformer shield to the neutral lead of the primary. However, a grounded shield still offers some differential mode protection; when a transformer includes only a single shield, the best compromise is to ground it. Higher isolation transformers incorporate a second shield so that one can be connected to ground and the other to the neutral lead of the primary.

Much of the isolation provided by the transformer can be lost if it is improperly mounted. The primary and secondary leads should not be in parallel along the same side of the transformer, proximity and parallelism of the leads can produce enough coupling to null the effect of the transformer's internal shield(s).

An additional defence against conducted interference is an ac power line filter. This filter generally provides adequate protection against continuous signals, and its low-pass nature attenuates transients by removing their high frequency components.

A power line filter shorts differential mode interference from the live to the neutral lead of the ac mains. Common mode interference should be either attenuated by a common mode choke or shunted into the ground system through filter capacitors. As always, the effectiveness of a common mode filter depends in large part on how small the inductance in the filter's ground lead can be made.

Transient signals can be particularly disruptive to microprocessor-based equipment. Transients in excess of 1 kV are not rare, and adequate precautions should be made to negate their effects.

For some sites it might be desirable to have AC supplies at frequencies other than are generally available (for example 400 Hz) in which case a generator may be installed. This should be considered as a threat to the site and adequate precautions should be taken regarding the isolation and filtering of such supplies.

9.5.3 Ancillary equipment

Free field test sites (normally remote from buildings, etc.) will need to be heated if they are not "seasonal sites" i.e. sites used when ambient conditions are comfortable for test site personnel. The provision of heating should be considered as a potential problem for such sites as it will place a drain on the electrical supplies. Passive heating with simple on/off switches is better than electronically controlled heating (as might be found in air conditioning) which should be avoided. If air conditioning is used special care should be taken with filtering and shielding any sources that might conduct or radiate interference.

Some sites may require pumps to remove excess water, especially those sites with a shielded enclosure or test laboratory built beneath the ground plane of an Open Area Test Site. Again the generation of interference from these should be considered a threat to the operation of the site.

Lighting is another area that should not be overlooked. Fluorescent or strip lights should not be used, but passive lighting types (carbon or tungsten filament etc.) with simple on/off switches should be used.

With all these resources drawing on the mains supply it should be established that the stability of the mains supplies are adequate to cope with the various current demands. A three or four hundred metre cable run is unlikely to cope with these demands if it is made of 13 A mains cable.

Another potential threat to the sites is telephones lines. Telephone lines should be isolated or filtered before they enter the site to avoid interference being conducted into the site and then possibly radiated around the site.

Unused and spare equipment should remain remote from the test site, either outside the outer limit, or below the ground plane, so as not to interfere with or degrade the quality of the measurement.

Plugs and sockets need to be made available at the turntable, and at the antenna mast and where possible the associated cables (both power and signal) should run under the ground plane or outside of the screen. The antenna cables should preferably be semi-rigid cables terminated in "N" type connectors. Cabling for the EUT (control and power leads) need special attention to avoid field coupling. As a result these cables need to be carefully dressed. This is discussed more in the method of test, but the importance of this aspect cannot be overstated as this can introduce more than 10 dB of variation into the result. To overcome some of these problems optical interfaces are sometimes used.

10 Test equipment

10.1 Introduction

Every item of test equipment in a measurement configuration will, in some way, contribute uncertainty to the measurement. For example the signal generator might drift in frequency, the cables may interact with the radiated fields, the dipoles with poor absorber materials etc.

Temperature effects on test equipment are normally the concern of the test site engineer with an outside or exposed test site. This is especially true when the equipment may be exposed to direct sunlight, since most equipment manufacturers have a +30°C upper limit on their temperature ranges. Above this, manufacturers normally operate a reduced or non guaranteed "typical" value of uncertainty. Test equipment housing can play an important part in reducing uncertainties caused by temperature changes.

The stability, accuracy, calibration and verification of all test site equipment are part of a responsible attitude to measurement quality. Without these, no site, however well constructed, will be suitable for repeatable measurements with time. For example, the configuration of modular test equipment may not be the same for measurements separated by time on the same device, and there may be some equipment incompatibility. Equally the different equipment may introduce electromagnetic compatibility problems as a result of its different response to radiated interference or indeed it may radiate interference itself.

Maintaining the quality of the measuring equipment should be as routine as for the test site itself, namely regular maintenance, calibration and daily system checks. The procedures in manufacturers' handbooks should be adhered to at all times, since particular problems can occur with certain types of test equipment. Allowance and consideration should be made for this.

This review of test equipment begins with the most common component of any measurement system, namely the interconnecting radio frequency cables.

10.2 Cables

Whereas an open two wire system is useful at lower frequencies (DC power leads, audio leads, etc.) and in short lengths up to about 100 MHz, at these higher frequencies serious losses can occur due to radiation and to skin effect in the conductors.

To overcome radiation losses, a closed field configuration is used in which the inner conductor is surrounded by an outer cylindrical sheath (i.e. coaxial cable). This has advantages in that the fields are confined within the outer conductor whilst the inner conductor is also shielded from outside interference. The medium between the conductors can be air or some other dielectric material (see figure 98).

The purpose of any cable is to carry energy from a source to a load. The efficiency with which the coaxial line does this is dependent (amongst other things) upon the mode in which it propagates energy. Such modes can be described in terms of their electrical and magnetic field patterns within the line, and each mode refers to a specific relationship between the orientation of the electric field, the magnetic field and the direction of propagation vectors of the electromagnetic wave.

A coaxial cable provides the means for more than one mode of propagation. The most commonly used mode, known as the dominant mode, is that in which both the electric and magnetic fields posses single components only which are perpendicular to each other and lie entirely in planes transverse to the direction of propagation. This wave is called a Transverse ElectroMagnetic (TEM) wave.

Other modes of propagation, which are not commonly used outside waveguides, are referred to as Transverse Electric (TE), Transverse Magnetic (TM) and hybrid modes.

The usable frequency band of the dominant mode in coaxial cable is from dc upwards and is only limited by the highest frequency at which it is the only propagating mode. Above this frequency the non-transverse electromagnetic (or waveguide type) modes can propagate.

The non-transverse electromagnetic modes can only propagate when the average circumference is roughly one wavelength. To ensure that they do not exist at a particular frequency, the cable diameter should be decreased in line with this limitation. This will ensure there is no longitudinal component of the field (as in rectangular waveguide), and as a result, this dominant mode is usable from dc to beyond the frequency of interest.

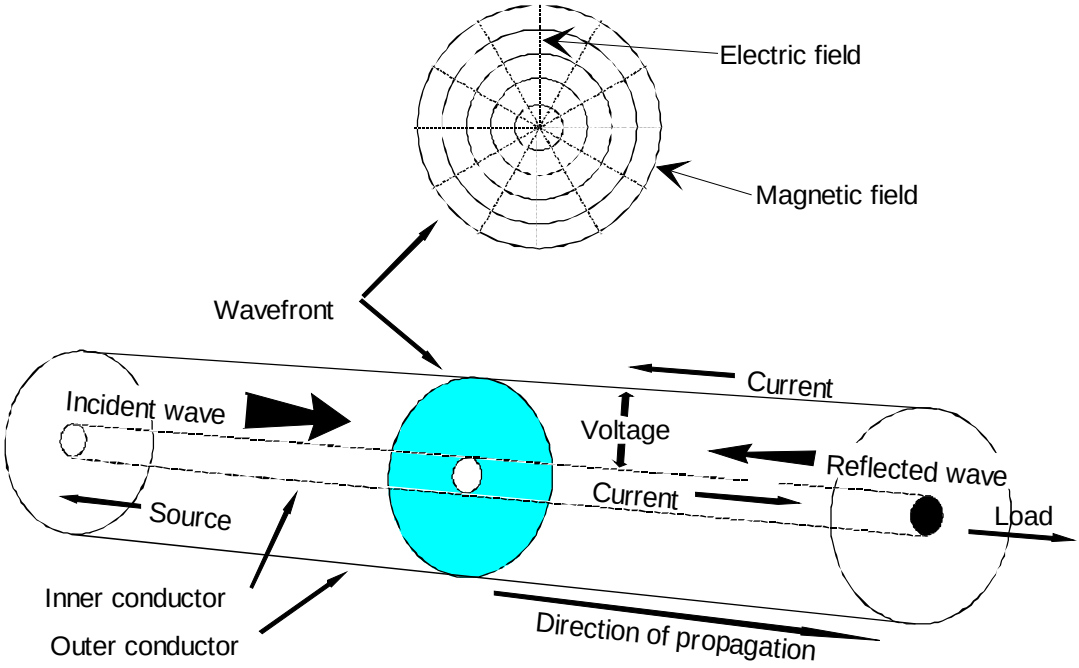

Figure 98: The electromagnetic wave in a coaxial cable

Other phenomena occur in coaxial cable as the frequency increases. One of the most important is the so-called "skin effect", i.e. the restriction of current flow to the outermost layers of a conductor as a result of the internal forces exerted by the alternating electric and magnetic fields. The problem of increasing concentration of current due to the decreasing cross-sectional area increases with frequency. For the centre conductor of a coaxial line, the decrease in available area results in higher resistance and hence reduced power handling. Figure 99 shows schematically the effects of using higher frequencies. To avoid moding problems, the cable diameter needs to be reduced, whilst the reduction in skin depth produces an associated drop in the cable's power handling capability.

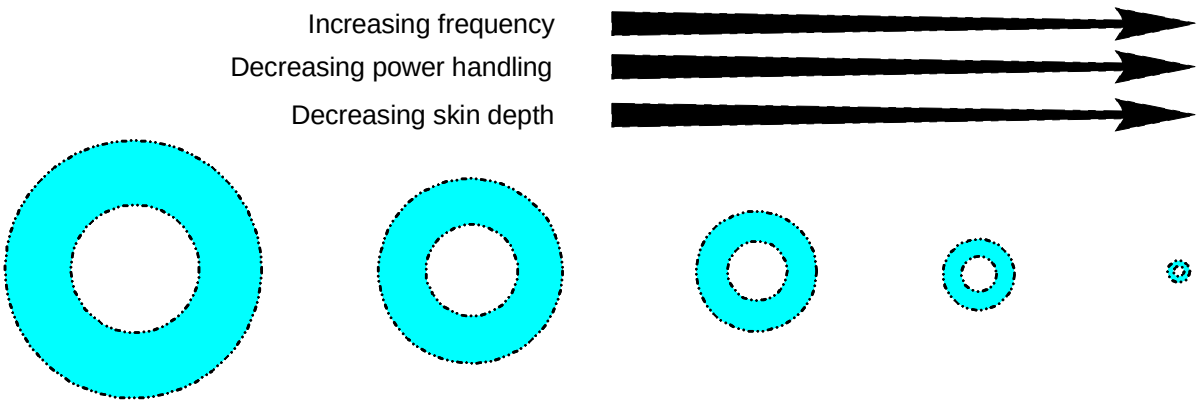

Figure 99: Coaxial cable diameter variation effects

Coaxial cable is widely used because it results in a very well controlled low loss environment for electromagnetic waves, since they are totally confined by the sheath or outer conductor. Amongst other benefits of the coaxial cable is that it is easily modelled theoretically allowing cable losses and cable impedances to be calculated, in practice giving good agreement with measured values. Power handling can be a problem at high frequencies.

The cables and connectors within a test facility can cause many uncertainties if they are not adequately considered. Some examples which affect performance either in the short or long term are:

- differences in the qualities due to the use of very expensive cable and cheap connectors (or vice versa);
- possible damage from the wheels of trolleys, feet of personnel, etc. due to the use of underground or protected cables which surface in the measurement area;
- cables that have sharp bends or kinks in them due to increased VSWR problems;
- cables that have no protection for the connectors when they are not in use;
- cables that are under mechanical stress can elongate or distort producing impedance changes;
- grade of cable is important, often for long term stability. Semi-rigid cables are better than flexible ones, for example, under a ground plane where no flexibility but good environmental performance is necessary;
- cable length can be a limiting factor in higher frequency applications when the cable losses are high. This has a direct effect on system sensitivity;
- cable connectors (for example, soldered, crimped etc.) may deteriorate with time.

Cable performance will generally be degraded by any of the above mechanisms and hence they all affect the accuracy and repeatability with which measurements can be made. Regular maintenance is vital to the long term stability of a test site. Some less obvious mechanisms are now discussed.

10.2.1 Cable attenuation

Cable attenuation plays an important part in test site operation. It can reduce unwanted reflections when it is high, but as a consequence also reduces sensitivity. Alternatively if it is low it will not reduce system sensitivity as much but equally it will offer less protection against any reflection problems. Cable attenuation is frequency dependant because the skin effect reduces the available cross sectional area of the centre conductor. This can limit the maximum generated field strengths in degradation tests.

Generally the cable with the least attenuation should be used, as attenuators can be added to reduce reflection problems.

10.2.2 Cable coupling

A common mechanism for introducing uncertainty into any measurement is electromagnetic coupling into the cables. This coupling can have differing effects depending on the length of the cable and where it is in the system. Cables are usually the longest parts of the test set-ups and as such they can make good receiving or transmitting antennas. This is bad news for the measurement engineer.

Because the wave contains both electric and magnetic fields, mixed coupling to the cable occurs. The induced voltage is very dependant on the orientation, with respect to the cable, of the electric and magnetic fields and in the general case, the voltage at the two ends of the cable will not be the same. This creates problems regarding cable positioning, screening and leakage.

For the case of a cable feeding an antenna (whether the antenna is receiving or transmitting), the signal will energize the free falling cable behind the antenna, which can act as a parasitic element i.e. it can couple to the antenna, either reflecting or directing the incident energy. The antenna and parasitic element behave as coupled circuits with self and mutual impedance depending on their lengths and spacing. The phase angle of the induced shield current relative to the antenna depends on the position of the cable and on its effective length. As the major effect of this is addition and subtraction of the wanted signal brought about by the phase differences, the placement of the cable can be critical to reducing its impact on the measurement configuration. Cable positioning is only a problem when coupling can occur. If the cables are positioned correctly minimal coupling will result. The presence of the parasitic element also loads the antenna and as a result the antennas input impedance can change.

Cable leakage probably has the least effect on the measured results except in extreme cases of signal attenuation, (i.e. excessive antenna factors equivalent to losses of over 60 dB. An example of this is the antenna factor of a loop antenna at 10 Hz being in the order of 70 dB, or detecting a magnetic field by the voltage it induces which is subjected to an attenuation of 51,5 dB). If the cable screening is not sufficiently high, serious measurement uncertainties can result.

As an example, consider the degradation test illustrated in figure 100 which requires a 10 V/m field at the EUT. The field is generated via an amplifier and automatically controlled via a feedback loop containing an antenna monitoring the field strength. If, in this theoretical system, the antenna factor is 25 dB and the cable screening, because of damage, loose connectors etc., is only providing 15 dB of isolation, the field strength at the EUT will be approximately 10 dB below what it is thought to be (that is only about 3 V/m) although the system will indicate 10 V/m.

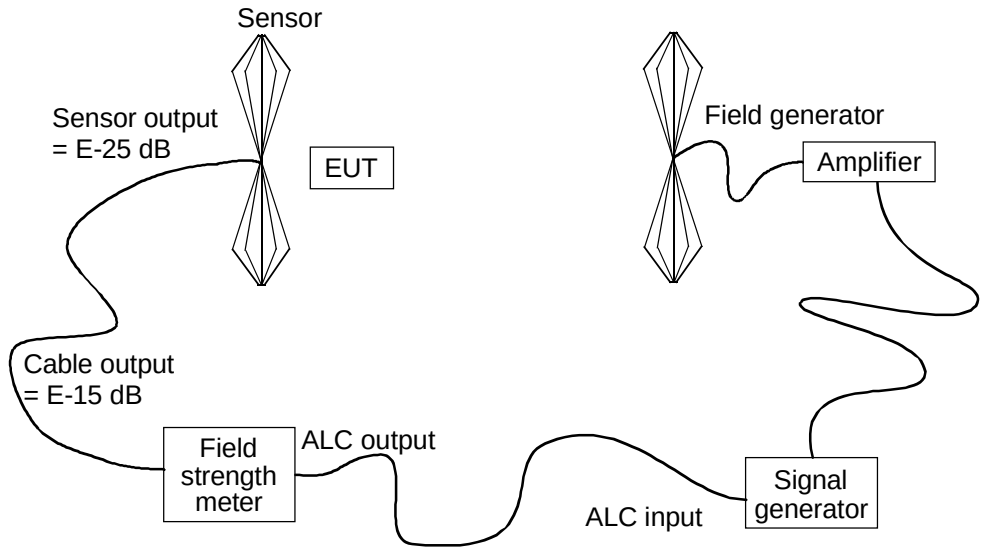

Figure 100: Example of cable screening affecting a degradation test

Imagine now the same system, but this time the cable is secure and not creating problems due to its screening effectiveness, but it is, however, coupling to the antenna by being parallel to it, for example, in the same way that a parasitic element couples to a linearly polarized antenna. The actual coupling factor will determine the actual effect. Obviously this is an unwanted effect that is likely to lead to an unquantifiable error and should be avoided.

10.2.3 Cable shielding

Externally, poor cable sheath earthing can have a major impact on the screening effectiveness of cables. The degree of screening is also affected by the skin effect, particularly at low frequencies, where the sheath can be thinner than a skin depth. In these cases the current flowing in the sheath can be considered to be uniformly distributed throughout its thickness. At higher frequencies, skin effect restricts the current flow to within a few skin depths of the outer surface. This enables the cable sheath to provide good protection at these higher frequencies.

Internally, due to skin effect most of the return current flows on the inside of the sheath. Since this is the surface closest to the centre conductor (in which the signal current flows), this situation gives the greatest mutual inductance.

When the return current flows on the inside of the sheath, high values of shielding effectiveness are obtained. The penetration of external fields will similarly be limited to a few skin depths of the outer surface, and in this way there is no mixing of the return current and the unwanted interference. The limiting factor is usually the presence of any apertures, such as the gaps found between strands in a braided sheath. Similarly poor grounding will cause return current flow on the outside of the sheath, no matter how impenetrable it has been made.

10.2.4 Transfer impedance

Surface transfer impedance is defined as "The quotient of the voltage induced in the centre conductor of a coaxial line per unit length by the current on the external surface of the coaxial line IEC 60050-161 [15].

In the case of figure 101, the impinging wave shown strikes the outer sheath and induces a current I_s on the outer surface. This gives rise to an induced voltage V_i in the centre conductor. In symbols the surface transfer impedance Z_t is:

$$Z_t = \left(\frac{V_i}{I_s} \right) \ \Omega/m$$

At low frequencies, the surface transfer impedance tends to be high because current flows throughout the whole thickness of the screen. With increasing frequency however, skin effect causes the current density within the screen to move away from the inside surface and concentrate increasingly within the outer layers. The result of this behaviour with frequency, is that V_i reduces with increasing frequency and the surface transfer impedance decreases. In the limit, as the frequency tends to infinity, the skin depth tends to zero, along with V_i and the surface transfer impedance.

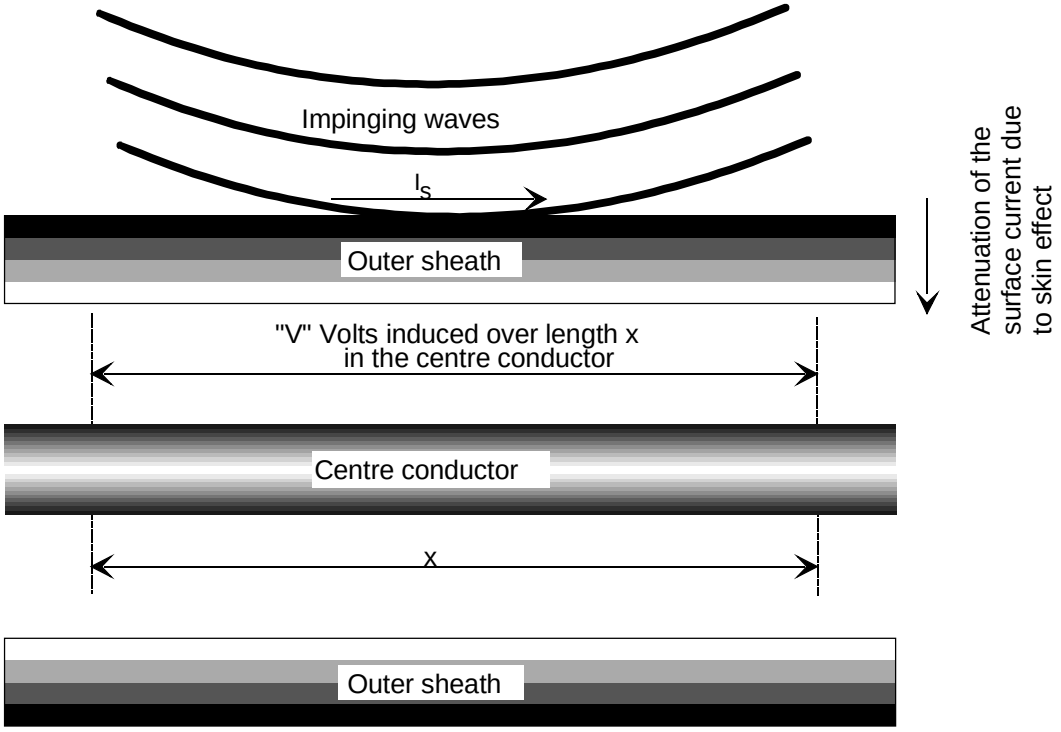

Figure 101: Coaxial cable in an interfering field

In practise, skin depth (see clause 9.3.5) is dependent not only on frequency but also the permeability and conductivity of the materials involved. For example, ferrous metals have smaller skin depths, as do higher conductivity ones.

Where it is necessary to confine, or reject, magnetic fields, Ferro-magnetic materials are used. These offer relative permeabilities ranging from 10 to 100 000 or more which significantly reduces the skin depth at low frequencies. Table 24 lists some of these materials.

Table 24: Permeability of various materials

Material	Relative Permeability (μ)		Material	Relative Permeability (μ_r)
Supermalloy	100 000		4 % Silicon Iron	500
78 Permalloy	8 000		Hiperco	650
Purified Iron	5 000		50 % Nickel Iron	1 000
Conetic AA	20 000		Commercial Iron	200
4-79 Permalloy	20 000		Cold rolled Steel	180
Mumetal	20 000		Nickel	100
Hypernick	4 500		Stainless steel	200
Hot rolled Silicon Steel	1 500		Rhometal	1 000

The smaller the skin depth, the better the shielding and the lower Z_t. The construction of the screen also determines its shielding quality. For example a solid screen is much better than a braided one. However, a solid screen is not practical in cases where some flexibility is required in the cable. Figure 102 shows the variation of surface transfer impedance with frequency for different screen types.

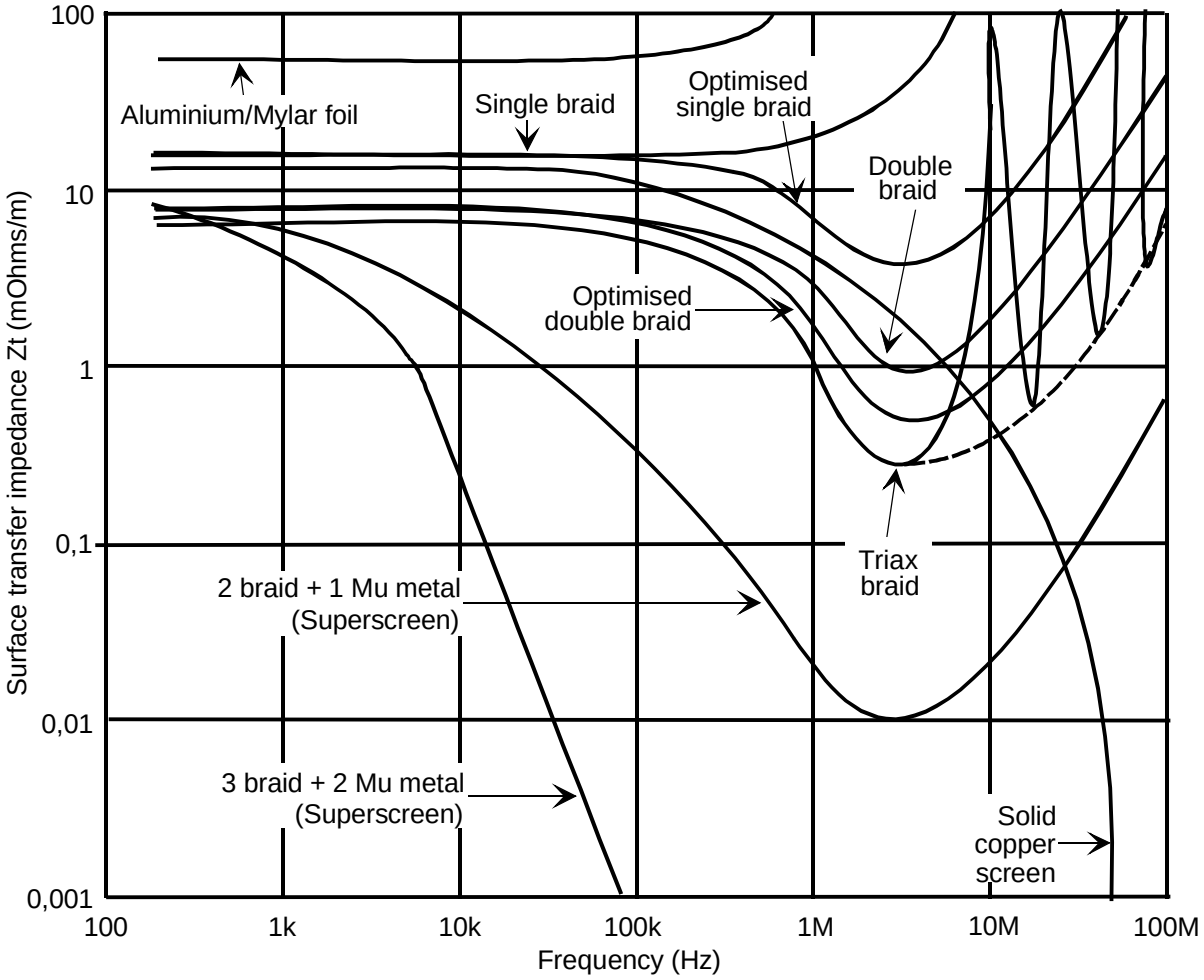

Figure 102: Variation of surface transfer impedance with frequency for different screen types

For the types shown in figure 102:

- The **aluminium/mylar foil** sheath has a high value of transfer impedance and increases rapidly with frequency.
- The **single braid** copper sheath extends the frequency range by a decade over the aluminium/Mylar cable.

- The **optimized single braid** copper sheath extends the frequency range by two decades over the aluminium/Mylar cable.
- The **double braid** and **optimized double braid** copper sheath again provide an increase in performance over the previous types.
- The **tri-axial** cable copper sheath provides slightly better performance to a few MHz, but then the transfer impedance swings between values, depending on the actual construction of the cable.
- The **two braid and single Mu metal** screen provides up to four orders improvement of the transfer impedance on the aluminium/mylar foil cable, most notably at lower frequencies where the higher permeability of the mu metal provides lower transfer impedance due to the effect of the permeability in reducing the skin depth.
- The **solid copper** screen has approximately the same transfer impedance at low frequencies as any of the non-ferrous sheaths, but due to its solid construction it does not suffer any of the capacitive or inductive effects that occur with braided cables and therefore the skin depth continues to decrease with increasing frequency as in the ideal case.
- The **three braid and two mu metal** screen provides the best overall performance of those compared, mainly due to the double mu metal screen performance at low frequencies. This cable provides five sheaths as opposed to the single braids described earlier.

The most commonly used cable for fixed installation is the cable with a solid copper sheath. For this sheath the skin effect makes the transfer impedance tend to the ideal value of zero. However a major cause of problems with solid sheathed cables, and indeed in the construction of any cable, is the termination of the cables at the connector or bulkhead. If the external surface of the sheath of the cable is not provided with a 360° electrical contact, then the transfer impedance will be increased by many orders. This effect is illustrated in figure 103.

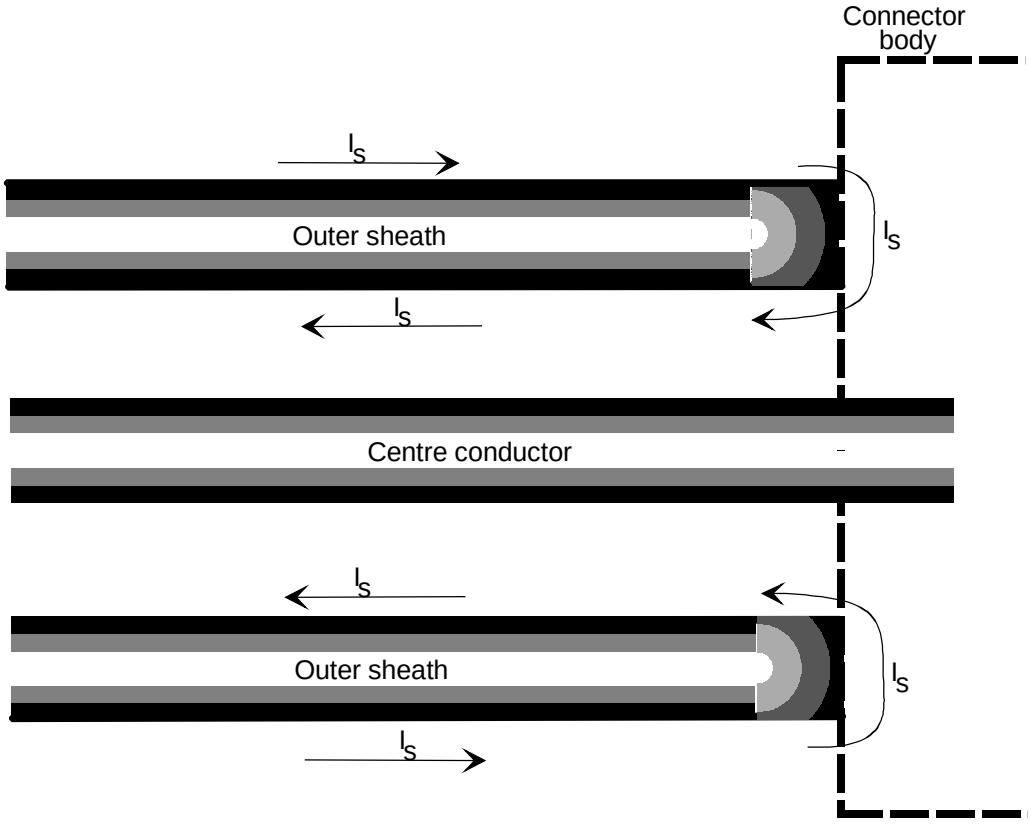

Figure 103: Poor cable sheath bonding

Figure 103 shows that, where the cable sheath is not terminated by a 360° electrical bond, the surface current flows through the unbounded section directly into the inside of the cable sheath thus completely bypassing the advantages that skin depth and a solid sheath gives in screening the centre conductor.

The transfer impedance of a solid sheath is sometimes referred to as the diffusion impedance Z_D.

In the case of braided cables, the weave of the braid will introduce an inductive element which will result in a mutual inductance between the sheath and the inner conductor. This factor M_{12} will always be to the detriment of the transfer impedance thus:

$$Z_t = Z_D + j\,\omega M_{12}$$

Connectors also have a transfer impedance and in practice there is little point using a good quality cable if a poor quality, high transfer impedance, connector is fitted. The transfer impedance of the interconnecting cable is only as good as its highest transfer impedance, anywhere along its length.

For frequencies above a few MegaHertz, the skin effect causes most of the return current to flow on the inside of the sheath because this surface is closest to the centre conductor. As stated above, the skin effect separates the currents flowing on the inside and outside of a shield. Thus, for high-frequency currents, the outside of the shield can be essentially thought of as a different conductor than the inside.

10.2.5 Improving cable performance with ferrite beads

Ferrite is a ferromagnetic ceramic material. Its susceptibility and permeability are dependant on the field strength and magnetization curves (which have hysterisis). Its magnetic characteristics can be affected by pressure, temperature, field strength, frequency and time. Its mechanical and electromagnetic characteristics depend heavily on the sintering process used to form the ferrite. It is hard (physically), brittle (as are all ceramics) and will chip and break if handled roughly.

The distinction between "hard" and "soft" ferrite's lies in the ferrite's magnetic properties. A "soft" ferrite does not retain significant magnetism, whereas a "hard" ferrite's magnetism is permanent.

Ferrites are predominantly used in two basic types of application. These are low level, power and electromagnetic interference suppressers. Each of these applications requires different characteristics from the ferrite material. In the case of test cables, ferrites are used as electromagnetic interference suppressers by being clamped onto the cables normally at regular, closely spaced intervals.

10.2.5.1 Impedance

The impedance of a ferrite core is considered to be a series combination of the inductive reactance ($j\omega L_s$) which is a function of the material's permeability, and the loss resistance (R_s), both of which are frequency dependant.

High permeability ferrites (μ_r greater than 2 000) have relatively high impedances at low frequencies levelling off after about 10 MHz. Low permeability ferrites (μ_r below 100) have a relatively low impedance that increases with frequency beyond 500 MHz.

The total loss tangent (tan δ) is a measure of the energy lost or incurred as the magnetization alternates. The real part of the permeability ($U_r^{/}$) of ferrites range from less than 40 to over 10 000. In almost all cases $U_r^{/}$ of the material initially remains constant with increasing frequency, but then it rises to a maximum value after which it falls rapidly. The material's loss component $U_r^{//}$ rises to a peak as $U_r^{/}$ falls. The higher the permeability the lower the frequency at which this occurs, producing an upper optimum frequency above which the ferrite's efficiency is reduced significantly.

These effects are very frequency dependent. At dc, the inductive reactance is zero, since there is no alternating current, which means the magnetization stays constant and no losses result for hysterics. At low frequencies, however, it is the inductive reactance which tend to dominate, producing attenuation by reflection. At high frequencies the loss resistance tends to dominate and in contrast to lower frequencies, attenuation is produced by absorption in the ferrite. In general the higher the permeability, the lower the optimum attenuation frequency. The lower the permeability the higher the optimum attenuation frequency.

In the presence of high intensity fields or large currents, the ferrite material will saturate, at which point the ferrite loses its blocking properties and becomes relatively transparent.

Ferrite beads are highly effective particularly against common-mode current when clamped over cables since they act as high resistance blocks to the passage of high frequency currents. For low frequency or dc currents, the ferrite device is virtually transparent, and has minimal effect.

When the current, returning from the load along the inside of the shield reaches the source end of the cable, some of it will flow into the source itself whilst the rest will flow back along the outside of the shield towards the load. This current now flows in the same direction as the signal current and is therefore a common mode current (see figure 104). The same situation exists for the coaxial line coupling to the antenna balun, however, in this case it does not have to be reflected from the load first. An antenna (usually a balanced device) should normally be connected to a coaxial cable (unbalanced), with or without impedance matching. However, the inner and outer conductors of the coaxial line do not couple to the antenna in the same way and a net current flows in the outer sheath, or shield, of the coaxial cable. The amount of current is determined by the shield's impedance to ground. The higher the impedance the less current flow. A balun is the device that is used to transform from a balanced to an unbalanced line and can be helpful at increasing the shield impedance. A good match gives negligible shield current whilst a bad match will increase it to significant proportions.

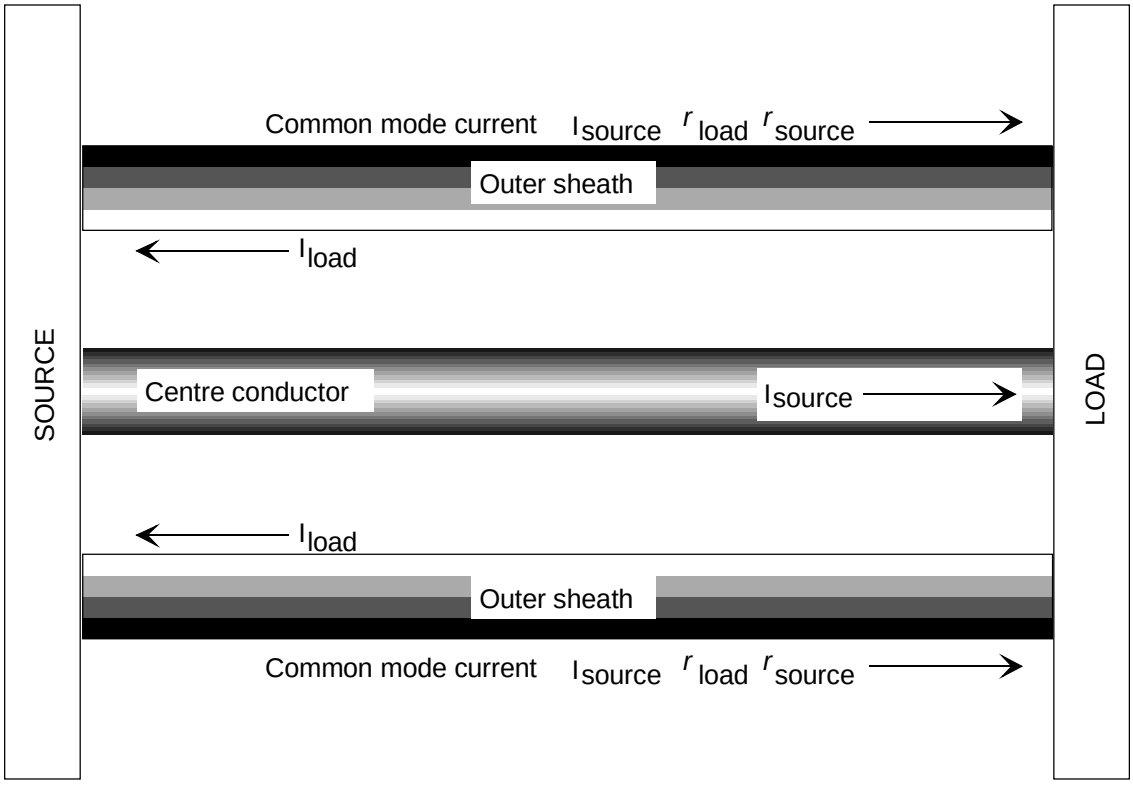

Figure 104: Common mode current on a cable

The ability of the balun to match the impedance of the antenna to the coaxial line at all frequencies is critical to the relative level of the shield current. A common mode current flows due to this imbalance. The amount of imbalance in the balun is frequency dependant and therefore the level of the current is also frequency dependant.

A single ferrite bead on a cable acts as a RF choke whose impedance is proportional to frequency. The resulting effect is that increasing the frequency increases the series impedance to currents flowing through the shield.

A common mode choke, as shown in figure 105a, attenuates common-mode current flow by increasing the impedance along the outside of the shield. Unlike other techniques for reducing radiated emissions resulting from common mode currents, the success of this approach does not depend on finding a low impedance ground. However, it usually curbs the cable emissions by only 6 dB to 10 dB.

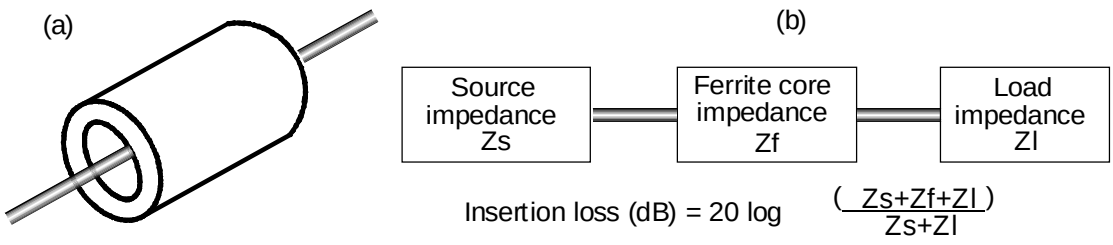

Figure 105: Improving common mode rejection with ferrite beads

The term "high frequencies" in this case tends towards frequencies greater than 1 MHz. The inner and outer surfaces of the shield are isolated from each other by skin effect at frequencies above this.

Ferrites may be regarded as high frequency resistors and the choice of ferrite material is based on the frequency range to be suppressed. When used for common mode suppression they are chosen for their lossy characteristics. The higher the value of loss angle, over the broadest frequency range, the better the material behaves as an attenuator. The ideal ferrite for cables is one which only absorbs power and dissipates it as heat. This is best illustrated for the balun case where reflecting the power back into the balun will obviously increase the problem and should be avoided.

All ferro-magnetic materials begin to lose their ability to conduct magnetic lines of flux as they approach saturation and become increasing transparent. Ferro-magnetic materials should never be used at, or close to, their saturation points. All soft magnetic materials are affected by strain, permeability falling off rapidly with increasing strain. These materials therefore are susceptible to stresses such as dropping, banging, or processes such as drilling and cutting. Magnetic materials have a greater absorption loss than non-magnetic materials, particularly at lower frequencies when the permeability is large. Caution should be exercised when high values of absorption loss are obtained for magnetic materials calculated using fixed dc values for permeability and conductivity, since these parameters vary considerably with frequency.

Other cables on a test site are those required to operate the equipment, for example signal cables, power cables and equipment control leads. These all act as antennas or parasitic elements at given frequencies depending on their configuration, type of cable etc., and can strongly influence the outcome of a particular measurement. In attempts to reduce the problems for measurements, ferrite beads may be used to reduce the effects or fibre optics can be used to overcome the metallic content of the cables and any of its effects.

10.2.6 Equipment interconnection (mismatch)

When two or more items of RF test equipment are connected together a degree of mismatch occurs. Associated with this mismatch there is an uncertainty component as the precise interactions are unknown. Mismatch uncertainties are calculated in the present document using *S*-parameters and full details of the method are given in annex D of TR 102 273-1-2 [12]. For our purposes the measurement set-up consists of components connected in series, i.e. cables, attenuators, antennas, etc. and for each individual component in this chain, the attenuation and VSWRs need to be known or assumed. The exact values of the VSWRs (which in RF circuits are complex values) are usually unknown at the precise frequency of test although worst case values will be known. It is these which should be used in the calculations. This approach will generally cause the calculated mismatch uncertainties to be worse (or more conservative) than they actually are. There are three different circuit configurations in the test methods given in parts 2 to 7 of the present document that give rise to these problems. The uncertainty contributions which arise from mismatch are given the representative symbols as follows:

u_{j35} is used throughout all parts of the present document for the uncertainty contribution associated with the mismatch: reference measurement.

NOTE 1: This uncertainty only contributes to verification procedures. It results from the interaction of the VSWRs of the components in the reference measurement i.e. the arrangement in which the signal generator is directly connected to the receiving device (via cables, attenuators and an adapter) to obtain a reference signal level. Due to load variations (antennas replacing the adapter in the second stage of the procedure) the uncertainty contributions are not identical in the two stages of the verification procedure and hence do not cancel.

u_{j36} is used throughout all parts of the present document for the uncertainty contribution associated with the mismatch: transmitting/substituting part.

NOTE 2: This uncertainty contributes to test methods and verification procedures. The transmitting part refers to the signal generator, cable, attenuator and antenna. This equipment configuration is used for the transmitting part of a free field test site verification procedure, the transmitting part of a stripline verification procedure (where the antenna is replaced by the stripline input), the transmitting part of the substitution measurement in a transmitter test method and in the field generation part in a receiver test method.

u_{j37} is used throughout all parts of the present document for the uncertainty contribution associated with the mismatch: receiving/measuring part.

NOTE 3: This uncertainty contributes to test methods and verification procedures. The receiving part refers to the antenna, attenuator, cable and receiving device. This equipment configuration is used for the receiving part of a free field test site verification procedure, the receiving part of a stripline verification procedure (where the antenna is a monopole), the receiving part of the substitution measurement in a transmitter test method and when measuring the field in a receiver test method.

10.3 Signal generator

The signal generator is used as the transmitting source for test site verification procedures, the substitution source for emission measurements and the transmitting source for sensitivity type tests. The signal generator's output level should remain constant for the duration of the tests. Any variation in the output level will result directly in an uncertainty in the received level and therefore a variation in either the site attenuation value or the substituted value. For site attenuation measurements the output level uncertainty contributes equally to both the reference measurement and the actual measurement (since, once set, its level stays unchanged) and therefore cancel in the calculations. However, this is not the case for emission (substitution) measurements where the generator output is compared with an EUT emission and therefore absolute level uncertainty for the generator needs to be known and included in the uncertainty calculations.

The uncertainty associated with the absolute level of the signal generator output is how accurately an absolute level can be set at the generator output. In certain measurements the output level accuracy of the generator is critical, as in, for example, a substitution measurement.

u_{j38} is used throughout all parts of the present document for the uncertainty contribution associated with the signal generators absolute output level uncertainty.

In other cases, such as referenced measurements (as in the verification case) the generator's output level is unimportant providing it remains constant. Variations in the absolute level due to temperature, load and supply variations etc. will occur however and an uncertainty contribution for output level stability is included to take this into account.

u_{j39} is used throughout all parts of the present document for the uncertainty contribution associated with the signal generators output level stability.

NOTE: When u_{j38} is included in the uncertainty calculations, u_{j39} can be disregarded as stability is part of the absolute level.

10.4 Attenuators

An attenuator on the measuring or test antenna provides isolation between the antenna output and the receiver input, whereas an attenuator on the substitution antenna (transmitting antenna) provides isolation between the signal generator output and the antenna input. In both cases the attenuator is used to prevent significant multiple reflections between two potentially badly matched devices. Attenuators used in this fashion can also be placed between receive antenna outputs and the inputs to high gain amplifiers as the amplifier helps to improve the dynamic range of the measurement whilst the attenuator prevents significant VSWR problems.

10.4.1 Attenuators used in test site verification procedures

The attenuation value is nominal and contributes equally to both the reference measurement and the actual measurement when site verification measurements are made. Any associated uncertainty in its loss value therefore cancels in the calculations.

10.4.2 Attenuators used in test methods

The test equipment layouts for the EUT measurement and substitution stages of a test method, are not always the same, therefore the uncertainty contributions do not always cancel. On the one side, the test antenna's attenuator is involved in both stages and hence its uncertainty contribution cancels. However the substitution antenna's attenuator is only involved in the substitution stage of the measurement and its uncertainty contribution therefore does not cancel.

u_{j40} is used throughout all parts of the present document for the uncertainty contribution associated with the insertion loss of an attenuator.

NOTE 1: For the attenuator associated with the test antenna this uncertainty contribution is common to both stage one and stage two of the measurement. Consequently, this uncertainty contribution is assumed to be zero due to the methodology.

NOTE 2: For the attenuator associated with the substitution or measuring antenna this uncertainty contribution is taken either from the manufacturer's data sheet or from the combined standard uncertainty figure of its measurement.

NOTE 3: Where the field strength in a stripline is determined from the results of the verification procedure, for the attenuator associated with the stripline input this uncertainty contribution is taken either from the manufacturer's data sheet or from the combined standard uncertainty figure of its measurement.

NOTE 4: Where a monopole or three-axis probe is used to determine the field strength, for the attenuator associated with the stripline input this uncertainty contribution is assumed to be zero due to the methodology.

NOTE 5: Where a monopole is used to determine the field strength, for the attenuator associated with the monopole antenna this uncertainty contribution is taken either from the manufacturer's data sheet or from the combined standard uncertainty figure of its measurement.

10.4.3 Other insertion losses

Other items of test equipment contribute measurement uncertainty in the same way as attenuators. These include cables, adapters and antenna baluns.

Each of these has an insertion loss at a given frequency which acts as a systematic offset. Knowing the value of the insertion loss allows the result to be corrected by the offset. However, there is an uncertainty associated with this insertion loss which is equivalent to the uncertainty of the loss measurement. This uncertainty contribution can be taken either from the manufacturer's data sheet or from the combined standard uncertainty figure of the loss measurement.

u_{j41} is used throughout all parts of the present document for the uncertainty contribution associated with the insertion loss of a cable.

NOTE 1: For the cable associated with the test antenna, this uncertainty contribution is common to both stage one and stage two of the measurement. Consequently, the uncertainty contribution is assumed to be zero due to the methodology.

NOTE 2: For the cable associated with the substitution or measuring antenna, this uncertainty contribution is taken either from the manufacturer's data sheet or from the combined standard uncertainty figure of its measurement.

NOTE 3: Where the field strength in a stripline is determined from the results of the verification procedure, for the cable associated with the signal generator this uncertainty contribution is taken either from the manufacturer's data sheet or from the combined standard uncertainty figure of its measurement.

NOTE 4: Where a monopole or three-axis probe is used to determine the field strength, for the cable associated with the signal generator this uncertainty contribution is assumed to be 0,00 dB due to the methodology.

NOTE 5: Where a monopole is used to determine the field strength, for the cable associated with the monopole antenna this uncertainty contribution is taken either from the manufacturer's data sheet or from the combined standard uncertainty figure of its measurement.

u_{j42} is used throughout all parts of the present document for the uncertainty contribution associated with the insertion loss of an adapter.

NOTE 6: This uncertainty contribution is taken either from the manufacturers data sheet or from the combined standard uncertainty figure for insertion loss measurement.

u_{j43} is used throughout all parts of the present document for the uncertainty contribution associated with the insertion loss of an antenna balun.

NOTE 7: This standard uncertainty of the contribution is 0,10 dB.

10.5 Antennas

An antenna is a device which converts a radiated field strength in V/m or A/m to a conducted power level and vice versa. Its technical characteristics can be described by a number of parameters typically gain, polarization, radiation pattern and input impedance. These, along with other parameters that affect the accuracy of a test site measurement are discussed below.

10.5.1 Antenna factor

The antenna factor for a particular antenna relates the output voltage appearing at its terminals to the electric (or magnetic) field strength in which it is immersed. It is a factor which takes into account the directivity, all internal and mismatch losses, the effects of any integral circuitry and is specified at a particular frequency. Its value is subject to an uncertainty which can contribute to measurements of field strength in test methods.

u_{j44} is used throughout all parts of the present document for the uncertainty contribution associated with the antenna factor of a transmitting, receiving or measuring antenna.

NOTE 1: The antenna factor contributes only to the radiated part of a verification procedure and the field measurement part of a test method.

NOTE 2: For ANSI dipoles the value should be obtained from table 25. For other antenna types the figures should be taken from manufacturers data sheets. If a figure is not given the standard uncertainty is 1,0 dB.

Table 25: Uncertainty contribution: antenna factor of the transmitting, receiving or measuring antenna

Frequency	Standard uncertainty of the contribution
30 MHz ≤ frequency < 80 MHz	1,73 dB
80 MHz ≤ frequency < 180 MHz	0,60 dB
frequency ≥ 180 MHz	0,30 dB

10.5.2 Gain

An antenna's gain is a measure of its ability to direct power in a particular direction and is usually specified in dB relative to an isotropic radiator in the far-field. Some manufacturers supply measured gain calibration curves with their antennas whilst others supply typical figures only. Whatever the case, the figures given are never quoted with an uncertainty of less than 0,25 dB, and 1 dB would be a more usual figure. This uncertainty will be compounded if the quoted far-field figures are subsequently used for tests carried out in the nearfield.

The gain of the antenna is assumed constant, but with an associated uncertainty depending on the frequency of operation. Where tuned half-wavelength dipoles are employed, constructed as detailed in ANSI C63.5 [1], a shortened dipole is used from 30 MHz - 70 MHz inclusive. At all these frequencies the 80 MHz arm length (0,889 m) is used attached to the 20 MHz - 65 MHz balun for all test frequencies in the 30 MHz - 60 MHz band and to the 65 MHz - 180 MHz balun for 70 MHz.

u_{j45} is used throughout all parts of the present document for the uncertainty contribution associated with which the gain of the substitution or test antenna is known at the frequency of test.

NOTE 1: The gain for some antennas is sometimes quoted relative to a half wavelength dipole. As a result the gain figure will be 2,15 dB less than the figure quoted against an isotropic radiator. Therefore, for every calculation involving gain, care should be taken to ensure that the right figures are used.

NOTE 2: During verification procedures using ANSI dipoles the value of this uncertainty is 0,00 dB. For other antenna types the figures should be taken from manufacturers data sheets. If a figure is not given the standard uncertainty is 0,6 dB. For test methods using ANSI dipoles the value should be obtained from table 26. The uncertainty degrades for lower frequencies due to, amongst other things, dipole shortening.

Table 26: Uncertainty contribution: gain of the antenna

Frequency	Standard uncertainty of the contribution
30 MHz ≤ frequency < 80 MHz	1,73 dB
80 MHz ≤ frequency < 180 MHz	0,60 dB
frequency ≥ 180 MHz	0,30 dB

10.5.3 Tuning

Uncertainty is introduced into any test in which dipoles are used, as a result of the uncertainty of setting of the correct length of the dipole arms.

u_{j46} is used throughout all parts of the present document for the uncertainty contribution associated with the inaccurate tuning of the antenna.

10.5.4 Polarization

Most antennas used on test sites (dipoles, bicones, LPDAs, waveguide horns, etc.) are termed linearly polarized, i.e. the electric vector is assumed to be contained in a single plane. However, few practical antennas exhibit true linear polarization since there is usually an orthogonal (cross-polarized) component present. For the general case this produces elliptical polarization. Using the term "axial ratio" for the ratio between the co-polarized and cross polarized components of the electric vector, the maximum signal is only received [2], when the polarization of the incident wave generated by the transmitting antenna has:

- the same axial ratio;
- the same sense, and;
- the same spatial orientation.

as the polarization of the receiving antenna in that direction. Uncertainties on test sites result from any of the above conditions not being met.

A useful device enabling the magnitude of the polarization loss to be calculated is the Poincaré sphere shown in figure 106, on the surface of which every possible polarization can be represented (see figure 106a).

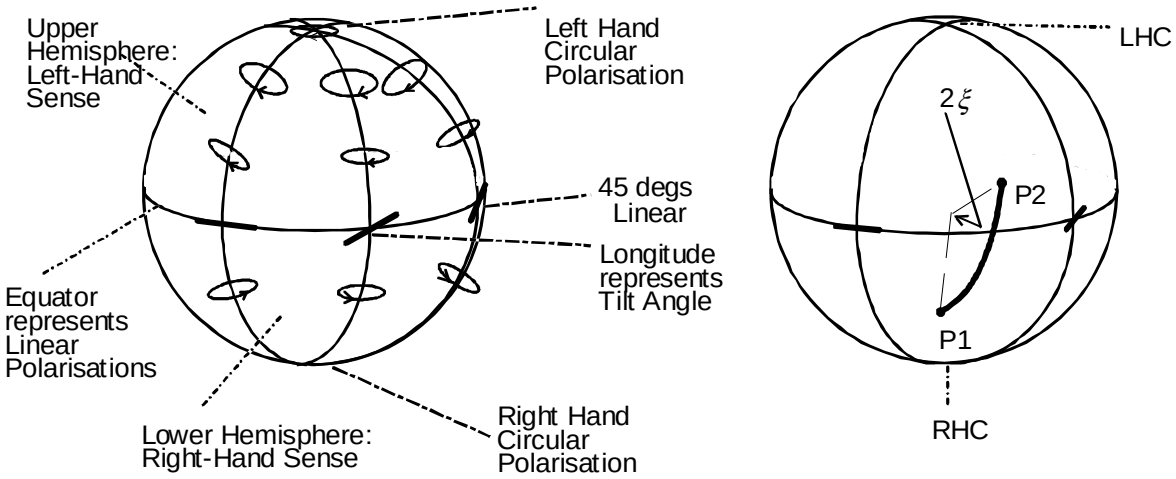

Figure 106: a) The Poincaré Sphere and b) Usage to determine Polarization Loss

If the polarizations of both the transmit and receive antennas are known and can be represented by points P1 and P2 as shown in figure 106b, the polarization loss, η_p, can be calculated from:

$$\eta_p = \cos^2 \xi$$

where 2ξ is the angle between the polarizations on the surface of the sphere.

10.5.5 Phase centre

The phase centre of an antenna (or any other radiating structure) is the point from which it can be considered to radiate. If the antenna (or radiating structure) was rotated about this point, the phase of the received/transmitted signal would not change. The phase centre of both a dipole and biconic antenna is in the centre of its two arms, for an LPDA it should be assumed to be halfway along its longitudinal axis and for a waveguide horn it is the centre of its open mouth.

10.5.6 Input impedance

The input impedance of an antenna is, in general, the complex combination of the radiation resistance, line lengths, loss resistance and matching section (if any). If the input impedance of the antenna is mismatched to its feed line then full power is not transmitted. Equally, if, in free Space, the antenna is perfectly matched to its feed but is then placed too close to another antenna or ground plane, the mutual coupling which results will change its input impedance, again resulting in power loss.

10.5.7 Temperature

Any surface at a temperature greater than absolute zero produces radiation which can contribute to the overall noise detected by an antenna. In general, on an unprotected Open Area Test Site the receive antenna will be pointing at the sky which is usually regarded as being at an equivalent temperature for microwave frequencies of between 100 and 150° Kelvin. This figure increases with decreasing frequency and at 25 MHz can be as high as 10 000° Kelvin due to various electrical discharges in the atmosphere. The contribution this makes towards system noise can be calculated from [5]:

$$P_r = kT_A \Delta f$$

where:

P_r is the antenna noise power (Watts);

k is Boltzmann's constant (1,38 x 10^{-23} Joules/ Kelvin);

T_A is the antenna temperature (Kelvin);

Δf is the bandwidth (Hertz).

In general, this tends to have very little contribution to measurement uncertainty, given the general sensitivities of the EUTs, even when wide measurement bandwidths are involved.

10.5.8 Nearfield

Reactive and radiated near-fields have been discussed in clause 7. Measurement uncertainty may be high in these regions due to the presence of numerous field components and a non-uniform phase front. Mutual coupling also occurs in this region resulting in possible impedance changes and the consequent mismatching of antennas to their feed lines.

10.5.9 Farfield

The far-field has also been discussed in clause 7 and is the region in which, wherever possible, all radiated measurements should be carried out. In this region the amplitude and phase distributions of the field incident on the receive antenna are sufficiently uniform for no significant uncertainties in the received power levels. Generally, this distance is taken to be:

$$2(d_1+d_2)^2/\lambda$$

where d_1 and d_2 are either the sizes of the EUT and the test antenna used or the sizes of the two antennas (in verification or substitution). λ is the wavelength.

10.5.10 Non-uniform field pattern

If, during testing, the field impinging on the antenna is not as uniform as the field under which it was calibrated, the signal appearing at its terminals will be other than expected. Given that, in general, the field distribution is an unknown quantity, the antenna's output will usually contain an associated uncertainty. The extent of the uncertainty will vary with the frequency, polarization, measurement geometry and the electrical and mechanical properties of the source. This factor is of particular relevance on test sites possessing a ground plane, because the field is modified by the reflecting surface.

To illustrate the effects of a ground plane on the fields across an antenna, figure 107 shows a biconic antenna in two orientations. The vertical biconic antenna suffers from nulls in the field (vertical polarization) across the physical size of the antenna and phase errors due to inadequate separation distance at the frequency of operation.

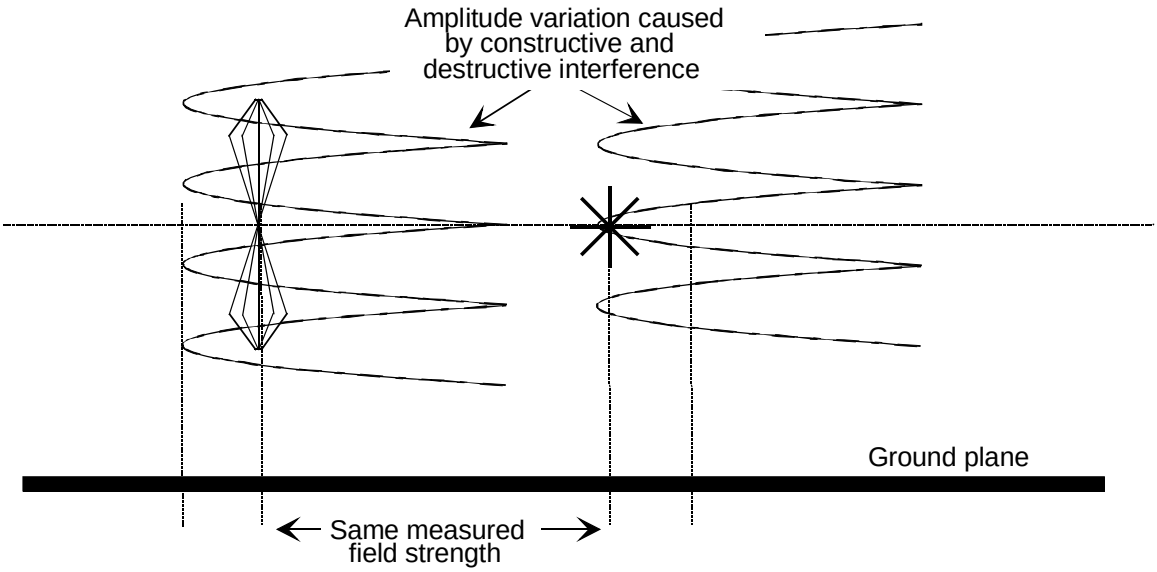

Figure 107: Field distribution over a ground plane

Contrast this testing environment generated on a ground-reflecting range, to that provided by an ideal Anechoic Chamber offering the same range length, see figure 108, the illuminating electric field is reasonably constant in both amplitude and phase along the entire length of the antenna, the variations being dependent on the radiation pattern of the test antenna in the vertical plane and the overall geometry for amplitude and phase respectively.

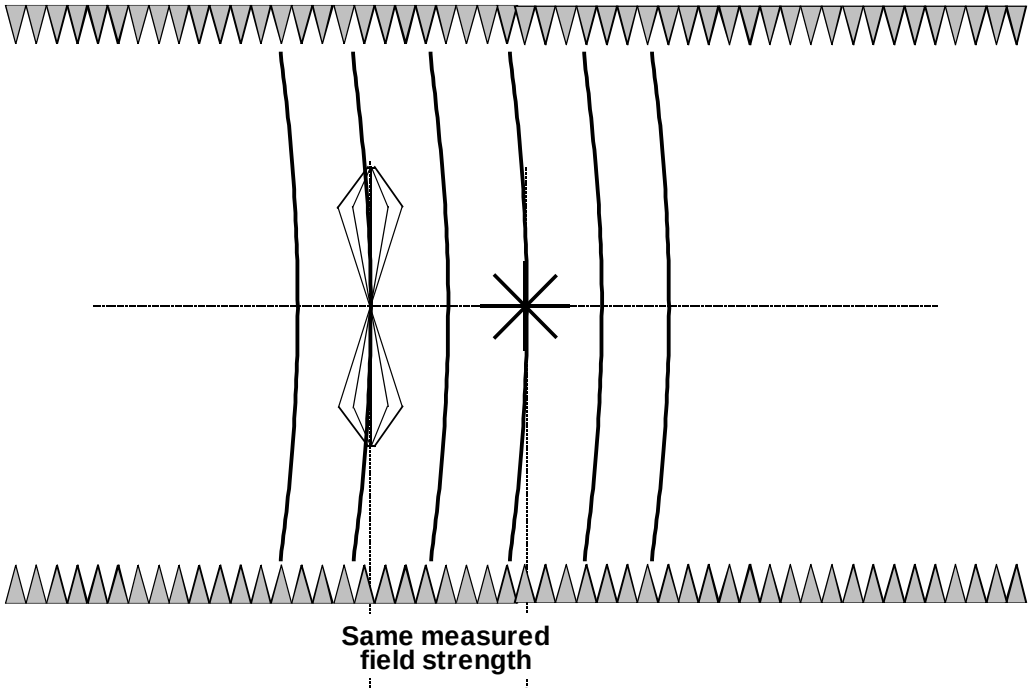

Figure 108: Field distribution in an Anechoic Chamber

If the antenna is small compared to either a wavelength or the variations of the field, the possible error is very much reduced. Conversely, the use of a large antenna (i.e. with high directivity) will give inaccurate readings even though it will tend to shield its aperture, to a greater or lesser degree, from those field components not in the direction of maximum directivity i.e. ground reflection.

10.5.11 Mutual coupling to the surroundings

An antenna will receive energy back from any reflective ground plane over which it is placed. This will induce additional currents within the antenna, thereby changing its input impedance. The radiation pattern is also affected. These effects reduce with increasing directivity in the vertical plane e.g. a vertically polarized dipole couples less to the ground plane than a horizontally polarized one.

Using an antenna close to a ground plane or anechoically lined screened room wall will result in mutual coupling between the antenna and any image. The mutual coupling varies depending on the distance between the antenna and the reflecting surface. The mutual coupling between the antenna and its images in the absorber panels is dependant on the quality of the absorbing panels. Where pyramidal absorbing panels only are used (i.e. no ferrite tiles or grids), the magnitude of the uncertainty is dependent not only on the absorber depth at the test frequency but also on angle of incidence. Under these conditions the characteristics of the antenna will diverge from the calibrated values supplied by the manufacturer. An EUT will also experience changes to its characteristics.

10.6 Spectrum analyser and measuring receiver

Different types of test equipment are used to measure the received signal, the main types being the spectrum analyser and the measuring receiver. It is important therefore to know the main differences between these two receiving devices for a better understanding of how they can introduce uncertainties through improper use.

The spectrum analyser has only a low pass filter on its input which results in frequencies from dc to just above the cut off frequency entering the analyser's circuits. As a result, any signal(s) in this band can enter the spectrum analyser in addition to the one being analysed on the display by the operator, causing possible overload. Overloading the spectrum analyser causes linearity problems, especially in the front end mixer, affecting the accuracy of the measurement. Phantom signals can also be produced.

The measuring receiver does not completely overcome these problems, but it does minimize them by limiting the spectral power incident on the input by using, for example, a band pass filter situated before the mixer.

The type of intermediate filter found in a spectrum analyser also differs from those in a measuring receiver. Receivers use flat topped filters with narrow 2,5:1 shape factors, whereas a spectrum analyser uses Gaussian shaped filters with wider 11:1 shape factors. Typically, there may be three choices of intermediate frequency filter bandwidths on a measuring receiver, against ten on a spectrum analyser.

A spectrum analyser presents the information about the input signals on a two-dimensional display, where frequency is swept against amplitude. Measuring receivers normally present information as a direct readout either as a meter deflection or as a numerical display or both.

The advantages receivers have over general purpose spectrum analysers are that:

- receivers provide adequate overload protection, in the form of RF preselection;
- receivers provide the appropriate range of intermediate frequency bandwidths;
- receivers provide the appropriate range of detectors;
- receivers are equipped with a more comprehensive calibration source;
- receivers retain manual control of the sweep speed, for more careful signal analysis purposes;
- receivers allow the operator to monitor signals at a fixed frequency allowing the peak amplitude to be detected;
- receivers generally have lower noise figures;
- receivers generally have better accuracies than spectrum analysers.

Conversely general purpose spectrum analysers have advantages over receivers, these are that:

- spectrum analysers are capable of sweeping across their entire frequency range in one sweep, very much quicker than a receiver;
- spectrum analysers provide many more selections of intermediate frequency bandwidths, offering a more complete signal analysis capability;
- spectrum analysers offer peak and average detection modes, where the peak amplitudes of a spectrum can be measured very much quicker than a receiver;
- spectrum analysers provide more comprehensive calibration routines than the receiver, but are not useful for electromagnetic interference measurements, specifically.

Generally spectrum analysers are clumsy to set up for manual operation and very few offer a manual frequency sweep capability. However, in practice, an operator can set up a spectrum analyser to monitor single frequencies, and by using the "Maximum Hold" display function, display only the peaks in amplitude, detected over time.

Both types of receiving device are used to measure the received signal level, either as an absolute level or as a reference level. It can contribute uncertainty components in two ways: absolute level uncertainty where the measurement of field strength is involved or in a verification procedure where a range change in the receiving device occurs between stages one and two, and non-linearity where the linearity of the receiving device (as given by the manufacturer) is applicable to the difference in the levels recorded in the two stages of the procedure.

u_{j47} is used throughout all parts of the present document for the uncertainty contribution associated with the absolute level of the receiving device.

NOTE 1: During free field test site verification procedures: the absolute level uncertainty is not applicable in stage one but should be included in stage two if the receiving device's input attenuator has been changed. This uncertainty contribution should be taken from the manufacturer's data sheet.

NOTE 2: During test methods: only applicable in the electric field strength measurement stage for a receiving equipment. This uncertainty contribution should be taken from the manufacturer's data sheet.

NOTE 3: During stripline verification: the absolute level uncertainty is not applicable in stage one but may be included in stage two if the receiving device's input attenuator has been changed. This uncertainty contribution should be taken from the manufacturer's data sheet.

NOTE 4: During stripline test methods: only applicable in the electric field strength measurement stage for a receiving equipment. This uncertainty contribution should be taken from the manufacturer's data sheet.

u_{j48} is used throughout all parts of the present document for the uncertainty contribution associated with the receiving device linearity.

NOTE 5: This uncertainty only contributes to verification procedures.

NOTE 6: During free field test site verification procedures: the linearity of the receiving device (as given by the manufacturer) is applicable to the difference in the levels recorded in the two stages of the procedure.

NOTE 7: During stripline verification: the linearity of the receiving device (as given by the manufacturer) is applicable to the difference in the levels recorded in the two stages of the procedure.

A further source of uncertainty is the mismatch between the receiving device's input and the cable connecting it to either the attenuator or antenna. The receiver input VSWR interacts with the cable VSWR in both the reference and actual measurements. However it is not necessarily the same value in each case. If the input attenuator setting on the receiving device remains constant throughout both the reference measurement and the actual measurement, (for a substitution measurement) the mismatch uncertainty cancels. If not (an absolute level is being measured) the mismatch uncertainty should be included.

10.6.1 Detector characteristics

An average detector is a detector, the output voltage of which is the average value of the magnitude of the envelope of an applied signal or noise [1]. Average detection occurs when the video bandwidth is less than the intermediate frequency bandwidth. A ratio may be defined of the (intermediate frequency bandwidth): (video bandwidth), and the greater the ratio, the greater the averaging effect will be (see figure 109a). The spectrum analyser scan rate should be adjusted to be compatible with the smallest bandwidth in the measurement otherwise distortion will occur as the filter time constants will not have been achieved if the sweep is too fast.

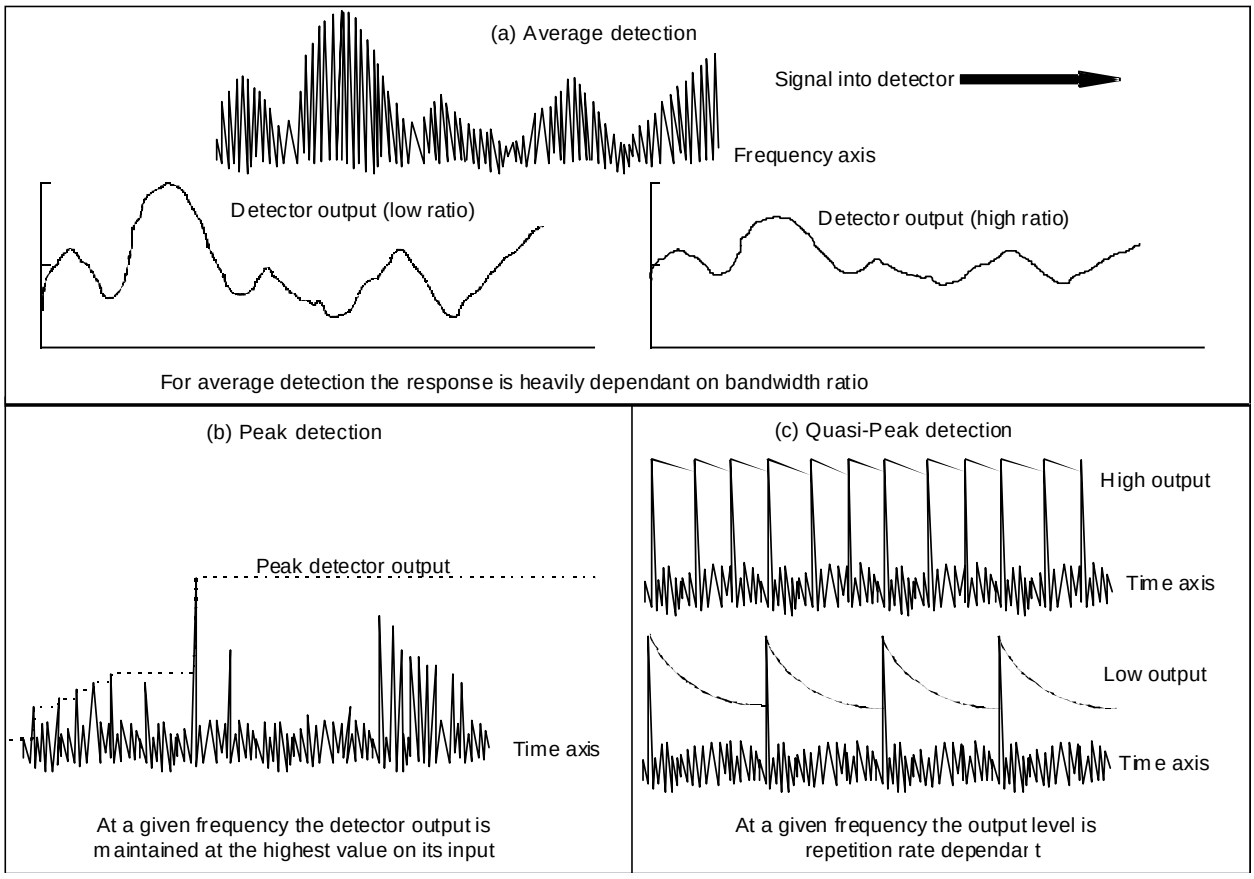

Figure 109: Detector modes

A Peak detector is a detector, the output voltage of which is the true peak value of an applied signal or noise [1]. Peak detection occurs when the detector simply maintains on its output the highest value detected on its input. On a spectrum analyser the video bandwidth is set to a value greater than the intermediate frequency bandwidth, and an envelope detector is used to measure the peak value of the envelope, see figure 109b.

A Quasi peak detector is a detector having specified electrical time constants that, when regularly repeated pulses of constant amplitude are applied to it, delivers an output voltage that is a fraction of the peak value of the pulses, the fraction increasing towards unity as the pulse repetition rate is increased. Quasi-peak detection represents an attempt to quantify the degree of annoyance caused by a source of electromagnetic interference and its value is dependant upon the two main factors of peak amplitude and repetition rate. For an arbitrary waveform the quasi-peak value will always be equal to or less than the peak value, see figure 109c.

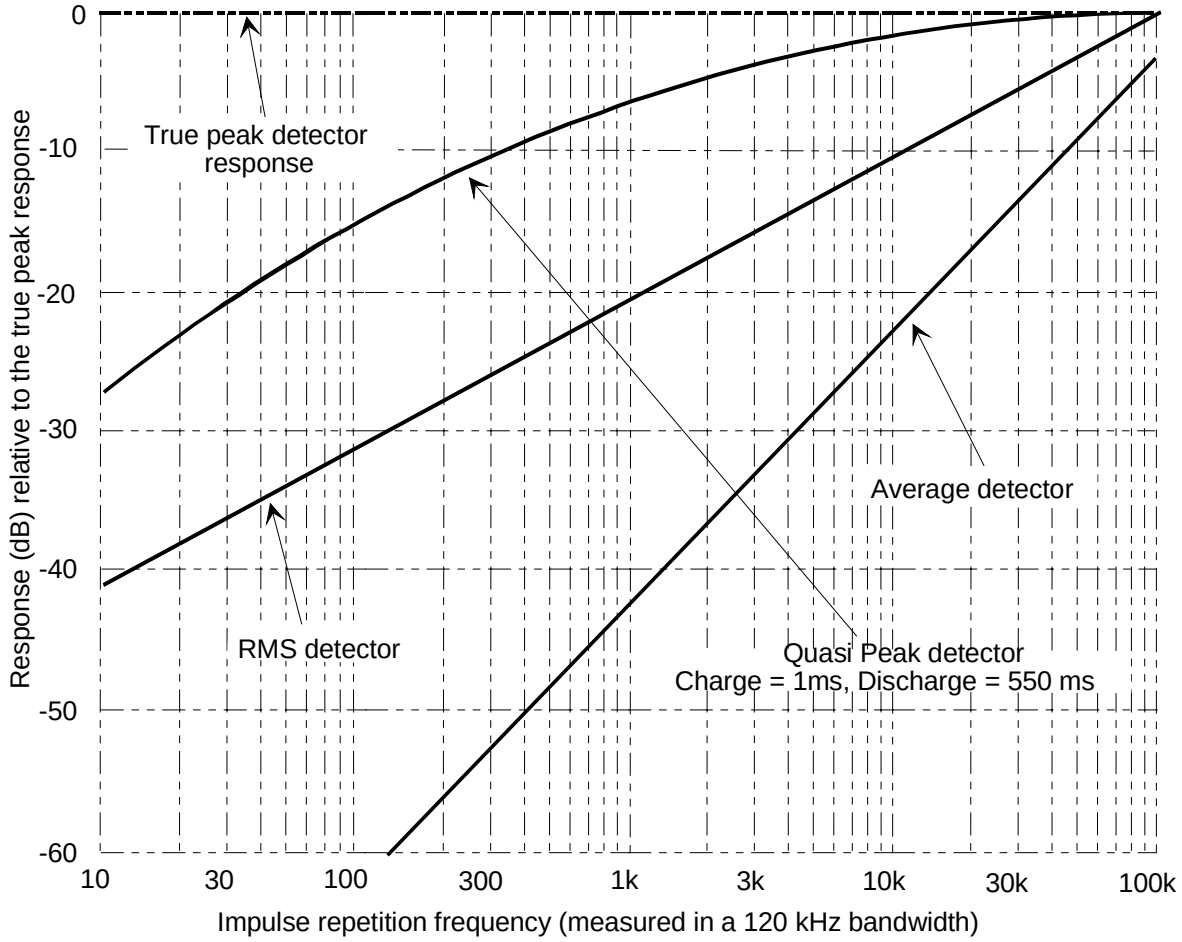

Figure 110: Ratio of different detector outputs verses impulse repetition frequency

An RMS detector is a detector the output voltage of which is the RMS value of an applied signal or noise [1]. A crest factor should be specified with the detector, e.g. to a specified maximum crest factor. RMS Detection, for any type of broadband input spectrum *RMS Value ∝ (Bandwidth)* and so the measured value may always be normalized to any specified bandwidth by a simple calculation involving the actual bandwidth used and the normalized bandwidth.

These are summarized in figure 110.

10.6.2 Measurement bandwidth

The measurement bandwidth can significantly affect the outcome of a measurement. For a purely sinusoidal wave, an increase or decrease in measurement bandwidth has no effect on the measured value, other than the relative passband loss of the selected bandwidth. For a broadband signal, however, the measurement bandwidth will affect the measured result all the time that the measured signal bandwidth is larger than the measurement bandwidth.

For emission measurements, emissions are described as being broadband or narrowband and coherent or incoherent. Generally a narrowband emission is one whose bandwidth is less than some previously defined reference bandwidth. In measurement terms this means the 3 dB bandwidth points are less than the 3 dB bandwidth of the receiving device. A broadband emission is one whose bandwidth is greater than the chosen reference bandwidth. In measurement terms this means the 3 dB bandwidth points are greater than the 3 dB bandwidth of the receiving device. See figures 111 and 112.

A coherent emission is one whose neighbouring frequency increments are related in both amplitude and phase (e.g. computer clocks). The neighbouring frequency increments of an incoherent emission have no relation in either phase or amplitude. These emissions are randomly distributed in frequency (e.g. the emissions from gas discharge lamps or noise diodes).

A narrowband signal (see figure 111) may be determined by the following methods:

- if the measured amplitude remains constant when reducing the intermediate frequency bandwidths;
- if the receiver is offset in frequency by half its 3 dB bandwidth and the change in level is greater than 3 dB;
- if the line spacing remains constant with slower sweep times;
- if when changing from a peak to an RMS detector, the signal level changes by less than 3 dB.

A broadband signal (see figure 112) may be determined by the following methods:

- if the measured amplitude of the signal changes with increasing intermediate frequency bandwidth;
- if the line spacing changes with sweep speed;
- if the receiver is offset in frequency by half its 3 dB bandwidth and the change in level is less than 3 dB;
- if when changing from a peak to an RMS detector, the signal level changes by more than 3 dB.

An aid to the identification of a broadband signal is when there is an apparent 20 dB increase in amplitude level, for a ten-fold increase in intermediate frequency bandwidth. This will always be the case until the intermediate frequency bandwidth approaches the bandwidth of the measured signal.

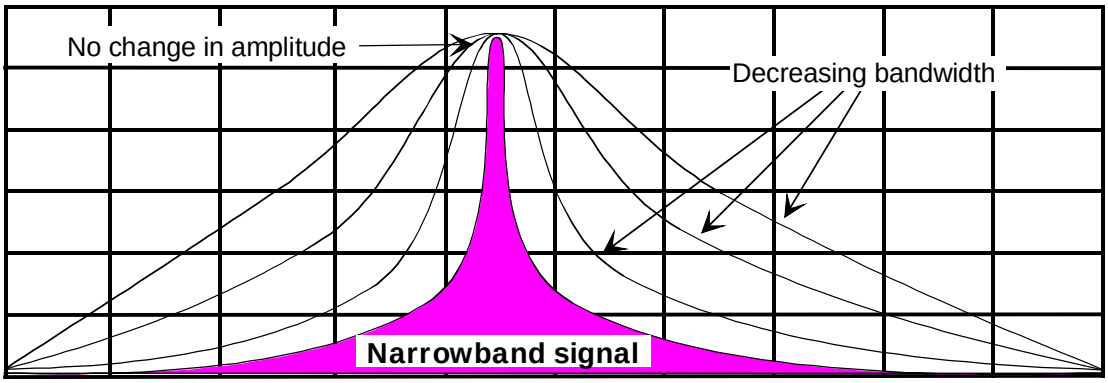

Figure 111: Narrowband signal characteristics

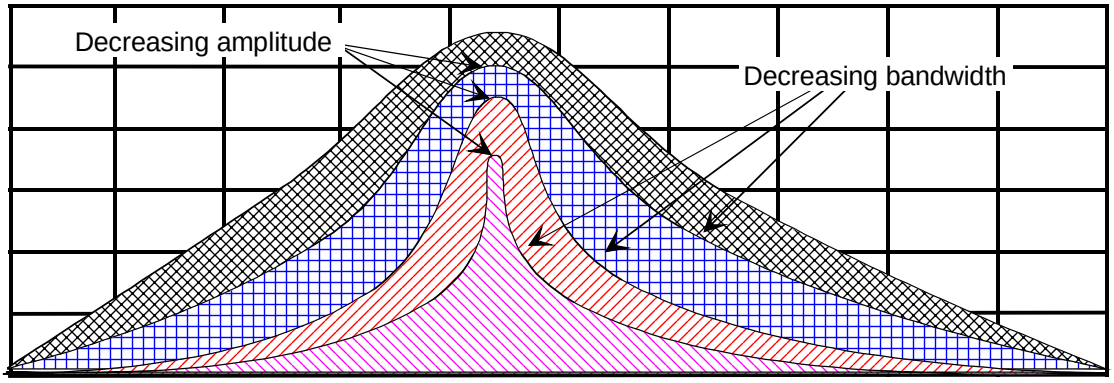

Figure 112: Broadband signal characteristics

General purpose spectrum analysers by themselves may not be suitable to perform compliance emission measurements. Consideration should be given to performance improvements such as the RF front end preselection, intermediate frequency bandwidths, both frequency band and shape, the intermediate frequency dynamic range, detector selections, display time constants and dynamic range. In order to overcome some of the current disadvantages some manufacturers have designed upgrades to the standard equipment. For example to overcome the problem of front end overload, a preselector can be added externally to the analyser. The RF preselector includes a comprehensive range of extra facilities necessary to upgrade the general purpose spectrum analyser to provide it with the equivalent performance of a measuring receiver.

With these additions spectrum analysers meet the requirements for most measurements, including quasi peak detection and CISPR specified bandwidths. The upgrade can also provide a loudspeaker and additionally, switches enabling some active devices to be turned on and off. This assists the operator to decide if an emission is an ambient, or is being radiated by the device under test.

10.6.3 Receiver sensitivity

The minimum discernible signal on a receiver is a signal that is just above the receiver noise floor, the receiver noise floor itself being bandwidth dependant. A method is required to calculate the receiver noise floor in a given bandwidth.

The source of the noise floor is thermal effects. The random motion of electrons in a resistor *"R"* Ω at an absolute temperature *"T"* Kelvin exhibits a random noise voltage across its terminals. The power spectral density of this noise voltage is given by Planck's distribution law: see [4]

$$P_n = \frac{4hfRB_W}{e^{\left(\frac{hf}{KT}\right)} - 1}$$

where:

T = temperature in Kelvin (normally taken as 293);

K = Boltzmann's constant (1,38 x 10^{-23});

B_W = measurement bandwidth of the receiver;

10^3 = multiplication factor from Watts to milliWatts.

For normal temperatures and for frequencies below the optical range this can be approximated by: see [4]

$$P_n = 4KTRB_W$$

This approximation is independent of frequency and hence is referred to as a white noise spectrum. The thermal noise delivered to a load of input impedance Z_{in} is: see [4]

$$P = \frac{4KTRB_W}{\left|R + Z_{in}\right|^2} R_{in}$$

where R_{in} is the resistive component of Z_{in}. If $Z_{in} = R$ which is the case for maximum power transfer, then: [4]

$$P = KTB_W$$

From this information the theoretical noise floor of a receiver can be calculated from:

Theoretical noise floor = 10 log $\sqrt{KTB_W}$ (10^3) dBm

This formula was used to calculate the graph of figure 113.

As an example for a particular measurement the dBm sensitivity for a measurement bandwidth of 1 MHz is calculated from:

$$10 \log (293 \times 1{,}38 \times 10^{-23} \times 1 \times 10^6 \times 10^3) = -113{,}9 \text{ dBm}$$

This is the minimum possible level for the receiver. However additional components within the receiver (which consists of more than just a resistor!) raise the noise floor above this level. For the purposes of the following calculations a receiver noise figure is taken as 12 dB and that for a spectrum analyser as 25 dB.

Also the above measurement has an assumed associated separation distance of 5 m. At 5 m the path loss is 60,40 dB.

The substitution power (sinewave) required to appear above the noise floor is therefore
(-113,9 + 60,40 + 12,0) dB = -41,53 dBm.

Now -41,53 dBm = 70,27 nW, which is the minimum discernible level in this particular case. Any specification level less than this means it is physically impossible to carry out the measurement.

This figure is increased considerably when using a spectrum analyser which may have a noise figure of 25 dB in which case the above calculation would render 1 410 nW. This analysis gives no consideration to the ambient levels at a particular facility or the gain of any antenna or preamplifiers which may be used.

The whole calculation can be carried out using the simple formula below:

Minimum discernible level = $10 \log (KTB_W \times 10^3) + 20 \log (4\pi d/\lambda) + R_{nf} + G_r$ dBm

where:

R_{nf} = Receiver noise figure;

G_r = Receive antenna gain (assumes the antenna has negligible noise figure).

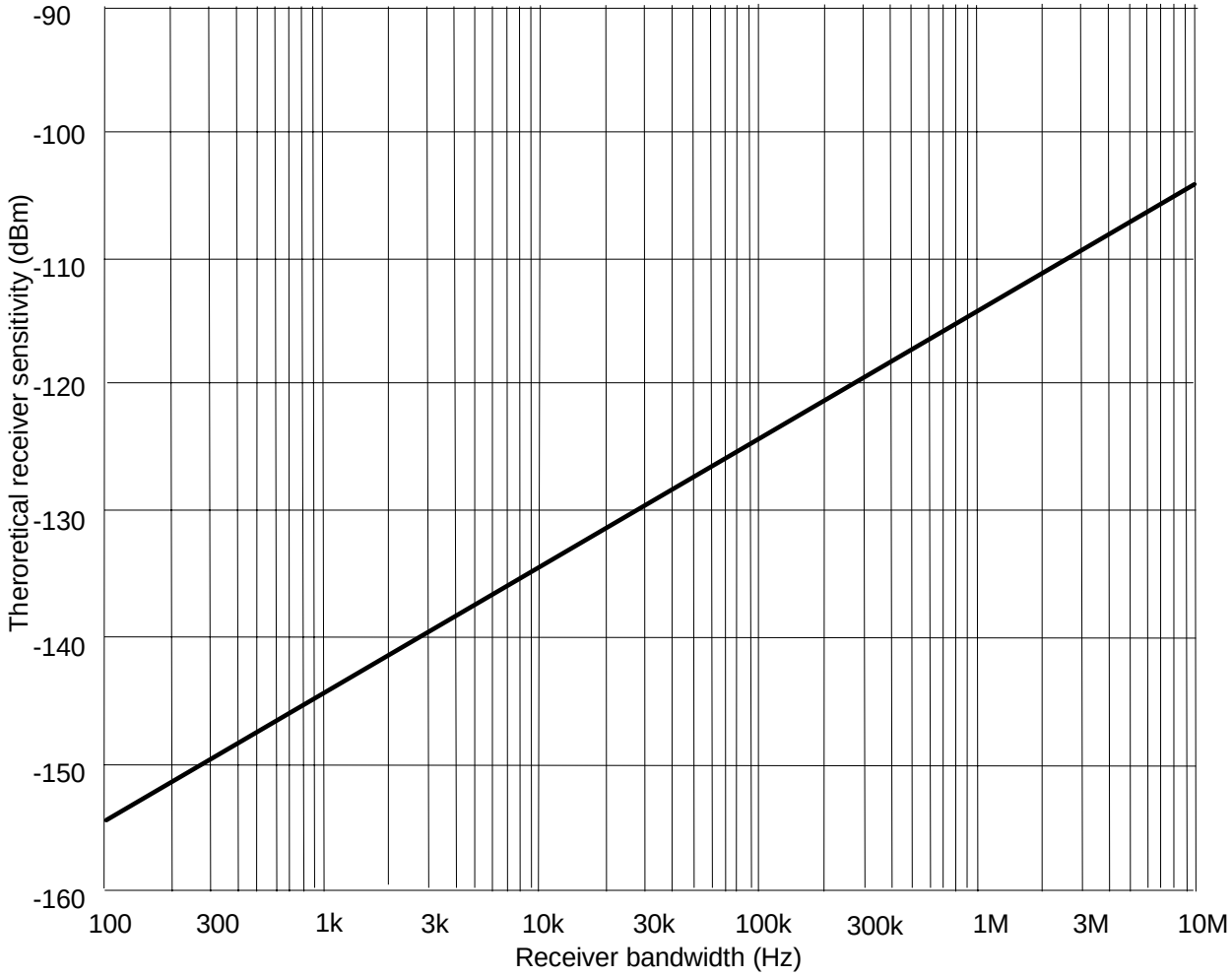

Figure 113: Receiver theoretical noise floor for a given bandwidth

10.6.4 Measurement automation

The complete measuring receiver, based on a spectrum analyser, is a complex instrument. Manufacturers often provide powerful automation software packages in order to take some of the difficulties away from the operator. By developing libraries of predetermined test set ups, and limit lines, the display can be processed from a standard linear frequency sweep, to the logarithmic sweep, generally shown in the specifications.

The advent of computer automation has significantly increased the speed at which the test operator can perform test measurements. This has a direct bearing on the cost of performing these measurements and the increase in throughput offsets the initial higher investment in automating the test equipment.

Automatic control software can normally be integrated into a complete system comprising two controller/motor assemblies, one for the turntable and one for the antenna mast. The software can then control the rotation and if necessary the peak search. This has the advantage over a manual system that the test will always be carried out in the same sequence and the method employed will always be the same.

This automatic set up has to be verified at least initially, enabling any software bugs to be removed. All modes of operation need to be checked, e.g. detector modes (RMS, peak, quasi-peak, etc.), detector response time and sweep time. After verification, regular checks are required to ensure that nothing has inadvertently deteriorated and that all remotely controlled mechanical actuators are operating correctly.

In most cases, the investment in an automatic system based on a spectrum analyser with the appropriate upgrades, is easier than a combination of measuring receivers.

10.6.5 Power measuring receiver

For the measurement of transmitter adjacent channel power, a power measuring receiver is required. There are three types of power measuring receivers in common usage, they are:

- an adjacent channel power meter with mechanical filters;
- a spectrum analyser;
- a measuring receiver with digital filters.

Adjacent channel power meter: The transmitter under test is connected to an adjacent channel power meter through a matching and attenuating network. This method involves the measurement of the transmitter adjacent channel power by off-setting an IF filter which has a very well-defined shape.

The meter consists of a mixer, an IF filter, an amplifier, a variable attenuator and a level indicator. The local oscillator signal to the adjacent channel power meter is supplied from a low noise signal generator.

Caution should be exercised when a non-symmetrical filter is used. In these cases the receiver needs to be designed such that the tighter tolerance filter slope is used close to the carrier. This type of equipment is used to measure adjacent channel power in systems employing channel spacings of 10 kHz, 12,5 kHz, 20 kHz and 25 kHz.

The uncertainty of this measurement is of the order of ±3 dB to 4 dB.

Spectrum analyser: The transmitter under test is connected to a spectrum analyser via a matching and attenuating network and the ERP is recorded as reference. The adjacent channel power is calculated from spectrum analyser reading (9 samples) by means of Simpson's Rule. This method is usually employed for channel spacings outside the land mobile range, such as 50 kHz or 100 kHz.

The uncertainty of this measurement is of the order of ±2 dB to 3 dB.

Measuring receiver with digital filters: The transmitter under test is connected to a measuring receiver with digital filters through a matching and attenuating network as in the adjacent channel power meter method above.

This method involves the measurement of the transmitter adjacent channel power by sampling the power in the adjacent channels. The measuring receiver with digital filters is normally for 10 kHz, 12,5 kHz, 20 kHz and 25 kHz channel spacing.

The uncertainty of this measurement is of the order of ±0,5 dB to 1 dB.

u_{j49} is used throughout all parts of the present document for the uncertainty contribution associated with the power measuring receiver.

10.7 EUT

The ideal EUT is a radiating (or receiving) device which is infinitesimal and therefore has an isotropic field pattern which is stable with time. In practice, however, the EUT will have a physical extent. This causes uncertainties in the distance to the test antenna as there is no standard way of determining the position of the radiating source within the EUT, or its changing position whilst the equipment is rotated. Also in real life an EUT is not stable with time. It is influenced by environmental parameters such as temperature, humidity, and air pressure. These variations can have significant effects on the long term stability of the EUT. It also changes in time due to, for example, self heating (as a result of the duty cycle) and falling output power due to battery characteristics. Equally, the EUT may be burst or frequency agile, in which case the time to measure power levels, frequencies, etc. is limited. All these factors may cause additional measurement uncertainties.

u_{j50} is used throughout all parts of the present document for the uncertainty contribution associated with the influence of the ambient temperature on the ERP of the carrier.

u_{j51} is used throughout all parts of the present document for the uncertainty contribution associated with the influence of the ambient temperature on the spurious emission level.

Degradation detection uncertainty contributes to receiver test methods and is the resulting RF level uncertainty associated with the uncertainty of measuring 20 dB SINAD, 10^{-2} BER of a bit stream or 80 % message acceptance ratio. The magnitude can be obtained from the method described in TR 100 028 [11]. For example, if 20 dB SINAD is measured then a value for the standard uncertainty of the RF level of 7,83 % is obtained from TR 100 028 [11]. This should then be transformed to the logarithmic form (annex C).

u_{j52} is used throughout all parts of the present document for the uncertainty contribution associated with the degradation RF level uncertainty when measuring SINAD, bit stream or message acceptance ratio.

NOTE 1: This uncertainty only contributes to receiver test methods and is the resulting RF level uncertainty associated with the uncertainty of measuring 20 dB SINAD, 10^{-2} BER of a bit stream or 80 % message acceptance ratio.

The EUT can be affected by the level of the actual power supply as well as by the supply cabling. As cables are made of metal they may change the radiation patterns and if it is not possible to exactly repeat the position of the cables, they can cause poor repeatability of the measurement.

u_{j53} is used throughout all parts of the present document for the uncertainty contribution associated with the influence of setting the power supply on the ERP of the carrier.

u_{j54} is used throughout all parts of the present document for the uncertainty contribution associated with the influence of setting the power supply on the spurious emission level.

u_{j55} is used throughout all parts of the present document for the uncertainty contribution associated with the mutual coupling to the power leads.

NOTE 2: Modifications to the EUT for testing purposes is sometimes required. This only applies to devices with integral antennas. At least two samples are required for testing, one that has been modified for parametric (conducted) testing and one that has not (for radiated tests). Individually they provide results for two different samples.

An artificial antenna (or RF load) is sometimes required in (I)-ETSs or ENs for cabinet radiation tests. This is another area that is often overlooked. The only stated requirement (usually) is that it should be relatively small compared to the EUT and no account is usually paid to any of the characteristics of the load. The load is therefore unlikely to have a measured frequency response above 1 GHz. So the question arises "Does this load act as a radiator at frequencies from 1 GHz to 12,75 GHz". For example, if the equipment has an emission outside the required specified limit at, say, 6 GHz, is this due to the EUT or is it due to the EUT interacting with the load? ETSs refer to "a 50 Ω substantially non-reactive, non-radiating power attenuator which is capable of safely dissipating the power in the transmitter". The generic terms "non reactive" and "non radiating" are meaningless when applied to a load without a specified frequency range. Their definition should, as a minimum, cover the required frequency range for the cabinet radiation test.

Drive equipment instructions (manufacturer supplied) should be precise and allow the test engineer to be able to exercise the different modes of operation of the EUT and determine if there are any EUT malfunctions. The operating instructions should indicate, where applicable, the status of the EUT, the length of transmission of information, etc.

Repeatability of settings (i.e. integral software control of, e.g. power level) is another possible source of uncertainty. Therefore software version status should be included in documentation of the results where appropriate.

10.7.1 Battery operated EUTs

Battery operated EUTs require special attention during testing. For example, how will the battery pack affect the measured results?

Normally the relevant standard requires that the power source of the EUT should be replaced by a test power source, capable of producing normal and extreme test voltages as stated in the relevant specifications. The supply voltage to the EUT should be set to the appropriate value as specified by the manufacturer. This should be measured on a digital voltmeter connected to the power terminals of the EUT and the level maintained constant throughout the test.

The internal impedance of the test source should be low enough for its effect on the test results to be negligible. This statement can often cause problems when for example a manufacturer uses the battery plate impedance to limit carrier power in "cheap" EUTs.

For EUT using other power sources, or capable of being operated from a variety of power sources, the extreme test voltages would normally be those agreed between the EUT manufacturer and the authority and should be recorded with the test results.

Ideally, the unit should not be tested with batteries powering it as the batteries discharge during testing with the result that emissions and carrier power levels reduce during the test in a largely undefined way.

To avoid this situation, two steps are possible:

- The first is to monitor the battery with a DVM, which ensures the supply levels but introduces cables to the EUT which could adversely affect the results. Also, what change in EUT performance results if the battery voltage is lower at the test completion than at the start?

- The second is to power the EUT with an independent power supply whose output is monitored at the battery terminals of the EUT. This again introduces cables to the EUT, which could adversely affect the results, but the supply voltage can be maintained constant throughout the test.

The second solution appears only marginally better than the first. It gives confidence that the power supply level remains constant throughout the test but we still have cables going into the equipment.

One solution is to carry out the test on the EUT using a power supply, and if an emission level is above the specification limit, re-test using fully charged batteries. This is the most common solution and is much better than testing on batteries alone.

Other considerations are:

- How many emissions that pass when using a power supply are subsequently tested with a battery to see if they fail?

- Typically, for hand portables, the battery pack often forms a significant part of the volume of the radio and, being metallic, it can have a major effect on the emissions. The problem here is how to test the radio so as not to adversely effect the results due to the omission of the battery pack.

- Any battery storage compartments should be filled with "spare" batteries. Where an EUT is powered only by battery, these should remain in place (with tape over their terminals) and power leads connected to the supply terminals in the equipment.

10.8 Frequency counter

The frequency of the device may be measured by several means. Amongst these, the purpose built frequency counter and the frequency readout on a spectrum analyser are the most common. The frequency counter will be specified by,

amongst other things, crystal stability, temperature drift and ageing rate. Similarly the spectrum analyser will be specified by a crystal stability, resolution bandwidth and sweep width.

Whichever method is used, there will be an uncertainty associated with the measured frequency due to the instrumentation.

u_{j56} is used throughout all parts of the present document for the uncertainty contribution associated with the measured frequency due to the absolute reading of the frequency counter.

If the frequency reading is fluctuating, then an uncertainty exists due to the ability to read the correct value. When this variation occurs an average frequency reading has to be estimated by the engineer.

u_{j57} is used throughout all parts of the present document for the uncertainty contribution associated with the measured frequency due to estimating the average reading of the frequency counter.

10.9 Salty man/salty-lite and Test Fixtures

Salty man/Salty-lite: The human body has a significant effect on the electrical performance of a body worn equipment. For test purposes the artificial human body should simulate the average human body. Two main types of artificial human bodies are used in testing salty man and salty-lite.

u_{j58} is used throughout all parts of the present document for the uncertainty contribution associated with the human simulation of the salty man/salty-lite.

NOTE 1: This is the difference between the average human being and the artificial one used in the test methods on free field test sites. Its value should be obtained from table 27.

Table 27: Uncertainty contribution: human simulation

Test Facility	Frequency Range	Standard Uncertainty
Salty man	30 MHz to 150 MHz	0,58 dB
	150 MHz to 1 000 MHz	1,73 dB
Salty-lite in Anechoic Chamber	100 MHz to 150 MHz	1,73 dB
	150 MHz to 1 000 MHz	0,58 dB
Salty-lite in Open Area Test Site or Anechoic Chamber with Ground Plane	70 MHz to 150 MHz	1,73 dB
	150 MHz to 1 000 MHz	0,58 dB

The presence of the Salty man/Salty-lite can also lead to uncertainty due to enhanced field strengths and de-tuning of the EUT, both of which are dependant on the spacing away from the Salty man/Salty-lite.

u_{j59} is used throughout all parts of the present document for the uncertainty contribution associated with the field enhancement and de-tuning of the EUT on the Salty man/Salty-lite.

Test Fixtures: A Test Fixture is a type of test site which enables the performance of an integral antenna equipment to be measured at extreme conditions. The close physical proximity of the Test Fixture to the EUT can result in mutual interaction, causing performance changes to the EUT.

u_{j60} is used throughout all parts of the present document for the uncertainty contribution associated with the effect on the EUT of the Test Fixture.

NOTE 2: During testing at extremes of temperature, the Test Fixture is placed with a climatic facility. Such a facility usually has metallic walls which can act as reflection sources and form a resonant cavity. Both effects can modify the internal field uniformity, leading to uncertainties in measurements made within the facility.

u_{j61} is used throughout all parts of the present document for the uncertainty contribution associated with the climatic facility effect on the EUT in tests using a Test Fixture.

10.10 Site factors

The construction and type of facility will contribute uncertainties, normally by coupling and reflection, that make the measured result differ from the ideal characteristic. For example, the variation between measured site attenuation from the ideal performance in an Anechoic Chamber is a function of the amount of suppression of the wall and ceiling reflections and any unaccounted for coupling effects between the two antennas used. The performance of pyramidal absorbers, in turn, change with a number of parameters i.e. thickness, angle of incidence, separation of the pyramidal cone tips, etc. Site factors cover all those uncertainties and generally over any reflection and measurement influences not accounted for elsewhere.

10.11 Random uncertainty

All measurements are subject to random variations. Random uncertainty should be assessed from multiple measurements of the same measurand.

u_{i01} is used throughout all parts of the present document for the uncertainty contribution associated with random uncertainty (the estimated or measured effect that randomness has on the final result of a measurement).

10.12 Miscellaneous

Acoustic interfaces are often used for EUT such as paging receivers where the expected response is simply a tone. The acoustic coupler complexity may range from a plastic tube with no calibration required (as it is only the sound of the tone that is needed) to fairly sophisticated acoustic couplers with which, for example, distortion measurements are made.

10.12.1 Personnel

The personnel operating a test site should have been trained in an appropriate manner and, preferably, have a basic understanding of the physics involved. They should also be fully acquainted with the particulars of each measurement. It should be noted, however, that there have been occasions when even experienced engineers have provided a major source of measurement error. For example, when on temporary secondment to a new team, it has been assumed, wrongly, that the engineer was fully aware of the requirements of a measurement procedure and, as a result adequate briefing was not given.

A further source of uncertainty can be introduced by other teams working in the near vicinity, perhaps with equipment which radiates (whether by accident or design), and with no knowledge or understanding of the tests conducted on the test site. Co-ordination of the teams of engineers is vital, in this circumstance, to remove unnecessary measurement uncertainties.

The relationships between the members of a test site measurement team can be a further source of measurement error. Problems related to a particular measurement or a particular procedure may, for a reason due to either the management of the team or personnel problems within the team, not be communicated throughout that team with the end result that errors occur.

Improvisation and individualism are some behaviour characteristics to be discouraged. For example when a particular adapter, cable, etc. goes missing or is unserviceable, it should be replaced by a fully calibrated part and not by the first one that comes to hand. Similarly, the last letter of a procedure needs to be adhered to with no short cuts being made. Impatient behaviour, whether as a result of an engineer's nature or due to time or cost pressures, can produce blunders and measurement errors at some time and should similarly be discouraged.

To an extent, the ideal test engineer is difficult to find. On the one hand, he/she is required to be knowledgeable and capable of thinking for himself/herself, whilst on the other hand he/she needs be fully prepared to follow, exactly, the instructions laid down in the test procedures. These are somewhat contradictory personal qualities and are almost certain to produce errors unless adequate quality control is employed.

Over familiarity with a test procedure is another factor which can lead to errors since the test engineer may tend not to devote full concentration to a task he/she has carried out many times before. Similarly, a test site known to provide accurate results can result in complacency within the engineer and, for example, a cable close to hand may be used rather than a better, calibrated one which may involve some time to locate.

Boredom, as a result of the test engineer's mind not being giving enough to occupy it, can lead to inadequate attention being paid, with inevitably, errors resulting. It should be a requirement that each engineer is given a sufficiently demanding role within any given test procedure to prevent this occurring.

In general, the engineers carrying out the measurements on a test site can be a major source of measurement uncertainty. It is suggested that the only way to adequately eliminate the associated uncertainties is for a rigorous quality control procedure to be in operation. This should involve checking the conditions under which the tests were conducted and ensuring that all aspects of the relevant procedure were adhered to.

10.12.2 Procedures

Making a measurement on a test site can be a very time consuming task because many predefined procedures have to be carried out. These procedures (involving positioning, calibration, peaking, substitution, etc.) needs to be very precise and detailed to ensure a correct and reproducible result of the measurement. This is due to the fact that various test sites have different procedure and the results are not inter-comparable in all cases.

For example, the results from an Open Area Test Site with a metal ground plane and the results from an Anechoic Chamber will almost certainly be different for the same device. Therefore the measurement procedures need to be followed to the smallest detail.

10.12.3 Methods

Typically the current (I)-ETSs and ENs requiring radiated measurements will give test facility details in their annex A. Annex A of these standards state for example for Open Area Test Sites:

The test site shall be on a **reasonably level surface or ground**. At one point on the site, a **ground plane of at least 5 m diameter shall be provided**. In the middle of this ground plane, a non-conducting support, capable of rotation through 360° in the horizontal plane, shall be used to support the test sample at 1,5 m above the ground plane. The **test site shall be large enough to allow the erection of a measuring or transmitting antenna at a distance of λ/2 or 3 m, whichever is the greater.** The distance actually used shall be recorded with the results of the tests carried out on the site.

Sufficient precautions shall be taken to ensure that reflections from extraneous objects adjacent to the site and ground reflections do not **degrade** the measurements results.

There are a few bolded phrases, these are all open to varying interpretation. The uncertainties are in the meanings of "reasonably", "sufficient" and "degrade".

Suppose a ground plane is constructed in good faith, of 5 m diameter (see figure 114), and a spurious emission test is to be performed.

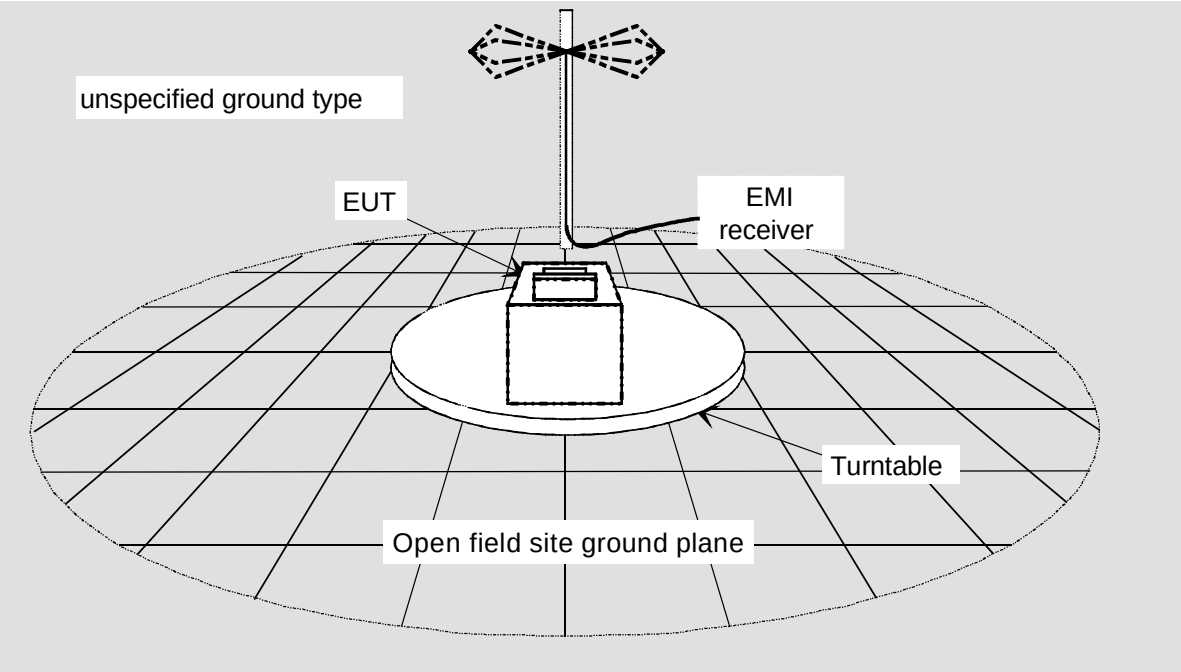

Figure 114: Typical emission set up on a ground plane

Suppose the engineer discovers an emission at 30 MHz, and sets up a substitution measurement as shown in figure 115 to measure its level.

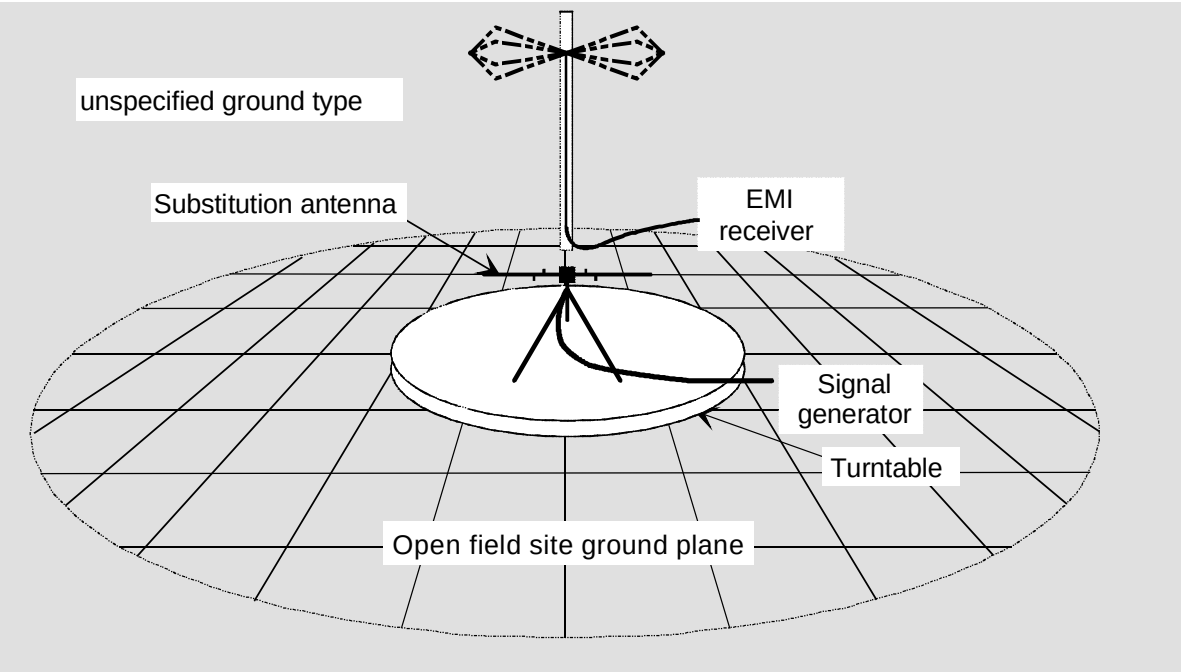

Figure 115: Substitution measurement

He then remembers from annex A of the testing standard "a distance of λ/2 or 3 m, whichever is the greater" and realizes that this is 5 m at 30 MHz and returns to the first configuration to remake the measurement at 5 m. Now, however, he realizes that:

- at a measuring distance of 5 m, for an EUT located in the middle of a 5 m diameter ground plane, the ground plane edge is the ground plane reflection point;
- that the measuring antenna is now remote from the ground plane over an unspecified ground type;

- that he is involved in a very complex (difficult to analyse) measurement set up and wishes he had a larger ground plane.

wherever possible, test methods should be unambiguous and need as little "interpretation" as possible.

10.12.4 Specifications

When defining limits for specifications, a certain amount of care should be exercised regarding the practicalities of a given measurement. An example of a limit of substituted power is:

- substituted power limit: 20 nW;
- frequency: 5 GHz;
- separation distance: 5 m;
- measurement bandwidth: 1 MHz.

What does all this mean? Specifically, what signal level do we have to detect at the receiver?

20 nW = -47,0 dBm, which is the limit value at the substitution antenna.

The formula for path loss (between isotropic antennas) is:

$$\text{Path loss} = 20 \log (4\pi d/\lambda)$$

and in this case (5 m separation at 5 GHz) the path loss is:

$$20 \log (20\pi/0{,}06) = 60{,}4 \text{ dB}$$

This gives a signal level of -47 dBm + (-60,40 dB) = -107,4 dBm at the receiver input.

This requires a fairly sensitive receiver although improvements can be brought about by including the gain of antennas. Additionally it is possible to improve these figures with the use of pre-amplifiers.

There are many more problems like this with procedures, methods and specifications. For instance during measurement on a test site with a ground plane it is not sufficient to elevate the test antenna to the height where the peak is **normally** found. The peaking procedure needs to be carried out in **every** case. Unpredictable influences (i.e. the EUT itself) may cause the peaking height to change.

Other more general considerations are listed below.

- the measurement techniques used need to be very clear;
- the procedures need to be explicit and situations open to interpretation should be avoided;
- thoroughness is required by the inclusion of diagrams;
- full descriptions of methods;
- examples of all calculations that are required;
- specifications needs to be definitive and not under consideration.

These all fall in the domain of the writers of the testing standards.

History

Document history		
Edition 1	February 1998	Publication as ETR 273-1-1
V1.2.1	December 2001	Publication